ISSN: 2153-1196 Volume 10, Number 10, September 2019

Scientific Research Publishing

Journal of Modern Physics

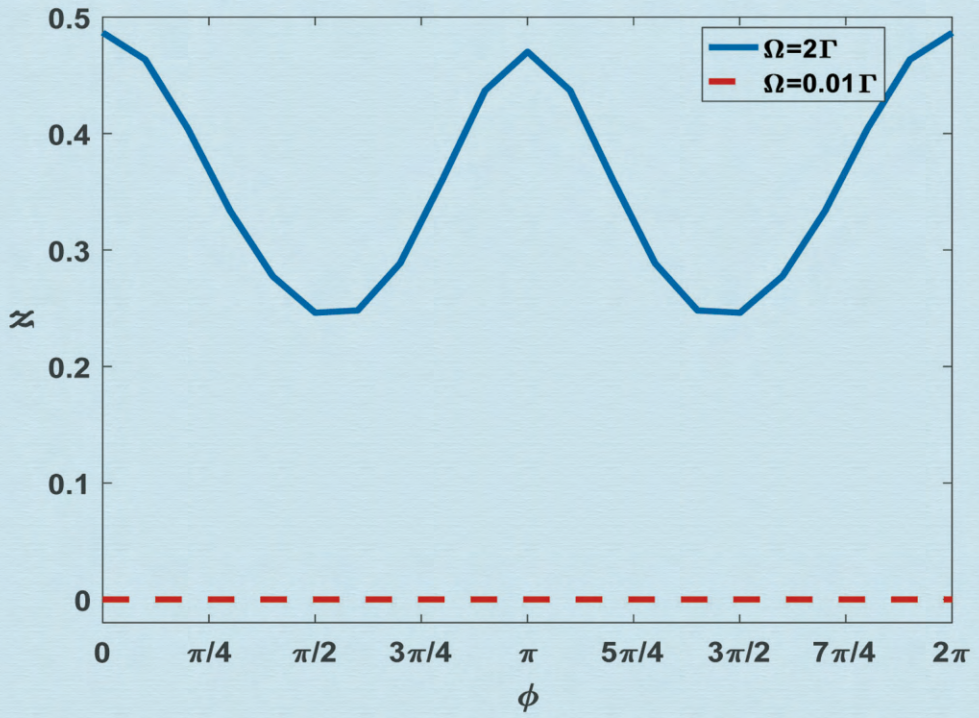

ISSN: 2153-1196
9 772153 119007 10

https://www.scirp.org/journal/jmp

Journal Editorial Board

ISSN: 2153-1196 (Print) ISSN: 2153-120X (Online)
https://www.scirp.org/journal/jmp

Editor-in-Chief

Editorial Board

Scientific Research Publishing

Journal of Modern Physics, 2019, 10, 1157-1298
https://www.scirp.org/journal/jmp
ISSN Online: 2153-120X
ISSN Print: 2153-1196

Table of Contents

Volume 10 Number 10 September 2019

The figure on the front cover is from the article published in Journal of Modern Physics, 2019, Vol. 10, No. 10, pp. 1177-1189 by Jing Wang, Yunan Wu and Wenyu Ji.

Journal of Modern Physics (JMP)
Journal Information

SUBSCRIPTIONS

The *Journal of Modern Physics* (Online at Scientific Research Publishing, https://www.scirp.org/) is published monthly by Scientific Research Publishing, Inc., USA.

Subscription rates:
Print: $89 per issue.
To subscribe, please contact Journals Subscriptions Department, E-mail: sub@scirp.org

SERVICES

Advertisements
Advertisement Sales Department, E-mail: service@scirp.org

Reprints (minimum quantity 100 copies)
Reprints Co-ordinator, Scientific Research Publishing, Inc., USA.
E-mail: sub@scirp.org

COPYRIGHT

PRODUCTION INFORMATION

For manuscripts that have been accepted for publication, please contact:
E-mail: jmp@scirp.org

Journal of Modern Physics, 2019, 10, 1157-1165
https://www.scirp.org/journal/jmp
ISSN Online: 2153-120X
ISSN Print: 2153-1196

Collapse of Bell's Theorem

Guangye Chen

Shanghai Jiao Tong University, Shanghai, China
Email: gychen@sjtu.edu.cn

How to cite this paper: Chen, G.Y. (2019) Collapse of Bell's Theorem. *Journal of Modern Physics*, **10**, 1157-1165.
https://doi.org/10.4236/jmp.2019.1010076

Received: July 30, 2019
Accepted: August 25, 2019
Published: August 28, 2019

Abstract

Bell's theorem founded on Bell's inequalities asserts that no local realistic theories can reproduce all quantum mechanical predictions for spin correlation of particle pairs. It is pointed out that the assumption of setting-independent probability makes Bell's inequalities not impose constraint on all local realistic models and thus constitutes a theoretical loophole of Bell's theorem. A counterexample is presented by showing that a local realistic model with appropriate probability density reproduces all quantum mechanical predictions. It becomes clear that experiments violate Bell's inequalities because the real correlation functions are not constrained by these inequalities. It is also exposed that, rigorous logical reasoning of counter factual deduction does not permit to exclude any premises of Bell's inequalities by a certain amount of experimental violations of these inequalities.

Keywords

Bell's Theorem, Bell's Inequalities, Local Realism, EPRB Experiment

1. Introduction

Bell's theorem has influenced some physics researches over a half of century. As the foundation of the theorem, Bell's original inequality [1] has inspired two variants CHSH (Clauser-Horne-Shimony-Holt) inequality and CH (Clauser-Horne) inequality for convenience of experimental implementation [2] [3]. Several authors also claimed proofs of the theorem without using inequality. These proofs include the GHZ (Greenberger-Horne-Zeilinger) paradox [4] and Hardy's paradox [5]. As all proofs without inequality commence with the quantum mechanical concept of entangled state, they involve inherent inconsistency in logic for experimental test to discriminate between quantum mechanical concepts and classical concepts. Therefore, we are confined to consider merely the original Bell's theorem founded on Bell's inequalities, which are derived totally from

classical concepts and have been used as criterions in most experimental tests.

Since the publication of Bell's seminal work, about twenty Bell experiments have been performed [6]. Majority of these experiments yielded outcomes violating one of Bell's inequalities and meantime agreeing with quantum mechanical predictions. During the earlier period, this experimental fact had been interpreted as the evidence of completeness of quantum mechanics or as a proof that no hidden variable theories exist, as then it had been often claimed that quantum mechanics overwhelms local realistic theories experimentally. Indeed, if quantum mechanics were proved a complete theory, not merely correct in predicting some properties of quantum systems, all weird properties arisen from its interpretation would be accounted as real physical phenomena. But proof of completeness of quantum mechanics seems far more difficult than the contrary. It was recognized many years later that violation of Bell's inequalities and proof of completeness of quantum mechanics are two irrelevant things. The objective of all Bell experiments was turned to exclude local realistic theories. Yet there has been no conclusive answer up to now. For the advocates of Bell's theory, the pending situation is caused by remaining loopholes for experimental tests of Bell's inequalities, despite the fact that the two main recognized loopholes were closed simultaneously in one experiment [7]. For other physicists, however, Bell's theorem is dubious due to the basic concepts or skeptical assumption underlying Bell's inequalities.

Negation of Bell's theorem is from computer simulations and theoretical analyses. Only theoretical aspect is exemplified here. Tipler showed that quantum non-locality does not exist if observed quantum particles and observer are both assumed to obey quantum mechanics as in the many-world interpretation [8]; Hess and Philipp demonstrated that Bell's theorem will be invalid if Bell's inequalities cover an extended parameter space that includes instrument parameters correlated by both time and setting dependencies [9] [10]. Although above viewpoints or alike have aroused argument or strong opposition from Bell's followers, they represent right stance against abandoning local realism, which is the fundamental believing in almost all other established scientific theories.

So far, the fact of experimental violations of Bell's inequalities has been established. This fact explains that Bell's inequalities are not applicable to the pertinent experiments. In other words, they are invalid in physics. Because their mathematical derivations are too simple to be suspected, it is deduced that at least one of their premises is wrong. [Here, we see that the verification of Bell's theorem is somewhat logically strange in comparison with that of other rules or theorems in physics. The involved problem will be discussed in the Section 3]. Some physicists think the attribute of local realism associated with the expression of the spin correlation function must be ruled out. However, the assumption of setting-independent probability can also be responsible for the situation. This point has long been ignored but is fatal to Bell's theorem. Without any further analysis, we immediately identify this assumption to be a theoretical loophole of the theorem, because it is not a necessary condition for locality. A set-

ting-dependent probability can also be factorized to guarantee the locality of a correlation function. Therefore, we are sure that Bell's inequalities do not impose constraint on all local models and for this reason their experimental violation cannot rule out locality theoretically.

Zhao showed the necessity of setting dependence of the probability [11]. While the assumption of setting-independent probability is indispensible for derivation of Bell's inequalities. Bell had indeed sensed that setting-independent probability might be one of the four possibilities invalidating his theorem [12]. He thus proposed a measure for compensation while the inequality was kept in use [13]. Regarding this issue, Clauser also proposed a countermeasure [2]. To evaluate the effect of these compensations is very difficult, but it is unlikely that they could make the Bell's inequality cover up all local models.

To avoid the mentioned problem, actually, one can circumvent Bell's inequalities by investigating a correlation function directly. That is, one can exploit a correlation function that obeys the general condition of locality and then examine its compatibility with experimental outcomes as well as quantum mechanical prediction. If the concerned properties of a correlation function can be worked out directly, why do we make a detour by investigating them through a fabricated constraint on it?

It has been demonstrated that quantum mechanical correlation could be reproduced by local models. To author's knowledge, Barut *et al.* advanced an instance with a simple model of a classical break-up process [14], and Gisin *et al.* with a local hidden variable model exploiting detection loophole [15]. As these demonstrations are not directly related to the correlation function in Bell's original proof, and do not reveal the flaw of Bell's inequalities, they do not disprove Bell's theorem.

In this paper, a counterexample to Bell's theorem is presented by demonstrating that a spin correlation function adopted from an extension of Bell's origin reproduces all quantum mechanical predictions under appropriate probability densities. It is explained that verification of Bell's theorem through certain amount of experimental violations of Bell's inequalities is logically prohibited even if these inequalities imposed constraint on all local models. In summary, the counterexample disproves Bell's theorem firmly, and the cause for which is that Bell's inequalities do not impose constraint particularly on real correlation functions.

2. The Counterexample

To avoid ambiguity, let us begin by making clear the precise scope of local realistic models that is referred in Bell's theorem. As generally understood and also explained by Greenberg *et al.* [16], "local realistic theories" means that there are no other restrictions except locality and reality on the probability density, the hidden variable and the measuring outcomes in the correlation expression in Bell's original proof. For conciseness, spin 1/2 of particle is tacitly assumed in

following discussion.

It is known that quantum mechanical prediction for the spin correlation of particle pairs in EPRB experiment is given by

$$\langle \Psi | \sigma_a \otimes \sigma_b | \Psi \rangle = -\boldsymbol{a} \cdot \boldsymbol{b} \tag{1}$$

where $\langle \Psi | = \left(|+\rangle \otimes |-\rangle - |-\rangle \otimes |+\rangle \right) \sqrt{1/2}$ is the singlet spin state for the two particles, and $\sigma_a = \boldsymbol{\sigma} \cdot \boldsymbol{a}$ and $\sigma_b = \boldsymbol{\sigma} \cdot \boldsymbol{b}$ are the components of Pauli spin operator $\boldsymbol{\sigma}$ in the directions of $\boldsymbol{a}$ and $\boldsymbol{b}$ respectively; $\otimes$ denotes the Kronecker product, $\boldsymbol{a}$ is the unit vector of the spin analyzer setting for particle 1 and $\boldsymbol{b}$ for that of particle 2; the single particle vectors $|+\rangle$ and $|-\rangle$ denote "spin up" and "spin down" with respect to some coordinate system.

On the other hand, Bell gave the correlation function of local realistic theories as [1]

$$\mathrm{P}(\boldsymbol{a},\boldsymbol{b}) = \int \rho(\boldsymbol{\lambda}) \mathrm{A}(\boldsymbol{a},\boldsymbol{\lambda}) \mathrm{B}(\boldsymbol{b},\boldsymbol{\lambda}) \mathrm{d}\boldsymbol{\lambda} \tag{2}$$

From the expression above Bell derived his inequality and found that quantum mechanical prediction does not obey it. This led to his famous theorem. It is easily found that the setting-independent probability in Equation (2) is indispensible for the derivation of Bell's inequality. As aforementioned, this premise limits the range of local models imposed by the inequality. In other words, that correlation of Equation (2) cannot reproduce the quantum mechanical prediction does not prevent the correlation given by other local models from reproducing all quantum mechanical predictions. Hence, we will extend the correlation of Equation (2) to a general form by considering a setting-dependent probability. Although the general correlation prohibits derivation of any Bell-type inequality, it can be used to solve the key concern whether local realistic model can yield prediction in agreement with experimental result as well as quantum mechanical prediction.

Before the formal proof, all terms in Equation (2) are explained as follows. $\mathrm{A}(\boldsymbol{a},\boldsymbol{\lambda})$ and $\mathrm{B}(\boldsymbol{b},\boldsymbol{\lambda})$ are two measuring outcomes for the spins of particle pairs respectively, which take the values either +1 or −1. $\mathrm{P}(\boldsymbol{a},\boldsymbol{b})$ is the spin correlation that is given as an expectation of the product $\mathrm{A}(\boldsymbol{a},\boldsymbol{\lambda})\mathrm{B}(\boldsymbol{b},\boldsymbol{\lambda})$ with the probability density $\rho(\boldsymbol{\lambda})$, which is commonly called the joint probability density. $\mathrm{P}(\boldsymbol{a},\boldsymbol{b})$ has been also termed as joint detection probability in many literatures, because the measuring outcomes have not dimension. $\boldsymbol{\lambda}$ is a hidden parameter introduced by Bell, ordinarily considered to be a vector with its terminal points uniformly distributed on the surface of a unit sphere.

It is known, the general condition of locality is expressed by the factorability of the probability [17]. So, when probability density depends on the settings, the general correlation is given by

$$\mathrm{P}(\boldsymbol{a},\boldsymbol{b}) = \int_{\Lambda} \rho_a(\boldsymbol{a},\boldsymbol{\lambda}) \rho_b(\boldsymbol{b},\boldsymbol{\lambda}) \mathrm{A}(\boldsymbol{a},\boldsymbol{\lambda}) \mathrm{B}(\boldsymbol{b},\boldsymbol{\lambda}) \mathrm{d}\boldsymbol{\lambda} \tag{3}$$

where Λ is the sample space of $\boldsymbol{\lambda}$, $\rho_a(\boldsymbol{a},\boldsymbol{\lambda})$ is the probability density for measuring $\mathrm{A}(\boldsymbol{a},\boldsymbol{\lambda})$, and $\rho_b(\boldsymbol{b},\boldsymbol{\lambda})$ for $\mathrm{B}(\boldsymbol{b},\boldsymbol{\lambda})$. It is evident that Bell's origi-

nal correlation is a special case of the correlation given by Equation (3). Besides its generality in locality, this general correlation highlights that the measurements are performed on two spatially-separate stations, while the correlation $\mathrm{P}(\boldsymbol{a},\boldsymbol{b})$ is merely a result of experimental data processing. Particularly, the measuring data at each station is allowed processing alone, so the statistical quantities of $\mathrm{A}(\boldsymbol{a},\boldsymbol{\lambda})$ and $\mathrm{B}(\boldsymbol{b},\boldsymbol{\lambda})$ can be calculated independently. For instance, the expectation of $\mathrm{A}(\boldsymbol{a},\boldsymbol{\lambda})$ is given as

$$\mathrm{E}(\mathrm{A}) = \int_{\Lambda} \rho_{\boldsymbol{a}}(\boldsymbol{a},\boldsymbol{\lambda})\mathrm{A}(\boldsymbol{a},\boldsymbol{\lambda})\mathrm{d}\boldsymbol{\lambda} \tag{4}$$

By the considerations above, the two probability densities must satisfy

$$\int_{\Lambda} \rho_{\boldsymbol{a}}(\boldsymbol{a},\boldsymbol{\lambda})\mathrm{d}\boldsymbol{\lambda} = 1 \quad \text{and} \quad \int_{\Lambda} \rho_{\boldsymbol{b}}(\boldsymbol{b},\boldsymbol{\lambda})\mathrm{d}\boldsymbol{\lambda} = 1 \tag{5a,5b}$$

respectively.

The ideal counter-correlation of particle pairs is also assumed

$$\mathrm{A}(\boldsymbol{a},\boldsymbol{\lambda})\mathrm{B}(\boldsymbol{a},\boldsymbol{\lambda}) = -1 \tag{6}$$

Following Bell's treatment, measuring outcomes can be designated

$$\mathrm{A}(\boldsymbol{a},\boldsymbol{\lambda}) = \mathrm{sign}(\boldsymbol{a}\cdot\boldsymbol{\lambda}) \quad \text{and} \quad \mathrm{B}(\boldsymbol{b},\boldsymbol{\lambda}) = -\mathrm{sign}(\boldsymbol{b}\cdot\boldsymbol{\lambda}) \tag{7a, 7b}$$

where sign(.) is the symbolic function.

Suppose that $\rho_{\boldsymbol{a}}(\boldsymbol{a},\boldsymbol{\lambda}) = \kappa_a|\boldsymbol{a}\cdot\boldsymbol{\lambda}|$ and $\rho_{\boldsymbol{b}}(\boldsymbol{b},\boldsymbol{\lambda}) = \kappa_b|\boldsymbol{b}\cdot\boldsymbol{\lambda}|$ respectively, where κ_a and κ_b are normalizing coefficients respective to each probability density. With these designations and assumptions, Equation (3) becomes simply

$$\mathrm{P}(\boldsymbol{a},\boldsymbol{b}) = -\kappa\int_{\Lambda}(\boldsymbol{a}\cdot\boldsymbol{\lambda})(\boldsymbol{b}\cdot\boldsymbol{\lambda})\mathrm{d}\boldsymbol{\lambda} \tag{8}$$

in which $\kappa = \kappa_a\kappa_b$, being not a normalizing coefficient for the so called joint probability (**Appendix 1**).

Then suppose that $\boldsymbol{\lambda}$ is a random vector with its terminal points distributing uniformly on the surface of a sphere with radius $r = 1/3\pi$ (**Appendix 2**), and denote it as $\boldsymbol{\lambda} = r(\cos\varphi\sin\theta, \sin\varphi\sin\theta, \cos\theta)$, where φ is the azimuthal angle and θ is the polar angle of the spherical coordinates, we have by inserting it in Equation (8)

$$\mathrm{P}(\boldsymbol{a},\boldsymbol{b}) = -\kappa(I_1 + I_2 + I_3 + I_4) \tag{9}$$

in which

$$I_1 = r^3\int_0^{2\pi}\int_0^{\pi}\left(a_1b_1\cos^2\varphi\sin^2\theta + a_2b_2\sin^2\varphi\sin^2\theta + a_3b_3\cos^2\theta\right)\sin\theta\mathrm{d}\varphi\mathrm{d}\theta,$$

$$I_2 = r^3\int_0^{2\pi}\int_0^{\pi}(a_1b_2 + a_2b_1)\sin\varphi\cos\varphi\sin^3\theta\mathrm{d}\varphi\mathrm{d}\theta,$$

$$I_3 = r^3\int_0^{2\pi}\int_0^{\pi}(a_1b_3 + a_3b_1)\cos\varphi\sin^2\theta\cos\theta\mathrm{d}\varphi\mathrm{d}\theta,$$

and

$$I_4 = r^3\int_0^{2\pi}\int_0^{\pi}(a_2b_3 + a_3b_2)\sin\varphi\sin^2\theta\cos\theta\mathrm{d}\varphi\mathrm{d}\theta,$$

where a_i and $b_i\,(i = 1,2,3)$ are components of $\boldsymbol{a}$ and $\boldsymbol{b}$, respectively.

Simple calculations yield $I_1 = (4\pi/3)r^3\boldsymbol{a}\cdot\boldsymbol{b}$ and $I_2 = I_3 = I_4 = 0$, and also

$\kappa_a = \kappa_b = 1/\left(2\pi r^2\right)$. Substituting these and $r = 1/3\pi$ into Equation (9), we finally obtain

$$\mathrm{P}(\boldsymbol{a},\boldsymbol{b}) = -\kappa_a \kappa_b I_1 = -\boldsymbol{a}\cdot\boldsymbol{b} \tag{10}$$

which is exactly the right side of Equation (1), what quantum mechanics predicts.

Quantum mechanical predictions may also include that the expectations of particle spin at each terminal are equal to zero, that is,

$$\mathrm{E}(\mathrm{A}) = \mathrm{E}(\mathrm{B}) = \mathbf{0} \tag{11}$$

These are readily confirmed. For example, we have

$$\mathrm{E}(\mathrm{A}) = \int \rho_a(\boldsymbol{a},\boldsymbol{\lambda})\mathrm{A}(\boldsymbol{a},\boldsymbol{\lambda})\mathrm{d}\boldsymbol{\lambda} = \kappa_a \int \left|\boldsymbol{a}\cdot\boldsymbol{\lambda}\right| sign(\boldsymbol{a}\cdot\boldsymbol{\lambda})\mathrm{d}\boldsymbol{\lambda} = \kappa_a \int (\boldsymbol{a}\cdot\boldsymbol{\lambda})\mathrm{d}\boldsymbol{\lambda} \tag{12}$$

and then substitution of $\boldsymbol{\lambda}$ as supposed previously and a calculation gives $\mathrm{E}(\mathrm{A}) = 0$.

Up to this point, we have presented the counterexample to Bell's theorem. Definitely, the correlation function that we have achieved, just like quantum mechanical prediction, is not constrained by Bell's inequalities. This is the true reason for experimental violation of these inequalities.

3. Logical Issue with Experimental Verification of Bell's Theorem

Let us scrutinize a logical issue with application of Bell's inequalities. We have made clear that Bell's inequalities only impose constraint on partial local models. Moreover, even if this flaw does not exist, there is also a logical obstacle with application of these inequalities. To exclude the premises of these inequalities by experimental violations belongs to the counter factual deduction of logical reasoning. However, to be rigorous, one will find in this logical deduction that a certain amount of experiments cannot substitute a theoretical proposition, because a theoretical proposition might involve indefinite or even infinite amount of experiments. Hence, to exclude the premises of Bell's inequalities by experimental violations of them is not permitted by rigorous logical reasoning.

4. Discussion of Bell's Model

In his seminal paper, Bell intended to implement the guessed EPR's idea of hidden variable model. As he stated, "...that idea will be formulated mathematically and shown to be incompatible with the statistical predictions of quantum mechanics." But his inequality and its variants are actually unrelated to hidden variable theory, because these inequalities are derived totally from classical concepts. The introduced parameter $\boldsymbol{\lambda}$ has nothing to do with completing the description of quantum mechanics though it has been termed hidden variable or parameter. The word of local hidden theories or models has concealed the inappropriateness of the assumption of setting-independent probability. Besides limiting the coverage of Bell's inequalities, actually, the setting-independent proba-

bility causes incompatibility with certain experimental observation. If the second moment of the outcome on one terminal is observed in the EPRB-type experiment with the photons of linear polarization, it will make the established fact like Malus' rule unpredictable. The demonstration is omitted here as it is very simple. Therefore, the assumption of setting-independent probability is inconsistent with what occurs in actual measuring process. Actually, that CHSH inequality was derived without any consideration of measuring process [18] has already hinted such inequality not for experimental test but to be a trivial mathematical relation.

5. Conclusions

As a necessary assumption of Bell's inequalities, the setting-independent probability makes these inequalities not impose constraint on all correlation functions representing local realistic models, and is also apparently false for actual experimental measurement. Existence of the counterexample further manifests that Bell's inequalities particularly do not impose constraint on real correlation functions. The revealed fatal flaw of these inequalities explains why they have been violated by experiments. Moreover, even if these inequalities had not the flaw, they would be useless for experiment because certain amount of experiments cannot substitute a theoretical proposition in counter factual deduction. It is concluded that, Bell's theorem is false because Bell's inequalities are trivial mathematical relations that, due to an unsuitable assumption of probability, lack essential connection with the real measuring process of the pertinent experiments.

Meanwhile, a point of view should be stated. Collapse of Bell's theorem does not deny the conflicts between classical concepts and some weird notions by the orthodox interpretation of quantum mechanics. And what Einstein had insisted that these conflicts are caused by incompleteness of quantum mechanics in description of microscopic systems appears rather reasonable.

Acknowledgements

The author wish to thank professor Karl Hess of the University of Illinois for a helpful proposal.

Conflicts of Interest

The author declares no conflicts of interest regarding the publication of this paper.

References

[1] Bell, J.S. (1964) *Physics Physique Fizika*, **1**, 195-200. https://doi.org/10.1103/PhysicsPhysiqueFizika.1.195

[2] Clauser, J.F., Horne, M.A., Shimony, A. and Holt, R.A. (1969) *Physical Review Letters*, **23**, 880-884. https://doi.org/10.1103/PhysRevLett.23.880

[3] Clauser, J.F. and Horne, M.A. (1974) *Physical Review D*, **10**, 526-535. https://doi.org/10.1103/PhysRevD.10.526

[4] Greenberger, D.M., Horne, M.A. and Zeilinger, A. (1989) Going beyond Bell's Theorem. In: Kafatos, M., Ed., *Bell's Theorem, Quantum Theory, and Conceptions of the Universe*, Kluwer Academic, Dordrecht, The Netherlands, 69-72. https://doi.org/10.1007/978-94-017-0849-4_10

[5] Hardy, L. (1993) *Physical Review Letters*, **71**, 1665-1668. https://doi.org/10.1103/PhysRevLett.71.1665

[6] Clauser, J.F. (2017) Bell's Theorem, Bell Inequalities, and the "Probability Normalization Loophole". In: Bertlmann, R. and Zeilinger, A., Eds., *Quantum [UN]Speakables II. The Frontiers Collection*. Springer, Cham, 451-484. https://doi.org/10.1007/978-3-319-38987-5_28

[7] Hensen, B., *et al.* (2015) *Nature*, **526**, 682-686. https://doi.org/10.1038/nature15759

[8] Tipler, F.J. (2014) *Proceedings of the National Academy of Sciences of the United States of America*, **111**, 11281-11286. https://doi.org/10.1073/pnas.1324238111

[9] Hess, K. and Philipp, W. (2001) *Proceedings of the National Academy of Sciences of the United States of America*, **98**, 14224-14227. https://doi.org/10.1073/pnas.251524998

[10] Hess, K. and Philipp, W. (2004) *Proceedings of the National Academy of Sciences of the United States of America*, **101**, 1799-1805. https://doi.org/10.1073/pnas.0307479100

[11] Zhao, H.L. (2013) *Journal of Experimental and Theoretical Physics*, **117**, 999-1010. https://doi.org/10.1134/S1063776113140070

[12] Bell, J.S. (1987) Speakable and Unspeakable in Quantum Mechanics. Cambridge, New York, 154.

[13] Bell, J.S. (1971) Introduction to the Hidden-Variable Question. In: d'Espagnat, B., Ed., *Foundations of Quantum Mechanics*, Academic, New York, 171-181.

[14] Barut, A.O. and Meystre, P. (1984) *Physics Letters*, **105**, 458-462.

[15] Gisin, N. and Gisin, B. (1999) *Physics Letters A*, **260**, 323-327. https://doi.org/10.1016/S0375-9601(99)00519-8

[16] Greenberg, D.M., Horne, M.A., Shimony, A. and Zeilinger, A. (1990) *American Journal of Physics*, **58**, 1131-1143. https://doi.org/10.1119/1.16243

[17] Clauser, J.F. and Shimony, A. (1978) *Reports on Progress in Physics*, 41, 1881-1927. https://doi.org/10.1088/0034-4885/41/12/002

[18] Hess, K. and Philipp, W. (2001) *Proceedings of the National Academy of Sciences of the United States of America*, **98**, 14228-14233. https://doi.org/10.1073/pnas.251525098

Appendix 1

Due to the two constraints Equations (5a) and (5b), the product $\rho_a(\boldsymbol{a},\boldsymbol{\lambda})\rho_b(\boldsymbol{b},\boldsymbol{\lambda})$ generally termed as the joint probability is actually not a normalized probability density. The proof is given as follows. The product can be conceived as a degenerated joint probability from $\rho_a(\boldsymbol{a},\boldsymbol{\lambda})\rho_b(\boldsymbol{b},\boldsymbol{\gamma})$ for two random variables $\boldsymbol{\lambda}$ and $\boldsymbol{\gamma}$, when $\boldsymbol{\gamma}$ goes to equate $\boldsymbol{\lambda}$ and both have the same sample space Λ. With this consideration, we have

$$1=\int_\Lambda\int_\Lambda \rho_a(\boldsymbol{a},\boldsymbol{\lambda})\rho_b(\boldsymbol{b},\boldsymbol{\gamma})\mathrm{d}\boldsymbol{\lambda}\mathrm{d}\boldsymbol{\gamma} > \int_\Lambda\int_\Lambda \rho_a(\boldsymbol{a},\boldsymbol{\lambda})\rho_b(\boldsymbol{b},\boldsymbol{\gamma})\delta(\boldsymbol{\lambda}-\boldsymbol{\gamma})\mathrm{d}\boldsymbol{\lambda}\mathrm{d}\boldsymbol{\gamma}$$

where $\delta(\cdot)$ is Dirac function. The most right part of the above is exactly $\int_\Lambda \rho_a(\boldsymbol{a},\boldsymbol{\lambda})\rho_b(\boldsymbol{b},\boldsymbol{\lambda})\mathrm{d}\boldsymbol{\lambda}$.

It is noted that all Bell inequalities were derived by that the joint probability fulfills the normalization condition. This normalization would be justified if the joint probability were for ordinary two random events. But the two random outcomes in the considered experiment are dependent on one parameter $\boldsymbol{\lambda}$ with the expectation of their product being not determined by a normalized joint probability, as demonstrated above. This exceptional property was not noticed in derivations of Bell's inequalities.

Appendix 2

We deliberately choose $r=1/3\pi$ rather than ordinarily $r=1$ to obtain a normalized correlation function in end, though this operation is essentially unnecessary. This means that a normalization of the correlation function is carried out in advance. Otherwise, it is readily found that the final correlation function will be $\mathrm{P}(\boldsymbol{a},\boldsymbol{b})=-(1/3\pi)\boldsymbol{a}\cdot\boldsymbol{b}$. In a view of geometry, a series of data represents a line, and the essence of a correlation coefficient represents the cosine of the angle made by two lines. The value of the cosine is independent of either length of the two lines. While a correlation function is the extension of the correlation coefficient when it depends on a variable. In practice, it is well known to an experimental physicist or an engineer of signal processing that a scaling of experimental data has to be carried out in order to verify a theoretical correlation function. This scaling is really equal to the normalization of a correlation function, entailing that the absolute magnitude of a correlation function makes nonsense or that correlation functions only different in magnitude are equivalent. Please excuse the author for the wordy explanations above, since some theorists might ignore this tiny issue. For instance, Bell did not treat $-(1/3)\boldsymbol{a}\cdot\boldsymbol{b}$ as equivalent to $-\boldsymbol{a}\cdot\boldsymbol{b}$ in his seminal paper [1].

Journal of Modern Physics, 2019, 10, 1166-1176
https://www.scirp.org/journal/jmp
ISSN Online: 2153-120X
ISSN Print: 2153-1196

Was There a Negative Vacuum Energy in Your Past?

George Chapline[1], James Barbieri[2]

[1]Lawrence Livermore National Laboratory, Livermore, CA, USA
[2]Retired, Naval Air Warfare Center, China Lake, CA, USA
Email: chapline1@llnl.gov, barbierijf@hughes.net

How to cite this paper: Chapline, G. and Barbieri, J. (2019) Was There a Negative Vacuum Energy in Your Past? *Journal of Modern Physics*, **10**, 1166-1176.
https://doi.org/10.4236/jmp.2019.1010077

Received: June 24, 2019
Accepted: August 27, 2019
Published: August 30, 2019

Abstract

We introduce a novel model for the origin of the observable universe in which a flat universe with a positive vacuum energy is proceeded by a flat universe with a negative vacuum energy. A negative vacuum energy is consistent with a supersymmetric ground state similar to that predicted by superstring theories. A positive vacuum energy could emerge as a result of the gravitational collapse of the negative vacuum energy universe when the matter temperature reaches a characteristic value where supersymmetry is strongly broken. In principle this allows one to derive all the features of our expanding universe from a single parameter: the magnitude of the pre-big bang negative vacuum energy density. In this paper, a simple model for the big bang is introduced which allows us to use the present day entropy density, and temperature fluctuations of the CMB, together with the present day density of dark matter, to predict the magnitude of the negative vacuum energy. This model for the big bang also makes a dramatic prediction: dark matter consists of compact objects with masses on the order of 10^4 solar masses. Remarkably this is consistent with numerical simulations for how the primordial fluctuations in the density of dark matter give rise to the observed inhomogeneous distribution of matter in our universe. Our model for the big bang also allows for the production of some compact objects with masses greater than 10^4 solar masses which are consistent with observations of massive compact objects at the center of the earliest galaxies.

Keywords

Gravitational Collapse, Cosmology, Dark Matter, Vacuum Energy, CMB

1. Introduction

One of the outstanding puzzles of modern theoretical physics is that classical

general relativity offers no clue as the fate of matter undergoing gravitational collapse or the state of matter prior to the "big bang". These puzzles are all the more perplexing because in quantum mechanics it is not possible for matter to simply appear or disappear. Previously we have drawn attention [1] [2] to the fact that the quantum critical phase transition theory of event horizons [3] provides a plausible explanation for the fate of matter undergoing gravitational collapse; namely most of the mass-energy is converted into vacuum energy resulting in the formation of a "dark energy star" [4]. Dark energy stars are distinguished from black holes in that their interiors resemble deSitter or Godel "interior" solutions [5] rather than a black hole space-times predicted by classical general relativity. In this paper, we offer a possible resolution of the enigma of what preceded the big bang by noting that a flat Robertson-Walker universe with a negative cosmological constant will naturally evolve via the same kind of quantum dynamics that resolves the problem of gravitational collapse to an expanding inhomogeneous universe containing radiation and dark matter. It was suggested some time ago by deSitter, Eddington, and Lemaitre [6] that the observable universe may not have had a singular beginning, but, instead may have originated from a finite size seed. Lemaitre suggested that this finite seed was a macroscopic quantum state which he called the "primeval atom". Cosmological models incorporating this idea make use of Lemaitre's examples of Robertson-Walker space-times with positive cosmological constant [7] [8]. In the following we describe a model for the origin of the expanding universe, in which the initial state of the observable universe is not a single quantum object, but an infinite assembly of quantum objects. It has already been noted [9] that such a two-phase cosmology provides a simple explanation for many of the observed features of our universe, including the entropy and temperature fluctuations of the cosmic microwave background. In this paper we describe how a 2-phase model for the initial state of our expanding universe can arise from the gravitational collapse of a flat Robertson-Walker universe with a negative cosmological constant. We also indicate how the parameters of the standard cosmological model as well the present day large scale inhomogeneous structure of our universe might be derived from a single parameter: the magnitude of the initial negative vacuum energy.The classical gravitational dynamics of a flat universe with a negative cosmological constant necessarily involves collapse to a density singularity. The acceleration of of the cosmological scale factor $R(t)$ in a flat Robertson-Walker universe with a cosmological constant is

$$\ddot{R} = -\frac{4\pi G}{3c^2}\left(\rho + 3p - 2\rho_\Lambda\right)R^2 \tag{1}$$

where ρ is the matter density, p is the matter pressure and ρ_Λ is the vacuum energy density. When the vacuum energy density ρ_Λ is negative and the matter is a relativistic gas of particles with an adiabatic index 4/3, Equation (1) has a simple analytic solution [8]:

$$R(\tau) = R_m\left[\frac{1-\cos 4\alpha\tau}{2}\right]^{1/4} \tag{2}$$

where τ is the usual Robertson-Walker universal time. The cosmological constant $\Lambda = -3\alpha^2 = 8\pi G\rho_\Lambda / c^2$. Regardless of it's maximum value the scale collapses to zero in a time $\tau_c \equiv \pi/4\alpha$. At the time $\tau = \pi/4\alpha$ when the scale factor is a maximum the total energy density $\rho + \rho_\Lambda = 0$. As τ approaches $\pi/2\alpha$ the energy density which is dominated by the matter density ρ approaches infinity. In Figure 1, we show the evolution of the scale factor for an initial scale factor $R_m = 10R_g$ where R_g is the initial gravitational radius for the matter. We also show the light sphere radius r_c for photons emitted at the initial time $\tau = \pi/4\alpha$. Equation (2). implies that a conformal radius

$$r_c/R = \sqrt{2}\, R_g/R_m\, F\left(\cos^{-1}\left(R/R_m\right)|\,\pi/4\right)$$

where F is an incomplete elliptic integral of the first kind. As is evident from Figure 1, photons emitted from any point in the negative cosmological constant universe are trapped, and according to Penrose and Hawking would require collapse to a singularity. On the other hand, we will assume that in reality a negative cosmological constant does not collapse to a singularity due to quantum effects.

2. Model for the Big Bang

Our hypothesis is that the same type of conversion of matter mass-energy to vacuum energy [10] that we previously been proposed [1] [2] as the reason for the avoidance of a singular end point for the gravitational collapse of massive stellar cores will also lead to the avoidance of a mass density singularity in a flat

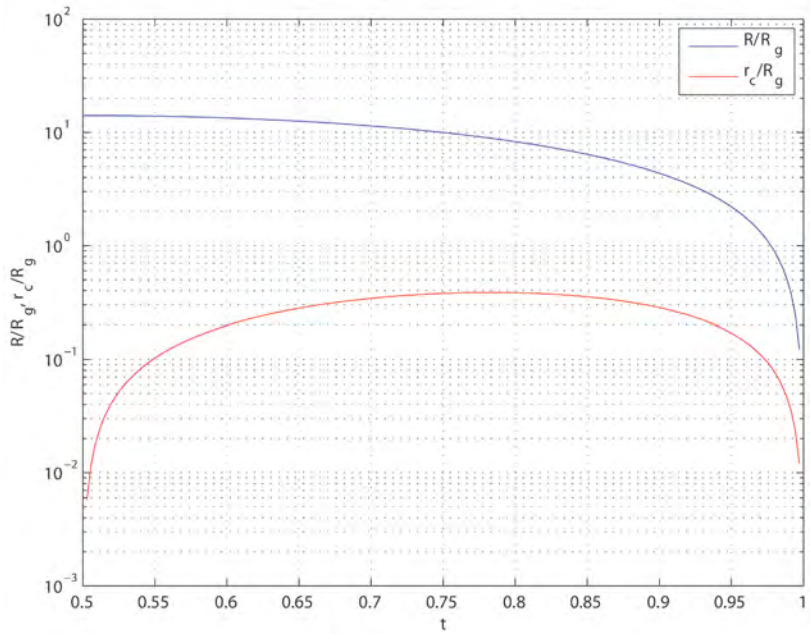

Figure 1. Time evolution of the scale factor in a radiation filled flat Robertson-Walker universe with a negative cosmological constant, together with the light sphere radius for photons emitted at the initial time $t = 0.5$. Time is measure in units of $\pi/2\alpha$, while the radii are measured in units of the initial matter gravitational radius C/α.

negative cosmological constant universe. In particular, we will argue that as a result of the ubiquitous formation of trapped surfaces in a flat negative cosmological constant universe most of the matter mass-energy will be transformed into positive vacuum energy, resulting in an expanding universe which resembles our universe. As a simple model for the conversion of most of the mass-energy of radiation in our negative cosmological constant universe to vacuum energy we propose replacing the usual conservation law for a Lemaitre universe with a constant cosmological constant with the equations

$$\frac{\mathrm{d}}{\mathrm{d}t}\left(\rho R^3\right)+p\frac{\mathrm{d}R^3}{\mathrm{d}t}=-\frac{\rho R^3}{\tau_c} \tag{3}$$

$$\frac{\mathrm{d}\rho_\Lambda}{\mathrm{d}t}=\frac{\rho}{\tau_c} \tag{4}$$

Numerical solutions of Equations (1), (3) and (4) are shown in Figure 2 and Figure 3. It can be seen that the acceleration of the Robertson-Walker scale factor switches from being negative to positive, indicating evolution from a collapsing to an expanding universe. Our model for the big bang consists of Equations (1), (3) and (4) together with the stipulation that after a time $\tau_c=\pi/2\alpha$ the vacuum energy created when the deSitter horizon is small compared to the Hubble radius does not contribute to a cosmological constant, but instead is encapsulated into a form of dark matter.

Of course the ultimate fate of matter undergoing gravitational collapse has been a long standing enigma. Following the seminal paper of Oppenheimer and Snyder, it had come to be widely accepted that the gravitational collapse of a sufficiently large mass would inevitably lead to the formation of an event horizon and a density singularity [11]. Moreover, it has generally been believed

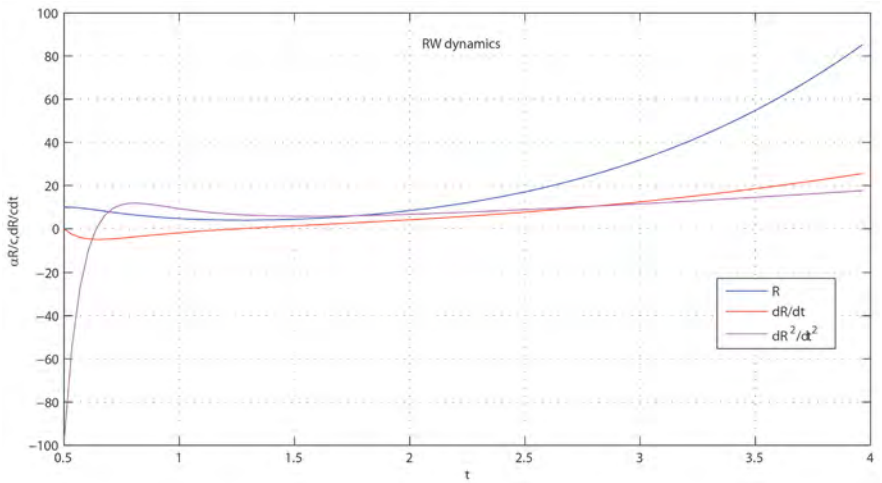

Figure 2. Evolution of a flat Robertson-Walker universe, initially with a negative cosmological constant and filled with radiation, but allowing for the radiation and vacuuum energy density to change according to Equations (3) and (4). Time is measured in units of $\pi/2\alpha$ while the radii are measured in units of the initial matter gravitational radius $R_g=C/\alpha$.

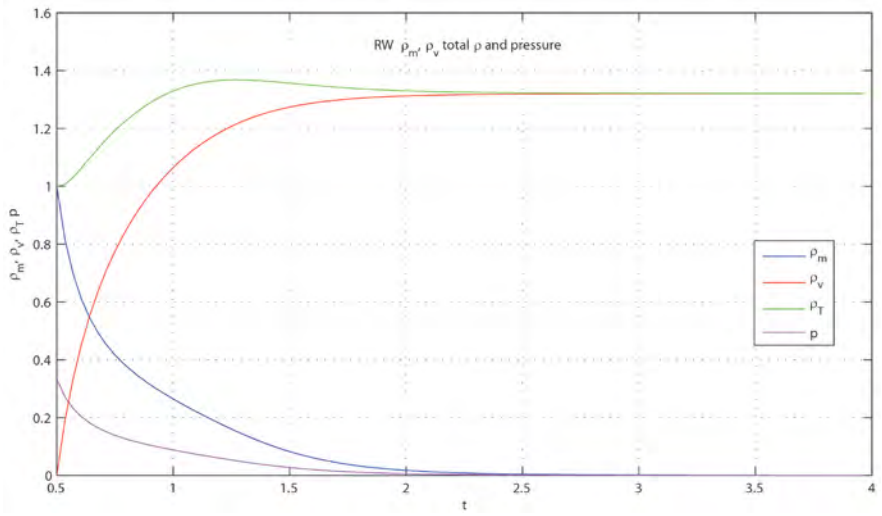

Figure 3. The matter, vacuum and total energy densities resulting from the collapse of a flat negative vacuum energy universe.

that these predictions will turn out to be correct even when quantum effects are taken into account, since the formation of an event horizon can take place in a region of space-time where the curvature is very small. On the other hand, there are several long standing puzzles connected with general relativistic picture of gravitational collapse. The most famous of these puzzles concerns the fact that in quantum mechanics information can never disappear. The most likely resolution of this paradox is that quantum effects profoundly affect the classical picture of matter in-falling smoothly through an event horizon. In particular, there are plausible arguments [3] [12] [13] that in a quantum theory of gravity the space-time inside an event horizon always resembles deSitter's "interior" solution of the Einstein equations [5].

3. Estimate of the Mass Range for Dark Matter MACHOs

A central central element for our argument that a negative cosmological constant evolves into an expanding universe that resembles our own is that, due to the well known instability of infinite deSitter space at the deSitter horizon [3], patches of space-time resembling deSitter interior solutions will appear throughout the collapsing universe. These "dark energy stars" are gravitationally stable, and will have a mass

$$M^* = 0.3\left[\left(\text{GeV}\right)^4 / \rho^*\right]^{1/2} M_\odot \tag{5}$$

where ρ^* is the positive vacuum energy created at the collapse time $\tau_c = \pi/2\alpha$ by the conversion of radiation energy in the collapsing negative cosmological universe into vacuum energy and $M_\odot$ is the mass of the sun. This mass is just the mass inside the deSitter horizon at the time τ_c. The two-phase picture for cosmology [14] where space-time is a mixture of ordinary vacuum and dark energy stars, emerges from our model in somewhat the same way that supersaturated steam consists of a mixture of water vapor and water droplets. It

is of course rather natural to imagine that in such a picture the initial energy densities of the dark matter and the cosmological vacuum may be comparable. The initial masses of the dark energy stars will be given by Equation (6) but because the spatial density of these dark energy stars will be very large, collisions and fluctuations in the spatial density of the primordial dark energy stars created at $\tau_c = \pi/4\alpha$ will cause them coalesce, (the details are discussed in Ref. [9]) leading to the formation of more massive compact objects. The reversal of the scale factor acceleration from negative to positive will result in a universe consisting of dark energy stars and radiation expanding in a Freidmann-like fashion. The maximum mass of these compact objects will be dictated by the time it takes for their spatial density to become too low for them to continue to coalesce (the details are discussed in Ref. [9]). We are immediately faced with the puzzle though that the expansion of a cloud of dark energy stars with an initial mass-energy density of ρ^* would lead to a present day density of matter that is many orders of magnitude greater than the observed matter density.

A possible resolution of this puzzle [9] is that when is that when the dark energy stars coalesce the surface area of the larger dark energy stars will be maximized in much the same a way that the total that the total surface area increases when two black holes coalesce. Because of this black hole-like behavior a large fraction of the mass-energy of dark energy stars is converted into thermal energy when they coalesce. Our model for the big bang is based on the assumption that this thermal radiation is released as freely as the streaming radiation when the photon frequency falls below a critical frequency ν_c where the radiation and the dark energy stars decouple. The value of this critical frequency was estimated in Ref.s [1] [2] [3]. If we assume that the gauge field coupling strength at the GUT scale $g^2 = 0.1$, this estimate for cutoff for strong interactions between dark energy stars and photons is $h\nu_c = 1\,\mathrm{GeV}\left(M_\odot/M\right)^{1/2}$ where M is the mass of the dark energy star.

In our model for the big bang transition between the very high temperature regime where there is strong coupling between the dark matter and radiation and the lower temperature regime where the dark matter and radiation are decoupled is assumed to be abrupt in the sense that for red shifts greater than certain red shift $1+z_r$, the radiation energy is stored as the mass-energy of dark energy stars with masses $M \gg M^*$, while for $1+z < 1+z_r$ we will assume that all the mass-energy of the primordial dark energy stars will have been converted into radiation and remanent dark energy stars with average mass M_{DM}. Taking into account the black hole-like relation between mass and surface area of a dark energy star the cosmological energy density of the dark matter as a function of red shift following the decoupling with radiation for $1+z < 1+z_r$ will be

$$\rho_{DM} = \rho_* \left(\frac{M^*}{M_{DM}}\right)^2 \left(\frac{1+z}{1+z_*}\right)^3 \tag{6}$$

where M_{DM} is the average mass of the dark energy star and $1+z_*$ is the red shift for the break-up of the initial positive vacuum energy state resulting from the collapse of the negative vacuum energy state, corresponding to the origin of

the observable universe. As an estimate for the red shift separating these two regimes we will use the value

$$1+z_r = \frac{0.37h\nu_c}{k_B T_{CMB}} \tag{7}$$

where the factor 0.37 accounts for the difference between the temperature and the mean photon energy and $T_{CMB} = 2.73\,\mathrm{K}$ is the present day temperature of the CMB. The radiation energy density for $1+z < 1+z_r$ will be given by

$$\rho_{rad} = \rho_*\left(\frac{1+z_*}{1+z_r}\right)\left(\frac{1+z}{1+z_*}\right)^4 \tag{8}$$

The radiation energy density is related to the radiation temperature T by the usual formula

$$\rho_{rad} = N(T)\frac{\pi^2}{30}\frac{(k_B T)^4}{(\hbar c)^3} \tag{9}$$

where $N(T)$ is the effective number of elementary particle species contributing to the radiation energy density at red shift $1+z$. Strictly speaking we should have taken into account $N(T)$ in our estimate, Equation (5), for the red shift marking the appearance of the CMB, but we have neglected this correction since it only depends on $N^{1/4}$.

Combining Equations (6)-(8) with the ratio of the present day mass-energy densities of dark matter (keV/cm^3) and the CMB (0.26 eV/cm^3) leads to the following relation between M_{DM} and M^*:

$$\left(\frac{M_{DM}}{M_\odot}\right)^{5/4} = 2\times 10^4\left(\frac{M^*}{M_\odot}\right) \tag{10}$$

Since in our model M^* is unconstrained, Equation (10) formally allows the transition from a dark energy star dominated universe to a radiation dominated universe to take place for any for M_{DM}. However this transition cannot occur so late that it interferes with the requirement that the cosmological production of of helium and other light elements hould be approximately the same as in the standard cosmological model. This limits the value of the transition red shift $1+z_r$ to be $>10^{10}$ and $M_{DM} < 2\times 10^4 M_\odot$. One may also invoke the limits on the present day abundance of MACHO objects set by gravitational micro-lensing [15] to say that M_{DM} should be $>10M_\odot$. In the following we will adopt as our *apriori* range for the average primordial compact object mass $2\times 10^4 M_\odot > M_{DM} > 10M_\odot$. For these nominal values of the dark matter masses the CMB originates at a red shift in the range $5\times 10^{11} > 1+z_r > 10^{10}$. The radiation temperature at redshift z_r would lie in the range $120\ \mathrm{MeV} > T(z_r) > 2.6\ \mathrm{MeV}$ which for the most part is above the temperature where the cosmological production of the light elements takes place

Equation (10) implies that our assumed range of dark matter masses the range of the initial primordial dark energy stars lie in the range $12M_\odot > M^* > 9\times 10^{-4} M_\odot$. The initial positive vacuum energy density ρ^* is

related to M^* by $\rho^* = 0.1(\mathrm{GeV})^4 \left(M_\odot / M^*\right)^2$, which just expresses the fact that for a dark energy star M is the mass of the vacuum energy inside the deSitter horizon. The limits on M^* derived from Equation (10) translates to $10^5 (\mathrm{GeV})^4 > \rho^* > 7\times 10^{-4} (\mathrm{GeV})^4$. Given the present day cosmological density of matter (2×10^{-30} gm/cc) the redshift where the dark energy stars were initially formed can be found from Equation (6) and lie in the range $5\times 10^{11} > 1+z_* > 210^{10}$ for our nominal range for M_{DM}. By construction the range for M^* and ρ^* just quoted are consistent with the present day density of dark matter. Our predicted present day mass spectrum extends to "intermediate masses" $>1000 M_\odot$ [16].

Equation (8) also yields a present day radiation temperature that is very close to the observed CMB temperature for all values of M_{DM} in our nominal range. Another very encouraging prediction of our model follows from the fact that the metric fluctuations created by the quantum instability of the positive vacuum energy state created by the big bang at the deSitter horizons have the Harrison-Zeldovich-Peebles form [17] [18] [19]:

$$\frac{\delta\rho}{\rho} \approx \epsilon_0 \left(R_0 k\right)^2 \tag{11}$$

where $R_0 = 2GM^*/c^2$ is the gravitational radius corresponding to the initial positive vacuum energy, $\epsilon_0 \sim 1$ is the metric fluctuation created on the scale R_0 by the formation of the objects with mass M^* and $\delta\rho/\rho$ is the fractional density fluctuation for scales $k^1 \gg R_0$. Because the speed of sound in an expanding universe of dark energy stars is very low, the density fluctuations will rapidly grow until the radiation is locked up the as the energy excited dark energy star becomes freely streaming. According to the Lifschitz formula [20] for the growth of the density fluctuations during a matter dominated period by the time the red shift reaches $1+z_r$ the fluctuations in the density of primordial dark energy stars with mass M^* will have grown by a factor $\left(1+z_*/1+z_r\right)$ independent of length scale. Taking this into account and averaging the density fluctuations as predicted by Equation (11) over all volumes that could have been have collapses by the time that the expanding universe had reached the beginning of the radiation dominated era at red shift $1+z_r$, we obtain (see Ref. [9] for details) as an estimate of the renormalized value of ε_0 at red shift $1+z_r$:

$$\epsilon_r \approx 3\epsilon_0 \left[\frac{1+z_r}{1+z_*}\right]^2 \tag{12}$$

For our assumed range of dark matter average masses our model for the big bang predicts

$$1.2\times 10^{-5} > \left(\frac{1+z_r}{1+z_*}\right)^2 > 10^{-6} \tag{13}$$

Considering the simplicity of our model these values are in remarkably good agreement with the observed value, $\delta T/T \sim 10^{-5}$, for the mean temperature

fluctuation of the CMB, which corresponds to $\epsilon_0 \sim 3\times 10^{-5}$. Taken literally Equation (12) suggests that the average dark matter compact object has a mass close to $10^4 M_\odot$.

It is of course a dramatic prediction of our model that dark matter consists of compact objects with masses on the order of $10^4 M_\odot$. Actually it is an old idea that dark matter consist of primordial black holes (PBHs) [21], although at the time this was proposed there was no preference for the typical masses of PBHs. Recently the idea that dark matter consists of compact objects has received renewed interest as a result of the failure to identify any stable elementary particles that might serve as a candidate for dark matter [22] [23] [24] [25]. Finally, it is certainly news worthy that our hypothesis that the initial vacuum energy was negative is consistent with superstring models for a supersymmetric ground state [16] [26].

4. Conclusion

Evidently, all of the features of the CMB as well as many features of dark matter follow from our hypothesis that the big bang created a positive vacuum energy with and energy density > $(\text{GeV})^4$. Rather amusingly our predictions for the nature of dark matter are *ipso facto* completely consistent with the observed inhomogeneity of matter at practically all scales. Indeed the actual state of the art for numerical simulation of the evolution of dark matter structures use point particles with a fixed mass typically in the range 10^3 - $10^4 M_\odot$ (for a review see [27] [28]). Furthermore in order to simulate the formation of galactic structures within the framework of the numerical models for the evolution of dark matter structures it is necessary to add primordial seed masses of about $10^5 M_\odot$ in order to obtain the observed galactic morphologies [28]. Of course it follows from our prediction that the dark matter compact objects were formed from the stochastic coalescence of primordial dark energy stars with a mass M^* that compact objects with mass greater than M_{DM} were also formed. In summary, it appears that our explanation for the big bang can simultaneously explain the energy density, entropy, and temperature fluctuations of the CMB, as well as virtually all details of the inhomogeneous matter structures.

Acknowledgements

The authors are very grateful to T. Axelrod, P. Frampton, C. Frenk, and A. Loeb for discussions regarding observational constraints on many solar mass dark matter constituents. This work was performed under the auspices of the US Department of Energy by Lawrence Livermore National Laboratory under Contract DE-AC52-07NA27344 and was supported by the LLNL-LDRD Program under Project No. 17-ERD-120.

Conflicts of Interest

The authors declare no conflicts of interest regarding the publication of this paper.

References

[1] Chapline, G. (2003) *International Journal of Modern Physics A*, **18**, 3587-3590. https://doi.org/10.1142/S0217751X03016380

[2] Chapline, G. and Barbieri, J. (2014) *International Journal of Modern Physics D*, **23**, Article ID: 1450025. https://doi.org/10.1142/S0218271814500254

[3] Chapline, G., Hohlfeld, E., Laughlin, R. and Santiago, D. (2001) *Philosophical Magazine B*, **81**, 235-254. https://doi.org/10.1080/13642810108221981

[4] Chapline, G. (2005) Dark Energy Stars. *Proceedings of the* 22*nd Texas Conference on Relativistic Astrophysics*, Stanford, CA, 12-17 December 2004, 1-4.

[5] Kramer, D., Stephani, H., MacCallum, M. and Heralt, E. (1980) Exact Solutions of Einstein Field Equations. Cambridge University Press, Cambridge.

[6] deSitter, W., Edditington, A.S. and Lemaitre, G. (1931) *Nature*, **127**, 704.

[7] Lemaitre, G. (1931) *Monthly Notices of the Royal Astronomical Society*, **bf91**, 493.

[8] Harrison, E.R. (1967) *Monthly Notices of the Royal Astronomical Society*, **137**, 69-79. https://doi.org/10.1093/mnras/137.1.69

[9] Chapline, G. (2010) Dark Energy Stars and the Cosmic Microwave Background. ArXiv:1004.0406.

[10] Feynman, R.P. (2003) Lectures on Gravitation. Westview Press, Boulder.

[11] Joshi, P. (2007) Gravitational Collapse and Spacetime Singularities. Cambridge University Press, New York. https://doi.org/10.1017/CBO9780511536274

[12] Mazur, P.O. and Mottola, E. (2004) *Proceedings of the National Academy of Sciences of the United States of America*, **101**, 9545-9550. https://doi.org/10.1073/pnas.0402717101

[13] Mazur, P.O. and Mottola, E. (2015) *Classical and Quantum Gravity*, **32**, Article ID: 215024. https://doi.org/10.1088/0264-9381/32/21/215024

[14] Chapline, G. and Mazur, P.O. (2007) A Two-Phase Model for Spacetime. 23*rd Pacific Coast Gravity Meeting*, Pasadena, CA, 16-17 March 2007.

[15] Alcock, C., *et al.* (1998) *The Astrophysical Journal*, **499**, 19.

[16] Chapline, G. and Barbieri, J. (2018) *Letters in High Energy Physics*, **1**, 17-20. https://doi.org/10.31526/LHEP.1.2018.04

[17] Harrison, E.R. (1970) *Physical Review D*, **1**, 2726-2730. https://doi.org/10.1103/PhysRevD.1.2726

[18] Zeldovich, Y.B. (1970) *Astronomy & Astrophysics*, **5**, 84-89.

[19] Peebles, P.J.E. and Yu, J.T. (1970) *Astrophysical Journal*, **162**, 815. https://doi.org/10.1086/150713

[20] Lifshitz, E.M. (1946) *Journal of Experimental and Theoretical Physics*, **16**, 587-602.

[21] Chapline, G. (1975) *Nature*, **253**, 251-252. https://doi.org/10.1038/253251a0

[22] Frampton, P. (2009) *Journal of Cosmology and Astroparticle Physics*, **2009**, 16. https://doi.org/10.1088/1475-7516/2009/10/016

[23] Clesse, S. and Garcia-Bellido, J. (2015) *Physical Review D*, **92**, Article ID: 023524. https://doi.org/10.1103/PhysRevD.92.023524

[24] Chapline, G. and Frampton, P.H. (2016) *Journal of Cosmology and Astroparticle Physics*, **11**, 916. https://doi.org/10.1088/1475-7516/2016/11/042

[25] Carr, B., Kuhnel, F. and Sandstad, M. (2016) *Physical Review D*, **94**, Article ID: 083504. https://doi.org/10.1103/PhysRevD.94.083504

[26] Ibanez, L.E. and Uranga, A.M. (2012) String Theory and Particle Physics. Cambridge University Press, New York.

[27] Frenk, C.S. and White, S.D.M. (2012) *Annalen der Physik*, **524**, 507-534. https://doi.org/10.1002/andp.201200212

[28] Schaye, J., *et al.* (2012) *Monthly Notices of the Royal Astronomical Society*, **446**.

Journal of Modern Physics, 2019, 10, 1177-1189
https://www.scirp.org/journal/jmp
ISSN Online: 2153-120X
ISSN Print: 2153-1196

Controlling Speedup Induced by a Hierarchical Environment

Jing Wang[1], Yunan Wu[1], Wenyu Ji[2*]

[1]School of Physics and Technology, University of Jinan, Jinan, China
[2]College of Physics, Jilin University, Changchun, China
Email: sps_wangj@ujn.edu.cn, *jiwy@jlu.edu.cn

How to cite this paper: Wang, J., Wu, Y.N. and Ji, W.Y. (2019) Controlling Speedup Induced by a Hierarchical Environment. *Journal of Modern Physics*, **10**, 1177-1189.
https://doi.org/10.4236/jmp.2019.1010078

Received: July 30, 2019
Accepted: August 31, 2019
Published: September 3, 2019

Abstract

Quantum speedup of an open quantum system can be induced by the non-Markovian effect of the environment. Although an environment with a higher degree of non-Markovianity may seem like it should cause a faster speed of quantum evolution, this seemingly intuitive thinking may not always be correct. To clarify this point, we give a mechanism for controlling speedup of a single qubit that is coupled to a hierarchical photonic-crystal (PC) environment, which contains a defect single-mode cavity and a semi-infinite one-dimensional (1D) waveguide. Via studying the dynamics of the qubit, we reveal that with a judicious choice of the qubit-cavity coupling strength and the memory time of the waveguide environment, a speed-up evolution can be achieved. In particular, we found that the quantum speedup is not entirely attributed to the non-Markovianity, but to the increase of the total amount of flow information. That is the intrinsic physical reason that the hierarchical environment may induce the speed-up process. Our results may open new perspectives for detecting quantum speedup in realistic environments.

Keywords

Non-Markovianity, Quantum Speed Limit Time, Photonic Crystal

1. Introduction

In the theory of open quantum systems, controlling evolution speed of quantum systems has recently attracted considerable attention, partially because of its domination in practical physical process and usefulness in technological applications, such as quantum computation [1] [2], quantum optical control [3] and suppressing quantum decoherence [4] [5]. For example, in order to reach the fastest computation time, one needs to speed up the quantum evolution. On the

other hand, if the quantum system is used as a quantum memory, the slowing down the noisy dynamical evolution will be desirable in order to gain longer coherence time [6]. In this connection, a lot of efforts have been made to realize controlling speedup in more general open systems. So far, many factors that can trigger quantum speedup have been found, for example, strong system-environment coupling [7], structured environments [8] and external classical driving fields [9].

In particular, the physical reason of quantum speedup for the above methods has been found to be the non-Markovian effect of environment, which can induce the information flowing from environment back to the system [10]-[15]. A good example of this is the situation where a qubit is coupled to a single environment with a Lorentzian spectrum [7]. In this setting, it has been found that, the non-Markovianity is able to speed up the evolution of open systems, and subsequently lead to a smaller quantum speed limit time (QSLT) bound [16], expressed as the minimum evolution time for a quantum system to go from an initial state to a target state. The QSLT plays a fundamental role in many operational tasks [1] [17] [18], and has close connection with quantum coherence [19] [20].

More specifically, a simple monotonic relationship between the degree of non-Markovianity and the actual evolution speed was presented in other physical models [21]. And this non-Markovian-assisted speedup feature can be infer from the behaviour of QSLT bound. In some sense, this may not seem surprising since one may intuitively reason that the evolution speed should be faster if the non-Markovianity is bigger. However, the transition from no-speedup to speedup dynamical process is still poorly understood if the environment is not formed by only a bath. So how to devise a feasible mechanism to speed up dynamical evolution of an open quantum system under multiple environments becomes extremely significant.

The purpose of this paper is to examine the relationship between the quantum speedup and the non-Markovianity in open quantum systems. To do so, we will consider a qubit (a two-level system) coupled to a hierarchical PC environment consisting of a defect single-mode cavity and a semi-infinite 1D waveguide. The qubit is only coupled to the cavity, which is in turn connected to the waveguide reservoir. The model under consideration can exhibit interesting crossover properties in the Markovian to non-Markovian transition [22] [23]. We are interested in the effect of the hierarchical environment on the evolution speed of the system. It should be point out that, in the absence of the waveguide environment, such as the case of a single qubit-cavity model, the speedup only takes place within the strong coupling regime [24]. Therefore, we carry out our study in both weak and strong qubit-cavity coupling regimes. As we shall show in this work, even in the weak coupling regime, obvious accelerating phenomenon can still occur by choosing an agreeable memory time, which can be characterized by the time taken by some information to travel from the system to the waveguide environment and back [25]. As for the mechanism of quantum speedup, some

unexpected and nontrivial results are found. The non-Markovianity, *i.e.*, the amount of backflow information, is only one of the reason for the quantum speedup. We illustrate that the increase of the total amount of flow information is the essential reason for the quantum speedup.

The work is organized as follows. In Section 2, we describe the system of interest. In Section 3, we construct the measure of actual speed of quantum evolution based on information geometric formalism, while in Section 4, we investigate how the hierarchical environment affects the speed of quantum evolution. In order to clarify the mechanism for quantum speedup, we explore the interrelationship between the non-Markovianity and the quantum speedup in Section 5. We summarize our conclusions in Section 6.

2. Physical Model

We consider a two-level atom (transition frequency ω_s) embedded in a planar PC platform consisting of a defect single-mode cavity and a semi-infinite 1D waveguide (see **Figure 1**). The atom is coupled to the defect cavity while the cavity is coupled to the 1D waveguide. That is to say, the qubit is coupled to a hierarchical environment. The total Hamiltonian of the open system can be written as ($\hbar = 1$).

$$H = \frac{\omega_s}{2}\sigma_z + \omega_c a^\dagger a + \sum_k \omega_k b_k^\dagger b_k + \Omega\left(\sigma_+ a + H.c.\right) + \sum_k \left(g_k b_k^+ a + H.c.\right), \quad (1)$$

where $\sigma_+ = \sigma_-^\dagger$ and σ_z are the transition and inversion operators of the atom; b_k ($b_k^\dagger$) and a ($a^\dagger$) are the annihilation (creation) operators for the kth field mode and the cavity mode, respectively; g_k is the coupling strength between the cavity mode and the kth waveguide field mode, which is characterized by the frequency ω_k. The frequency of the cavity mode is described with ω_c and Ω is the coupling strength between the atom and the cavity mode. We assume that the 1D PC waveguide along x-axis is semi-infinite, that is, the termination of the waveguide imposes a hard-wall boundary condition on the field. The waveguide with one end located at $x = 0$ is coupled to the defect cavity at $x = x_0$. In experiment, the strong coupling between PC defect cavities and PC waveguides has been realized [26]. For simplicity, we assume $\omega_s = \omega_c = \omega_0$. The photon dispersion relationship of the one end waveguide field can be given by [27]

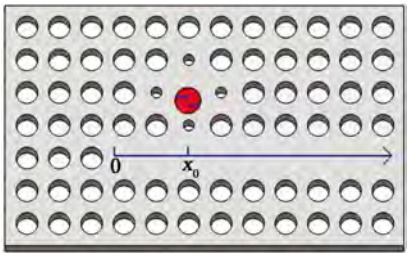

Figure 1. The implementation of the model. The qubit of interest is coupled to a defect cavity while the cavity is coupled at $x = x_0$ to a 1D semi-infinite waveguide, whose termination lies at $x = 0$.

$$\omega_k = \omega_0 + \upsilon\left(k - k_0\right), \tag{2}$$

where υ is the photon group velocity, and k_0 is the carrier wave vector with $\omega_{k0} = \omega_0$. Then the coupling strength between the cavity and the waveguide is

$$g_k = \sqrt{\Gamma\upsilon/\pi}\sin kx_0, \tag{3}$$

with the decay rate Γ of the cavity.

In the single-photon limit, the initial state is assumed to be $\left|\varphi(0)\right\rangle = \left|e,0_d,\tilde{0}\right\rangle$, which denotes the excited state of the atom with the cavity and the waveguide being in the vacuum state. After time $t > 0$, the total state can be generally written as

$$\left|\varphi(t)\right\rangle = A(t)\mathrm{e}^{-i\omega_0 t}\left|e,0_d,\tilde{0}\right\rangle + B(t)\mathrm{e}^{-i\omega_0 t}\left|g,1_d,\tilde{0}\right\rangle + \sum_k C_k(t)\mathrm{e}^{-i\omega_k t}\left|g,0_d,\tilde{1}_k\right\rangle, \tag{4}$$

where the state $\left|\tilde{1}_k\right\rangle$ ($\left|1_d\right\rangle$) accounts for the waveguide field mode (cavity mode) having one excitation. By putting the above equation into the Schrödinger equation, we obtain

$$\dot{A}(t) = -i\Omega B(t), \tag{5}$$

$$\dot{B}(t) = -i\Omega A(t) - i\sum_k g_k C_k(t)\mathrm{e}^{-i(\omega_k-\omega_0)t}, \tag{6}$$

$$\dot{C}_k(t) = -ig_k B(t)\mathrm{e}^{i(\omega_k-\omega_0)t}. \tag{7}$$

By formal time integration of Equation (7) and substituting it into the Equation (6), we can obtain

$$\dot{B}(t) = -i\Omega A(t) - \int_0^t f(t-t')B(t')\mathrm{d}t', \tag{8}$$

where $f(t-t') = \sum_k \left|g_k\right|^2 \mathrm{e}^{i(\omega_0-\omega_k)(t-t')}$ is the memory kernel of the waveguide reservoir. Through integrating of $f(t-t')$ over k and replacing this into Equation (8) we acquire

$$\dot{B}(t) = -i\Omega A(t) - \frac{\Gamma}{2}B(t) + \frac{\Gamma}{2}\mathrm{e}^{i\upsilon k_0 t_d}\mathrm{e}^{i\phi}B\left(t-t_d\right)\Theta\left(t-t_d\right), \tag{9}$$

where $\phi = 2k_0x_0$, $t_d = 2x_0/\upsilon$ is the memory time of the waveguide environment, which denotes the finite time taken by a photon to perform a round trip between the defect cavity and the mirror, and $\Theta(t)$ is the Heaviside step function. Clearly, for $t \geq t_d$, which ensures that the third term of the right hand side of Equation (9) is not zero, the dynamical evolution is greatly influenced by the phase ϕ. Specifically, due to the existence of the mirror, the light emitted in the present can interfere with the radiation in the pase. This interference process plays a key role in the dynamics of the open system, and can be witnessed by the factor $\mathrm{e}^{i\phi}$.

Performing the Laplace transformation for the Equations (5) and (9), we acquire

$$\tilde{A}(s) = \frac{1}{s + \dfrac{\Omega^2}{s + \dfrac{\Gamma}{2} - \dfrac{\Gamma}{2}\mathrm{e}^{i\phi}\mathrm{e}^{-st_d}}}. \tag{10}$$

By numerically solving the above equation, we can obtain the amplitude $A(t)$.

3. Measure of Dynamical Evolution Speed

The quantum speed of dynamical evolution for open quantum systems characterizes how fast a system under the environment driving can evolve. Via evaluating the speed of quantum evolution, one could use the method of differential geometry [28]. The geometric length between an initial state and its target state for open systems can be measured by using the Reimannian metric g^f, and then the squared infinitesimal length between two neighboring quantum states ρ and $\rho+\mathrm{d}\rho$ yields [29] [30]

$$\mathrm{d}s^2 = g^f(\mathrm{d}\rho, \mathrm{d}\rho). \tag{11}$$

We consider a evolved path ρ_0 and ρ_t with $t\in[0,\tau]$, the line element of the path can be given by $\mathrm{d}l = \sqrt{g^f(\partial_t\rho_t, \partial_t\rho_t)}\mathrm{d}t$. Hence, the instantaneous speed can be expressed as

$$S = \frac{\mathrm{d}l}{\mathrm{d}t} = \sqrt{g^f(\partial_t\rho_t, \partial_t\rho_t)}, \tag{12}$$

and the average speed is

$$V_a = \frac{1}{\tau}\int_0^\tau S\mathrm{d}t. \tag{13}$$

If the evolved state is in the form of its spectral decomposition, $\rho_t = \sum_k p_k |\phi_k\rangle\langle\phi_k|$ with $0 < p_k < 1$. The instantaneous speed can be rewritten as [28]

$$S = \sqrt{\sum_k \frac{|\dot{p}_k|^2}{4p_k} + \sum_{k\neq l} c^f(p_k, p_l)\frac{p_k(p_k-p_l)}{2}|\langle\phi_l|\dot{\phi}_k\rangle|^2}, \tag{14}$$

where $c^f(x,y)$ is a symmetric function defined as

$$c^f(x,y) = \frac{1}{yf(x/y)} \tag{15}$$

with $f(t)$ being the Morozova-Čencov (MC) function which fulfills $f(t) = tf(1/t)$ and $f(1)=1$ [31]. It is intuitively clear that the instantaneous speed of quantum evolution refers to two separate contributions as expressed in Equation (14). The first one, which is common to all the MC functions, depends only on the populations p_k of the evolved state. The second one, which is responsible for the chosen Riemannian metric, is instead only due to the coherence of the evolved state. Different types of MC functions $f(t)$ represent different Riemannian metrics employed to evaluate the evolution speed. It has been proven that [30] the Wigner-Yanase information metric with $f(t) = \left(1+\sqrt{t}\right)^2/4$ can lead to a definitely tighter QSLT for the amplitude damping dynamics in the form of Equation (1). Therefore, in the following we will focus on the Wigner-Yanase information metric.

4. Controllable of Quantum Speedup

In this section, we study the role of the hierarchical environment on the quantum speed of evolution. If the atomic system is initially in the state $|\Psi(0)\rangle = \beta|e\rangle + \sqrt{1-\beta^2}|g\rangle \quad (0 \le \beta \le 1)$, and the environment is in the vacuum state $|0_d, \tilde{0}\rangle$, the reduced density matrix of the atom at time t reads

$$\rho_a(t) = \begin{pmatrix} \beta^2 P_t & \beta\sqrt{1-\beta^2}\sqrt{P_t} \\ \beta\sqrt{1-\beta^2}\sqrt{P_t} & 1-\beta^2 P_t \end{pmatrix}, \tag{16}$$

where $P_t = |A(t)|^2$ denotes the excited state population of the atom. The spectral decomposition of $\rho_a(t)$ can be expressed as

$$\rho_a(t) = \sum_{k=\pm} p_k |\phi_k\rangle\langle\phi_k|, \tag{17}$$

with

$$p_\pm = (1 \pm \lambda)/2 \quad \text{and} \quad |\phi_\pm\rangle = \left(\alpha_\pm|e\rangle + |g\rangle\right)\Big/\sqrt{1+\alpha_\pm^2}$$

where $\lambda = \sqrt{1-4\beta^4(1-P_t)P_t}$ and $\alpha_\pm = \left(2\beta^2 P_t \pm \lambda - 1\right)\Big/\left(2\beta\sqrt{1-\beta^2}\sqrt{P_t}\right)$. According to Equations (14) and (17), we can investigate the speed of dynamical evolution in this open quantum system. It is easy to find that, for all the incoherent initial states such that $\beta = 1$, the instantaneous speed is independent on the choice of MC functions. That is to say, the second term of Equation (14) is identically zero in this case. The speed arises only from the population of the evolved state, and thus can be seen as the classical Fisher information metric [30]. In the following, we focus on the Wigner-Yanase information metric and consider two cases: 1) the atom-cavity coupling is in the weak coupling region with $\Omega < \Gamma$ and 2) the atom-cavity coupling is in the strong coupling region with $\Omega \ge \Gamma$.

We first consider the situation where the atom-cavity coupling is weak. **Figure 2(a)** shows the variation of the average speed of quantum evolution with respect to the phase ϕ for different memory time t_d with $\Omega = 0.01\Gamma$. Clearly, for each line (a fixed t_d), the minimum evolution speed occurs at the point where the phase $\phi = \pi$. Also, in the center region (from $\phi = \pi/2$ to $\phi = 3\pi/2$), the average speed slows down with the reduction of the memory time, while in other regions (from $\phi = 0$ to $\phi = \pi/2$, and from $\phi = 3\pi/2$ to $\phi = 2\pi$), decreasing the memory time will greatly increase the speed of quantum evolution. The changes of average speed V_a with respect to Ω and ϕ are plotted in **Figure 3(a)**. We find that, in the weak coupling regime determined by the inequality $\Omega < \Gamma$, increasing the atom-cavity coupling strength Ω, can speed up the quantum evolution for a given phase ϕ.

On the other hand, if the atom-cavity coupling is in the strong coupling regime with $\Omega \ge \Gamma$, the behavior of the evolution speed is different from the case where the coupling is weak. As shown in **Figure 2(b)** and **Figure 3(b)**, there is not a linear relationship between the speed of quantum evolution and the coupling strength. That is to say, periodicity of distribution about speedup region in the strong coupling case can be found. Thus, in the strong atom-cavity

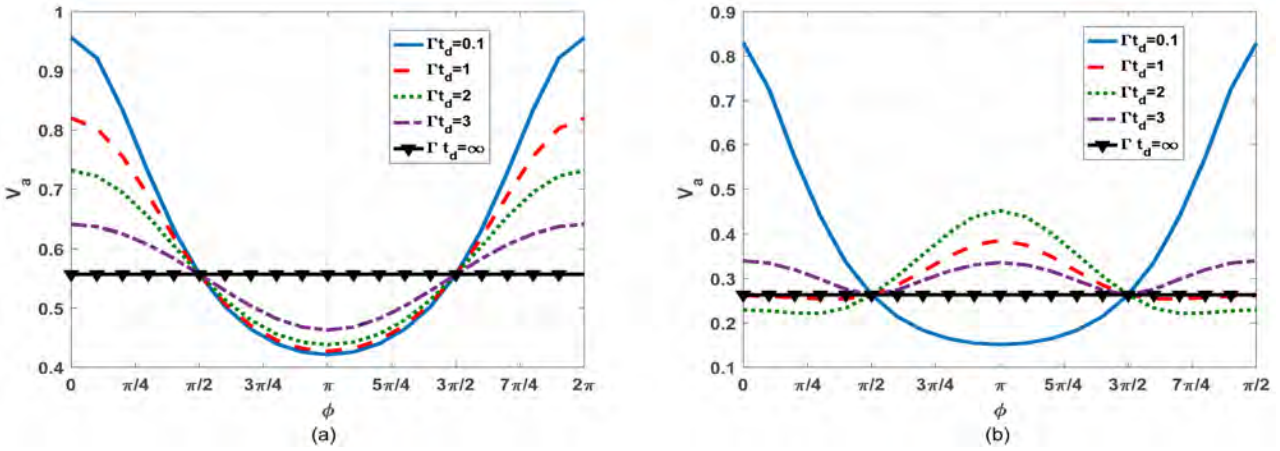

Figure 2. The average speed of quantum evolution V_a between the time zero and $\Gamma\tau = 10$ (in units of $1/\Gamma$) as a function of phase ϕ for various values of memory time Γt_d with $\beta = 1/\sqrt{2}$. (a) The atom-cavity coupling strength is weak with $\Omega = 0.01\Gamma$; (b) The atom-cavity coupling strength is strong with $\Omega = 2\Gamma$.

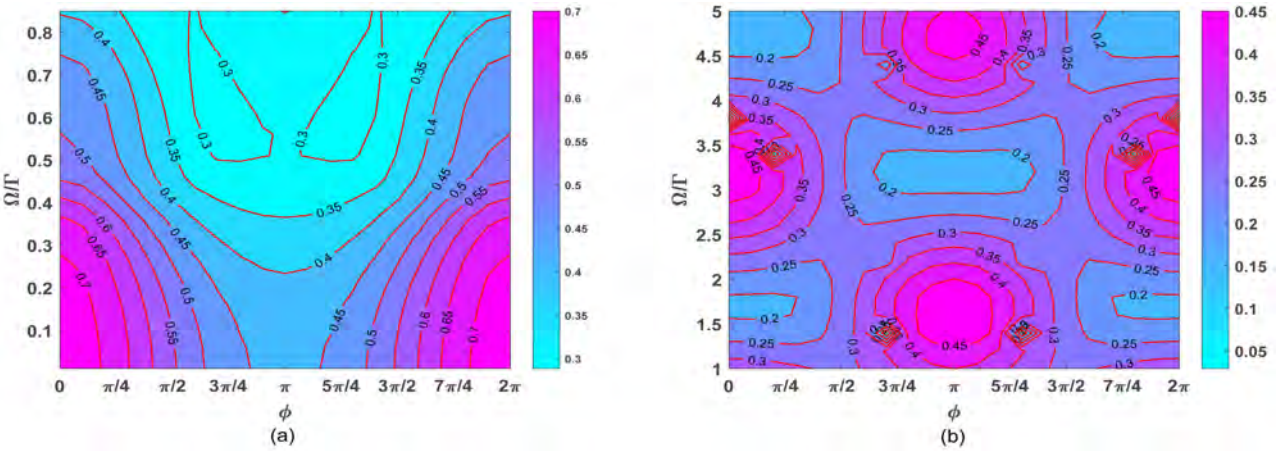

Figure 3. The average speed V_a as a function of ϕ and Ω for $\Gamma t_d = 2$ and $\beta = 1/\sqrt{2}$. (a) The atom-cavity coupling strength is in the weak coupling regime with $\Omega < \Gamma$; (b) The atom-cavity coupling strength is in the strong coupling regime with $\Omega \geq \Gamma$.

coupling regime, the speed of quantum evolution can be controlled to a speed-up or speed-down process.

Clearly, the evolution speed is greatly influenced by the memory time as well as the atom-cavity coupling. It should be noted that the above analysis only takes into account the situation where the memory time is shorter than the evolution time of the system, *i.e.*, $t_d < \tau$. In this case, the presence of the mirror mainly determines the evolution speed, which can be seen from the Equation (9). The emitted light will be reflected back and thus affect the evolution speed, owing to the feedback effect of the mirror. On the other hand, if the memory time is far longer than the evolution time, the emitted light will not been reflected back when the quantum system has already decayed. As expected, the average speed has no change with varying the phase ϕ, as shown in **Figure 2**. This is due to the fact that the light emitted in the past cannot interfere with the light emitted

in the present [22]. In this limiting regime with $\Gamma t_d \gg 1$, the waveguide behaves as being infinite, hence as a fully Markovian reservoir for the cavity. Accordingly, this system is actually reduce to a qubit coupled to lossy cavity.

5. Mechanism of Quantum Speedup

Previous results [7] [8] show that the non-Markovian effect of the reservoir can lead to speedup of quantum evolution. In order to understand the mechanism of quantum speedup in our model, in what follows we further study the relationship between the evolution speed and the non-Markovianity.

The non-Markovian effect means that the environment would cause the information flowing from environment back to the quantum system. When considering the framework to characterize non-Markovianity proposed by Breuer, Lane and Piilo [32], the total amount of information flowing back to the system is defined as

$$\aleph = \max_{\rho_{1,2}(0)} \int_{\sigma>0} \mathrm{d}t\sigma\left(t, \rho_{1,2}(0)\right), \tag{18}$$

where $\sigma\left(t, \rho_{1,2}(0)\right) = \frac{\mathrm{d}}{\mathrm{d}t} D\left(\rho_1(t), \rho_2(t)\right)$ denotes the changing rate of the trace distance $D\left(\rho_1(t), \rho_2(t)\right) = \frac{1}{2} tr\left|\rho_1(t) - \rho_2(t)\right|$ between states $\rho_{1,2}(t)$ evolving from their respective initial states $\rho_{1,2}(0)$. The rate $\sigma\left(t, \rho_{1,2}(0)\right)$ can be used to monitor the flow direction of information. It is negative for an information flowing from system to the environment, and positive for the information flowing in the opposite direction. Based on this, an evolution is non-Markovian if and only if $\sigma\left(t, \rho_{1,2}(0)\right) > 0$ for a pair of initial states. For our model, the optimal pair of initial states has been proven to be $\rho_{1,2}(0) = \left|\pm\right\rangle\left\langle\pm\right|$ [33], where $\left|\pm\right\rangle = \frac{1}{\sqrt{2}}\left(\left|e\right\rangle \pm \left|g\right\rangle\right)$.

When the atom-cavity coupling is weak, the speed that the information flowing out of the qubit is far lower than the evolution speed of the environment, so the backflow of information cannot happen, and thus the non-Markovianity converges to zero over the entire range of phase, as shown in **Figure 4** (dashed line). However, in the strong coupling regime with $\Omega = 2\Gamma$, the evolution of the atom has disturbed the environment, which eventually results in the backflow of information, *i.e.*, the non-Markovian effect. Thus we see a oscillating variation relationship between the non-Markovianity and the phase.

It is worth noting that the reason of the quantum speedup is not just due to the non-Markovian effect of the environment. By contrasting the average speed shown in **Figure 2(a)** and the non-Markovianity shown in **Figure 4** (dashed line), we can find that evolution speed varies depending on the value of ϕ in the weak atom-cavity coupling regime. Instead, the non-Markovianity remains unchanged when the coupling strength is weak. That is to say, the non-Markovianity, *i.e.*, the backflow of information, cannot seen an essential reflection to the speedup of quantum evolution.

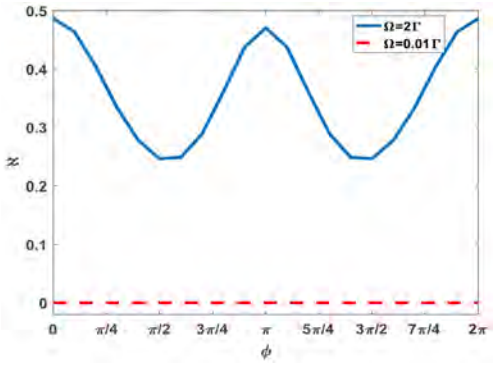

Figure 4. The non-Markovianity as a function of ϕ for various values of atom-cavity coupling strength Ω with $\Gamma t_d = 2$ and $\beta = 1/\sqrt{2}$.

Note that regarding to the measure of the non-Markovianity, the calculation is based on that one proposed in [32]. There are several other measures of the non-Markovianity, which is not agree with each other generally. However, it has been proven that they are equivalent for the dynamics in the form of the Equation (16). Therefore, our conclusion is invariant with respect to the definition of the non-Markovianity.

The total amount of flow information consists of two parts: the information flowing from system to environment and the information backflow from environment to the system. Why only the backflow information will speed up the quantum evolution? What is the effect of the information flowing from system to the environment on the evolution speed?

In what follows we focus on these questions. Based on the measure of non-Markovianity, the absolute value of changing rate $\left|\sigma\left(t,\rho_{1,2}(0)\right)\right|$ describes the changing of information, which consists the information flowing from system to environment and the reverse flow. Thus, the total amount of flow information can be defined as

$$\aleph_{\text{total}} = \max_{\rho_{1,2}(0)} \int \mathrm{d}t \left|\sigma\left(t,\rho_{1,2}(0)\right)\right|. \tag{19}$$

Figure 5 shows the $\aleph_{\text{total}}$ as a function of ϕ for various values of memory time t_d. It is interesting to find that the $\aleph_{\text{total}}$ exhibits the same behavior as the average speed of evolution. In detail, the decrease (increase) of $\aleph_{\text{total}}$ will lead to the speed-down (speed-up) process of quantum evolution. Take the case in the weak-coupling regime (**Figure 5(a)** and **Figure 2(a)**) as examples, when $\Omega = 0.01\Gamma$ and $\Gamma t_d = 2$, we find that the changing trend of $\aleph_{\text{total}}$ and the V_a are the same, while the value of non-Markovianity is always zero, as shown in **Figure 4** (dashed line). That is to say, the change of evolution speed is due to the flow of information from system to environment in this case. As shown in **Figure 6(a)**, we find a small decay of atomic excited-sate population due to the information flowing out. The decaying-degree of population P_t increase with decreasing the phase ϕ (in the region from $\phi = 0$ to $\phi = \pi$), and thus lead to the speedup of quantum evolution. It is also confirm that the minimum speed occurs at $\phi = \pi$ in the weak-coupling case (see **Figure 2(a)**).

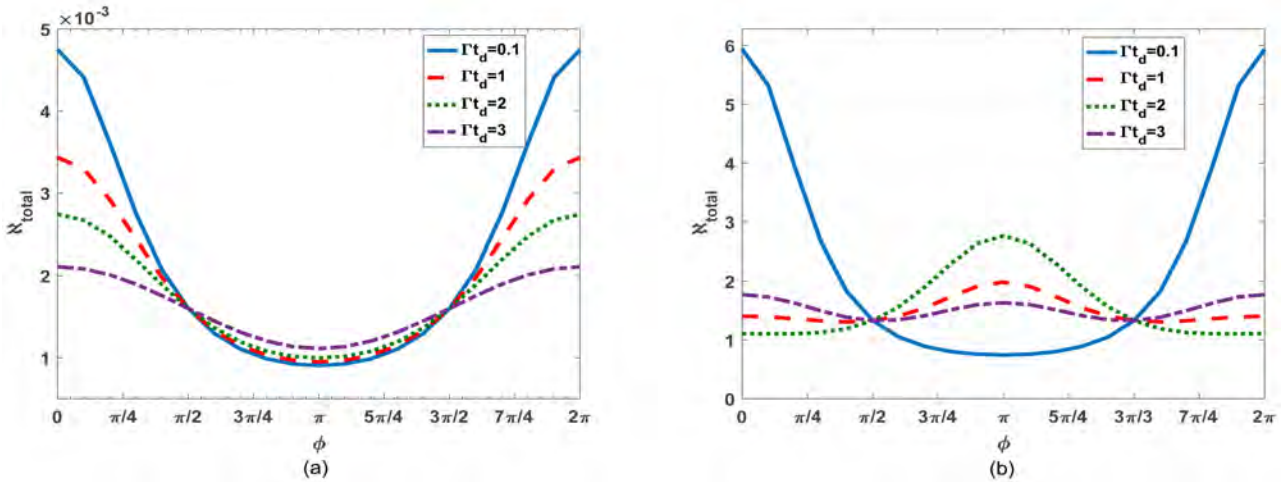

Figure 5. The total amount of flow information $\aleph_{\text{total}}$ between time zero and the time $\Gamma t = 10$ as a function of ϕ for various values of memory time t_d with $\beta = 1/\sqrt{2}$. (a) The atom-cavity coupling strength is weak with $\Omega = 0.01\Gamma$; (b) The atom-cavity coupling strength is strong with $\Omega = 2\Gamma$.

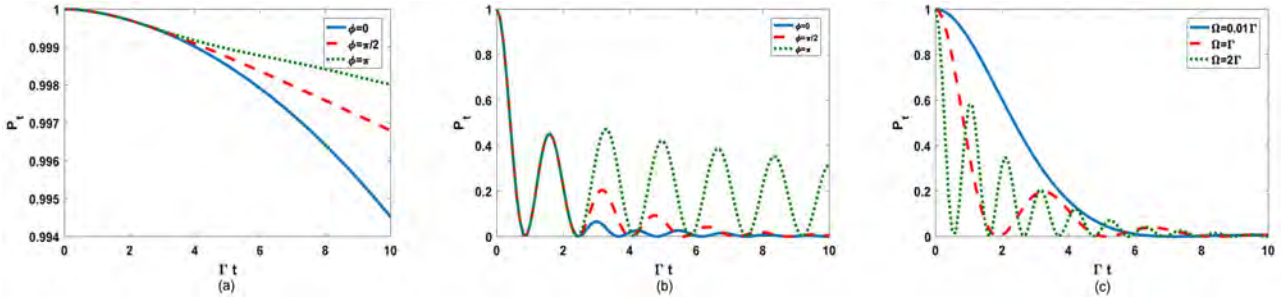

Figure 6. The time dependence of the atomic excited state population P_t with $\beta = 1/\sqrt{2}$. (a) The atom-cavity coupling strength is weak with $\Omega = 0.01\Gamma$ and $\Gamma t_d = 2$; (b) The atom-cavity coupling strength is strong with $\Omega = 2\Gamma$ and $\Gamma t_d = 2$; (c) The limit case with $\Gamma t_d \gg 1$.

While in the strong-coupling case with $\Omega = 2\Gamma$ and $\Gamma t_d = 2$, the backflow of information happens, which can result in the partial atomic re-excitation, as shown in **Figure 6(b)**. In this case, the speed of quantum evolution depends on the total amount of flow information $\aleph_{\text{total}}$. This is a newly noticed phenomenon. Overall, a remarkable result we find that, the changing in the evolution speed is attribute to the flow of information, regardless of the direction in which the information flows.

Our conclusion applies also to the more standard and basic case of an atom in a lossy cavity, which corresponds to the limit case with $\Gamma t_d \gg 1$. As shown in **Figure 6(c)**, P_t exhibits a monotonic decay in the weak atom-cavity coupling, while the strong atom-cavity couplings can lead to the backflow of information, and thus increase the $\aleph_{\text{total}}$. Accordingly, the strong atom-cavity couplings can speed up the quantum evolution (see **Figure 2(a)** and **Figure 2(b)**).

6. Conclusion

In summary, we have studied a two-level atom that is coupled to a hierarchically

structure environment consisting of a PC defect cavity and a semi-infinite 1D waveguide. We investigated how the atom-cavity coupling and the memory time affect the quantum speedup. We found that the information flow volume consisting the information flowing from system to environment and the backflow information is the main physical reason of the speed-up process. The potential candidates which can verify our prediction can be systems such as InGaAa quantum dots coupled to a GaAs PC membrane [34], and nitrogen-vacancy (N-V) centers embedded in a two-dimensional planar PC [35].

Funding

This work was supported by the Young Foundation of Shandong province (Grant number ZR2017QA002) and Doctoral Foundation of University of Jinan (Grant No. XBS1325).

Conflicts of Interest

The authors declare no conflicts of interest regarding the publication of this paper.

References

[1] Caneva, T., Murphy, M., Calarco, T., Fazio, R., Montangero, S., Giovannetti, V. and Santoro, G.E. (2009) *Physical Review Letters*, **103**, Article ID: 240501. https://doi.org/10.1103/PhysRevLett.103.240501

[2] Lloyd, S. (2000) *Nature* (*London*), **406**, 1047-1054. https://doi.org/10.1038/35023282

[3] Hegerfeldt, G.C. (2014) *Physical Review A*, **90**, Article ID: 032110. https://doi.org/10.1103/PhysRevA.90.032110

[4] Georgescu, I.M., Aahhab, S. and Noir, F. (2014) *Reviews of Modern Physics*, **86**, 153. https://doi.org/10.1103/RevModPhys.86.153

[5] Frey, M.R. (2016) *Quantum Information Process*, **15**, 3919-3951. https://doi.org/10.1007/s11128-016-1405-x

[6] Julsgaard, B., Sherson, J.I., Cirac, J., Fiurášek, J. and Polzik, E.S. (2000) *Nature* (*London*), **406**, 1047-1054. https://doi.org/10.1038/35023282

[7] Deffner, S. and Lutz, E. (2013) *Physical Review Letters*, **111**, Article ID: 010402. https://doi.org/10.1103/PhysRevLett.111.010402

[8] Xu, Z.Y., Luo, S., Yang, W.L., Liu, C. and Zhu, S. (2014) *Physical Review A*, **89**, Article ID: 012307. https://doi.org/10.1103/PhysRevA.89.012307

[9] Zhang, Y.J., Hsn, W., Xia, Y.J., Cao, J.P. and Fan, H. (2015) *Physical Review A*, **67**, Article ID: 032112.

[10] Laine, E.M., Breuer, H.P., Piilo, J., Li, C.F. and Guo, G.C. (2012) *Physical Review Letters*, **108**, Article ID: 210402. https://doi.org/10.1103/PhysRevLett.108.210402

[11] Zhang, W.M., Lo, P.Y., Xiong, H.N., Yu, M.W.-Y. and Nori, F. (2012) *Physical Review Letters*, **109**, Article ID: 170402. https://doi.org/10.1103/PhysRevLett.109.170402

[12] Cianciaruso, M., Maniscalco, S. and Adesso, G. (2017) *Physical Review A*, **96**, Article ID: 012105. https://doi.org/10.1103/PhysRevA.96.012105

[13] Man, Z.X., Xia, Y.J. and Lo Franco, R. (2018) *Physical Review A*, **97**, Article ID: 062104. https://doi.org/10.1103/PhysRevA.97.062104

[14] Man, Z.X., Xia, Y.J. and Lo Franco, R. (2015) *Physical Review A*, **92**, Article ID: 012315. https://doi.org/10.1103/PhysRevA.92.012315

[15] Kabuss, J., Krimer, D.O., Rotter, S., Stannigel, K., Knorr, A. and Carmele, A. (2015) *Physical Review A*, **92**, Article ID: 053810. https://doi.org/10.1103/PhysRevA.92.053801

[16] Anandan, J. and Aharonov, Y. (1990) *Physical Review Letters*, **65**, Article ID: 1697. https://doi.org/10.1103/PhysRevLett.65.1697

[17] Giovannetti, V., Lloyd, S. and Maccone, L. (2011) *Nature Photonics*, **5**, 222-229. https://doi.org/10.1038/nphoton.2011.35

[18] Dener, S. and Lutz, E. (2010) *Physical Review Letters*, **105**, Article ID: 170402. https://doi.org/10.1103/PhysRevLett.105.170402

[19] Marvian, I., Spekkens, R.W. and Zanardi, P. (2016) *Physical Review A*, **93**, Article ID: 052331. https://doi.org/10.1103/PhysRevA.93.052331

[20] Streltsov, A., Adesso, G. and Plenio, M.B. (2017) *Reviews of Modern Physics*, **89**, Article ID: 041003. https://doi.org/10.1103/RevModPhys.89.041003

[21] Behzadi, N., Ahansaz, B., Ektesabi, A. and Faizi, E. (2017) *Physical Review A*, **95**, Article ID: 052121. https://doi.org/10.1103/PhysRevA.95.052121

[22] Tufarelli, T., Kim, M.S. and Ciccarello, F. (2014) *Physical Review A*, **90**, Article ID: 012113. https://doi.org/10.1103/PhysRevA.90.012113

[23] Man, Z.X., An, N.B. and Xia, Y.J. (2014) *Physical Review A*, **90**, Article ID: 062104. https://doi.org/10.1103/PhysRevA.90.062104

[24] Liu, H.B., Yang, W.L., An, J.H. and Xu, Z.Y. (2016) *Physical Review A*, **93**, Article ID: 020105. https://doi.org/10.1103/PhysRevA.93.020105

[25] Tufarelli, T., Ciccarello, F. and Kim, M.S. (2013) *Physical Review A*, **87**, Article ID: 013820. https://doi.org/10.1103/PhysRevA.87.013820

[26] Faraon, A., Waks, E., Englund, D., Fushman, I. and Včković, J. (2007) *Applied Physics Letters*, **90**, Article ID: 073102. https://doi.org/10.1063/1.2472534

[27] Shen, J.T. and Fan, S.H. (2005) *Optics Letters*, **30**, 2001-2003. https://doi.org/10.1364/OL.30.002001

[28] Bengtsson, I. and Zyczkowski, K. (2006) Geometry of Quantum States: An Introduction to Quantum Entanglement. Cambridge University Press, Cambridge. https://doi.org/10.1017/CBO9780511535048

[29] Petz, D. and Hasegawa, H. (1996) *Letters in Mathematical Physics*, **38**, 221-225. https://doi.org/10.1007/BF00398324

[30] Pires, D.P., Cianciaruso, M., Cleri, L.C., Adesso, G. and Soares-Pinto, D.O. (2016) *Physical Review X*, **6**, Article ID: 021031. https://doi.org/10.1103/PhysRevX.6.021031

[31] Kubo, F. and Ando, T. (1980) *Mathematische Annalen*, **246**, 205-224. https://doi.org/10.1007/BF01371042

[32] Breuer, H.P., Laine, E.M. and Piilo, J. (2009) *Physical Review Letters*, **103**, Article ID: 210401. https://doi.org/10.1103/PhysRevLett.103.210401

[33] Wissmann, S., Karlsson, A., Laine, E.M., Piilo, J. and Breuer, H.-P. (2012) *Physical Review A*, **86**, Article ID: 062108. https://doi.org/10.1103/PhysRevA.86.062108

[34] Yoshie, T., Scherer, A., Hendrickson, J., Khitrova, G., Gibbs, H.-M., Rupper, G., Ell, C., Shchekin, O.-B. and Deppe, D.-G. (2004) *Nature*, **432**, 200-203.

https://doi.org/10.1038/nature03119

[35] Faraon, A., Santori, C., Huang, Z., Acosta, V.M. and Beausoleil, R.G. (2012) *Physical Review Letters*, **109**, Article ID: 033604. https://doi.org/10.1103/PhysRevLett.109.033604

Journal of Modern Physics, 2019, 10, 1190-1208
https://www.scirp.org/journal/jmp
ISSN Online: 2153-120X
ISSN Print: 2153-1196

The Contradiction between Two Versions of Quantum Theory Could Be Decided by Experiment

María Esther Burgos

Faculty of Sciences, University of Los Andes, Mérida, Venezuela
Email: mburgos25@gmail.com

How to cite this paper: Burgos, M.E. (2019) The Contradiction between Two Versions of Quantum Theory Could Be Decided by Experiment. *Journal of Modern Physics*, **10**, 1190-1208.
https://doi.org/10.4236/jmp.2019.1010079

Received: June 10, 2019
Accepted: September 9, 2019
Published: September 12, 2019

Abstract

The incompatibility of Orthodox Quantum Mechanics with philosophical realism poses a serious challenge to scientists upholding such a philosophical doctrine. The desire to find a solution to this and other conceptual problems that quantum mechanics confronts has motivated many authors to propose alternative versions to Orthodox Quantum Mechanics. One of them is the Spontaneous Projection Approach, a theory grounded on philosophical realism. It has been introduced in previous papers and, with a few exceptions, it yields experimental predictions coincident with those of Orthodox Quantum Mechanics. One of these exceptions is analyzed in detail. The difference in predictions becomes apparent in a suggested experiment which could put both theories to the test.

Keywords

Philosophical Realism, Orthodox Quantum Mechanics, Spontaneous Projection Approach, Quantum Measurement Problem

1. Introduction and Outlook

Realism is a philosophical doctrine that revolves around two theses: the first (or ontological thesis) is that the world exists by itself as opposed to being the product of human mind; the second (or epistemological thesis) is that it can be known gradually and approximately [1]. Among authors adopting realism let us mention Albert Einstein and Mario Bunge. For Einstein, "The belief in an external world independent of the perceiving subject is the basis of all natural science" [2]. For Bunge, "Epistemological realism is the family of epistemologies which assume that a) the world exists independently of the knowing subject, and

b) the task of science is to produce maximally true conceptual models of reality..." ([3] pp. 191-192).

In 1930, Paul Dirac published the first formulation of quantum mechanics [4]. Two years later John von Neumann published *Mathematische Grundlagen der Quantenmechanik* [5]. These first versions of quantum theory share two characteristics: 1) the state vector $|\psi\rangle$ (wave function ψ) describes the state of an individual system, and 2) they involve two laws of change of the state of the system: spontaneous (natural) processes, governed by the Schrödinger equation; and measurement processes, ruled by the projection postulate. Many other versions of quantum theory followed. Those where $|\psi\rangle$ describes the state of an individual system *and* the projection postulate is included among its axioms are generally called standard, ordinary or Orthodox Quantum Mechanics (OQM), sometimes referred to as the *Copenhagen Interpretation*.

On the one hand, OQM is very successful a theory. "[It has provided] a strikingly successful recipe for doing calculations that accurately described the outcomes of experiments... [It has been] instrumental in predicting antimatter, understanding radioactivity (leading to nuclear power), accounting for the behavior of materials such as semiconductors, explaining superconductivity and describing interactions such as those between light and matter (leading to the invention of the laser) and of radio waves and nuclei (leading to magnetic resonance imaging). Many successes of quantum mechanics involve its extension, quantum field theory, which forms the foundations of elementary particle physics..." [6].

On the other hand, OQM contravenes philosophical realism. This is particularly clear as concerns its projection postulate. Scientists upholding philosophical realism have criticized this postulate because it introduces a subjective element into the theory: either it invokes an observer placed above the laws of nature ([3], pp. 191-202) or it appeals to the interaction between the quantum system and a macroscopic measuring device (built, of course, by human beings). Referring to this issue Max Jammer points out: "As long as quantum mechanics one-body or many-body system does not interact with macroscopic bodies, as long as its motion is described by the deterministic Schrödinger time-dependent equation, no events could be considered to take place in the system... If the whole physical universe were composed only of microphysical entities, as it should be according to the atomic theory, it would be a universe of evolving potentialities (time-dependent ψ functions) but not of real events" ([7], p. 474).

It is worth noting that well-known scientists dealing with quantum mechanics renounce philosophical realism, either implicitly or explicitly. Let us mention two of them: Niels Bohr and Asher Peres. The last one declares: "Quantum theory is not an objective description of physical reality" ([8], p. 423) and "any attempt to inject realism in physical theory is bound to lead to inconsistencies" [9]. In his analysis of Bohr's philosophy Aage Petersen asserts: "When asked whether the algorithm of quantum mechanics could be considered as somehow mirroring an underlying quantum world, Bohr would answer: 'There is no

quantum world. There is only an abstract quantum physical description. It is wrong to think that the task of physics is to find out how nature *is*. Physics concerns what we can say about nature'." [10].

Taking philosophical realism as a starting point, a Spontaneous Projection Approach (SPA) to quantum theory was formulated some years ago [11]. This approach was recently modified to account for quantum processes in the general case, including those where the Hamiltonian depends explicitly on time [12]. It is worth noting that SPA overcomes the main flaws of OQM [12] and in general yields experimental predictions coincident with those of OQM. There are, however, a few exceptions which could be exploited to confront both theories. This is the principal aim of our present study.

The contents of this paper are as follows: In Section 2, we reproduce the formulations of OQM and SPA, highlight their similarities and differences, mention some contributions aiming to solve the measurement problem and refer one of them in detail. In Section 3, we deal with a case where SPA and OQM yield different experimental predictions. We consider a silver atom in the ground state placed in a uniform constant magnetic field $\boldsymbol{B}$. Starting with the atom in a given state we find 1) the evolution of its state assuming the validity of OQM; and 2) the possible changes of its state assuming the validity of SPA. The resulting contradiction could be decided by means of a suggested experiment. Section 4 is devoted to the discussion and conclusions.

2. OQM, SPA and the Measurement Problem

2.1. Formulation of OQM

The formulation of quantum mechanics due to von Neumann (OQM) ([7], p. 5) ([13], pp. 215-222) includes the primitive (undefined) notions of *system, state and physical quantity* (or observable). Its postulates are:

I) To every system ζ corresponds a Hilbert space *Hb* whose vectors (state vectors, wave functions) $|\psi\rangle$ completely describe the states of the system.

II) To every physical quantity $\mathcal{A}$ corresponds uniquely a self-adjoint operator *A* acting in *Hb*. It has associated the eigenvalue equations

$$A\left|\alpha_k^{\nu}\right\rangle = \alpha_k \left|\alpha_k^{\nu}\right\rangle \tag{1}$$

(ν is introduced in order to distinguish between the different eigenvectors that may correspond to one eigenvalue α_k), and the closure relation

$$\sum_{k,\nu}\left|\alpha_k^{\nu}\right\rangle\left\langle\alpha_k^{\nu}\right| = \mathcal{J} \tag{2}$$

is fulfilled (here $\mathcal{J}$ is the identity operator). If either *k* or ν is continuous, the respective sum has to be replaced by an integral.

III) *Spontaneous processes are continuous*. The evolution in time *t* of the state vector $|\psi(t)\rangle$ is governed by the Schrödinger equation

$$i\hbar\frac{\mathrm{d}}{\mathrm{d}t}\left|\psi(t)\right\rangle = H(t)\left|\psi(t)\right\rangle \tag{3}$$

where $H(t)$ is the Hamiltonian of the system, $\hbar$ Planck's constant divided by 2π and i the imaginary unit.

Comment: The Schrödinger equation is a deterministic law. The solution $|\psi(t)\rangle$ of Equation (3) which corresponds to the initial condition $|\psi(0)\rangle$ is *unique*. The system's state evolves according to the equation

$$|\psi(t)\rangle = U(t,0)|\psi(0)\rangle \tag{4}$$

where $U(t,0)$ is the *evolution operator* corresponding to the Hamiltonian $H(t)$; more details in ([4], p. 109) ([13], p. 308) ([14], p. 137).

IV) For a system in the state $|\psi\rangle$ the probability that the result of a measurement of $\mathcal{A}$ lies between α_1 and α_2 is $\|\eta\|^2$, where $\|\eta\|$ is the norm of $|\eta\rangle = (\mathcal{J}_{\alpha_2} - \mathcal{J}_{\alpha_1})|\psi\rangle$ and $\mathcal{J}_\alpha$ is the resolution of the identity belonging to A.

V) Projection postulate. If a measurement of $\mathcal{A}$ yields a result between α_1 and α_2, then the state of the system immediately after the measurement is an eigenfunction of $(\mathcal{J}_{\alpha_2} - \mathcal{J}_{\alpha_1})$.

2.2. Formulation of SPA

The formulation of SPA includes the primitive notions of *system, state, physical quantity and probability* [12]. Its postulates are:

A) Agrees word for word with postulate I of OQM.

B) Agrees word for word with postulate II of OQM.

C) *Spontaneous processes can be either continuous or discontinuous*. In continuous processes the evolution in time of the state vector $|\psi\rangle$ is determined by the Schrödinger equation.

Comment (i): Equation (4) applies to processes that are continuous in the whole time interval $(0,t)$. In cases where this equation is satisfied, we shall say that in the interval $(0,t)$ *the system remains in the Schrödinger channel*.

Comment (ii): Let the Hamiltonian of the system be

$$H(t) = \varepsilon + \lambda(t) \tag{5}$$

where ε is the sum of all the terms of the Hamiltonian which do not depend explicitly on time t and $\lambda(t)$ includes every term of the Hamiltonian depending explicitly on t. If $\lambda(t) = 0$, a self-adjoint operator A fulfilling

$$\frac{\partial A}{\partial t} = 0 \tag{6}$$

$$[A, \varepsilon] = 0 \tag{7}$$

is a constant of the motion.

Definition of preferential states: The system in the state $|\psi(t)\rangle$ has tendency to jump to the eigenstates of operators satisfying Equations (6) and (7) whether $\lambda(t) = 0$ or not [12]. If there is *a unique set* of $N \geq 2$ orthonormal vectors: $|\varphi_1\rangle, |\varphi_2\rangle, \cdots, |\varphi_N\rangle$ ($\{N_\varphi\}$ for short) such that the normalized state of the system ζ at time t can be written

$$\left|\psi(t)\right\rangle = \sum_j \gamma_j(t)\left|\varphi_j\right\rangle \tag{8}$$

where 1) $\gamma_j(t) = \left\langle \varphi_j \middle| \psi(t)\right\rangle \neq 0$ for every $j = 1,2,\cdots,N$; 2) at least $(N-1)$ vectors belonging to the set $\{N_\varphi\}$ are eigenstates of ε; and 3) *every* self-adjoint operator A for which Equations (6) and (7) are valid satisfies the relation

$$\left\langle \psi(t)\middle| A \middle|\psi(t)\right\rangle = \sum_j \left|\gamma_j(t)\right|^2 \left\langle \varphi_j \middle| A \middle| \varphi_j \right\rangle \tag{9}$$

we shall say that $\{N_\varphi\}$ *is the preferential set* of ζ in the state $\left|\psi(t)\right\rangle$ and the members of $\{N_\varphi\}$ will be called *its preferential states*.

Comment (iii): The validity of Equation (9) ensures the statistical sense of conservation laws [11]. Note that, by definition, the preferential set does not depend on $\lambda(t)$ [12].

D) If the system ζ in the state $\left|\psi(t)\right\rangle$ *has no preferential set*, it remains in the Schrödinger channel.

E) If the system ζ in the normalized state $\left|\psi(t)\right\rangle$ *has the preferential set* $\{N_\varphi\}$, in the small time interval $(t, t+\mathrm{d}t)$ it can either remain in the Schrödinger channel or jump to one of its preferential states $\left|\varphi_k\right\rangle$ with probability

$$\mathrm{d}P_k(t) = \left|\gamma_k(t)\right|^2 \frac{\mathrm{d}t}{\tau(t)} \tag{10}$$

where

$$\tau(t)\Delta\varepsilon(t) = \frac{\hbar}{2} \tag{11}$$

and

$$\left[\Delta\varepsilon(t)\right]^2 = \left\langle \psi(t)\middle|\varepsilon^2\middle|\psi(t)\right\rangle - \left[\left\langle \psi(t)\middle|\varepsilon\middle|\psi(t)\right\rangle\right]^2 \tag{12}$$

Comment: The probability that the system will remain in the Schrödinger channel during the time interval $(t, t+\mathrm{d}t)$ is

$$\mathrm{d}P_S(t) = 1 - \frac{\mathrm{d}t}{\tau(t)} \tag{13}$$

see [12]. If the parameter τ defined by Equation (11) is constant, the state $\left|\psi(t)\right\rangle$ may be considered as an unstable state that can decay to *one* of its N preferential states [11] [15] [16]. In this case the probability that the system will remain in the Schrödinger channel during the interval $(0,t)$ is a decreasing exponential

$$P_S(t) = \mathrm{e}^{-t/\tau} \tag{14}$$

with relaxation time τ.

2.3. OQM, SPA and Other Contributions Aiming to Solve the Measurement Problem

OQM assumes that there are two kinds of processes: spontaneous processes and

measurement processes. In spontaneous processes the evolution of the state vector is governed by the Schrödinger equation; in measurement processes the changes of the state vector are ruled by the projection postulate.

On the one hand, since the Schrödinger equation involves a derivative of the state vector $|\psi(t)\rangle$ with respect to time *t*, in spontaneous processes $|\psi(t)\rangle$ must be continuous. On the other hand, Postulate C of SPA states that in continuous processes the evolution in time of the state vector $|\psi(t)\rangle$ is determined by the Schrödinger equation. *Continuous processes are governed by the Schrödinger equation in SPA as well as in OQM.*

It is worth stressing that continuous processes are not restricted to cases where the system in the state $|\psi(t)\rangle$ has no preferential set. Even if the system in the state $|\psi(t)\rangle$ has a preferential set, the dominant process in a small time interval $(t, t+\mathrm{d}t)$ is the Schrödinger evolution; see Equation (13). According to Equation (14) the Schrödinger evolution is also the dominant process for $t \ll \tau$. Spontaneous projections seldom occur.

OQM measurements are somehow related to SPA projections. Let us highlight their similarities: SPA projections as well as OQM measurements 1) yield discontinuities of the state vector; 2) instantaneously break down certain superposition of different states; 3) violate conservations laws but respect their statistical sense [16] [17]; 4) imply a kind of action-at-a-distance [16] [18]; and 5) collide with determinism [16] [19].

The main difference between SPA and OQM is that while according to SPA the state vector $|\psi(t)\rangle$ may spontaneously jump to one of its preferential states, *e.g.* $|\varphi_n\rangle$ (see Equation (8)), OQM ensures that $|\psi(t)\rangle$ remains continuous until a measurement is performed.

Let A be the operator representing the physical quantity $\mathcal{A}$ to be measured and $|\alpha_j\rangle$ the eigenvector of A corresponding to the eigenvalue α_j (for simplicity we refer to the discrete non-degenerate case). The state vector $|\psi(t)\rangle$ can be expanded

$$|\psi(t)\rangle = \sum_j c_j(t)|\alpha_j\rangle \tag{15}$$

where $c_j(t) = \langle\alpha_j|\psi(t)\rangle$. OQM states that the probability that the measurement of $\mathcal{A}$ will yield the result α_n and so (according to the projection postulate) $|\psi(t)\rangle$ will jump to $|\alpha_n\rangle$ is

$$p_n(t) = |c_n(t)|^2 \tag{16}$$

According to SPA the probability that in the small time interval $(t, t+\mathrm{d}t)$ the state vector $|\psi(t)\rangle$ will jump to the preferential state $|\varphi_n\rangle$ is

$$\mathrm{d}P_n(t) = |\gamma_n(t)|^2 \frac{\mathrm{d}t}{\tau(t)} \tag{17}$$

see Equation (10). If the relaxation time τ and $|\gamma_n(t)|^2 = |\gamma_n|^2$ are constant in the interval $(0,t)$, the probability that $|\psi(t)\rangle$ will jump to $|\varphi_n\rangle$ in this interval

is

$$P_n(t) = |\gamma_n|^2 \left(1 - e^{-t/\tau}\right) \tag{18}$$

[11]. For $t \gg \tau$, it results

$$P_n(t \gg \tau) \simeq |\gamma_n|^2 \tag{19}$$

The similarity of the mathematical expressions for the probabilities given by (16) and (19) is worth stressing.

Even if it is not clear what a measurement is [20], the notion of measurement is included in two of the five postulates of OQM formulation. In any case, collapses or something similar to collapses are necessary to avoid paradoxes such as that of Schrödinger's cat ([7], pp. 216-217). "Because of the linearity of the Schrödinger evolution there is no mechanism to stop the evolution and yield a single result for the measurement" ([14], p. 264). However, "in common life as well as in laboratories, one never observe superposition of results; we observe that Nature seems to operate in such a way that a single result always emerges from a single experiment; this will never be explained by the Schrödinger equation, since all that it can do is to endlessly extend its ramifications into the environment, without ever selecting one of them only" [21]. The rule compelling $|\psi(t)\rangle$ to remain continuous as long as no measurements are performed poses a serious problem for OQM. By contrast, assuming that spontaneous projections are natural processes, SPA succeeds in stopping the endless ramifications resulting from Schrödinger evolution.

The issues just mentioned are at the very heart of the measurement problem. In previous articles we dealt with several proposed solutions to this problem. Among them, 1) Margenau's contribution ([7], pp. 226-227) was addressed in [16]; 2) The statistical interpretation of quantum mechanics [22] [23] was addressed in [16]; 3) Bohm's theory [24] [25] was addressed in [11]; 4) Many-worlds interpretation [26] [27] was addressed in [16]; 5) The consistent histories approach to quantum mechanics [28] [29] was addressed in [11]; 6) Decoherence [30] [31] was addressed in [16]; 7) The theory of spontaneous localizations [32] [33] was addressed in [11]; 8) Bell's Beables for quantum field theory [34] was addressed in [15]; 9) Sudbery's privileged observables [35] was addressed in [15]; and 10) Sudbery's preferred observables [36] was addressed in [15]. Some of them as well as SPA involve dynamical reduction models.

2.4. SPA Preferential Sets and Sudbery's Preferred Observables

Among the contributions appearing in the previous list the closest to SPA is Sudbery's theory of preferred observables. Let us highlight their similarities and differences with SPA.

In his article entitled Diesse Verdammten Quantenspringerei, Anthony Sudbery asserts: "*there are no events in quantum theory*. The nearest thing to an event described in the basic theory is the result of a measurement... There is no way that the theory can describe events, like the Ω^- decay… which happen spon-

taneously and are passively recorded by the waiting experimenter… Nevertheless, textbooks do purport to derive decay rates for such events from the general principles of quantum mechanics. The derivation goes like this. To describe a decay $A \to B + C$, we start at time $t = 0$ with a state $|A\rangle$ in which the unstable particle A is certain not to have decayed, and follows its time evolution, governed by the Hamiltonian H, to a superposition of the initial state and a state of the decay products B and C:

$$e^{-iHt/\hbar}|A\rangle = a(t)|A\rangle + b(t)|BC\rangle \tag{20}$$

The general principles of quantum mechanics are then supposed to yield the interpretation that $|b(t)|^2$ is the probability that by time t there has been a transition from particle A to particles $B + C$. But where does this notion of a 'transition' come from? It appears nowhere in the general principles of the theory as usually stated. The literal application of these principles to the state (20) gives only the statement that if a measurement is made at time t (to determine, say, whether a particle of type B is present) then $|b(t)|^2$ is the probability that the result of the measurement will be positive. The inference that something discontinuous (a transition) happened between time 0 and time t is completely unwarranted. According to the official principles, quantum systems evolve continuously (as the time dependence of (20) shows), and quantum jumps occur only when provoked by the intervention of an experimenter" [36].

Sudbery adds: "The procedure that starts with the time-depending state vector (20), produces from it a time-dependent probability $P(t)$, interprets this as a probability of something *having happened,* and, on the strength of this interpretation, derives from $P(t)$ a transition probability per unit time, certainly ends up with an empirical adequate result" [36]. The problem Sudbery wants to discuss is that of formulating the theory so as to make this argument as sound as its conclusion. To do so, he claims, "transitions must be given a fundamental role in the theory; one of its basic postulates should be of the form 'If the system [however broadly conceived it] is in the state ψ at time t, there is a probability $T_{\varphi\psi}(t)\mathrm{d}t$ that it will take a transition to state φ between t and $t + \mathrm{d}t$.' Such a postulate, if it is to be fundamental, would need to be accompanied by a clear statement of exactly what the eligible states φ, ψ are" [36].

In order to formulate a postulate concerning transitions, Sudbery adopts a suggestion made by Bell [34]. "The basic idea is that there is a set of special physical quantities, which have a fundamental status; Bell liked to call them beables... These quantities always have definite values which change stochastically according to transition probabilities determined by the solutions to the Schrödinger equation. Equivalently, one can replace the special quantities by a special set of subspaces of space states, namely their eigenspaces, and the actual values of special quantities by a vector (the projection of the full space vector) in the corresponding subspace" [36]. These subspaces are called the viable subspaces.

By adopting Bell's transition probabilities, Sudbery succeeds in giving a satisfactory description of the decay process. But, he points out, "Bell's formulation of quantum mechanics does not exists until one has specified the viable subspaces. In this respect, it is no improvement on the conventional formulation, which does not exist until one has specified precisely which physical arrangement constitutes 'measurement'… If one is aspiring to give an absolute description of the physical world, there seems to be no good empirical or theoretical reason why any particular set of physical quantities should have fundamental status" [36]. Nevertheless, he adds, "if arbitrary choices cannot be avoided, we must consider how to live with them" [36].

SPA fulfills all the requirements stated by Sudbery: According to Postulate E, if the system is in the state $|\psi(t)\rangle$ and $|\varphi_k\rangle$ is one of its preferential states, the probability that it will take a transition from $|\psi(t)\rangle$ to $|\varphi_k\rangle$ between t and $t+\mathrm{d}t$ is

$$\mathrm{d}P_k(t)=\left|\gamma_k(t)\right|^2\frac{\mathrm{d}t}{\tau(t)} \tag{21}$$

where $\gamma_k(t)=\langle\varphi_k|\psi(t)\rangle$. SPA explicitly says what states $|\psi(t)\rangle$ and $|\varphi_k\rangle$ are; neither special physical quantities nor viable subspace are necessary for SPA to exist. Physical quantities represented by operators satisfying Equations (6) and (7) have a fundamental status; but as opposed to Bell's beables neither their choices are arbitrary nor they have definite values at all times.

3. A Case Where SPA and OQM Yield Different Experimental Predictions

In this section we shall deal with a case where SPA and OQM yield different experimental predictions. Let us consider a silver atom in the ground state placed in a uniform constant magnetic field $\boldsymbol{B}$. We choose Oz axis along $\boldsymbol{B}$. Let S_z be the operator representing the z-component of the atom's spin $\boldsymbol{S}$. The eigenvectors of S_z corresponding to the eigenvalues $+\frac{\hbar}{2}$ and $-\frac{\hbar}{2}$ will be denoted $|+_z\rangle$ and $|-_z\rangle$ respectively. They satisfy the equations

$$S_z|+_z\rangle=+\frac{\hbar}{2}|+_z\rangle \tag{22}$$

$$S_z|-_z\rangle=-\frac{\hbar}{2}|-_z\rangle \tag{23}$$

$$\langle+_z|-_z\rangle=\langle-_z|+_z\rangle=0 \tag{24}$$

$$\langle+_z|+_z\rangle=\langle-_z|-_z\rangle=1 \tag{25}$$

$$|+_z\rangle\langle+_z|+|-_z\rangle\langle-_z|=\mathcal{J} \tag{26}$$

Let $\boldsymbol{u}$ be a unitary vector defined by the angles ϑ and φ (Figure 1). The operator representing the u-component of $\boldsymbol{S}$ will be denoted S_u. Its eigenvector corresponding to the eigenvalue $+\frac{\hbar}{2}$ satisfies the equation

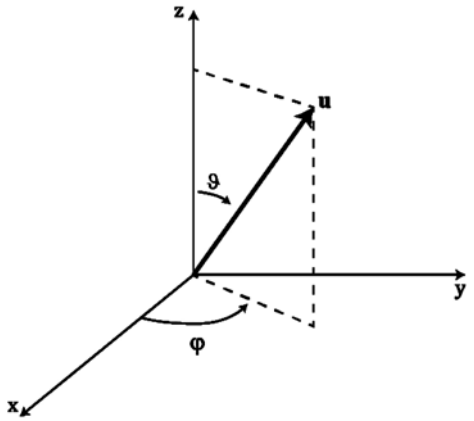

Figure 1. The unitary vector $\boldsymbol{u}$ is defined by the angles ϑ and φ.

$$S_u\left|+_u\right\rangle = +\frac{\hbar}{2}\left|+_u\right\rangle \tag{27}$$

and its expansion on the basis of the eigenvectors of S_z is

$$\left|+_u\right\rangle = \cos\frac{\vartheta}{2}\mathrm{e}^{-i\varphi/2}\left|+_z\right\rangle + \sin\frac{\vartheta}{2}\mathrm{e}^{i\varphi/2}\left|-_z\right\rangle \tag{28}$$

See for instance ([13], p. 395).

We shall refer only to spin states. The Hamiltonian of a silver atom in the ground state placed in a uniform magnetic field is time-independent and can be written

$$\varepsilon = \omega S_z \tag{29}$$

where

$$\omega = -gB \tag{30}$$

is the Larmor frequency, g the gyromagnetic ratio of the silver atom in the ground state and B the modulus of the magnetic field ([13], p. 403). Taking into account Equation (29), the eigenvalue equations of this Hamiltonian can be written

$$\varepsilon\left|+_z\right\rangle = E_+\left|+_z\right\rangle = +\frac{\hbar\omega}{2}\left|+_z\right\rangle \tag{31}$$

$$\varepsilon\left|-_z\right\rangle = E_-\left|-_z\right\rangle = -\frac{\hbar\omega}{2}\left|-_z\right\rangle \tag{32}$$

where E_+ and E_- are the eigenvalues of ε.

Magnetic fields are never completely uniform and the wave functions of atoms always have a certain extension. The Hamiltonian given by Equation (29) is a valid approximation only in cases where the magnetic field can be considered uniform in a region much larger than the region where the wave function of the atom takes on appreciable values; in these cases the eigenvectors of ε coincide with the eigenvectors of S_z. In contrast, if the magnetic field does not fulfill this requirement, the Hamiltonian of the atom is not given by Equation (29) and its eigenvectors do not coincide with the eigenvectors of S_z.

Let the initial state of the atom be $|\psi(0)\rangle = |+_u\rangle$. We shall find the state $|\psi(t)\rangle$ for $t > 0$: 1) assuming the validity of OQM; and 2) assuming the validity of SPA.

3.1. Evolution of the State Vector Assuming the Validity of OQM

This evolution is ruled by the Schrödinger equation, which is a deterministic law. If $|\psi(0)\rangle = |+_u\rangle$, per Equations (28), (31) and (32), the state at time t will be

$$|\psi(t)\rangle = \cos\frac{\vartheta}{2}e^{-i\varphi/2}e^{-i\omega/2}|+_z\rangle + \sin\frac{\vartheta}{2}e^{i\varphi/2}e^{i\omega/2}|-_z\rangle \tag{33}$$

Let $\boldsymbol{w}(t)$ be the unitary vector defined by the angles

$$\Theta(t) = \vartheta \tag{34}$$

$$\Phi(t) = \varphi + \omega t \tag{35}$$

The vector $\boldsymbol{w}(t)$ turns about the Oz axis with the Larmor frequency and spends a time

$$T_L = \frac{2\pi}{\omega} \tag{36}$$

to complete a tour.

Let S_w be the $w(t)$-component of $\boldsymbol{S}$ and $|+_w\rangle$ its eigenvector corresponding to the eigenvalue $+\frac{\hbar}{2}$. On the basis of the eigenvectors of S_z it can be expanded

$$|+_w\rangle = \cos\frac{\vartheta}{2}e^{-i\varphi/2}e^{-i\omega t/2}|+_z\rangle + \sin\frac{\vartheta}{2}e^{i\varphi/2}e^{i\omega t/2}|-_z\rangle \tag{37}$$

The state $|\psi(t)\rangle$ given by Equation (33) coincides with $|+_w\rangle$ ([13], p. 405). In a region where the magnetic field is uniform the atom performs a Larmor precession with frequency ω. In particular, at $t = T_L$, $\boldsymbol{w}(T_L) = \boldsymbol{w}(0) = \boldsymbol{u}$ and $|\psi(T_L)\rangle = |\psi(0)\rangle = |+_u\rangle$.

According to OQM the atom remains in the Schrödinger channel and at time T_L recovers its initial state.

3.2. Possible Changes to the State Vector Assuming the Validity of SPA

In SPA spontaneous processes are not necessarily ruled by a deterministic equation. If the system has the preferential set $\{N_\varphi\}$, it can either remain in the Schrödinger channel or jump to one of its preferential states. Thus, the same initial state $|\psi(0)\rangle$ may give rise to different states $|\psi(t)\rangle$.

Let the condition $0 < \vartheta < \pi$ be satisfied. The set $\{|+_z\rangle, |-_z\rangle\}$ fulfills all the conditions required to be the preferential set of the silver atom in the state $|\psi(t)\rangle$ given by Equation (33); see Section 2.2. A straightforward calculation yields

$$\langle\psi(t)|\varepsilon|\psi(t)\rangle = \left(\frac{\hbar\omega}{2}\right)\cos\vartheta \tag{38}$$

$$\left\langle \psi(t)\left|\varepsilon^2\right|\psi(t)\right\rangle = \left(\frac{\hbar\omega}{2}\right)^2 \tag{39}$$

$$\Delta\varepsilon = \left(\frac{\hbar\omega}{2}\right)\sin\vartheta \tag{40}$$

$$\frac{1}{\tau} = \omega\sin\vartheta \tag{41}$$

As τ is constant, in the time interval $(0,t)$ the atom can either remain in the Schrödinger channel with probability

$$P_S(t) = \mathrm{e}^{-t/\tau} = \mathrm{e}^{-\omega t\sin\vartheta} \tag{42}$$

or decay to one of its preferential states ($\left|+_z\right\rangle$ and $\left|-_z\right\rangle$). If it remains in the Schrödinger channel, at $t = T_L$ it will recover its initial state $\left|+_u\right\rangle$. The corresponding probability is

$$P_S(T_L) = \mathrm{e}^{-T_L/\tau} = \mathrm{e}^{-\omega T_L\sin\vartheta} = \mathrm{e}^{-2\pi\sin\vartheta} \tag{43}$$

According to SPA the probability that the atom will remain in the Schrödinger channel is a decreasing exponential with relaxation time τ. The probability that it will recover its initial state at time T_L decreases when the polar angle ϑ increases.

3.3. Testing OQM vs. SPA Experimental Predictions

In the case of a silver atom in a uniform magnetic field, the experimental predictions of SPA are radically different from those yielded by OQM. This contradiction could be decided by means of the experiment described in (Figure 2).

1) Atoms leaving the oven *O* are collimated and move along the *y*-axis.

2) They are prepared by the filter *F* in the eigenstate $\left|+_u\right\rangle$ of S_u given by Equation (28) with $\varphi = 0$

$$\left|+_u\right\rangle = \cos\frac{\vartheta}{2}\left|+_z\right\rangle + \sin\frac{\vartheta}{2}\left|-_z\right\rangle \tag{44}$$

Atoms in the state $\left|-_u\right\rangle$ are stopped in *F*; for details about how this filter works see ([14], pp. 16-17) [18] [37]. We assume, in addition, that at the exit of *F* the atoms travel with velocity υ.

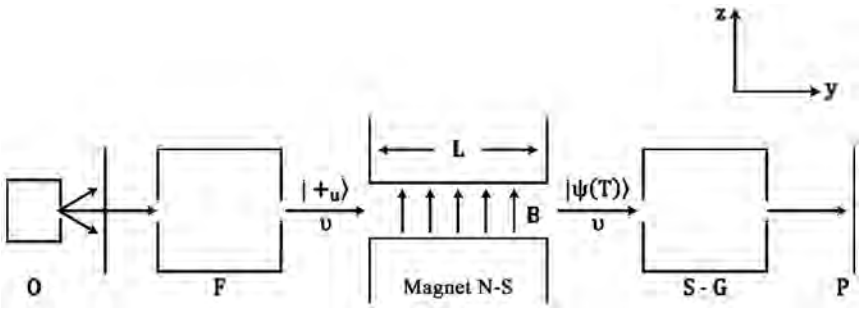

Figure 2. Schematic representation of the eperimental set-up. See text.

3) Atoms so prepared fly through a magnet $N-S$ of length L which generates a uniform magnetic field $\boldsymbol{B}$ pointing along the z-axis. Atoms entering one end of the magnet in the state $|\psi(0)\rangle = |+_u\rangle$ exit the other end in the state $|\psi(T)\rangle$ where

$$T = \frac{L}{\upsilon} \tag{45}$$

is the time an atom spends travelling through the magnet. The velocity of the atoms does not change during their passage through the magnet. By contrast, their spin states change, either as a result of Larmor precession or due to projection to one of their preferential states.

4) A Stern-Gerlach apparatus measures the u-component S_u of the spin $\boldsymbol{S}$ of the atoms in the state $|\psi(T)\rangle$.

5) The impacts of arriving atoms at plate P are recorded.

We shall choose L, υ and ω in such a way that the time T_L required to complete a precession tour equals the time T spent by the atom in the magnet. In other words, we shall impose the condition

$$\frac{L}{\upsilon} = \frac{2\pi}{\omega} \tag{46}$$

At the entrance as well as at the end of the magnet the magnetic field is strongly non uniform. Several authors have assumed that the evolution of a spin in a strongly non uniform magnetic field is ruled by the Schrödinger equation [37] ([38], pp. 593-598). According to SPA this is so if 1) either the atom does not have a preferential set; or 2) the atom has a preferential set, but the time it spends in such a region is so short that it "has no time" to be projected. We shall assume one of these two conditions fulfilled in the experiment just described.

3.3.1. If OQM Is Valid

The atom enters the magnet in the state $|\psi(0)\rangle = |+_u\rangle$. While flying through the magnet it precesses around the z-axis with the Larmor frequency ω, "it never aligns itself with the z-axis" ([14], p. 164). It will remain in the Schrödinger channel and at time T it will recover its initial state $|+_u\rangle$. Therefore, a measurement of S_u yields the result $+\frac{\hbar}{2}$ with certitude whatever the angle ϑ may be (**Figures 3(a)-(c)**).

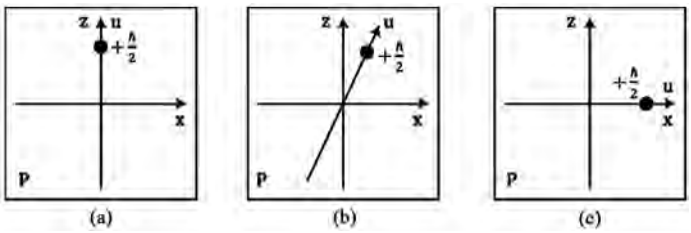

Figure 3. Registers on plate P of the measurement of S_u according to OQM. The result is $+\frac{\hbar}{2}$ with certitude whatever the polar angle may be: (a) $\vartheta \simeq 0$; (b) $\vartheta = \pi/6$; (c) $\vartheta = \pi/2$.

3.3.2. If SPA Is Valid

We assume, as above, that the atom enters the magnet in the state $|\psi(0)\rangle = |+_u\rangle$. When it flies through the magnet there are three possibilities:

1) It remains in the Schrödinger channel and at time T it recovers its initial state. Therefore $|\psi(T)\rangle = |+_u\rangle$.

2) It jumps to the preferential state $|+_z\rangle$ and remains in this state until it leaves the magnet. Therefore $|\psi(T)\rangle = |+_z\rangle$.

3) It jumps to the preferential state $|-_z\rangle$ and remains in this state until it leaves the magnet. Therefore $|\psi(T)\rangle = |-_z\rangle$.

The corresponding probabilities will be respectively denoted $P_S(T)$, $P_{+z}(T)$ and $P_{-z}(T)$. The relation

$$P_S(T) + P_{+z}(T) + P_{-z}(T) = 1 \tag{47}$$

is fulfilled.

A measurement of S_u performed on the atom in the state $|\psi(T)\rangle = |+_u\rangle$ yields the result $S_u = +\frac{\hbar}{2}$ with certitude. By contrast, if the atom is in the state $|\psi(T)\rangle = |+_z\rangle$, the measurement can yield either the result $S_u = +\frac{\hbar}{2}$ or the result $S_u = -\frac{\hbar}{2}$. The same applies for an atom in the state $|\psi(T)\rangle = |-_z\rangle$.

Let $\eta_{+z}\left(+\frac{\hbar}{2}\right)\left[\eta_{-z}\left(+\frac{\hbar}{2}\right)\right]$ be the probability that the measurement yields the result $S_u = +\frac{\hbar}{2}$ if the state of the atom were $|+_z\rangle\left(|-_z\rangle\right)$. The probability that a measurement of S_u yields the result $+\frac{\hbar}{2}$ whatever the state $|\psi(T)\rangle$ be is

$$\wp\left(+\frac{\hbar}{2}\right) = P_S(T) + P_{+z}(T)\eta_{+z}\left(+\frac{\hbar}{2}\right) + P_{-z}(T)\eta_{-z}\left(+\frac{\hbar}{2}\right) \tag{48}$$

and the probability that a measurement of S_u yields the result $-\frac{\hbar}{2}$ whatever the state $|\psi(T)\rangle$ be is

$$\wp\left(-\frac{\hbar}{2}\right) = P_{+z}(T)\eta_{+z}\left(-\frac{\hbar}{2}\right) + P_{-z}(T)\eta_{-z}\left(-\frac{\hbar}{2}\right) \tag{49}$$

with obvious notation. The relation

$$\wp\left(+\frac{\hbar}{2}\right) + \wp\left(-\frac{\hbar}{2}\right) = 1 \tag{50}$$

holds.

The following diagram illustrates the process just described.

$$|\psi(0)\rangle = |+_u\rangle \xrightarrow[\text{The atom goes through the magnet}]{} |\psi(T)\rangle \xrightarrow[S_u \text{ is measured}]{} +\hbar/2 \text{ or } -\hbar/2$$

The probabilities $\wp\left(+\frac{\hbar}{2}\right)$ and $\wp\left(-\frac{\hbar}{2}\right)$ depend on the polar angle ϑ. If

$\vartheta \simeq 0$, the same holds for the inverse of the relaxation time τ; see Equation (41). For $T \ll \tau$, the atom "has no time" to decay to one of its preferential states during its passage through the magnet. The probability that it will remain in the Schrödinger channel is $P_S(T) \simeq 1$. Hence

$$\wp\left(+\frac{\hbar}{2}\right) \simeq 1 \tag{51}$$

$$\wp\left(-\frac{\hbar}{2}\right) \simeq 0 \tag{52}$$

(Figure 4(a)). In this case the difference between SPA and OQM predictions is irrelevant.

When ϑ increases, the relaxation time τ and the probability $P_S(T)$ decrease and the sum $P_{+z}(T)+P_{-z}(T)$ increases, see Equations (41), (43) and (47). If the experiment is performed with a beam of atoms, the number of atoms abandoning the Schrödinger channel and exiting the magnet either in the state $|+_z\rangle$ or in the state $|-_z\rangle$ increases with ϑ.

A measurement of S_u performed on an atom in the state $|+_z\rangle$ may yield either the result $+\frac{\hbar}{2}$ or the result $-\frac{\hbar}{2}$; the same holds for an atom in the state $|-_z\rangle$. As the probability $\wp\left(-\frac{\hbar}{2}\right)$ increases, the probability $\wp\left(+\frac{\hbar}{2}\right)$ decreases; see Equation (50). Plate P registers the impacts corresponding to both results (Figure 4(b)).

If $\vartheta = \pi/2$, the probability that the atom will remain in the Schrödinger channel during its flight through the magnet is almost null. As $P_S(T) \simeq 0$, the sum $P_{+z}(T)+P_{-z}(T) \simeq 1$. Taking into account Equation (44), it is easily concluded that

$$P_{+z}(T) \simeq P_{-z}(T) \simeq \frac{1}{2} \tag{53}$$

If the atoms enter the magnet in the state $|\psi(0)\rangle = |+_u\rangle$, almost a half of them will decay to $|+_z\rangle$ and the other half will decay to $|-_z\rangle$ while flying through the magnet. A measurement of S_u performed on an atom in the state $|+_z\rangle$ may yield either the result $+\frac{\hbar}{2}$ or the result $-\frac{\hbar}{2}$ with the same probability. This assertion is also valid if the state of the atom is $|-_z\rangle$. As

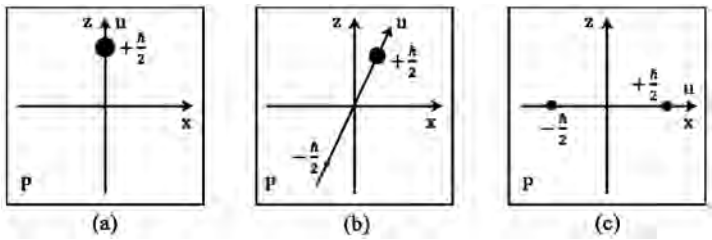

Figure 4. Registers on plate P of the measurement of S_u according to SPA. The results depend on the polar angle: (a) $\vartheta \simeq 0$; (b) $\vartheta = \pi/6$; (c) $\vartheta = \pi/2$.

$$\wp\left(+\frac{\hbar}{2}\right)\simeq\wp\left(-\frac{\hbar}{2}\right)\simeq\frac{1}{2} \tag{54}$$

the intensity of the traces on plate P corresponding to both results will be very similar (**Figure 4(c)**).

3.3.3. SPA Vs. OQM: Which One Is Valid (If Any)?

Taking into account the previous analysis we can assert that:

1) either all the atoms hit the same point on plate P (which depends on the polar angle ϑ), as shown in **Figure 3**; or

2) the atoms make impact in one of the two opposite points on plate P as shown in **Figure 4**; here the positions of the opposite points depend on the polar angle and the rate between the number of impacts corresponding to the eigenvalues $-\frac{\hbar}{2}$ and $+\frac{\hbar}{2}$ of S_u grows with ϑ.

In the first case we should conclude that when flying through the magnet $N-S$ no atoms abandon the Schrödinger channel. *The predictions of OQM would be confirmed*. In the second case we should conclude that when flying through the magnet $N-S$ some atoms do abandon the Schrödinger channel, the number of them exiting the magnet $N-S$ increases with the polar angle and takes a maximum for $\vartheta=\pi/2$. *The predictions of SPA would be confirmed*.

4. Discusion and Conclusions

John Bell points out: "In the beginning natural philosophers tried to understand the world around them. Trying to do that they hit upon the great idea of contriving artificially simple situations in which the number of factors involved is reduced to a minimum. Divide and conquer. Experimental science was born. But experiment is a tool. The aim remains: to understand the world. To restrict quantum mechanics to be exclusively about piddling laboratory operations is to betray the great enterprise. A serious formulation will not exclude the big world outside the laboratory" [20].

OQM is fine for all practical purposes. But besides excluding the big world outside the laboratory, its formulation lacks precision. The central notions of system, apparatus and measurement are neither included as primitive concepts nor defined in the theory. To circumvent this ambiguity—says Bell—discretion and good taste (born from experience) are needed ([39], p. 160). It would be perhaps possible to improve OQM by replacing these ambiguous notions. "However, the idea that quantum mechanics, our most fundamental physical theory, is exclusively even about the results of experiments would remain disappointing" [20].

SPA is a version of quantum theory grounded on philosophical realism. It is not about the results of experiments; it talks about what happens [16]. It has been precisely formulated [12]. The notion of system is introduced as a primitive concept and those of apparatus and measurement are not included in its formulation. Spontaneous and measurement processes are treated on the same

footing [16]. In SPA transitions to the continuum are spontaneous processes. The expressions of the probability density per unit interval of energy resulting from SPA and from OQM treatments coincide approximately and Fermi's golden rule is obtained [15].

In the framework of OQM, it is agreed that time-dependent perturbation theory (TDPT) must be used for solving *all* problems involving time, including spontaneous time-dependent processes. We have questioned TDPT on the following grounds: accounting for *spontaneous* time-dependent processes requires the application of a law (the projection postulate) which is not valid in such processes [40]. In the same direction, contradictions reminiscent of Zeno's paradoxes of motion have been pointed out [41]. By contrast, SPA has no relation with TDPT. Hence it does not confront these issues.

According to SPA the Schrödinger equation not only rules processes where the system has no preferential set, but it also rules most processes where the system does have a preferential set. Spontaneous projections seldom occur. It is worth noting that spontaneous projections and projections resulting from OQM measurements share several traits. In particular, the mathematical expressions for the corresponding probabilities are quite similar; see Section 2.3.

The rule forcing the state vector to remain continuous as long as no measurements are performed poses a serious problem for OQM. By contrast, assuming that spontaneous projections are natural processes, SPA succeeds in stopping the endless ramifications resulting from Schrödinger evolution; see Section 2.4. Hence if SPA is valid there should be no paradoxes such as that of Schrödinger's cat.

SPA exhibits several advantages over OQM, but OQM enjoys the prestige of old age. In order to put both theories to the test, in this paper we suggest an experiment where at least one of them should fail. We study the behavior of a silver atom, initially in an eigenstate of the u-component of the spin, placed in a uniform magnetic field.

Assuming the validity of OQM, in Section 3.1 we find the state of the atom at a certain time T_L.

Assuming the validity of SPA, in Section 3.2 we find the possible states of the atom at the same time T_L.

In this particular case, the experimental predictions of SPA are radically different from those yielded by OQM. The resulting contradiction could be decided by means of the experiment described in Section 3.3.

Until today OQM experimental predictions seem to have no exceptions. Should the experiment mentioned yield the results predicted by SPA, it would be the first time that OQM experimental predictions fail.

Acknowledgements

We are grateful to Professors D.R. Bes, J.C. Centeno, F.G. Criscuolo, C.A. Fernández Bareilles and F. Laloë for fruitful discussions. We are indebted to Professor D. A. Morales for a critical review of the manuscript. We thank

Mariana Delbue for her help with stylistic matters and Carlos Valero for his assistance with the figures and the transcription of the manuscript into LaTex.

Conflicts of Interest

The author declares no conflicts of interest regarding the publication of this paper.

References

[1] Burgos, M.E. (1987) *Foundations of Physics*, **17**, 809-812. https://doi.org/10.1007/BF00733269

[2] Einstein, A. (1931) James Clerk Maxwell: A Commemoration Volume. Cambridge University Press, Cambridge.

[3] Bunge, M. (1985) Treatise on Basic Philosophy, Vol. 7, Philosophy of Science & Technology. D. Reidel Publishing Company, Dordrecht, Boston, Lancaster.

[4] Dirac, P.A.M. (1958) The Principles of Quantum Mechanics. Clarendon Press Oxford, Oxford. https://doi.org/10.1063/1.3062610

[5] von Neumann, J. (1932) Mathematische Grundlagen der Quantenmechanik. Springer, Berlin.

[6] Tegmar, M. and Wheeler, J. (2001) *Scientific American*, **284**, 54-61. https://doi.org/10.1038/scientificamerican0201-68

[7] Jammer, M. (1974) The Philosophy of Quantum Mechanics. John Wiley & Sons, New York.

[8] Peres, A. (1993) Quantum Theory: Concepts and Methods. Kluwer Academic Publishers, Dordrecht.

[9] Peres, A. (1985) *Foundations of Physics*, **15**, 201-205. https://doi.org/10.1007/BF00735292

[10] Petersen, A. (1963) *Bulletin of the Atomic Scientists*, **19**, 8-14. https://doi.org/10.1080/00963402.1963.11454520

[11] Burgos, M.E. (1998) *Foundations of Physics*, **28**, 1323-1346. https://doi.org/10.1023/A:1018826910348

[12] Burgos, M.E. (2018) *JMP*, **9**, 1697-1711. https://doi.org/10.4236/jmp.2018.98106

[13] Cohen-Tannoudji, C., Diu, B. and Laloë, F. (1977) Quantum Mechanics. John Wiley & Sons, New York, London, Sydney, Toronto.

[14] Bes, D.R. (2004) Quantum Mechanics. Springer, Berlin. https://doi.org/10.1007/978-3-662-05384-3

[15] Burgos, M.E. (2008) *Foundations of Physics*, **38**, 883-907. https://doi.org/10.1007/s10701-008-9213-5

[16] Burgos, M.E. (2015) The Measurement Problem in Quantum Mechanics Revisited. In: Pahlavani, M., Ed., *Selected Topics in Applications of Quantum Mechanics*, INTECH, Croatia, 137-173. https://doi.org/10.5772/59209

[17] Burgos, M.E. (2010) *JMP*, **1**, 137-142. https://doi.org/10.4236/jmp.2010.12019

[18] Burgos, M.E. (2015) *JMP*, **6**, 1663-1670. https://doi.org/10.4236/jmp.2015.611168

[19] Born, M. (1971) The Born Einstein Letters, Letters 50, 53 and 81. The Mcmillan Press Ltd., London.

[20] Bell, J.S. (1990) *Physics World*, **3**, 33-40. https://doi.org/10.1088/2058-7058/3/8/26

[21] Laloë, F. (2001) *American Journal of Physics*, **69**, 655-701. https://doi.org/10.1119/1.1356698

[22] Ballentine, L.E. (1970) *Reviews of Modern Physics*, **42**, 358-381. https://doi.org/10.1103/RevModPhys.42.358

[23] Ballentine, L.E. (1972) *American Journal of Physics*, **40**, 1763-1771. https://doi.org/10.1119/1.1987060

[24] Bohm, D.A. (1952) *Physical Review*, **85**, 166-179. https://doi.org/10.1103/PhysRev.85.166

[25] Bohm, D.A. (1952) *Physical Review*, **85**, 180-193. https://doi.org/10.1103/PhysRev.85.180

[26] Everett, H. (1957) *Reviews of Modern Physics*, **29**, 454-462. https://doi.org/10.1103/RevModPhys.29.454

[27] Wikipedia, The Free Encyclopedia: Many-Worlds Interpretation.

[28] Griffith, R.B. (1984) *Journal of Statistical Physics*, **36**, 219-272. https://doi.org/10.1007/BF01015734

[29] Omnès, R. (1988) *Journal of Statistical Physics*, **53**, 893-932. https://doi.org/10.1007/BF01014230

[30] Zurek, W. (1991) *Physics Today*, **44**, 36-44. https://doi.org/10.1063/1.881293

[31] Zurek, W. (2003) *Reviews of Moders Physics*, **75**, 715-775. https://doi.org/10.1103/RevModPhys.75.715

[32] Ghirardi, G.C., Rimini, A. and Weber, T. (1986) *Physical Review D*, **34**, 470. https://doi.org/10.1103/PhysRevD.34.470

[33] Ghirardi, G.C., Rimini, A. and Weber, T. (1987) *Foundations of Physics C*, **18**, 1-27. https://doi.org/10.1007/BF01882871

[34] Bell, J.S. (1984) *CERN-TH*, **4035**, 159-166. https://doi.org/10.1142/9789812386540_0017

[35] Sudbery, A. (1984) *Annals of Physics*, **157**, 512-536. https://doi.org/10.1016/0003-4916(84)90070-8

[36] Sudbery, A. (2002) *Studies in History and Philosophy of Science. Part B: Studies in History and Philosophy of Modern Physics*, **33**, 387-411. https://doi.org/10.1016/S1369-8486(02)00003-1

[37] Feynman, R.P., Leighton, R.B. and Sands, M. (1963) Lectures on Physics, Vol. III. Addison-Wesley, Reading, Chapter 5.

[38] Bohm, D.A. (1951) Quantum Theory. Prentice-Hall, Princeton.

[39] Bell, M., Gottfried, K. and Veltman, M. (2001) John S. Bell on the Foundations of Quantum Mechanics. Word Scientific, Singapore. https://doi.org/10.1142/4757

[40] Burgos, M.E. (2016) *JMP*, **7**, 1449-1454. https://doi.org/10.4236/jmp.2016.712132

[41] Burgos, M.E. (2017) *JMP*, **8**, 1382-1397. https://doi.org/10.4236/jmp.2017.88087

Journal of Modern Physics, 2019, 10, 1209-1221
https://www.scirp.org/journal/jmp
ISSN Online: 2153-120X
ISSN Print: 2153-1196

Categories of Nonlocality in EPR Theories and the Validity of Einstein's Separation Principle as Well as Bell's Theorem

Karl Hess

Center for Advanced Study, University of Illinois, Urbana, IL, USA
Email: karlfhess@gmail.com

How to cite this paper: Hess, K. (2019) Categories of Nonlocality in EPR Theories and the Validity of Einstein's Separation Principle as Well as Bell's Theorem. *Journal of Modern Physics*, **10**, 1209-1221.
https://doi.org/10.4236/jmp.2019.1010080

Received: August 26, 2019
Accepted: September 9, 2019
Published: September 12, 2019

Abstract

Work on quantum entanglement is currently emphasizing the nonlocal nature of theories that attempt to explain spatially separated Einstein-Podolsky-Rosen (EPR) correlation experiments. It is frequently claimed that nonlocal instantaneous influences, or equivalently a breakdown of Einstein's separation principle, are a signature property of (quantum) entanglement. This paper presents a categorization of the various forms of nonlocality in physical theories. It is shown that, even for Einstein's theory of relativity, correlations of spatially separated measurements cannot be explained without the involvement of some nonlocal or global knowledge and facts. Instantaneous Influences at a distance are, however, in a special category of nonlocality and, as is well known, Einstein called them spooky. Following a separation of nonlocalities into four distinctly different categories 0, 1, 2, 3, with number 3 corresponding to theories containing instantaneous influences at a distance, I show that any theory of EPR experiments must be at least in category 1 or 2 and does not need to be in category 3. In particular, the Bell theorem, valid for category 0 theories, may be violated for categories 1 and 2 and does not require category 3 theories. Category 0 enforces Bell's theorem. However, it does not apply to relativistic theories of space like separated measurements.

Keywords

Bell's Theorem, Einstein's Separation Principle, EPRB Experiments

1. Introduction

The EPR Gedanken-experiments [1] were originally designed to show that quantum mechanics is either involving velocities higher than the speed of light in va-

cuum or is incomplete. Such experiments were later suggested by Bohm (EPRB), in a specific form, for correlated particles with spin and measurements with Stern-Gerlach magnets. The experiments have actually been performed with optical polarizers measuring correlated (commonly called entangled) photon pairs.

The incompleteness of quantum mechanics was suspected by Einstein, because of the possible existence of hidden variables in the theory of EPR experiments. However, John Stuart Bell [2] claimed that he could prove that no hidden variables can exist in any EPR-type theory that uses exclusively the physics of Einstein as opposed to quantum theory. (Bell used actually the phrase "classical physics" instead of the "physics of Einstein". The term "classical physics" is, however, not clearly defined and usually refers to physics that violates the Uncertainty Principle. Such violations are not permitted in the EPR Gedanken-experiment, which was constructed in a way to avoid violations of this established quantum principle.)

As a consequence of Bell's denial of the existence of hidden variables, the EPR logic leads necessarily to some violations of the limiting nature of the speed of light. This fact was only reluctantly accepted even by Bell himself, but is now accepted by a significant majority of the physics community who believes that entanglement does just that. It is widely assumed that instantaneous influences are exerted over arbitrary large distances between entangled particles or equivalently that entangled particles exhibit a "quantum nonlocality". They cannot be entirely separated but carry with them some properties that are rigidly connected to each other irrespective of space-like distances. Thus, Einstein's separation principle that is the basis of the EPR paper [1] is said to be violated by entanglement.

However, no experimental proof of instantaneous influences (or a violation of Einstein's separation principle) has ever been provided for any given entangled-particle-pair measurement. Nor can it ever be provided, because of the random outcome of the single measurement events. Any proof of instantaneity for a given pair would necessarily involve instantaneous information transfer at a distance, which contradicts the theory of relativity. Such possibility is indeed entertained by many science writers.

Experts on EPR questions, however, point to Bells theorem and to statistical experiments involving significant distances to justify their acceptance of such instantaneous influences. However, as we will see, Bells theorem depends sensitively on the actual meaning of the words "quantum nonlocality" as opposed to "local", words that are used when stating what the theorem means. A stalemate usually occurs at this point of discussions, because most of Bell's followers claim that the word "quantum nonlocality" is of a nature unknown to our macroscopic world and we can, therefore, not find any valid analogies about it.

It is the purpose of this paper to show that "nonlocalities" in physical theories (including Bell's) may be subdivided into 4 categories. The Bell theorem of the non-existence of hidden variables is shown to be valid in category 0 but may be violated in categories 1, 2 and 3. Only the theories of category 3 violate Einstein's

separation principle. This means that the Bell theorem is not sufficient to guarantee membership of any EPR theory in category 3.

2. Illustrations of the Nonlocal Content in Physical Theories

As the first example for nonlocal content consider Einsteins special relativity and corresponding experiments: we must assume that the speed of light in vacuum is the same everywhere in empty space. This nonlocal (global) knowledge is a postulate of special relativity. Furthermore and most importantly, any observable physical events in different macroscopic inertial systems are linked by their relative velocity and their theory must, therefore, involve nonlocal knowledge.

As a second example consider EPRB-type experiments and corresponding theories, which are about macroscopically detecting separate and distant measurement events corresponding to entangled pairs emanated from a common source. We encounter here the difficult task of asserting experimentally and theoretically which of the single detections have indeed originated from entangled pairs. The difficulties of this task arise because of the existence of quantum fluctuations that influence all measurements related to atomic and subatomic phenomena. This difficult task of pairing the single outcomes is the last step of the data formation process in EPRB experiments, which must produce data for the products of two distant measurement outcomes. That last step involves nonlocal knowledge and facts; a crucial point that is usually ignored.

It appears then that correlations of space-like separated measurements cannot be understood by a completely local theory, nor is the process of data formation completely local. However, Bell stated himself the following about the meaning of his **Theorem**: "But if [a hidden variable theory] is local it will not agree with quantum mechanics, and if it agrees with quantum mechanics it will not be local. This is what the [Bell] Theorem says".

Bell refers, of course, to the quantum mechanics of EPRB experiments and to experimental results that agree to a very good approximation with that quantum mechanics. Proving the Theorem involves a mathematical inequality [2] that contradicts quantum mechanics.

As we just have seen, all theories and experiments of spatially separated events must involve some nonlocal knowledge. Why, then, did Bell need a mathematical inequality to prove what he claims "the Theorem says"? The contradictions to Bells inequality [2] and similar Bell-type inequalities are the crux of Bells claim. One could restate Bells explanation of the meaning of his **Theorem** by:

"But if [a hidden variable theory] is local, it will obey Bell-type inequalities, and if it agrees with quantum mechanics it will not be local."

The above examples show, however, that nonlocal (global) knowledge is indeed involved in any non-trivial theory of correlations of separated systems and events. All EPRB-experimenters rely on some form of post-processing, which accomplishes the bringing together of the results of the single measurements and in itself requires a nonlocal knowledge of facts. Nonlocal (global) knowledge must be contained in any specific labelling of the experimental data that is used

for the pairing of distant events.

We must, therefore, ask what precisely the word "local" means in Bells theorem. Why is it not clear without any inequality and theorem that some nonlocality is involved in both theory and experimental data as soon as we talk about space-like separated measurements and their correlations? What kind of nonlocality did Bell actually identify by his inequality and why should this fact have any special significance? There also exist numerous text-book tutorials involving the two characters Alice and Bob, who have exclusively local knowledge and try to explain EPRB experiments. How can they work without any nonlocal knowledge and again what does nonlocal mean?

In order to answer these questions with precision, I propose the following categorization of local and nonlocal theories.

3. Categories of Nonlocality

I wish to define four mutually exclusive categories of locality or nonlocality of theories that correlate space-like distant events:

- **Category 0**: Any physical theory that exclusively uses local knowledge of facts and data that are immediately available to the local experimenters and only to them.
- **Category 1**: Any physical theory that uses nonlocal (global) knowledge of facts, which is precisely the same than (or physically equivalent to) the nonlocal (global) knowledge of facts that the formation and labeling of the experimental data necessarily involves. This category includes theories that consider the experimental processing of data, which originally have been obtained at two or more different locations, for the purpose of comparison.
- **Category 2**: Any physical theory that uses nonlocal (global) knowledge of facts beyond that of category 1 but is itself not contained in the theory-sets of category 3.
- **Category 3**: Any physical theory that involves a measurement event at one location that determines instantaneously the outcome of a measurement event at a space-like separated location. Both measurements must be related to two or more physical entities (such as electrons or photons) that are "nonlocally connected". The words "nonlocally connected" mean that the physical entities violate Einstein's separation principle as defined in [1]. This nonlocal connection is currently thought to describe the nature of entanglement.

As shown in the next section, categorizing the main theories of physics, including relativity and quantum mechanics, suggests the following epistemological acceptability of categories:

Theories of category 0 and 1 that are used to describe correlations of distant measurement events are entirely acceptable. Correlations of measurement events described by category 2 are acceptable, but call for investigations to transform the theory into category 1. Category 3 theories are the only theories that use nonlocal "knowledge" that is not exclusively about macroscopically measurable

facts. Therefore, theories of category 3 are not of the type that Mach found appropriate and venture into the realm of what Einstein called spooky. They can only be accepted if there is no viable theoretical path in categories 0, 1 and 2.

It was already discussed above and is illustrated in more detail below that there exist no nontrivial category 0 theories of correlations between space-like separated measurements. It will also be shown that the Bell theorem, which is clearly valid for category 0 theories, may be violated in theories of all other categories and does, therefore, not specifically require a theory of category 3.

4. Examples to Illustrate the Nonlocality-Categories

As a first example that illustrates nonlocal categories take Newtons theory of gravitation. This theory assumes an instantaneous gravitational force acting between the sun and planets. The experiments that attempt to confirm this theory, however, are all performed by optical observations, which have the speed of light in vacuum as upper limit. Newtons theory is, therefore neither of category 0 nor of category 1. Simplified model systems such as point-masses and a fixed sun may be put into category 2, with category 3 being a possibility that cannot necessarily be excluded for more complex models. Einstein transformed the theory of gravitation into category 1. The recent measurements of gravitational waves gave a brilliant confirmation to this fact.

Take as another example an experiment from Einsteins special relativity. Alice and Bob are flying in two separate spaceships. Each of their spaceships contains an identical clock fabricated before departure. Einsteins special relativity gives the theory of the clock-times that Alice and Bob may determine by measurements and observations. We do not need to repeat here Einsteins solution, which is given in many elementary texts. The theory uses only the global knowledge found by all actual experiments and that forms the basis of the experiments: the velocity of light in vacuum and the global validity of the same physical law independent of the uniform motion of the systems in question. Thus, according to our postulate, there is no need to suspect spooky influences. However, it is also clear that Alice and Bob could not determine the clock correlations without knowing anything of each other. The requirement of category 0 to use exclusively knowledge that is locally available to them also excludes the relative velocity of the other spaceship and the identity of the velocity of light in vacuum at all spatially separated locations. Membership in category 0 thus prevents any meaningful theory of clock rates that Alice and Bob would observe. For example, how could they form a theory for the probability that both clocks are pointing to times in the first quarter (12 - 3) without knowing anything about the other spaceship? How could they predict the clock-times when the spaceships are finally brought together again (compare to post-processing of data)? Actual measurements of the relative velocity of the other spaceship permits the explanation of the clock-times by a category 1 theory as Einstein has shown.

Many body quantum theory, our third example, is very complex. It certainly cannot be placed into category 0. Some quantum physics has used global gauge

fields, which would correspond to category 2 frameworks. Modern teachings tell us how global gauge fields may be promoted to local ones and put the theory into category 1, which is commensurate with the Machian design of quantum mechanics by some of its fathers. However, many researchers of the quantum entanglement area and all science writers, have moved quantum mechanics into category 3 on the basis of Bell's theorem; incorrectly as we will see.

5. Nonlocal Relativistic Factors Involved in EPRB Theories (Models)

From the above examples, we can deduce that the postulate of exclusively local knowledge (category 0) prevents Alice and Bob to find any relativistic theory of clock-rates in spaceships. Relativistic theories necessarily depend on the velocity of both spaceships (the relative velocity of the spaceships to each other). The return and reuniting of the spaceships involves also nonlocal factors. However, Einsteins relativity is clearly of category 1, because the relative velocity and the return of the spaceships are part of the experiments and the process to obtain the data (compare to post-processing of data in EPRB experiments).

It is worthwhile to note that the relativity of events in two or more space-like separated locations, taken in its most basic meaning of the word "relative", necessarily involves nonlocal facts. However, the relativity of space-like separated events does not mean that Einstein's separation principle is violated. Take for example a double-barrel that shoots bullets into two directions. The bullets hit wooden planks with different thickness and strength in two separate locations. The bullets are detected if and only if they break through the wooden planks. The question of how many pairs of bullets break through the planks on average cannot be theorized about if one does not know the thickness of the planks on both sides. Therefore, a theory of category 0 cannot explain this elementary experiment. (As an aside, the probability for both bullets of a pair to break through planks with different thickness is, in general, not equal to the product of the single probabilities to break through on the respective side (equality being a signature feature of Bell-type proofs.)

Deeper relativistic aspects come to light if we consider the actual interactions of the particles with the measurement equipment. Consider spin $\frac{1}{2}$ particles interacting with Stern-Gerlach magnets and attempt to explain the interaction in terms of Einstein's physics (we defer the quantization to a later choice of the range of possible experimental outcomes).

The single particles approaching the Stern-Gerlach magnet system obey a symmetry by rotations of 4π, while the macroscopic magnet-symmetry is for rotations by 2π. The total system of entangled pairs (in the singlet state) plus magnets has also a 2π rotational symmetry. Each single collision in the separate EPRB wings involves relativistic interactions of the incoming single particles (4π rotational symmetry) with those of the equipment (2π symmetry). Because of the existence of the (2π) rotational symmetry of the system as a whole, there must be

some "connection" for the macroscopic outcomes of the two separate single collisions that is noticeable over longer time periods. This connection must reflect, on average, the symmetry of the whole system (rotations by 2π).

If one aims, however, for a more detailed description of the measurement outcomes (data) including the single collisions, it is not sufficient to consider only the symmetry of the whole system. One needs then to consider the dynamics of the single collisions on each side and, in addition, a space-time correlation for the pair-outcomes describing the remnants of the overall symmetry "carried" by the single particles. A model of the single measurements on both sides that just includes the magnet directions without any trace of the space-time dynamics is certainly oversimplified. Even a very simple model of such a complex situation cannot work with a description that considers exclusively, in a dice-game-like manner, space-like entities. Any model that attempts to provide some realistic (if the word is permitted) description of the measurement outcomes needs at least to include some remnants of the space-time dynamics such as the measurement times in the laboratory system, as I have emphasized in several previous publications. The measurement time then carries the significance of representing the hidden or rather suppressed variable.

But what about Bell, who claims to have proven with his inequalities that hidden variables do not exist. Here lies one of my major points. Measurement times cannot and must not be included in Bell's theory. Walter Philipp and I have proven a theorem (theorem 2 in reference [3]) that means the following: Bell-type inequalities may be and even must be violated, if Bell's functions depend on the measurement times in addition to the magnet (polarizer) directions.

The quantum mechanical treatment has eliminated the use of space-time related effects for the single outcomes, because it does not consider the single outcomes and it uses the rotational symmetry of the whole system (2π) to calculate the averages over many experiments. The detailed dynamics of single particle equipment interactions are of no concern for what one can calculate, much to the advantage of the quantum theory. For interpretational questions, however, one must include invariably space-time, or equivalent concepts, in a more detailed way, because the macroscopic world of the data is currently only understandable in space-time or at least space and time. No better substitute has been offered yet. Space-time emerges, thus, as the "hidden" or rather suppressed variable. Its partial suppression in quantum theory permits us to "shut up and calculate".

6. Nonlocal Facts and Labeling of EPRB Measurement Data

To answer the question into which category theories of EPRB experiments may belong we need to know also nonlocalities that are necessarily used to label the data of these experiments.

Discussions of EPRB experiments frequently involve arguments with the two characters Alice and Bob that may be located arbitrarily far away from each other. They know everything about quantum physics and EPRB experiments but

they do not know anything about each other, because of the arbitrarily large distance between them, which may be light years. They must be able, however, to take data characterizing the EPRB measurements and label them. To be concrete, we consider the modern experiments of groups (e.g. [4]) that often use optical fibers to transmit and detect the single signals corresponding to photon pairs emanating from a common source and being detected after passing polarizers.

We assume here for the sake of argument that we have very long fibers, thousands of kilometers to each side so that a whole experimental sequence of measurements on many single pairs may be completed before Alice or Bob could obtain any information from each other. Alice and Bob, therefore, know nothing about each others measurements and have performed all their measurements independent from the other side. These measurements are taken with two randomly different polarizer directions denoted by unit vectors, $\boldsymbol{a}$ and $\boldsymbol{d}$ at Alice's location and $\boldsymbol{b}$ and $\boldsymbol{c}$ at Bob's, respectively. (Bells original theory deals with the special case $\boldsymbol{d} = \boldsymbol{b}$.)

Thus, we assume that Alice has been given the end of an optical fiber and a polarizer that measures the transmission of single photons from that fiber-end for a certain polarizer direction that Alice denotes e.g. by unit radius vectors $\boldsymbol{a}$ or $\boldsymbol{d}$ using her own coordinate system. Bob does the same with polarizer settings $\boldsymbol{b}$ or $\boldsymbol{c}$ defined in his respective coordinate system. They both create data when their detectors click and label the clicks with their own polarizer direction vector. (One can imagine an analogous experiment with spin 1/2 particles and Stern-Gerlach magnets.)

The goal of these EPRB experiments is to determine the frequency (related to the probability) of common clicks for the 4 different given setting pairs $\boldsymbol{a}, \boldsymbol{b}$; $\boldsymbol{a}, \boldsymbol{c}$; $\boldsymbol{d}, \boldsymbol{b}$ and $\boldsymbol{d}, \boldsymbol{c}$, in order to use these data to perform a so called Bell-test [4]. This determination is, as discussed above, impossible without the knowledge of further global facts. Assume for the moment, however, that we somehow are able to correctly pair detector clicks in the respective stations using a common vector space for the polarizer or magnet directions. Then we obtain certain frequencies and corresponding probabilities for each of the different polarizer-setting pairs.

Is it then possible to obtain the probabilities for detector clicks in both stations and compare them with the quantum result? The answer is no! We are still missing an important piece of information, because we do not know how the fibers have changed the polarization. To find this polarization change, we need to know for which pairs of polarizer settings all entangled pairs produce either a certain double click thus showing complete correlation (or equivalently anti-correlation as discussed in Bells original papers [2]). Knowledge of this latter fact is also an important part of Bells theory. Without this knowledge of the polarizer settings and detector ordering for complete correlation (or anti-correlation), neither Bells theory nor quantum theory can be related to the measurement results. How can Alice and Bob obtain this knowledge and label the data correspondingly? A relatively easy way is for Alice to take one setting-vector in

station one, say $\boldsymbol{a}$, and search in station 2 for the setting vector $\boldsymbol{a}^*$ that always leads to detector clicks when a click for $\boldsymbol{a}$ is obtained. This can, of course, only be achieved by letting Alice and Bob work together and know the outcomes of both stations, which represents a highly nonlocal procedure. To be complete, we also need to determine $\boldsymbol{d}^*$ as well as $\boldsymbol{b}^*$ and $\boldsymbol{c}^*$.

If we like to include the additional complication of quantum fluctuations and very large distances, we need to let Alice and Bob use certain additional tools, e.g. correlated clocks, in order to determine which of the clicks likely belong to pairs; or we need to invoke other additional global knowledge such as global thresholds. We can see from this discussion that nonlocality cannot easily be banned from the physics of correlations and we need a clear definition of which type of nonlocality is spooky as Einstein called it, and not scientifically permitted, and which type is permitted and must even be used to exorcise the spook and to demonstrate a natural correlation (or even causation).

7. Analytical Form of EPRB Theories of Category 3

EPRB theories that embrace Einstein's relativity and address separate measurements of entangled (or just correlated) pairs use the functions $A(\boldsymbol{j},\cdots)$ in one wing of the EPRB experiment and $B(\boldsymbol{j}',\cdots)$ in the other. The variable $\boldsymbol{j}$ may assume, for example, the values $\boldsymbol{a}$, $\boldsymbol{d}$ and $\boldsymbol{j}'$ may assume the values $\boldsymbol{b}$, $\boldsymbol{c}$. The domain of the functions includes thus a variable representing the magnet (or polarizer) settings and other variables that do not necessarily represent numbers but may represent more complex elements of physical reality such as space-time or objects in space-time.

The co-domain (range) of the functions is frequently taken as some outcome of spin-measurements such as up (+1) or down (−1) (quantization). However, it is clear that "up" is only well defined with respect to a given magnet (polarizer) setting and needs, from a more strict point of view, further labeling when multiple magnet (polarizer) settings are involved. It is not at all a priori clear whether or not "up (+1)" with an $\boldsymbol{a}$ direction of the magnet is physically or mathematically the same as "up (+1)" for a $\boldsymbol{b}$ direction of the magnet when multiple measurements with multiple magnet directions are involved. We do not address this point in most of the following discussions, but instead refer below to a publication that deals with complexities of the co-domain. Our main interests are related to questions regarding the domain of the functions A, B.

We ask ourselves the question whether there are distinct properties of the domain that signify the presence of instantaneous influences at a distance (a violation of Einstein's separation principle). The answer to this question is as follows.

The functions $A(\boldsymbol{j},\cdots)$ indicate the presence of instantaneous influences at a distance, or equivalently a breakdown of Einstein's separation principle, if and only if they are equivalent to functions $A'(\boldsymbol{j},\boldsymbol{j}',\cdots)$ *i.e.* functions that include explicitly the variable corresponding to the magnet settings of the other wing of the EPRB experiment. Obviously this condition is sufficient to describe an in-

stantaneous dependence on the magnet (polarizer) setting of the other side. It is also necessary, because otherwise no instantaneous change of the outcome value of A depending on magnet position can be achieved. Analogous reasoning applies for the functions B.

8. Category 1 and 2 EPRB Theories

In contrast to the immediately identifiable mathematical form of nonlocal category 3 theories, one cannot find a straightforward way to determine which mathematical form of functions puts the theory clearly into nonlocal category 1 or 2. The mathematical signatures of general global (nonlocal) knowledge that may be used in EPRB theories are numerous. Such signatures may be present in both domain and codomain of the functions. They also may shape the graph of the function and no specific and succinct criterium can be given for the function-forms that A, B must assume to be in nonlocal categories 1, 2 without detailed investigations of the involved specific physics.

Membership in a particular category other than 3 and 0 may only be deduced by extended physical reasoning. For example, the equipment settings $\boldsymbol{a}^*$ and $\boldsymbol{d}^*$ that guarantee the complete anti-correlation to the outcomes with Alices settings $\boldsymbol{a}$ and $\boldsymbol{d}$, respectively, must be known by Bob in order to properly label his measurement results. Therefore, a corresponding theory using Bobs nonlocal labeling belongs still to nonlocal category 1.

These complexities have impeded the detailed modeling of EPRB experiments by category 1 and 2 EPRB theories. However, several such theories are available in the literature and four examples are given in this section by pointing to references. It would be too complicated to report the detailed reasoning in these references but the main lines include the introduction of measurement time in the first two, the introduction of the mathematics of dynamical systems for the third and the explicit use of symmetries for the fourth. Finally I point to the conferences organized by Andrei Khrennikov for a world of further information.

In paper [5], the nonlocal knowledge involved is a globally known threshold for photon detection as well as a common vector space that is used in both EPRB wings to label the polarizer settings. Both pieces of global knowledge are also used by the experimenter and therefore the theory belongs to nonlocal category 1. No instantaneous influences are needed. The paper shows a clear contradiction to Bell-type inequalities and thus Bells theorem if it refers to nonlocalities of category 3.

In paper [6], the nonlocal knowledge involved is that of the magnet (polarizer) directions leading to perfect anticorrelation and the choice of a coordinate system for any given magnet or polarizer orientation of one experimental wing. This knowledge is used also by the experimenters and, therefore, up to this point the theory is of category 1. Furthermore, however, a global random function of time $rm(t)$ is used. The reason that Bell's theorem cannot capture such an approach related to measurement time is his assumption that puts all the variables of the domain of A as well as B on the same probability space. As shown by the

above mentioned theorem [3], measurement time and magnet settings cannot be on the same probability space. Global functions $rm(t)$ represent, of course, a remnant of nonlocality and are not used by experimenters. This puts the theory of this paper into category 2. However, such remnant nonlocalities (e.g. a global negative electron charge or any global symmetry) are completely different from instantaneous influences between one measurement event and a spatially distant event *i.e.* category 3.

For completeness, I like to add that the above considerations are not covering all the past and current work of dealing theoretically with EPRB experiments and finding contradictions to Bell-type inequalities.

For example, Luigi Accardi [7] has made early investigations of the dynamics of EPRB experiments in rigorous mathematical form.

Marian Kupczynski [8] has made many significant contributions and has recently closed the door on quantum nonlocality.

Joy Christian [9] used a more general codomain for the functions A, B as compared to the work described above, which only uses Bells original codomain of A, B = +1 or −1. Christian has attempted to show that his theory is within category 1. The complications of such assessment are beyond the scope of this discussion. However, as far as I understand it, Christians framework is at least in category 2 and certainly not in category 3.

Last, but not least, Andrei Khrennikov has made many important contributions in journals, books and conferences that he organized over decades. Many references to his work as well as papers of and references to other notables can be found in a special issue on this subject [10].

9. Conclusions

A quantum nonlocality violates Einstein's separation principle, and a theory that contains a quantum nonlocality is of category 3. I have shown, however, that nonlocal theories of category 1 and 2 exist that explain EPRB experiments and are based on Einstein's physics and the validity of his separation principle. These category 1 and 2 theories also agree with the quantum result for EPRB correlations and thus violate Bell-type inequalities. Bell's theorem stating that any local theory validates Bell-type inequalities is still correct. Completely local theories (category 0) do indeed validate Bell-type inequalities but cannot cover non-trivial relativisitc theories, because of the very definition of the word relativity, which requires viewing a system relative to another system (a nonlocal requirement). This nonlocality of relativistic theories is, however, not of category 3, which requires a breakdown of Einstein's separation principle.

A simplified explanation of these very formal distinctions and corollaries may be given in the following way. It is commonly assumed that entangled particles do not obey Einstein's separation principle, because the single particles carry properties that do not only depend on themselves but also on the other particles of the entangled system. This latter assertion is thought to invalidate Einstein's separation principle and is also seen as equivalent to the consequences of Bell's

theorem that requires nonlocality if one wishes to obtain the quantum result. These factors seem to present a shut and closed case for the Bell theorem and the concept of entanglement that violates Einstein's separation principle. Instead we are dealing here with a logical circle that can only be broken by the use of precise categorization as shown above.

The properties of the particle-pair that are not independent but nonlocal may just be properties of symmetry: the symmetry property of the single particles, the symmetry properties of the equipment with which they interact and the symmetry of the system as a whole. These various symmetries leave a trace in the single EPRB measurement outcomes for both measurement stations. As a consequence, the single-pair measurement outcomes are somehow linked to each other; a fact that may be described for interpretational purposes by the space-time dynamics of particle equipment interactions. In other words one needs to discuss details related to the dynamical interactions with the measurement equipment that quantum mechanics wisely avoids considering (at the risk of being incomplete). Considerations of many body interactions with the equipment help avoid any violation of Einstein's separation principle and remove the "weirdness" of quantum interpretations, at least as far as EPRB experiments and theories are concerned. Such considerations are, of course, of great complexity and reduce the effectiveness of quantum mechanics, which rests on the representation of polarizers and Stern-Gerlach magnets by unit vectors in three dimensional space. As I have shown, however, the mere addition of a time variable in the functions A and B (symbolizing correlated dynamic processes) is sufficient to avoid the pitfalls of model-oversimplification and allows violations of the Bell theorem in categories 1 and 2.

Acknowledgements

Louis Marchildon has provided very valuable comments for strengthening the manuscript. Hans De Raedt has helped, as always, with valuable discussions.

Conflicts of Interest

The author declares no conflicts of interest regarding the publication of this paper.

References

[1] Einstein, A., Podolsky, B. and Rosen, N. (1935) *Physical Review*, **16**, 777-780. https://doi.org/10.1103/PhysRev.47.777

[2] Bell, J.S. (1964) *Physics*, **1**, 195-200. https://doi.org/10.1103/PhysicsPhysiqueFizika.1.195

[3] Hess, K. and Philipp, W. (2005) *Foundations of Physics*, **35**, 1749-1767. https://doi.org/10.1007/s10701-005-6520-y

[4] Weihs, G., Jennewein, T., Simon, C., Weinfurther, H. and Zeilinger, A. (1998) *Physical Review Letters*, **81**, 5039-5043. https://doi.org/10.1103/PhysRevLett.81.5039

[5] De Raedt, H., Michielsen, K. and Hess, K. (2017) *Open Physics*, **15**, 713-733.

https://doi.org/10.1515/phys-2017-0085

[6] Hess, K. (2018) *Journal of Modern Physics*, **9**, 1573-1590. https://doi.org/10.4236/jmp.2018.98099

[7] Accardi, L. (1981) *Physics Reports*, **77**, 169-192. https://doi.org/10.1016/0370-1573(81)90070-3

[8] Kupczynski, M. (2018) *Entropy*, **20**, 877. https://doi.org/10.3390/e20110877

[9] Christian, J. (2018) *Royal Society Open Science*, **5**, Article ID: 180526. https://doi.org/10.1098/rsos.180526

[10] Hess, K., De Raedt, H.A. and Khrennikov, A. (2017) *Open Physics*, **15**, 572-576. https://doi.org/10.1515/phys-2017-0067

Journal of Modern Physics, 2019, 10, 1222-1234
https://www.scirp.org/journal/jmp
ISSN Online: 2153-120X
ISSN Print: 2153-1196

Plane Symmetric Solutions to the Nonlinear Spinor Field Equations in General Relativity Theory

A. Adomou[1,2*], Jonas Edou[1], Siaka Massou[1]

[1]Department of Theoretical Physics and Mathematics, University of Abomey-Calavi, Abomey-Calavi, Benin
[2]National Superior Institute of Industrial Technology, INSTI-Lokossa, National University of Sciences, Technology, Engineering and Mathematics of Abomey, Abomey, Benin
Email: *elietteadomou@gmail.com

How to cite this paper: Adomou, A., Edou, J. and Massou, S. (2019) Plane Symmetric Solutions to the Nonlinear Spinor Field Equations in General Relativity Theory. *Journal of Modern Physics*, **10**, 1222-1234.
https://doi.org/10.4236/jmp.2019.1010081

Received: June 7, 2019
Accepted: September 15, 2019
Published: September 18, 2019

Abstract

We have obtained exact static plane-symmetric solutions to the spinor field equations with nonlinear terms which are arbitrary functions of invariant $I_p = P^2 = \left(i\bar{\psi}\gamma^5\psi\right)^2$, taking into account their own gravitational field. It is shown that the initial set of the Einstein and spinor field equations with a power-law nonlinearity have regular solutions with a localized energy density of the spinor field only if $m = 0$ (m is the mass parameter in the spinor field equations). Equations with power and polynomial nonlinearities are studied in detail. In this case, a soliton-like configuration has negative energy. We have also obtained exact static plane-symmetric solutions to the above spinor field equations in flat space-time. It is proved that in this case soliton-like solutions are absent.

Keywords

Lagrangian, Static Plane-Symmetric Metric, Field Equations, Energy-Momentum Tensor, Charge Density, Current Vector, Soliton-Like Solution

1. Introduction

The consideration of the nonlinear generalization of classical field theory is the only possibility to overcome the shortcomings to the theory which considers elementary particles as materials points. Indeed, with this theory, it is impossible to get a finite quantity of mass, charge and spin of elementary particles as prouved experimentaly. In order to describe the elemetary particles, it is necessary

to take account the nonlinear terms in the field equations and their own gravitational field. In these conditions, we obtain the soliton-like solutions which are used in the formation of the fields configurations of elementary particles with limited total energy and localized energy density. The concept of soliton is more used in pure science for different purpose. It's studied by many authors in the gravitational theory. G.N. Shikin has investigated the basics of soliton theory in general relativity. In his work, he has formulated clearly the requirements to be fulfilled by soliton-like solutions [1]. In a remarkable paper on the soliton, A. Adomou and G. N. Shikin have obtained exact plane-symmetric solutions to the spinor field equations with nonlinear terms which are arbitrary functions of the invariant $S=\bar{\psi}\psi$, taking into account their own gravitational field. They have studied in detail equations with power and polynomial nonlinearities. They have shown that the initial set of the Einstein and spinor field equations with a power-law nonlinearity has regular solutions with a localized energy density of the spinor field only in the case of zero mass parameter in the spinor field, with a negative energy for the soliton-like configuration. They have also proved that the spinor field equation with a polynomial nonlinearity has a regular solution with positive energy. Their study has come out onto the non existence of soliton-like solutions in the flat space-time [2].

The plane-symmetric solitons of spinor and scalar fiels are studied by B. Saha and G. N. Shikin. They have considered a system of nonlinear spinor and scalar fields with minimal coupling in general relativity. The nonlinear term in the spinor field is given by an arbitrary function depending on the bilinear spinor forms $S=\bar{\psi}\psi$ and $P=\left(i\bar{\psi}\gamma^{5}\psi\right)$. As for the scalar lagrangian, it is chosen as an arbitrary function of the scalar invariant $\Omega=\phi_{,\alpha}\phi^{,\alpha}$ that becomes linear when $\Omega\to 0$. The spinor and scalar fields in question interact with each other by means of a gravitational field. The gravitational field is given by a plane-symmetric metric. They have obtained exact plane-symmetric solutions to the gravitational, spinor and scalar field equations. They have also investigated the role of gravitational field in the formation of the configurations with limited total energy,spin and charge. In general, they have proved that the choice of spinor field nonlinearity can lead to the elimination of scalar field contribution to the metric functions, but having it contribution to the total energy unaltered [3]. V. Adanhoum, A. Adomou, F. P. Codo and M. N. Hounkonnou have obtained spherical-symmetric soliton-like solutions of nonlinear spinor field equations in gravitational theory. The regularity properties of the obtained solutions as well as the asymptotic behavior of the energy and charge densities are studied [4].

The aim of the paper is to study the role of nonlinear spinor as well as the own gravitational field in the formation of configurations of elementary particles with localized energy density and limited total energy. In this optic, we choose the nonlinear terms in the spinor field equations which are arbitrary functions of $I_P=P^2=\left(i\bar{\psi}\gamma^{2}\psi\right)^{2}$.

The rest of the present research work is organized as follows. Section 2 deals

with fundamental equations and general solutions. In the first time, we have established gravitational and spinor fields equations, using the variational principle and usual algebraic manipulations. in the second time, we have obtained and analized the general solutions of the basic equations established. In Section 3, we have investgated in detail the polynomial nonlinearities equations. Section 4 addresses to the concluding remarks.

2. Fundamental Equations and Their General Solutions

The lagrangian of the nonlinear spinor and gravitational fields can be written in the form [3]:

$$L=\frac{R}{2\chi}+L_{Sp}=\frac{R}{2\chi}+\frac{i}{2}\left(\bar{\psi}\gamma^{\mu}\nabla_{\mu}\psi-\nabla_{\mu}\bar{\psi}\gamma^{\mu}\psi\right)-m\bar{\psi}\psi+L_{N}, \tag{1}$$

with R the scalar curvature and χ the Einstein's gravitational constant. The nonlinear term L_N in spinor lagrangian characterizes the self-interaction of a spinor field. $L_N=F\left(I_p\right)$ represents an arbitrary function depending on the invariant $I_p=\left(i\bar{\psi}\gamma^5\psi\right)^2$.

The metric of space-time admitting static plane-symmetric may be written as [1]:

$$\mathrm{d}s^2=\mathrm{e}^{2\gamma}\mathrm{d}t^2-\mathrm{e}^{2\alpha}\mathrm{d}x^2-\mathrm{e}^{2\beta}\left(\mathrm{d}y^2+\mathrm{d}z^2\right). \tag{2}$$

Here the speed of light C is taken to be unity and the metric functions α,β,γ depend exclusively on the spatial variable *x*. They satisfy the coordinate condition having the form:

$$\alpha=2\beta+\gamma. \tag{3}$$

The general form of Einstein equation is:

$$G_{\mu}^{\nu}=R_{\mu}^{\nu}-\frac{1}{2}\delta_{\mu}^{\nu}R=-\chi T_{\mu}^{\nu}, \tag{4}$$

where G_{μ}^{ν} is the Einstein's tensor; R_{μ}^{ν} is the Ricci's tensor; δ_{μ}^{ν} is the Kronecker's symbol and T_{μ}^{ν} is the energy-momentum tensor.

Taking into account the metric tensor $g_{\mu\nu}$, the larangian (1) and the variational principle, we obtain Einstein's field equations for the metric (2) under the coordinate condition (3) [5] [6]:

$$G_0^0=\mathrm{e}^{-2\alpha}\left(2\beta''-2\gamma'\beta'-\beta'^2\right)=-\chi T_0^0, \tag{5}$$

$$G_1^1=\mathrm{e}^{-2\alpha}\left(2\beta'\gamma'+\beta'^2\right)=-\chi T_1^1, \tag{6}$$

$$G_2^2=\mathrm{e}^{-2\alpha}\left(\beta''+\gamma''-2\beta'\gamma'-\beta'^2\right)=-\chi T_2^2, \tag{7}$$

$$G_2^2=G_3^3,\quad T_2^2=T_3^3. \tag{8}$$

Let us write down the spinor field equations for the functions ψ and $\bar{\psi}$ [2] [6]:

$$i\gamma^{\mu}\nabla_{\mu}\psi-m\psi+F'\left(I_p\right)\psi=0, \tag{9}$$

$$i\nabla_{\mu}\bar{\psi}\gamma^{\mu}+m\bar{\psi}-F'\left(I_p\right)\bar{\psi}=0, \tag{10}$$

with

$$F'\left(I_p\right)=2iP\frac{\partial F}{\partial I_p}\gamma^5. \tag{11}$$

The metric energy-momentum tensor of the spinor field is [5] [6]

$$T_\mu^\nu=\frac{i}{4}g^{\nu\rho}\left(\bar{\psi}\gamma_\mu\nabla_\nu\psi+\bar{\psi}\gamma_\nu\nabla_\mu\psi-\nabla_\mu\bar{\psi}\gamma_\nu\psi-\nabla_\nu\bar{\psi}\gamma_\mu\psi\right)-\delta_\mu^\nu L_{Sp} \tag{12}$$

where L_{sp} with respect to (9) and (10) takes the form

$$L_{Sp}=-\frac{1}{2}\left(\bar{\psi}\frac{\partial L_N}{\partial\bar{\psi}}+\frac{\partial L_N}{\partial\psi}\psi\right)+L_N=-2I_P\frac{\partial F\left(I_p\right)}{\partial I_p}+F\left(I_p\right). \tag{13}$$

From (13), let us write explicitly the nonzero components of the tensor T_μ^ν:

$$T_0^0=T_2^2=T_3^3=-L_{Sp}=2I_p\frac{\partial F\left(I_p\right)}{\partial I_p}-F\left(I_p\right) \tag{14}$$

$$T_1^1=\frac{i}{2}\left(\bar{\psi}\gamma^1\nabla_1\psi-\nabla_1\bar{\psi}\gamma^1\psi\right)+2I_p\frac{\partial F\left(I_p\right)}{\partial I_p}-F\left(I_p\right). \tag{15}$$

In (9), (10) and (12), ∇_μ denotes the covariant derivative of spinor, having the form [3] [4] [7] [8]

$$\nabla_\mu\psi=\frac{\partial\psi}{\partial x^\mu}-\Gamma_\mu\psi\quad\text{or}\quad\nabla_\mu\bar{\psi}=\frac{\partial\bar{\psi}}{\partial x^\mu}+\Gamma_\mu\bar{\psi} \tag{16}$$

where Γ_μ are the spinor affine connection matrices.

In curved space-time, the Dirac's matrices γ^μ are defined in the following way.

Using the egalities

$$g_{\mu\nu}\left(x\right)=e_\mu^a\left(x\right)e_\nu^b\left(x\right)\eta_{ab},$$
$$\gamma_\mu\left(x\right)=e_\mu^a\left(x\right)\bar{\gamma}_a, \tag{17}$$

where $\eta_{ab}=diag\left(1,-1,-1,-1\right)$, $\bar{\gamma}_a$ are Dirac's matrices in flat space-time, $e_\mu^a\left(x\right)$ are tetradic 4-vectors, we obtain:

$$\gamma^0=\mathrm{e}^{-\gamma}\bar{\gamma}^0,\quad\gamma^1\left(x\right)=\mathrm{e}^{-\alpha}\bar{\gamma}^1,\quad\gamma^2=\mathrm{e}^{-\beta}\bar{\gamma}^2,\quad\gamma^3=\mathrm{e}^{-\beta}\bar{\gamma}^3. \tag{18}$$

From

$$\Gamma_\mu\left(x\right)=\frac{1}{4}g_{\rho\mu}\left(\partial_\mu e_\sigma^b e_a^\rho-\Gamma_{\mu\sigma}^\rho\right)\gamma^\delta\gamma^\sigma, \tag{19}$$

we get

$$\Gamma_0=-\frac{1}{2}\mathrm{e}^{-2\beta}\bar{\gamma}^0\bar{\gamma}^1\gamma',\quad\Gamma_1=0,\quad\Gamma_2=\frac{1}{2}\mathrm{e}^{-\beta-\gamma}\bar{\gamma}^2\bar{\gamma}^1\beta',\quad\Gamma_3=\frac{1}{2}\mathrm{e}^{-\beta-\gamma}\bar{\gamma}^3\bar{\gamma}^1\beta' \tag{20}$$

The Dirac's matrices $\bar{\gamma}^a$ in flat space-time are chosen as in [8] [9].

Using Einstein's sommation, we find

$$\gamma^\mu\Gamma_\mu=-\frac{1}{2}\mathrm{e}^{-\alpha}\alpha'\bar{\gamma}^1. \tag{21}$$

Taking into account the obtained expression for $\gamma^\mu\Gamma_\mu$ (21), we can rewrite

the Equations (9) and (10) as follows

$$i\mathrm{e}^{-\alpha}\overline{\gamma}^{1}\left(\partial_{x}+\frac{1}{2}\alpha'\right)\psi-m\psi+2iP\frac{\partial F\left(I_{p}\right)}{\partial I_{p}}\gamma^{5}\psi=0, \tag{22}$$

$$\mathrm{e}^{-\alpha}\left(\partial_{x}+\frac{1}{2}\alpha'\right)\overline{\psi}\overline{\gamma}^{1}+m\overline{\psi}-2iP\frac{\partial F\left(I_{p}\right)}{\partial I_{p}}\overline{\psi}\gamma^{5}=0. \tag{23}$$

Further setting $\psi(x)=V_{\delta}(x)$ with $V_{\delta}(x)=\begin{pmatrix}V_{1}(x)\\V_{2}(x)\\V_{3}(x)\\V_{4}(x)\end{pmatrix}$, for the components of spinor field one deduces the following set of equations from (22)

$$V_{4}'+\frac{1}{2}\alpha'V_{4}+im\mathrm{e}^{\alpha}V_{1}-2PF'\left(I_{p}\right)\mathrm{e}^{\alpha}V_{3}=0. \tag{24}$$

$$V_{3}'+\frac{1}{2}\alpha'V_{3}+im\mathrm{e}^{\alpha}V_{2}-2PF'\left(I_{p}\right)\mathrm{e}^{\alpha}V_{4}=0. \tag{25}$$

$$V_{2}'+\frac{1}{2}\alpha'V_{2}-im\mathrm{e}^{\alpha}V_{3}+2PF'\left(I_{p}\right)\mathrm{e}^{\alpha}V_{1}=0. \tag{26}$$

$$V_{1}'+\frac{1}{2}\alpha'V_{1}-im\mathrm{e}^{\alpha}V_{4}+2PF'\left(I_{p}\right)\mathrm{e}^{\alpha}V_{2}=0. \tag{27}$$

The functions V_{1}, V_{2}, V_{3} and V_{4} are connected by the relations

$$V_{1}^{2}-V_{2}^{2}-V_{3}^{2}+V_{4}^{2}=cste \quad \text{and} \quad \overline{V}_{1}V_{4}+\overline{V}_{2}V_{3}=\overline{V}_{3}V_{2}+\overline{V}_{4}V_{1}. \tag{28}$$

The set of Equations (24)-(27), leads to the system of equations for invariant functions $S=\overline{\psi}\psi$, $P=i\overline{\psi}\gamma^{5}\psi$ and $R=\overline{\psi}\overline{\gamma}^{5}\overline{\gamma}^{1}\psi$:

$$S'+\alpha'S+4F'\left(I_{p}\right)P\mathrm{e}^{\alpha}R=0 \tag{29}$$

$$R'+\alpha'R+2m\mathrm{e}^{\alpha}P+4F'\left(I_{p}\right)P\mathrm{e}^{\alpha}S=0 \tag{30}$$

$$P'+\alpha'P+2m\mathrm{e}^{\alpha}R=0 \tag{31}$$

Immediately, the solution of the system of equations of the invariant functions is

$$P^{2}-R^{2}+S^{2}=C\mathrm{e}^{-2\alpha(x)}, \tag{32}$$

$$C=const.$$

Using the spinor field equation in the form (9) and the conjugate one in the form (10), we obtain the following expression for T_{1}^{1} from (15):

$$T_{1}^{1}=mS-F\left(I_{p}\right) \tag{33}$$

Let us now solve the Einstein equation. In view of $T_{0}^{0}=T_{2}^{2}$, the difference $\begin{pmatrix}0\\0\end{pmatrix}$ - $\begin{pmatrix}2\\2\end{pmatrix}$ of the Einstein equations leads to

$$\beta''-\gamma''=0. \tag{34}$$

By integrating, the Equation (34) has the solution

$$\beta(x)=\gamma(x)+Ax \tag{35}$$

where A is the integration constant; another integration constant has been chosen equal to zero since the functions β and γ depend only of the spatial

variable *x*.

From (3), we have

$$\alpha'' = 2\beta'' + \gamma''. \tag{36}$$

Taking into account (34), we obtain from (36) the following equalities

$$\beta''(x) = \frac{1}{3}\alpha''(x), \quad \gamma''(x) = \frac{1}{3}\alpha''(x). \tag{37}$$

The solutions to the Equation (37) using (3) and (35) lead to the following expressions for $\beta(x)$ and $\gamma(x)$:

$$\beta(x) = \frac{1}{3}\left(\alpha(x) + Bx\right), \quad \gamma(x) = \frac{1}{3}\left(\alpha(x) - 2Bx\right) \tag{38}$$

where B is the integration constant. Taking into account the expressions (35) and (38), we deduce easily $A = B$.

The Equation (6) being the first integral of (5) and (7), is a first order differential equation. Inserting (38) into (5) and substituting the result into (33), we get the Eintein equation $\begin{pmatrix} 1 \\ 1 \end{pmatrix}$ under the form

$$\left(\alpha'\right)^2 - A^2 = -3\chi \mathrm{e}^{2\alpha}\left[mS - F\left(I_p\right)\right]. \tag{39}$$

In order to solve the Equation (39), it is necessary to choose massless spinor field, *i.e.*, $m = 0$ according to unified nonlinear spinor theory of Heisenberg. The mass term should be obtained after quantization. For details, refer to [10] [11] and references therein.

From (31), for $m = 0$, $\alpha' = -\frac{1}{P}\frac{\mathrm{d}P}{\mathrm{d}x}$. Therefore (39) becomes

$$\frac{\mathrm{d}P}{\sqrt{A^2P^2 + 3\chi C_0^2 F\left(I_p\right)}} = \pm \mathrm{d}x. \tag{40}$$

Thus, the general exact solutions of Einstein equations and nonlinear spinor field equations are:

$$\int \frac{\mathrm{d}P}{\sqrt{A^2P^2 + 3\chi C_0^2 F\left(I_p\right)}} = \pm\left(x + x_0\right), \quad x_0 = cste. \tag{41}$$

Let us remark that the general solutions depend on the analytics explicits forms of $F\left(I_p\right)$. Indeed knowing $F\left(I_p\right)$, we can find $P(x)$ from (41). If $P(x)$ is known, we can determine $\alpha(x)$ from (31) and if $\alpha(x)$ is known, we can determine easily $\beta(x)$ and $\gamma(x)$ from (38).

Taking into account $P(x) = C_0 \mathrm{e}^{-\alpha(x)}$, we can establish the regular properties of the obtained solutions and on the other hand to establish the regularity of the metric functions and the matter fields in the whole space-time. Studying the energy density T_0^0, we can establish the localization properties of the solutions and the finiteness of The total energy [2] [8].

Let us resolve the spinor field equations in the following paragraph . We can get a concrete form of the functions V_δ by solving Equations (24)-(27) in a

more compacte form if we pass to the functions $V_\delta = \mathrm{e}^{-\frac{\alpha}{2}} W_\delta$, $\delta = 1,2,3,4$:

$$W_4'(x) - \phi(x) W_3(x) = 0 \tag{42}$$

$$W_3'(x) - \phi(x) W_4(x) = 0 \tag{43}$$

$$W_2'(x) + \phi(x) W_1(x) = 0 \tag{44}$$

$$W_1'(x) + \phi(x) W_2(x) = 0 \tag{45}$$

With $\phi(x) = 2F'(I_p)P\mathrm{e}^{\alpha}$. Let us find from the set of first-order Equations (42)-(45) to a set second-order equations for the functions W_1, W_2, W_3, W_4.

We have:

$$W_1'' - \frac{\phi'}{\phi} W_1' - \phi^2 W_1 = 0 \tag{46}$$

$$W_2'' - \frac{\phi'}{\phi} W_2' - \phi^2 W_2 = 0 \tag{47}$$

$$W_3'' - \frac{\phi'}{\phi} W_3' - \phi^2 W_3 = 0 \tag{48}$$

$$W_4'' - \frac{\phi'}{\phi} W_4' - \phi^2 W_4 = 0 \tag{49}$$

The solution of the Equation (46) is

$$W_1(x) = C_1 \exp\left(\int \phi(x)\mathrm{d}x\right) + iC_2 \exp\left(-\int \phi(x)\mathrm{d}x\right) \tag{50}$$

where C_1 and C_2 are integration constants.

From (45), the solution of the Equation (47) is

$$W_2(x) = -C_1 \exp\left(\int \phi(x)\mathrm{d}x\right) + iC_2 \exp\left(-\int \phi(x)\mathrm{d}x\right). \tag{51}$$

Solving analogously Equations (48) and (49), we obtain the following expressions for W_3 and W_4:

$$W_3(x) = C_3 \exp\left(\int \phi(x)\mathrm{d}x\right) + iC_4 \exp\left(-\int \phi(x)\mathrm{d}x\right), \tag{52}$$

$$W_4(x) = C_3 \exp\left(\int \phi(x)\mathrm{d}x\right) - iC_4 \exp\left(-\int \phi(x)\mathrm{d}x\right) \tag{53}$$

with C_3 and C_4 are integration constants.

Let us determine the link between the integration constants C, C_0, C_1, C_2, C_3 and C_4 which are in the solutions of Einstein's and spinor fields equations.

From $V_\delta = \mathrm{e}^{-\frac{\alpha}{2}} W_\delta$, we get

$$P = 4\left(C_1 C_4 - C_2 C_3\right)\exp(-\alpha), \tag{54}$$

$$R(x) = 2\left[\left(C_2^2 - C_4^2\right)\exp\left(-2\int \phi(x)\mathrm{d}x\right) + \left(C_3^2 - C_1^2\right)\exp\left(2\int \phi(x)\mathrm{d}x\right)\right]\exp(-\alpha), \tag{55}$$

$$S(x) = 2\left[\left(C_1^2 - C_3^2\right)\exp\left(2\int \phi(x)\mathrm{d}x\right) + \left(C_2^2 - C_4^2\right)\exp\left(2\int \phi(x)\mathrm{d}x\right)\right]\exp(-\alpha). \tag{56}$$

Substituting the expressions (50), (51), (52) and (53) obtained previously in (32), we have

$$C = 16\left(C_1C_2 - C_3C_4\right)^2. \tag{57}$$

Later, comparing the expression of $P(x)$ in (54) and $P(x) = C_0 e^{-\alpha}$, we have

$$C_0 = 4\left(C_1C_4 - C_2C_3\right). \tag{58}$$

Thus, we have obtained the general solutions of the Equations (46)-(49) which contain four arbitrary constants C_1, C_2, C_3 and C_4.

In the following section, we shall analyze the general solutions obtained in the previous section choosing the nonlinear term in the concrete form.

3. Analysis of the Results: Concrete Form of Nonlinear Term in Spinor Lagrangian

Let us study the solution to linear Equation (Dirac's equation). Note that this solution is necessary for comparing with solutions to nonlinear spinor equations in order to clarify the influence of nonlinear terms in the nonlinear field equations in the formation of configuation of elementary particles.

In the linear case $L_N = 0$ for $m = 0$ we have from (22)

$$ie^{-\alpha}\overline{\gamma}^1\left(\partial_x + \frac{1}{2}\alpha'\right)\psi = 0 \tag{59}$$

Taking into account (41), we get

$$P(x) = C_0 e^{-A(x+x_0)} \tag{60}$$

As $P(x) = C_0 e^{-\alpha}$, from (60), we obtain the expression of the metric function:

$$\alpha(x) = A(x + x_0) \tag{61}$$

From (38), we find the following expressions of β and γ:

$$\beta(x) = \frac{2}{3}A(x + x_0) \tag{62}$$

$$\gamma(x) = -\frac{1}{3}A(x + x_0) \tag{63}$$

With $L_N = 0$, the energy density is

$$T_0^0 = 0 \tag{64}$$

From (64) it follows that, the energy density of the system is not localized. In sum, the soliton-like solutions are absent in the linear case.

Let us now consider a concrete type of nonlinear spinor field equation in the form $L_N = F\left(I_p\right) = \lambda P^{2n}$ where λ is a nonlinearity parameter and n is a power of nonlinearity. In the first case, For $n = 1$, we find Heisenberg-Ivanenko type nonlinear spinor field equation [10]

$$ie^{-\alpha}\overline{\gamma}^1\left(\partial_x + \frac{1}{2}\alpha'\right)\psi - m\psi + 2iP\lambda\gamma^5\psi = 0, \tag{65}$$

Substituting $F\left(I_P\right) = \lambda I_P = \lambda P^2$ into (41), we obtain the similar expression as for a linear spinor field, only now the constant A^2 is replaced by $A^2 + 3\chi\lambda C_0^2$.

We have

$$P(x) = C_0 \mathrm{e}^{(x+x_0)\sqrt{A^2+3\chi\lambda C_0^2}} \tag{66}$$

From the relation $P = C_0 \mathrm{e}^{-\alpha}$, we get

$$\alpha(x) = -(x+x_0)\sqrt{A^2+3\chi\lambda C_0^2}. \tag{67}$$

According to the equality (38), we define the functions $\beta(x)$ and $\gamma(x)$ as follows

$$\beta(x) = \frac{1}{3}\left[-(x+x_0)\sqrt{A^2+3\chi\lambda C_0^2} + Ax\right] \tag{68}$$

$$\gamma(x) = -\frac{1}{3}\left[(x+x_0)\sqrt{A^2+3\chi\lambda C_0^2} + 2Ax\right] \tag{69}$$

The invariant $I_P = P^2$ and the functions $g_{00} = \mathrm{e}^{2\gamma}$, $g_{11} = -\mathrm{e}^{2\alpha}$, $g_{22} = g_{33} = -\mathrm{e}^{2\beta}$ are regular in all space.

The energy density T_0^0 has the following expression:

$$T_0^0 = C_0^2 \mathrm{e}^{2(x+x_0)\sqrt{A^2+3\chi\lambda C_0^2}} \tag{70}$$

hence we obtain for $\varepsilon(x)$ the energy density per unit invariant volume

$$\varepsilon(x) = T_0^0\sqrt{-3_g} = C_0^2 \mathrm{e}^{2(x+x_0)\sqrt{A^2+3\chi\lambda C_0^2}} \mathrm{e}^{\frac{2}{3}Ax} \tag{71}$$

We conclude from (70) and (71) that a localization of the energy density and the energy density per unit invariant volume are absent. The total energy diverges. The Equation (65) has no soliton-like solution.

In the second case when $F(I_P) = \lambda P^{2n}$ and $n > 1$, From (41), we have

$$P(x) = \left\{\frac{A}{\sqrt{3\chi\lambda C_0^2}\sinh\left[A(n-1)x\right]}\right\}^{\frac{1}{n-1}}; n > 1. \tag{72}$$

From (14), the energy density is

$$T_0^0 = \lambda(2n-1)\left\{\frac{A}{\sqrt{3\chi\lambda C_0^2}\sinh\left[A(n-1)x\right]}\right\}^{\frac{2n}{n-1}}; n > 1. \tag{73}$$

We remark that, from $L_N = \lambda P^{2n}$; (72) and (73), when $x \to 0$, $P(x) \to \infty$ and $T_0^0 \to \infty$.

It follows that the energy density is not localized and the total energy does not finite value.

When $\lambda = -\Lambda^2$, from the relation (41), we deduce that:

$$P(x) = \left\{\frac{A}{\sqrt{3\chi\Lambda^2 C_0^2}\cosh\left[A(n-1)x\right]}\right\}^{\frac{1}{n-1}} \tag{74}$$

From (74), it follows that $P(x)$ has its maximum value $\left\{\frac{A}{\sqrt{3\chi\Lambda^2 C_0^2}}\right\}^{\frac{1}{n-1}}$;

$n>1$ when $x=0$ and $P(x)\to 0$ when $x\to\pm\infty$. In this case T_0^0 is

$$T_0^0=-\Lambda^2(2n-1)\left\{\frac{A}{\sqrt{3\chi\Lambda^2C_0^2}\cosh\left[A(n-1)x\right]}\right\}^{\frac{2n}{n-1}};n>1 \tag{75}$$

From the expression (75), it follows that the energy density T_0^0 of a nonlinear spinor field is negative and localized in space when the nonlinear term of the equation is chosen under the form $L_N=F(I_p)=-\Lambda^2P^{2n}$ with $-\Lambda^2<0$ [2] [12] [13].

The energy density per unit invariant volume is:

$$\varepsilon(x)=T_0^0\sqrt{-3_g}=-\Lambda^2(2n-1)C_0^{\frac{5}{3}}\left\{\frac{A}{\sqrt{3\chi C_0^2\Lambda^2}\cosh\left[A(n-1)x\right]}\right\}^{\frac{-4n}{3(n-1)}}\mathrm{e}^{\frac{2}{3}Ax} \tag{76}$$

From (76), it follows that the energy density is negative and localized. Indeed, when $A>0$; $n>1$ and for $x\to\pm\infty;\varepsilon\to 0$. Furthermore, $\varepsilon(x)$ has its minimal value $-\Lambda^2(2n-1)C_0^{\frac{5}{3}}\left\{\frac{A}{\sqrt{3\chi C_0^2\Lambda^2}}\right\}^{\frac{-4n}{3(n-1)}}$ when $x=0$.

The total energy of spinor field is defined by

$$E_f=\int_{-\infty}^{+\infty}\varepsilon(x)\mathrm{d}x=\int_{-\infty}^{+\infty}T_0^0\sqrt{-3_g}\,\mathrm{d}x.$$

Thus

$$E_f=\int_{-\infty}^{+\infty}-\Lambda^2(2n-1)C_0^{\frac{5}{3}}\left\{\frac{A}{\sqrt{3\chi C_0^2\Lambda^2}\cosh\left[A(n-1)x\right]}\right\}^{\frac{-4n}{3(n-1)}}\mathrm{e}^{\frac{2}{3}Ax}\mathrm{d}x<\infty. \tag{77}$$

$\varepsilon(x)$ is a regular, negative and localized function therefore the total energy E_f is limited and negative.

Since the obtained solution is regular and has a localized energy density T_0^0, the total energy E_f negative, limited and the metric functions regular and limited, it is a soliton-like solution. Moreover, this solution can be used to describe the configuration of the elementary particles.

From (50)-(53), we can obtain the concrete form of the functions $V_\delta(x)$ in their more compact form.

$$V_1(x)=\left(C_1\mathrm{e}^{\sigma(x)}+iC_2\mathrm{e}^{-\sigma(x)}\right)\cdot\mathrm{e}^{-\frac{\alpha}{2}}. \tag{78}$$

$$V_2(x)=\left(-C_1\mathrm{e}^{\sigma(x)}+iC_2\mathrm{e}^{-\sigma(x)}\right)\cdot\mathrm{e}^{-\frac{\alpha}{2}}. \tag{79}$$

$$V_3(x)=\left(C_3\mathrm{e}^{\sigma(x)}+iC_4\mathrm{e}^{-\sigma(x)}\right)\cdot\mathrm{e}^{-\frac{\alpha}{2}}. \tag{80}$$

$$V_4(x)=\left(C_3\mathrm{e}^{\sigma(x)}-iC_4\mathrm{e}^{-\sigma(x)}\right)\cdot\mathrm{e}^{-\frac{\alpha}{2}}. \tag{81}$$

where C_1; C_2; C_3 and C_4 are integration constants. Furtermore,

$\mathrm{e}^{-\frac{\alpha}{2}} = \left[P(x)/C_0\right]^{\frac{1}{2}}$ with $P(x)$ defined by the expression (74).

$$\sigma(x) = \int \Phi(x)\mathrm{d}x = 2\int F'(I_P)C_0\mathrm{d}x = -\frac{2nA}{3\chi C_0(n-1)}\tanh\left[A(n-1)x\right] \quad (82)$$

$P(x)$ is a regular function, then $\sigma(x)$ and $V_\delta(x)$ are also the regular functions.

In sum, for a massless field (*i.e.* $m = 0$) and $F(I_p) = -\Lambda^2 I_p^n$; $n > 1$; the solutions of the equations of the spinor and gravitational fields have an energy density $\varepsilon(x)$ and total energy E_f negative, regular and localized.

Let us now study the influence of the proper gravitational field in the formation of the configuration of elementary particles.

In order to determine the role of the own gravitational field in the formation of regular localized solutions of soliton-like type to nonlinear spinor field equations, it is necessary to consider solutions to Equation (9) in flat space-time when $\beta = \alpha = \gamma = 0$ in (2). In this case, from (41) we get

$$P = C_0 = cste. \quad (83)$$

The explicit form of $V_\delta(x)$ is:

$$V_1(x) = \left(C_1\mathrm{e}^{Mx} + iC_2\mathrm{e}^{-Mx}\right). \quad (84)$$

$$V_2(x) = \left(-C_1\mathrm{e}^{Mx} + iC_2\mathrm{e}^{-Mx}\right). \quad (85)$$

$$V_3(x) = \left(C_3\mathrm{e}^{Mx} + iC_4\mathrm{e}^{-Mx}\right). \quad (86)$$

$$V_4(x) = \left(C_3\mathrm{e}^{Mx} - iC_4\mathrm{e}^{-Mx}\right). \quad (87)$$

where $\sigma(x) = Mx$; $M = cste$ and $T_0^0 = cste$.

We deduce that, the proper gravitational field of elementary particles plays an important role in the aim to obtain the regular solutions which possess a localized energy density and limited total energy of the nonlinear equations with the nonlinear term depending on P^2.

The last point is addressed to the spinor current vector and the total charge. Using the general solutions of the Equations (24)-(27), we can write the components of the spinor current vector $j^\mu = \bar{\psi}\gamma^\mu\psi$:

$$j^0 = \psi^+\bar{\gamma}^0\gamma^0\psi$$

$$j^0 = \left(V_1^*V_1 + V_2^*V_2 + V_3^*V_3 + V_4^*V_4\right)\mathrm{e}^{-\alpha-\gamma}.$$

$$j^0 = \left[C_1^2\cosh^2\sigma(x) + C_2^2\cosh^2\sigma(x) + C_1^2\sinh^2\sigma(x) + C_2^2\sinh^2\sigma(x)\right]\mathrm{e}^{-\alpha-\gamma}. \quad (88)$$

$$j^1 = \psi^+\bar{\gamma}^0\gamma^1\psi.$$

$$j^1 = \left[V_1^*V_4 + V_2^*V_3 + V_3^*V_2 + V_4^*V_1\right]\mathrm{e}^{-2\alpha}.$$

$$j^1 = 0. \quad (89)$$

$$j^2 = \psi^+\bar{\gamma}^0\gamma^2\psi.$$

$$j^2 = i\left[V_1^*V_4 + V_2^*V_3 + V_3^*V_2 + V_4^*V_1\right]\mathrm{e}^{-2\alpha}.$$

$$j^2 = -2\left[C_1^2 \cosh\sigma(x)\sinh(x) - C_2^2 \cosh\sigma(x)\sinh\sigma(x)\right]\mathrm{e}^{-\alpha-\beta}. \quad (90)$$

$$j^3 = \psi^+ \overline{\gamma}^0 \gamma^3 \psi$$

$$j^3 = \left[V_1^* V_3 - V_2^* V_4 + V_3^* V_1 - V_4^* V_2\right]\mathrm{e}^{-\alpha-\gamma}.$$

$$j^3 = 0. \quad (91)$$

Since the field configuration is chosen to be static plane symmetric, the spatial components of the spinor current vanishes. Alone the component j^0 is non-zero. This assumption leads to the following relations between the constants:

$$j^1 = j^2 = j^3 = 0 \quad \text{and} \quad j^2 = 0 \Rightarrow C_1 = C_2 = a. \quad (92)$$

The component j^0 defines the charge density of spinor field that has the following chronometric-invariant form given by the expression

$$\rho(x) = \left(j_0 j^0\right)^{\frac{1}{2}} = 2a^2 \cosh\left[2\sigma(x)\right]\mathrm{e}^{-\alpha}. \quad (93)$$

The total charge of the spin is defined by

$$Q = \int_{-\infty}^{+\infty} \rho(x)\sqrt{3_{-g}}\,\mathrm{d}x \quad (94)$$

The spin tensor is given by the expression as in [9] [11]

$$S^{\mu\nu,\lambda} = \frac{1}{4}\overline{\psi}\left\{\gamma^\lambda \sigma^{\mu\nu} + \sigma^{\mu\nu}\gamma^\lambda\right\}\psi. \quad (95)$$

The spatial density of the spin tensor $S^{ik,0}, i,k = 1;2;3$ from (95) is:

$$S^{ik,0} = \frac{1}{4}\overline{\psi}\left\{\gamma^0\sigma^{ik} + \sigma^{ik}\gamma^0\right\}\psi = \frac{1}{2}\overline{\psi}\gamma^0\sigma^{ik}\psi. \quad (96)$$

Here i, j, k take the value 1, 2, 3 and $i \neq j \neq k$. Thus, for the projection of spin vector on the x, y and z axis, we get:

$$S^{23,0} = \left[V_1^* V_2 + V_2^* V_1 + V_3^* V_4 + V_4^* V_3\right]\mathrm{e}^{-\alpha-2\beta-\gamma} \quad (97)$$

$$S^{31,0} = \left[V_1^* V_2 - V_2^* V_1 + V_3^* V_4 - V_4^* V_3\right]\mathrm{e}^{-2\alpha-\beta-\gamma} \quad (98)$$

$$S^{12,0} = \left[V_1^* V_1 - V_2^* V_2 + V_3^* V_3 + V_4^* V_4\right]\mathrm{e}^{-2\alpha-\beta-\gamma} \quad (99)$$

Thus, we have

$$S^{12,0} = S^{13,0} = 0. \quad (100)$$

$$S^{23,0} = a^2 \cosh\left[2\sigma(x)\right]\mathrm{e}^{-\alpha}. \quad (101)$$

From (101) the chronometric invariant spin tensor is defined by:

$$S_{chI}^{23,0} = \left(S_{23,0}S^{23,0}\right)^{\frac{1}{2}} = a^2 \cosh\left[2\sigma(x)\right]\mathrm{e}^{-\alpha}. \quad (102)$$

We remark that the total charge and total spin are not limited because from (93), $\rho(x)$ is not a localized function since when $x \to \pm\infty$, we have $\rho(x) \to \pm\infty$. Thus, we can note that the nonlinearity of the spinor field equation and the consideration of the proper gravitational field of the elementary particles are the necessary conditions but not sufficient in order to obtain the limited total charge and total spin to confirm what are got experimentaly.

4. Concluding Remarks

In this research work, we have obtained the analytic general solutions of nonlinear spinor and gravitational fields equations which are regular, localized energy density and finite total energy. These solutions are soliton like solutions. They can be used in order to describe the configuration of elementary particles. In flat space-time and linear cases, the soliton like solutions are absent. The role of the own gravitational field is crucial for the formation of soliton-like configuration of nonlinear spinor fields. In the case of the study of polynomial nonlinearities $L_N = \lambda P^{2n}$, $n > 1$, we remark that the obtained solutions are regular, localized energy density and finite quantity of total energy in the exclusively case where $\lambda = -\Lambda^2$. Emphasize that the total charge and total spin are not limited in the all metric case. Our perspective, in the forthcomming research work, is to examine the spherical symmetric soliton-like solutions to the spinor field equations with nonlinear terms $L_N = F\left(I_P\right)$ which are arbitrary functions of $I_P = \left(i\bar{\psi}\gamma^5\psi\right)^2$.

Conflicts of Interest

The authors declare no conflicts of interest regarding the publication of this paper.

References

[1] Shikin, G.N. (1995) Theory of Solitons in General Relativity. URSS, Moscow.

[2] Adomou, A. and Shikin, G.N. (1998) *Izvestia VUZov*, *Fizika*, **41**, 69.

[3] Saha, B. and Shikin, G.N. (2003) *Czechoslovak Journal of Physics*, **54**, 597-620. https://doi.org/10.1023/B:CJOP.0000029690.61308.a5

[4] Adanhoum, A., Adomou, A., Codo, F.P. and Hounkonnou, M.N. (2012) *Journal of Modern Physics*, **3**, 935. https://doi.org/10.4236/jmp.2012.39122

[5] Brill, D. and Wheeler, J. (1957) *Reviews of Modern Physics*, **29**, 465. https://doi.org/10.1103/RevModPhys.29.465

[6] Zhelnorovich, V.A. (1982) Spinor Theory and Its Applications in Physics and Mechanics. Nauka, Moscow.

[7] Saha, B. and Shikin, G.N. (1996) *International Journal of Modern Physics A*, **15**, 1481. https://doi.org/10.1016/S0217-751X(00)00066-5

[8] Adomou, A., Alvarado, R. and Shikin, G.N. (1995) Izvestiya Vuzov. Fizika, 863-868.

[9] Bogoliubov, N.N. and Shirkov, D.V. (1976) Introduction to the Theory of Quantized Fields. Nauka, Moscow.

[10] Heisenberg, W. (1966) Introduction to Unified Field Theory of Elementary Particles. Interscience Publishers, London.

[11] Schweber, S. (1961) Introduction to Relativistic Quantum Field Theory. Harper and Row, New York.

[12] Weyl, H. (1950) *Physical Review*, **77**, 699-701.

[13] Rybakov, Yu.P., Shikin, G.N. and Saha, B. (1997) *International Journal of Theoretical Physics*, **36**, 1475-1494. https://doi.org/10.1007/BF02435941

Journal of Modern Physics, 2019, 10, 1235-1246
https://www.scirp.org/journal/jmp
ISSN Online: 2153-120X
ISSN Print: 2153-1196

AC Recombination Velocity in the Back Surface of a Lamella Silicon Solar Cell under Temperature

Youssou Traore[1], Ndeye Thiam[2], Moustapha Thiame[3], Amary Thiam[1], Mamadou Lamine Ba[2], Marcel Sitor Diouf[1], Ibrahima Diatta[1], Oulymata Mballo[1], El Hadji Sow[1], Mamadou Wade[2], Grégoire Sissoko[1]

[1]Laboratory of Semiconductors and Solar Energy, Physics Department, Faculty of Science and Technology, University Cheikh Anta Diop, Dakar, Senegal
[2]Laboratory of Sciences and Techniques of Water and Environment, Polytechnic School of Thiès, Thiès, Senegal
[3]University Assane SECK, Ziguinchor, Senegal
Email: gsissoko@yahoo.com

How to cite this paper: Traore, Y., Thiam, N., Thiame, M., Thiam, A., Ba, M.L., Diouf, M.S., Diatta, I., Mballo, O., Sow, E.H., Wade, M. and Sissoko, G. (2019) AC Recombination Velocity in the Back Surface of a Lamella Silicon Solar Cell under Temperature. *Journal of Modern Physics*, **10**, 1235-1246.
https://doi.org/10.4236/jmp.2019.1010082

Received: August 26, 2019
Accepted: September 20, 2019
Published: September 23, 2019

Abstract

The ac recombination velocity of the excess minority carriers, in the back surface of a silicon solar cell with a vertical junction connected in series, is developed through Einstein's law giving the diffusion coefficient of minority carriers according to temperature, through mobility. The frequency spectrum of both, amplitude and phase, are produced for the diffusion coefficient and the recombination velocity in the rear face, in order to identify the parameters of equivalent electric models.

Keywords

Vertical Multi-Junctions, Solar Cell, AC Back Surface Recombination Velocity, Temperature, Bode and Nyquist Diagrams

1. Introduction

Vertical multi-junctions (VMJ) silicon solar cells have an architecture that is an alternative for collecting minority carriers with low-diffusion length [1] [2] [3] [4] [5].

Two types of VMJ solar cells are developed, by a succession of npp or pnn junctions. The VMJ-P has connections in parallel, between bases and connections between emitters. Thus a base type (p) is surrounded by two emitters allowing the collection of minority carriers at close range, leading to the increase

of photocurrent [6] [7] [8]. The VMJ-S, presents a succession of npp+ or pnn+ solar cells, connected in series, allowing increasing the electrical voltage [9].

The VMJ is designed to operate under light concentration to generate more minority carriers, thereby increasing voltage or current production. In this situation, temperature is an important factor that influences the operating performance of the solar cell, through the physical mechanisms that are important to study [10]. In this work, the ac recombination velocity in the rear face (p/p+) of the solar cell, is determined and studied in temperature using the frequency spectrum of its amplitude and phase.

2. Theory

The structure of the serially connected vertical multi-junctions silicon solar cell, under monochromatic illumination in frequency modulation, is given by **Figure 1** [11].

The unit of the solar cell extracted from the series representation, is a npp+ structure, the base of which is studied by variation in the temperature T (**Figure 2**).

The continuity equation relating to the excess minority carriers density $\delta(x,z,T,t)$ in the base at temperature T, and under monochromatic illumination in frequency modulation, is given by the relationship [12] [13]:

$$D(\omega,T)\times\frac{\partial^2\delta(x,z,\omega,T,t)}{\partial x^2}-\frac{\delta(x,z,\omega,T,t)}{\tau}=-G(z,\omega,t)+\frac{\partial\delta(x,z,\omega,T,t)}{\partial t} \quad (1)$$

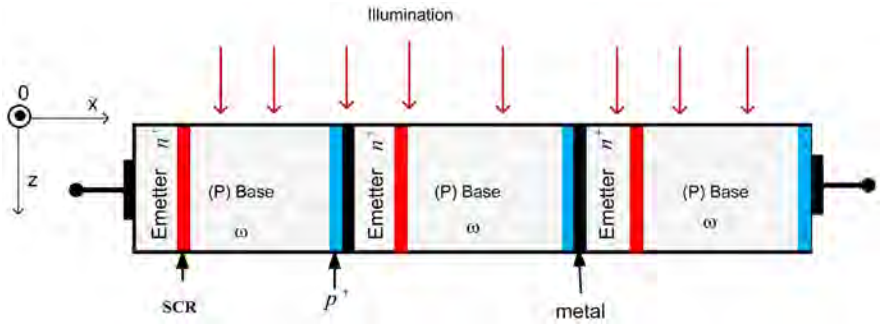

Figure 1. Schematic of a series-connected vertical multi-junction solar cells.

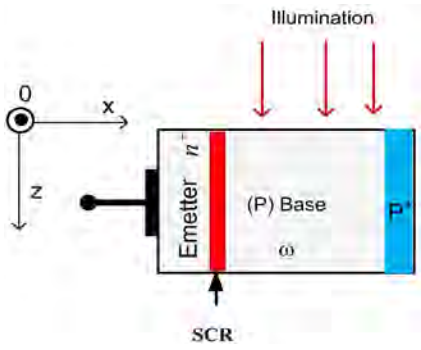

Figure 2. Across section of the vertical junction.

The density of photogenerated carriers is written according to the space coordinates (x, z) and the time t as:

$$\delta(x,z,t)=\delta(x,z)\exp(-j\omega t) \tag{2}$$

The minority carriers generation rate at depth z in the base and at any point of abscis x, under the modulation frequency ω of the incident wave, is given by the relationship:

$$G(z,\omega,t)=g(z)\exp(-j\omega t) \tag{3}$$

where $g(z)$ is the steady stateminority carriers generation rate at the z depth induced in the base by a monochromatic light of incident flow $\phi(\lambda)$, respectively with monochromatic absorption and reflecting coefficients $\alpha(\lambda)$ and $R(\lambda)$. It is then written by the following relation:

$$g(z)=\alpha(\lambda)\cdot(1-R(\lambda))\cdot\phi(\lambda)\cdot\exp(-\alpha(\lambda)\cdot z) \tag{4}$$

With τ the excess minority carrier lifetime in the base.

$D(\omega,T)$ is the complex diffusion coefficient of excess minority carrier in the base at T-temperature. Its expression is given by the relationship [14]:

$$D(\omega,T)=\frac{D(T)(1-j\cdot\omega^2\tau^2)}{1+(\omega\tau)^2} \tag{5}$$

$D_0(T)$ is the temperature-dependent diffusion coefficient given by Einstein's relationship [15]:

$$D(T)=\mu(T)\cdot\frac{K_b\cdot T}{q} \tag{6}$$

T is the temperature in Kelvin, K_b the Boltzmann constant:

$$K_b=1.38\times10^{-23}\ \mathrm{m^2\cdot kg\cdot S^{-2}\cdot K^{-1}} \tag{7}$$

The minority carrier mobility coefficient [16] expressed according to the temperature, is given by:

$$\mu(T)=1.43\times10^{9}T^{-2.42}\ \mathrm{cm^2\cdot V^{-1}\cdot s^{-1}} \tag{8}$$

By replacing the Equations (2) and (3) in the Equation (1), the continuity equation for the excess minority carriers density in the base is reduced to the following relationship:

$$\frac{\partial^2\delta(x,z,\omega,T)}{\partial x^2}-\frac{\delta(x,z,\omega,T)}{L^2(\omega,T)}=-\frac{G(x,z)}{D(\omega,T)} \tag{9}$$

$L(\omega,T)$ is the complex diffusion length of excess minority carrier in the base; ilest donné par :

$$L(\omega,T)=\frac{\sqrt{D(\omega,T)\tau}}{\sqrt{1+j\cdot\omega\cdot\tau}} \tag{10}$$

(ω, T) is the ac minority carriers diffusion coefficient in the base under the influence of temperature and the minority carrier lifetime in the base.

Thus the solution of the Equation (9) is given by the following expression of the ac density of minority carriers:

$$\delta(x,\omega,T,z) = A\cosh\left(\frac{x}{L(\omega,T)}\right) + B\sinh\left(\frac{x}{L(\omega,T)}\right) + \frac{L^2(\omega,T)}{D(\omega,T)}\cdot\alpha_t\left(1-R(\lambda)\right)\cdot\phi(\lambda)\cdot\exp(\alpha_t\cdot z) \tag{11}$$

Coefficients A and B are determined from conditions at the base space boundaries, *i.e.* at the junction ($x = 0$) and in the rear ($x = H$) and are expressed by:

1) At, $x = 0$, at the junction emitter-base (n/p) surface

$$D(\omega,T)\cdot\left.\frac{\partial\delta(x,z,T,\omega)}{\partial x}\right|_{x=0} = Sf\cdot\delta(x,z,T,\omega)\big|_{x=0} \tag{12}$$

2) At, $x = H$, the back surface (p/p+)

$$D(\omega,T)\cdot\left.\frac{\partial\delta(x,z,\omega)}{\partial x}\right|_{x=H} = -Sb\cdot\delta(x,z,T,\omega)\big|_{x=H} \tag{13}$$

where Sf is the junction surface recombination velocity [17]. It can be represented into the sum of two terms. We then get:

$$Sf = Sf_O + Sf_j \tag{14}$$

Sf_O, defines the lost electrical charges velocity at the junction surface and is related to shunt resistance in establishing the electric model equivalent to the illuminated solar cell [17] [18].

Sf_j is the velocity of the flow of electrical charges that crosses through the external charge and defines the solar cell operating point [18].

Sb is the excess minority carrier recombination velocity at the rear surface of the solar cell's base (p/p+) [19]. It characterizes the electric field in this area (low-high junction), which allows the return of minority carrier to the junction to participate in the photocurrent.

3. Results and Discussions

3.1. Diffusion Coefficient: Bode and Nyquist Diagrams for Différent Temperatures

The amplitude and phase of the diffusion coefficient under different temperatures, are represented versus frequency, through the **Figure 3** and **Figure 4**.

For a given temperature, the diffusion coefficient is maximum and virtually constant when the frequency is low. Indeed, in a quasi-static regime the diffusion of minority carriers is not influenced by the frequency which explains the level observed. On the other hand, in a dynamic frequency regime, repeated arousals lead to a problem of relaxation of the solar cell which is a blocking factor for the diffusion of minority carriers. In addition, an increase in temperature decreases the diffusion of minority carriers. The diffusion is more sensitive to temperature in a quasi-static regime.

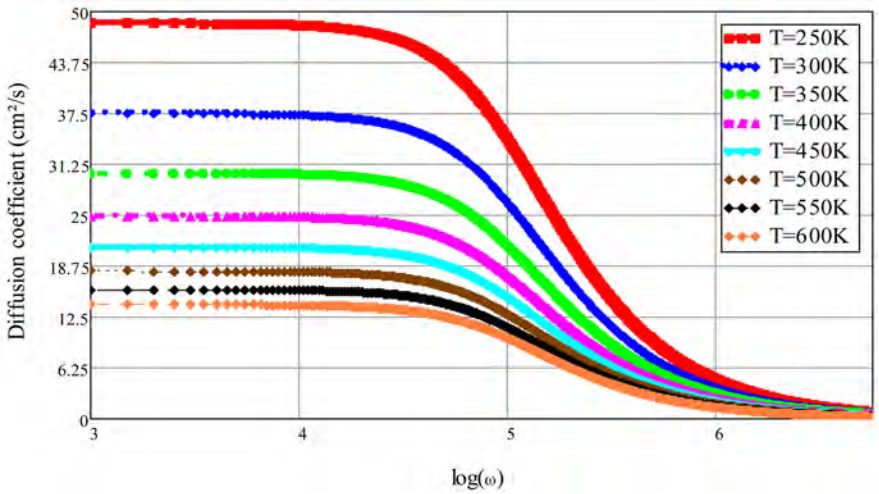

Figure 3. Diffusion coefficient versus frequency for different temperatures.

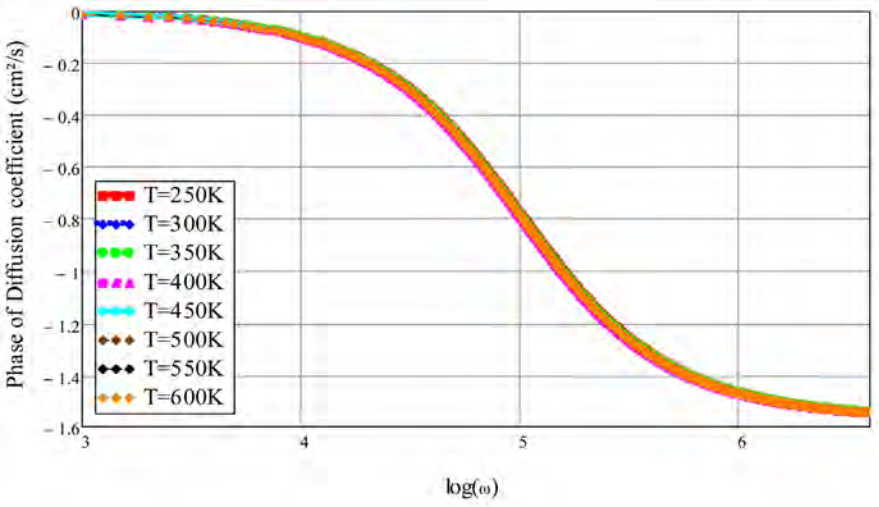

Figure 4. Diffusion coefficient phase versus frequency for different temperatures.

In a dynamic frequency regime, the problem of relaxation in the solar cell, blocks the diffusion of the minority carriers which gives a negative phase of the diffusion coefficient. The Nyquist diagram is shown in Figure 5.

We find that the radius of the semicircles decreases according to the temperature with a shift from the center of the circles to the origin of the axes. The semicircle indicates a resistor in parallel with a capacitor, so gives rise to a single time constant. The deformation of the semicircles, corresponds to a time constant, time dependent. The exploitation of the half-circle radius allows to determine electrical parameters characteristic of the equivalent electric model.

3.2. Photocurrent

The density of photocurrent at the junction is obtained from the density of minority carriers in the base and is given by the following expression:

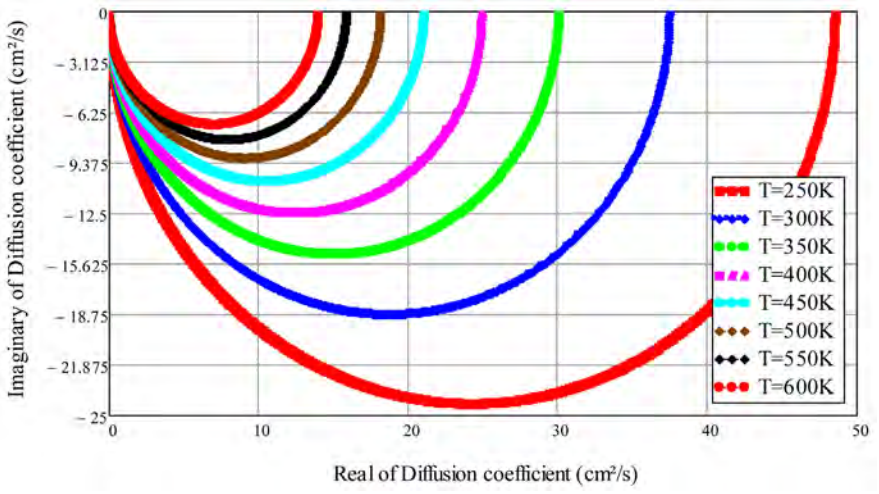

Figure 5. Imaginary component versus real component of diffusion coefficient for different temperatures.

$$J_{Ph}(\omega,T,Sf,Sb)=q\cdot D(\omega,T)\cdot\left.\frac{\partial\delta(x,\omega,T,Sf,Sb)}{\partial x}\right|_{x=0} \tag{15}$$

where q is the elementary electron charge.

Figure 6 shows ac photocurrent density versus the junction surface recombination velocity for different temperatures.

3.3. Deduction of the $Sb(\omega, T)$ Expression

The representation of photocurrent density according to the junction recombination velocity of minority carriers shows that, for very large *Sf*, a bearing sets up and corresponds to the short-circuit current density (Jphsc). So in this junction recombination velocity interval, we can write [20]:

$$\frac{\partial J_{ph}(\omega,T,Sf,Sb)}{\partial Sf}=0 \tag{16}$$

The solution of this equation leads to expressions of the ac recombination velocity in the back surface, given by:

$$Sb1(\omega,T)=\frac{D(\omega,T)\cdot\sinh\left(\dfrac{H}{L(\omega,T)}\right)}{L(\omega,T)\cdot\left[\cosh\left(\dfrac{H}{L(\omega,T)}\right)-1\right]} \tag{17}$$

$$Sb2(\omega,T)=-\frac{D(\omega,T)}{L(\omega,T)}\cdot\tanh\left(\frac{H}{L(\omega,T)}\right) \tag{18}$$

Previous studies have looked at the second solution given to the Equation (18). Our study will consider this second solution, whose module and phase are represented versus the logarithm of the modulation frequency by the **Figure 7** and **Figure 8**, for different temperatures.

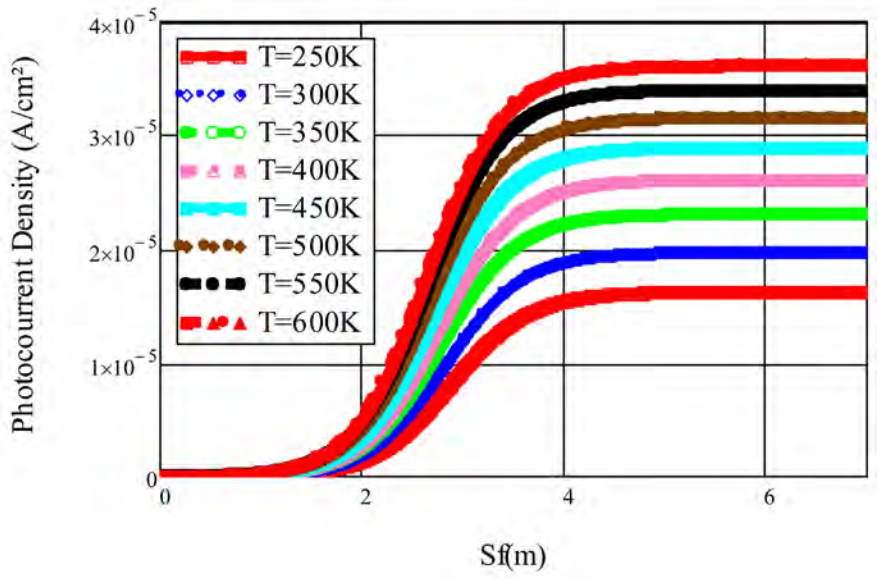

Figure 6. Photocurrent density versus junction surface recombination velocity under temperature influence. $\omega = 10^5$ rad/s, $H = 0.025$ cm; $z = 0.017$ cm; $\lambda = 0.9$ μm.

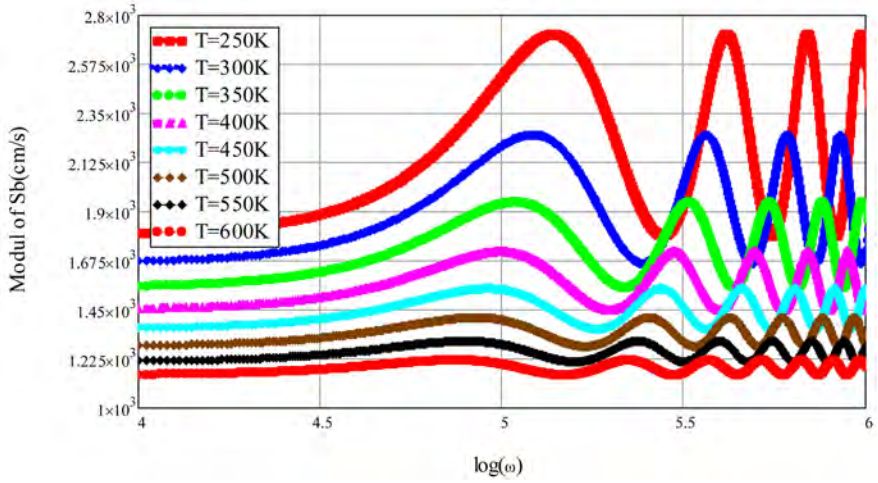

Figure 7. Module of Sb versus frequency for different temperatures.

Ac Sb in complex form (real and imaginary components) is presented by analogy of the effect of Maxwell-Wagner-Sillars (MWS) model [21] [22] [23] and can be written as:

$$Sb(\omega,T) = Sb'(\omega,T) + J \cdot Sb''(\omega,T) \tag{19}$$

We define the ac phase for a given temperature, as following equation:

$$\tan\left(\phi(\omega,T)\right) = \frac{Sb''(\omega,T)}{Sb'(\omega,T)} \tag{20}$$

$Sb_{ampl}(\omega,T)$ and $\phi(\omega,T)$ correspond for a given temperature T, to the amplitude and phase component of ***Sb***.

At low frequencies (≤10^4 rad/s), the stationary regime is observed and gives constant amplitudes for each T. These amplitudes decrease with the temperature T. Beyond the frequency ($\gg 10^4$ rad/s), the cut-off frequency (ω_c, $sb(T)$) is determined for each temperature. It is noted that the cut-off frequency decreases with the temperature T, as does the amplitude ($\boldsymbol{Sb_{ampl}}$) and on the other hand the frequency ($\omega_{Sb}(T)$) of oscillations increases, in the part corresponding to the dynamic regime(See Table 1).

The phase is represented versus the logarithm of the modulation frequency. The part corresponding to the dynamic regime shows sinusoidal oscillations between positive and negative values of the phase, amplitude (Φampl) that decreases with the temperature T and the frequency of oscillations (ω_Φ), which on the other hand increases with the temperature T (See Table 2).

Figure 9 produces the Niquyst diagram of the excess minority carrier recombination velocity for different temperatures. The radius of the resulting circles decreases with temperature, with a shift from the center of the circles to the origin of the axes (See Table 3 and Table 4).

Figure 10 and Figure 11 show that the sb recombination velocity decreases with temperature. Indeed, when the temperature is above the optimum temperature (Topt-300 K) [24], thermal agitation leads to the exponential evolution of umklapp processes that predict a temperature dependence of thermal conductivity

Table 1. Ac Sb periods for different temperatures.

T(K)	250	300	350	400	450	500	550	600
ω_c (rad/s)	$10^{4.34}$	$10^{4.38}$	$10^{4.33}$	$10^{4.24}$	$10^{4.23}$	$10^{4.24}$	$10^{4.06}$	$10^{4.18}$
$Sb\,(T)$ (cm/s)	1837.1	1813.1	1583.9	1523.8	1377	1295.5	1240	1156.3
Sb, ampl (cm/s)	2711.3	2118.7	1940.9	1650.4	1547.4	1414.5	1280.5	1218.6
ω (rad/s)	$10^{5.14}$	$10^{5.00}$	$10^{5.04}$	$10^{4.91}$	$10^{4.96}$	$10^{4.93}$	$10^{4.82}$	$10^{4.87}$

Table 2. Ac Sb, phase period for different temperatures.

T(K)	250	300	350	400	450	500	550	600
Φ ampl	0.20	0.15	0.11	0.08	0.06	0.04	0.03	0.02
ω_Φ (rad/s)	$10^{4.85}$	$10^{4.79}$	$10^{4.74}$	$10^{4.70}$	$10^{4.67}$	$10^{4.64}$	$10^{4.61}$	$10^{4.57}$

Table 3. Maximum amplitude of the imaginary part of Sb for different temperatures.

T(K)	250	300	350	400	450	500	550	600
$ImSb_{max}$ (cm/s)	459.96	293.63	195.11	132.75	92.77	65.36	47.41	34.63

Table 4. Parallel resistors characterizing Sb for different temperatures.

T(K)	250	300	350	400	450	500	550	600
$Re\,(Sb\,(\mathrm{cm/s}))$	2712	2252	1941	1717	1547	1415	1307	1219
$\frac{1}{Re\left(Sb\left(\mathrm{cm/s}\right)\right)\cdot 10^{-5}}$	36.873	44.405	51.52	58.241	64.641	70.671	76.511	82.034

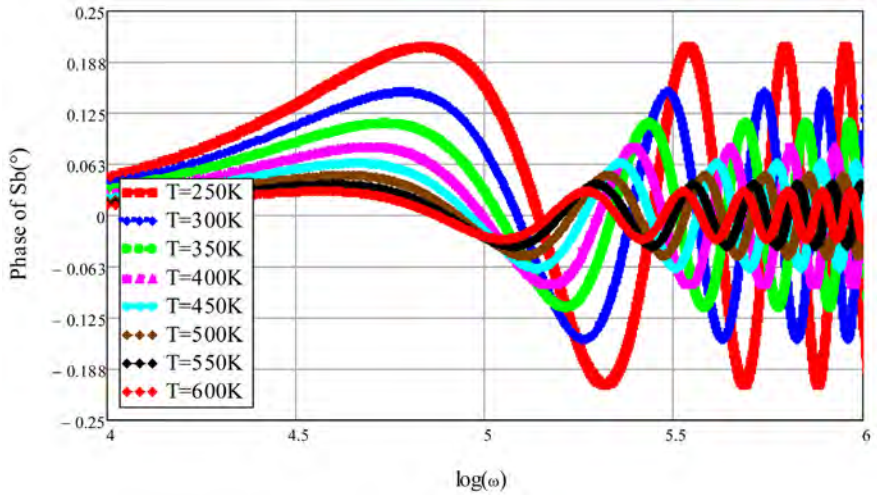

Figure 8. Phase of Sb versus frequency for different temperatures.

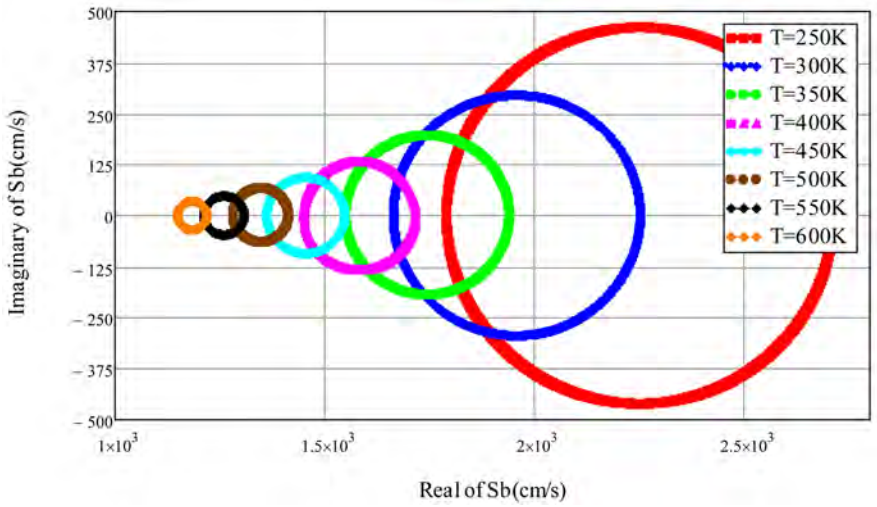

Figure 9. Imaginary compoment versus real compoment of Sb for different Temperatures.

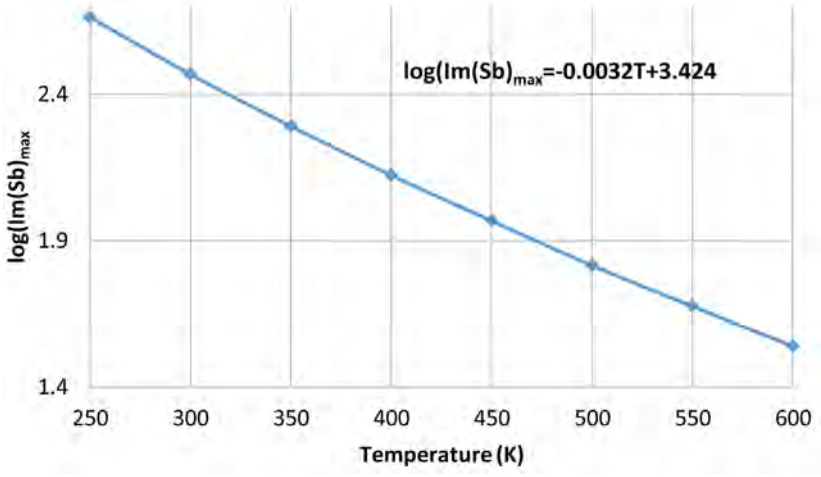

Figure 10. Log(Im(Sb)) versus of temperature.

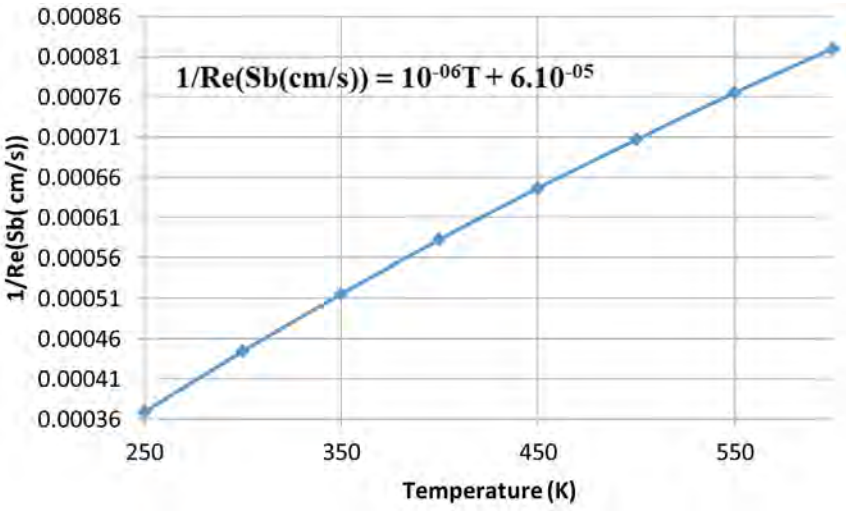

Figure 11. Reciprocal of Sb real part versus temperature.

in $1/T$ [25] [26] [27]. This decreases the mobility of excess minority carriers and results in a decrease in the diffusion coefficient [25] which increases recombination.

The negative phase of the ac Sb recombination velocity and the determination of electrical parameters, with the Bode and Nyquist diagrams, characterizing Sb, allow to determine the equivalent electric model [28] [29].

4. Conclusion

The solar cell's ac back surface (p/p+) recombination velocity that controls the recombination of the excess minority carrier has been determined. Thus, the spectroscopy method allowed the study of the Bode and Nyquist diagrams and extracted certain electrical parameters characterizing the equivalent electric model. The effect of temperature on back surface recombination velocity was explained by umklapp processes.

Conflicts of Interest

The authors declare no conflicts of interest regarding the publication of this paper.

References

[1] Nam, L.Q., *et al.* (1992) *International Journal of Solar Energy*, **11**, 273-279. https://doi.org/10.1080/01425919208909745

[2] Yadav, P., Pandey, K., Tripathi, B., Kumar, C.M., Srivastava, S.K., Singh, P.K. and Kumar, M. (2015) *Solar Energy*, **122**, 1-10. https://doi.org/10.1016/j.solener.2015.08.005

[3] Wise, J.F. (1970) Vertical Junction Hardened Solar Cell. U.S. Patent 3, 690-953.

[4] Gover, A. and Stella, P. (1974) *IEEE Transactions on Electron Devices*, **21**, 351-356. https://doi.org/10.1109/T-ED.1974.17927

[5] Mazhari, B. and Morkoç, H. (1993) *Journal of Physics A*, **73**, 7509-7514.

https://doi.org/10.1063/1.353998

[6] Gueye, M., Diallo, H.L., Moustapha, A.M., Traore, Y., Diatta, I. and Sissoko, G. (2018) *World Journal of Condensed Matter Physics*, **8**, 185-196. http://www.scirp.org/journal/wjcmp https://doi.org/10.4236/wjcmp.2018.84013

[7] Ngom, M.I., Thiam, A., Sahin, G., El Moujtaba, M.A.O., Faye, K., Diouf, M.S. and Sissoko, G. (2015) *International Journal of Pure & Applied Sciences & Technology*, **31**, 65-75.

[8] Diallo, H.L., Dieng, B., Ly, I., Dione, M.M., Ndiaye, M., Lemrabott, O.H., Bako, Z.N., Wereme, A. and Sissoko, G. (2012) *Research Journal of Applied Sciences, Engineering and Technology*, **4**, 2626-2631.

[9] Terheiden, B., Hahn, G., Fath, P. and Bucher, E. (2000) The Lamella Silicon Solar Cell. 16*th European Photovoltaic Solar Energy Conference*, Glasgow, 1-5 May 2000, 1377-1380.

[10] Dieme, N., Zoungrana, M., Mbodji, S., Diallo, H.L., Ndiaye, M., Barro, F.I. and Sissoko, G. (2014) *Research Journal of Applied Sciences, Engineering and Technology*, **7**, 2559-2562. https://doi.org/10.19026/rjaset.7.567

[11] Xing, Y., Han, P., Wang, S., Liang, P., Lou, S., Zhang, Y., Hu, S., Zhu, H., Mi, Y. and Zhao, C. (2013) *Science China Technological Sciences*, **56**, 2798-2807. https://doi.org/10.1007/s11431-013-5378-z

[12] Heinbockel, J.H. and Walker, G.H. (1988) Three-Dimensional Models of Conventional and Vertical Junction Laser-Photovoltaic Energy Converters. NASA-TM-403919880014727.

[13] Sarfaty, R., Cherkun, A., Pozner, R., Segev, G., Zeierman, E., Flitsanov, Y., Kribus, A. and Rosenwaks, Y. (2011) Vertical Junction Si Micro-Cells for Concentrating Photovoltaics. *Proceedings of the* 26*th European Photovoltaic Solar Energy Conference and Exhibition*, Hamburg, 5-6 September 2011, 145-147.

[14] Sze, S.M. (1981) Physics of Semiconductor Devices. John Wiley & Sons, Hoboken.

[15] Mohammad, S.N. (1987) *Journal of Applied Physics*, **61**, 767-772. https://doi.org/10.1063/1.338230

[16] Kunst, M. and Sanders, A. (1992) *Semiconductor Science and Technology*, **7**, 51-59. https://doi.org/10.1088/0268-1242/7/1/009

[17] Sissoko, G., Museruka, C., Corréa, A., Gaye, I. and Ndiaye, A.L. (1996) *Renewable Energy*, **3**, 1487-1490.

[18] Sissoko, G., Nanéma, E., Corréa, A., Biteye, P.M., Adj, M. and Ndiaye, A.L. (1996) *Renewable Energy*, **3**, 1848-1851.

[19] Bocande, Y.L., Corréa, A., Gaye, I., Sow, M.L. and Sissoko, G. (1994) Bulk and Surfaces Parameters Determination in High Efficiency Si Solar Cells. *Proceedings of the World Renewable Energy Congress*, Vol. 3, 1698-1700.

[20] Stamboulis, A., Baillie, C.A. and Peijs, T. (2001) *Composites Part A*, **32**, 1105-1115. https://doi.org/10.1016/S1359-835X(01)00032-X

[21] Maxwell, J.C. (1982) Electricity and Magnetism. Calerdon, Oxford, 1.

[22] Lestriez, B. and Maazouz, A. (1998) *Polymer*, **39**, 6733-6742. https://doi.org/10.1016/S0032-3861(98)00093-7

[23] Bottcher, C.J.F. and Bordewijik, P. (1979) *Advances in Molecular Relaxation and Interaction Processes*, **14**, 161-162. https://doi.org/10.1016/0378-4487(79)80023-0

[24] Mane, R., Ly, I., Wade, M., Datta, I., Douf, M.S., Traore, Y., Ndiaye, M., Tamba, S.

and Sissoko, G. (2017) *Energy and Power Engineering*, **9**, 1-10. https://doi.org/10.4236/epe.2017.91001

[25] Berman, R. (1951) *Nature*, **168**, 277-280. https://doi.org/10.1038/168277a0

[26] Casimir, H.B.G. (1938) *Physica*, **5**, 495-500. https://doi.org/10.1016/S0031-8914(38)80162-2

[27] Kittel, C. (1972) Introduction à la Physique de l'état Solide. 284-285.

[28] Fatimata, B.A., Seibou, B., Wade, M., Diouf, M.S., Ly, I. and Sissoko, G. (2016) *International Journal of Electronics & Communication*, **4**, 1-11.

[29] El Hadji, N., Sahin, G., Thiam, A., Dieng, M., Diallo, H.L., Ndiaye, M. and Sissoko, G. (2015) *Journal of Applied Mathematics and Physics*, **3**, 1522-1535. https://doi.org/10.4236/jamp.2015.311177

Journal of Modern Physics, 2019, 10, 1247-1254
https://www.scirp.org/journal/jmp
ISSN Online: 2153-120X
ISSN Print: 2153-1196

Disentanglement of a Singlet Spin State in a Coincidence Stern-Gerlach Device

Per-Olof Westlund[1], **Håkan Wennerström**[2]

[1]Department of Chemistry, Theoretical Chemistry, Umeå University, Umeå, Sweden
[2]Department of Physical Chemistry, Lund University, Lund, Sweden
Email: per-olof.westlund@umu.se

How to cite this paper: Westlund, P.-O. and Wennerström, H. (2019) Disentanglement of a Singlet Spin State in a Coincidence Stern-Gerlach Device. *Journal of Modern Physics*, **10**, 1247-1254.

https://doi.org/10.4236/jmp.2019.1010083

Received: May 8, 2019
Accepted: September 20, 2019
Published: September 23, 2019

Abstract

We analyze the spin coincidence experiment considered by Bell in the derivation of Bells theorem. We solve the equation of motion for the spin system with a spin Hamiltonian, H_z, where the magnetic field is only in the z-direction. For the specific case of the coincidence experiment where the two magnets have the same orientation the Hamiltonian H_z commutes with the total spin I_z, which thus emerges as a constant of the motion. Bells argument is then that an observation of spin up at one magnet A necessarily implies spin down at the other B. For an isolated spin system A-B with classical translational degrees of freedom and an initial spin singlet state there is no force on the spin particles A and B. The spins are fully entangled but none of the spin particles A or B are deflected by the Stern-Gerlach magnets. This result is not compatible with Bells assumption that spin 1/2 particles are deflected in a Stern-Gerlach device. Assuming a more realistic Hamiltonian $H_z + H_x$ including a gradient in x direction the total I_z is not conserved and fully entanglement is not expected in this case. The conclusion is that Bells theorem is not applicable to spin coincidence measurement originally discussed by Bell.

Keywords

Bells Theorem, Disentanglement, Stern-Gerlach Coincident Measurement, Singlet Spin State

1. Introduction

In 1966, Bell [1] presented an analysis of a thought experiment based on independent measurements of the spin state of two initially correlated particles. Using an example advocated by Bohm and Aharonov [2] he described the experiment as follows:

> Consider a pair of spin-one-half particles formed somehow in the singlet spin state and moving freely in opposite direc-

> tions. Measurements can be made, say by Stern-Gerlach magnets, on selected components of the spins $\sigma_{\mathbf{A}}$ and $\sigma_{\mathbf{B}}$. If measurement of component $\sigma_{\mathbf{A}} \cdot \vec{a}$ where $\vec{a}$ is some unit vector, yield the value +1 then, according to quantum mechanics, measurements of $\sigma_{\mathbf{B}} \cdot \vec{a}$ must yield the value -1 and vice versa. Now we make the hypothesis, and it seems one at least worth considering, that if the two measurements are made at places remote from one another the orientation of the magnet does not influence the result obtained with the other. Since we can predict in advance the result of measuring any chosen component of $\sigma_{\mathbf{B}}$, by previously measuring the same component of $\sigma_{\mathbf{A}}$ it follows that the result of any such a measurement must actually be predetermined [1].

In the present paper, we aim at scrutinizing the arguments used by Bell using recent advances [3] in the formal description of the Stern-Gerlach experiment [4]. A crucial question from our perspective, concerns the anticipated correlation between the observations in the two magnets. Bell's analysis is based on the assumption that the initial spin singlet state is preserved during the passage through the two Stern-Gerlach devises. We argue below that there is a coupling between the spin and translational degrees of freedom caused by inhomogeneities in the magnet field. This coupling leads to changes in the spin state and a partial disentanglement of the initial singlet state.

2. The Stern-Gerlach Setup and Its Application to Coincidence Measurements

The essential ingredients in a Stern-Gerlach experiment is i) a source of spin particles, for simplicity we consider $I = 1/2$ particles. The source should give particles of as well-defined speed as possible. Through a slit system particles are selected to propagate in a narrow solid angle, chosen here to be in the y-direction. The particles then enter the gap of a magnet where the main component, B_z of the field B is perpendicular to the direction of propagation. The field B is inhomogeneous with a gradient $\frac{dB_z}{dz}$ in the z-direction. It follows from Maxwells laws that there is also a matching gradient in some other direction; in the SG case the x-direction. Using such a setup Stern and Gerlach observed [4] that silver atoms, later realized to have spin 1/2, were deflected an amount $\pm\Delta z$ in the gradient. Only these two alternatives were observed and the degree of deflection was later found to be consistent with estimates of the magnetic moment associated with the spin of an electron. The, empirical, conclusion was that the silver atoms passed through the magnet as if they were either in the $I_z = +1/2$ or $I_z = -1/2$ state, with equal probability. In the conventional, textbook analysis of the experiment the translational motion is described classically and one leaves the question open of how a spin of initially unspecified polarization appears as polarized along the direction of the magnetic field [5]. By analyzing how the predicted outcome of the experiment depended on the relative orientation of the two magnets Bell found that the expected observation at one magnet depended on the orientation of the second magnet in spite of the fact that there was no direct physical interaction between the

particles once they had left the source. This observation, later coined *Bells theorem*, has given rise to a large discussion concerning non-locality effects in quantum systems. [6] In later years the discussion of this effect has mainly been concentrated on photon systems. The present paper is solely concerned with the discussion of the original coincidence spin measurement argument.

Consider the special case when the two magnets have the same orientation in the xz-plane chosen to be the z direction. According to the original SG observation the spin particle reaches the detector of magnet A at say position $+\Delta z$ indicating that $I_{zA} = +1/2$. What is the expected observation for the other particle of the pair at the second magnet? Following Bohms reasoning Bell concluded that by necessity $I_{zB} = -1/2$ for this particle and it then should be observed at $-\Delta z$ in the second magnet. To see the basis for this conclusion considered first the spin Hamiltonian

$$H_z \equiv H_{zA} + H_{zB} = [-\gamma\hbar[B_z + \frac{dB_z}{dz}z(t)]I_z + [-\gamma\hbar[B_z + \frac{dB_z}{dz}z(t)]I_z. \quad (1)$$

where γ and $\hbar$ have their usual meaning. Equation (1) is typically used to analyze the SG experiment in elementary texts. It follows that the total spin in the z-direction $I_z = I_{zA} + I_{zB}$ commutes with the Hamiltonian and I_z is a constant of the motion. For a singlet state, $|S_0\rangle$, it has a value $I_z = 0$ so $I_{zA} = 1/2$ implies $I_{zB} = -1/2$, or vice versa. By necessity there is, within the magnet, also a field in the x-direction and thus two terms

$$H_x \equiv H_{xA} + H_{xB} = [-\gamma\hbar\frac{dB_z}{dx}x(t)I_x]_A + -\gamma\hbar\frac{dB_z}{dx}x(t)I_x]_B \quad (2)$$

in the spin Hamiltonian. Bohm argued that the gradient in the x-direction was of negligible consequence [7,8] so that it is a good approximation to analyze the experiment on the basis of a further simplified Hamiltonian H_z. Still I_z is strictly not a constant of the motion.

The analysis of the coincidence experiment by Bell is based on two basic arguments. The first is the empirical finding of the SG experiment that a spin 1/2 particle is deflected an amount $\pm\Delta z$. The second is that for parallel orientations of the two magnets the total spin I_z is conserved which follows theoretically using the Hamiltonian H_z. The dependence of the outcome on the relative orientation of the two magnets then follows in a straightforward way. We note that the two basic arguments have different origins; one empirical and one theoretical.

3. Describing the Stern-Gerlach Experiment through the Hamiltonian H_z

It is implicit in the Hamiltoinan H_z that the translational degrees of freedom are described classically. We now investigate to which extent this Hamiltonian describes the dynamics of spin particles in the SG magnet. In contrast to the original SG experiment the initial spin state is known and represented by an entangled singlet in the coincidence setup. The equation of motion for the spin "density operator", $\sigma(t)$,

is

$$\frac{d}{dt}\sigma(t) = -\frac{i}{\hbar}[H_z, \sigma(t)] \tag{3}$$

To illustrate our point it is sufficient to consider the special case with only one Stern-Gerlach device. Then

$$H_z = H_{zA} \tag{4}$$

For two I = 1/2 particles there are 16 spin density operator components. For the case with a magnetic field solely along the z-direction only four components couple; $|S_0 >< S_0|, |S_0 >< T_0|, |T_0 >< S_0|, |T_0 >< T_0|$. Here $|S_0\rangle$ denotes the singlet state and $|T_0\rangle$ the triplet state with $S_z = 0$. The equation of motion,

$$\frac{d}{dt}\begin{bmatrix} \sigma_{AB}(t)_{|S_0><S_0|} \\ \sigma_{AB}(t)_{|S_0><T_0|} \\ \sigma_{AB}(t)_{|T_0><S_0|} \\ \sigma_{AB}(t)_{|T_0><T_0|} \end{bmatrix} = \tag{5}$$

$$\frac{1}{2}\begin{bmatrix} 0 & -i\omega_A(z) & i\omega_A(z) & 0 \\ -i\omega_A(z) & 0 & 0 & i\omega_A(z) \\ i\omega_A(z) & 0 & 0 & -i\omega_A(z) \\ 0 & i\omega_A(z) & -i\omega_A(z) & 0 \end{bmatrix}\begin{bmatrix} \sigma_{AB}(t)_{|S_0><S_0|} \\ \sigma_{AB}(t)_{|S_0><T_0|} \\ \sigma_{AB}(t)_{|T_0><S_0|} \\ \sigma_{AB}(t)_{|T_0><T_0|} \end{bmatrix}$$

where $\omega_A(z) \equiv -\gamma_A[B_z^A + \frac{dB_z^A}{dz_A} z_A]$. With the initial condition $\rho(0)_{|S_0><S_0|} = 1$, the solution is (see SI)

$$\begin{aligned} \sigma_{AB}(t)_{|S_0><S_0|} &= \tfrac{1}{2}(1 + cos(\omega_A(z)t) \\ \sigma_{AB}(t)_{|S_0><T_0|} &= -\tfrac{1}{2}(i * sin(\omega_A(z)t) \\ \sigma_{AB}(t)_{|T_0><S_0|} &= \tfrac{1}{2}(i * sin(\omega_A(z)t) \\ \sigma_{AB}(t)_{|T_0><T_0|} &= \tfrac{1}{2}(1 - cos(\omega_A(z)t) \end{aligned}$$

The force, F_A, on the particle A is

$$F_A = \frac{dB_z}{dz}_A \langle I_{z,A}\rangle(t) = 0 \tag{7}$$

since

$$\langle I_{z,A}\rangle(t) = \frac{1}{2}[tr_B\{\sigma_{AB}(t)_{|S_0><T_0|}\} + tr_B\{\sigma_{AB}(t)_{|T_0><S_0|}\}] = 0 \tag{8}$$

It follows that there is no net force on the particles and the Hamiltonian $H_{zA}(H_z)$ is thus inadequate for predicting the empirically based anticipated outcome of the experiment. On the other hand the calculation show that the two separated spins A and B are completely entangled. This indicates that there is an internal inconsistency in Bell's original argument. The Hamiltonian used to motivate that I_z is a constant of motion is inadequate to explain why one observe a spin dependent deflection of particles emerging from a non-magnetic singlet spin state.

4. Implications of Recent Description of the SG Experiment

There has in recent years appeared several theoretical accounts of the SG experiment [9]- [14]. Although clearly different in the approaches

they share the common feature that it is necessary to include a quantum description of the translational motion or other degrees of freedom to account for the observation of two distinct positions $\pm\triangle z$ at the detector for a spin 1/2 particle. This further corroborates the conclusion of the previous section that the Hamiltonian H_z of Equation (1) is inadequate for describing the SG-experiment. A more adequate Hamiltoinan [13, 14] for describing the experiment can be written

$$H = \vec{p}/2m + \gamma\vec{S}\cdot\vec{B}(\hat{r}) \tag{9}$$

where $B(\hat{r})$ is the magnetic field and the hat$(\hat{r})$ is to denote that the spatial coordinate is an operator in the Hamiltonian. In most discussions of the SG experiment the focus is on the magnetic field inside the magnet, neglecting the gradient in the x-direction so that

$$B = B_z + \frac{dB_z}{dz}\hat{z} \tag{10}$$

Based on this expression for the magnetic field the outcome of the S-G experiment is adequately predicted. Using a perturbation approach we [3] could also show that the effect of the gradient in the x-direction is to reduce the deviation for spin particles with initial positions slightly off center. This calculation corroborates Bohms original assertion that the x-gradient has only a small influence. However, it is causing the mouth-like shape found at the detector in the original experiment. When applied to the coincidence measurement the Hamiltonian (9) with the expression for the magnetic field (10), for the respective particles, gives a system where the total spin I_z is conserved. However, there is an important factor missing in the expression for the magnetic field in Equation (10), which refers to the conditions inside the magnet. There is necessarily a zone close to the entrance of the gap of width D in the magnet where the z-component of the field grows from zero to B_z. From Maxwells equations it follows that there are also a gradient of corresponding magnitude in the y-direction, as well as a small contribution from the asymmetry in the x-direction. In [3] we have presented an approximate analytical expression for the field outside the magnet, $y \leq 0$.

$$\begin{aligned} B_z(y,z) &\approx \frac{B_0}{\pi}\{\arctan(\frac{z+D}{y}) - \arctan(\frac{z-D}{y}), \\ B_y(y,z) &\approx -\frac{B_0}{2\pi}\ln\{\frac{y^2+(z+D)^2}{y^2+(z-D)^2},\} \\ B_x &\approx 0. \end{aligned} \tag{11}$$

Using the expression (11) for the field in the Hamiltonian (9) it follows that the commutator becomes

$$[H, I_z] = \gamma(I_{xA}B_{yA}(\hat{y},\hat{z}) + I_{xB}B_{yB}(\hat{y},\hat{z})). \tag{12}$$

This shows that I_z is not a constant of the motion since the commutator of Equation (12) is not zero. To further emphasize the existence of a coupling between spin and translation we note that there is an effect on the momentum in the y-direction in the entrance zone. This is evident from the nonzero value of the commutator $[H, p_y]$, caused by the y-dependence of both B_z and B_y in Equation (11). In the entrance phase there is thus, in general, an energy transfer between spin and translation degrees of freedom.

It is a considerable challenge to solve the equation of motion for the combined spin-translation degrees of freedom. Lacking such a solution we consider possible implications of the coupling between spin and translation by analyzing how the spin energy levels vary as the initially strongly coupled spins separate and move towards their respective magnets. For the sake of illustration let the two magnets be positioned as symmetrically as possible. As the two spin particles move apart they still interact through a dipolar coupling, while the stronger J-coupling is vary local. The dipolar coupling results in two non-degenerate states, $|S_0\rangle$ and $|T_0\rangle$, both with I_z=0, but with different permutation symmetry. In addition there is a degenerate level with states $|T_1\rangle$ and $|T_{-1}\rangle$. As the particles separate the dipolar coupling becomes negligible while there is a growing Zeeman term from the magnetic field. In this limit, and assuming the z-component of the field to be the largest one, the $|T_1\rangle$ and $|T_{-1}\rangle$ levels are separated by a frequency $2\omega(y)$, while the $|S_0\rangle$ and $|T_0\rangle$ states are degenerate with an energy half way between the other levels (See Figure 1). With a perfect symmetry between the two magnets an initial singlet state will remain in that state throughout the passage. However, it is not feasible to have microscopically identical fields in the two magnets. A difference in the z-components of the magnetic fields will result in a mixing of the $|S_0\rangle$ and $|T_0\rangle$ states, while the I_z component is conserved at a value zero. A difference in the B_x or B_y components result in a breaking of the symmetry with respect to both parity and I_z. In Figure 1 it is seen that the energy level for the singlet state by necessity crosses either the level for the $|T_{-1}\rangle$ state, as in the figure, or for the $|T_1\rangle$ state, for a different choice of the sign of the gyromagnetic ratio.

One approach to handle the problem of treating the quantum effects of the translational degree of freedom is to use adiabatic approximation. In the specific example of Figure 1 the adiabatic reasoning would predict that the initial $|S_0\rangle$ state will experience an avoided crossing in the presence of a coupling term and continue in the $|T_1\rangle$ state as the particles enter the magnet. As expected neither the parity nor the I_z value is conserved during the crossover. This argument shows, by example, a realistic mechanism for how the I_z value of the initial singlet state can change during the entrance of the magnet, by referring to the common phenomenon of avoided level crossing .

5. Conclusion

We have analyzed the arguments leading to the formulation of Bells theorem for spin coincidence measurements. The proof of the theorem has two central ingredients. The rule, based on the original Stern-Gerlach observation, that on exit from the SG-setup a spin 1/2 particle is either in the $I_z = +1/2$ or$I_z = -1/2$ state. The second essential feature is that the total spin in the z-direction I_z is conserved. This conservation rule follows from the Hamiltonian Equation (1) usually used in simplified discussions of the SG experiment. However, using the Hamiltonian of Equation (1) and the known initial spin state the equation of motion for the spin can be solved and we find that there is no net force acting on the particle passing through the magnet, as expected for a non-magnetic state. This indicates that there is an internal inconsistency of the original proof of Bells theorem. Recent work [3], [10]- [12] has shown that it is necessary to include a quantum description of the translational motion or other degrees of freedom in order to account for the observed SG effect. The empirical rule used

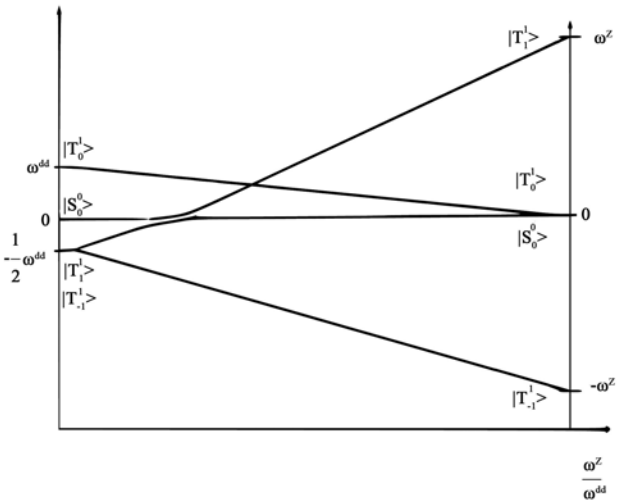

Figure 1. The energy level at zero magnetic field with the eigenstates $|S_0^0\rangle$, $|T_0^1\rangle$, $|T_1^1\rangle$ and $|T_{-1}^1\rangle$ with the dipole-dipole energy ω^{dd}. Increasing Zeeman energy ω^Z to the right, indicating how the energy leves change for the states when $\omega^Z \gg \omega^{dd}$.

by Bell can thus be theoretically derived, but using a different Hamiltonian than Bell used to conclude that I_z of the combined system is conserved. The coupling between spin and translation emerges from the spatial dependence of the magnetic field, which has components in more than one direction. It follows that the I_z of the combined system is not a constant of the motion. We further argue that the most significant deviation of the field from the main z-direction occurs on entering the magnet. The proof of Bells theorem thus rests on an approximation of unknown validity. We have given one illustration of the situation where using conventional argument, where the approximation is specifically giving a misleading result.

Acknowledgements

This work was supported by Swedish Research Council (VR).

Conflicts of Interest

The authors declare no conflict of interest.

References

[1] Bell, J.S. (1966) *Reviews of Modern Physics*, **38**, 447-452.

[2] Bohm, D. and Aharonov, Y. (1957) *Physical Review*, **108**, 1070. https://doi.org/10.1103/PhysRev.108.1070

[3] Wennerstrom, H. and Westlund, P.-O. (2017) *Entropy*, **19**, 186. https://doi.org/10.3390/e19050186

[4] Gerlach, W. and Stern, O. (1922) *Zeitschrift fr Physik*, **9**, 349-352. https://doi.org/10.1007/BF01326983

[5] Einstein, A. and Ehrenfest, P. (1922) *Zeitschrift fr Physik*, **11**, 31-34. https://doi.org/10.1007/BF01328398

[6] Schlosshauer, M., Ed. (2011) Elegance and Enigma. Springer Heidelberg, Dordrecht, London, New York.

[7] Bohm, D. (1952) *Physical Review*, **85**, 180. https://doi.org/10.1103/PhysRev.85.180

[8] Bohm, D. (1951) Quantum Theory. Dover Publications, New York, 326.

[9] Scully, M.O., Shea, R. and McCullen, J. (1978) *Physics Reports*, **43**, 485-498. https://doi.org/10.1016/0370-1573(78)90210-7

[10] Scully, M.O., Lamb Jr., W.E. and Barut, A. (1987) *Foundations of Physics*, **17**, 575-583. https://doi.org/10.1007/BF01882788

[11] Wennerstrom, H. and Westlund, P.-O. (2012) *Physical Chemistry Chemical Physics*, **14**, 1677-1684. https://doi.org/10.1039/C2CP22173J

[12] Wennerstromm H. and Westlund, P.-O. (2013) *Physics Essays*, **26**, 174-180. https://doi.org/10.4006/0836-1398-26.2.174

[13] Utz, M., Levitt, M.H., Cooper, N. and Ulbricht, H. (2015) *Physical Chemistry Chemical Physics*, **17**, 3867-3872. https://doi.org/10.1039/C4CP05606J

[14] Gomis, P. and Perez, A. (2016) *Physical Review A*, **94**, Article ID: 012103. https://doi.org/10.1103/PhysRevA.94.012103

Journal of Modern Physics, 2019, 10, 1255-1270
https://www.scirp.org/journal/jmp
ISSN Online: 2153-120X
ISSN Print: 2153-1196

New Concept of Physics Energy Behaviour and Its Application in Cosmology to Define Gravity Value from Einstein's Relativity

Khelalfa Houssam[1,2]

[1]LGCE of University of Jijel, Jijel, Algeria
[2]Department of Engineering & Applied Science of K.E.C Laboratory, Jijel, Algeria
Email: khelalfahoussam@gmail.com, kec.geotech@gmail.com

How to cite this paper: Houssam, K. (2019) New Concept of Physics Energy Behaviour and Its Application in Cosmology to Define Gravity Value from Einstein's Relativity. *Journal of Modern Physics*, **10**, 1255-1270.
https://doi.org/10.4236/jmp.2019.1010084

Received: May 22, 2019
Accepted: September 20, 2019
Published: September 23, 2019

Abstract

The goal is to define Quantum Gravity Value by combination between our new concept about physics energy behaviour [1] and Einstein relativity's Theory [2]. Our theory is based on the existence of a relationship between energy and vacuum! So it can be considered that the energy is a function of the vacuum ratio (ν). Therefore, we can say that vacuum ratio constitutes a part of space-time. With simple mathematical formula, we can easily obtain the equation of the Energy Vacuum. This gives us the distribution of the energy Vacuum (E) into two parts are inversely proportional from our vacuum energy diagram, the effective energy that the sole responsible for Curvature of space-time fabric, and the lost energy that the responsible of the Gravitational waves [3]. From these equations, we can find that the relationship with Energy and Vacuum ratio is linear which are compatible with Quantum Mechanics laws and Maintains the energy conservation principle. It is also observed that the equations obtained through our theory are Combining relativity and Quantum Mechanics into one continuum. If we take the equations of our theory, we can easily obtain from Curvature of Space-Time Fabric, the Gravity value equation which equals to the square root of energy multiply times the square of the vacuum ratio. On other hand, a curvature matrix and a Time Dilation's Circle are proposed, which gives us a new method to facilitate the calculations of the parameters involved in the Space-Time Curvature.

Keywords

Energy, Vacuum Ratio, Relativity, Quantum Mechanics, Quantum Gravity, Cosmology, New Theory

1. Introduction

Energy (E) is one of the obsessions of humanity concerns since antiquity. The feasibility of formulating the Singularity of Nature was enunciated by Einstein's mathematical formula, demonstrating the equivalency of energy and mass ($E = m * c^2$) [4]-[9]. Despite that statement of principle, it has proven difficult to achieve this goal scientifically by directly merging Relativity and Quantum Mechanics into one continuum [10] [11]. It has been realized that there are four forces in the universe: gravity, electromagnetism, weak and powerful nuclear forces. The universe according to Stephen Hawking is Energy, space and time [12] [13]. Perhaps there is a fifth force in the universe; the force of the Vacuum represented with the vacuum ratio (v)?! "Gravity is one of the mysteries to be solved in order to get a complete understanding of how the Universe works. So, what is gravity and where does it come from? To be honest, we're not entirely sure" [14]. In general relativity, the universe has three dimensions of space and one of time and putting them together we get four-dimensional space-time, which gravity as an emergent effect from the space-time curvature associated with distributions of energy. "Matter tells space how to bend; space tells matter how to move" [15]. Despite intense efforts over the last years, it is far from clear at this time what a consistent theory of quantum gravity will look like and what its main features will be [16]. Although many books and articles on quantum gravity and graviton have been published, but no explanation has yet been provided. In fact, old definition of gravity [17] is not able to solve quantum gravity problem. It means we need a new definition of gravity that should be based on developing old theories and experimental evidences and resolve the renormalization problem [18]. This research is concerned with the unification of general relativity and quantum mechanics into a theory of quantum gravity value.

2. New Concept

The relation of the Space-Time Fabric to a Cosmic Energy impact during their interaction is very complex (**Figure 1(a)**). This may be the reason for the slow progress in the development of a rational method for Curvature of Space-Time Fabric analysis. Very few theoretical models are available. From US; another theory [1] (**Figure 1(b)**) of the interaction between Space-Time Fabric and Cosmic Energy has been proposed to facilitate analysis of Gravitational Waves results, (**Figure 1(c)**). Our theory is based on the existence of a reflection of a part of the energy received by the matrix of the Space-Time Fabric to be interacted with Cosmic Energy (**Figure 1(b)**), which implies a distribution of energy in two parts Equation (1), the effective energy (E'), which is solely responsible for Space-Time Curvature, and the lost energy (E_L) responsible for resultant Gravitational Waves:

$$E = E' + E_L \tag{1}$$

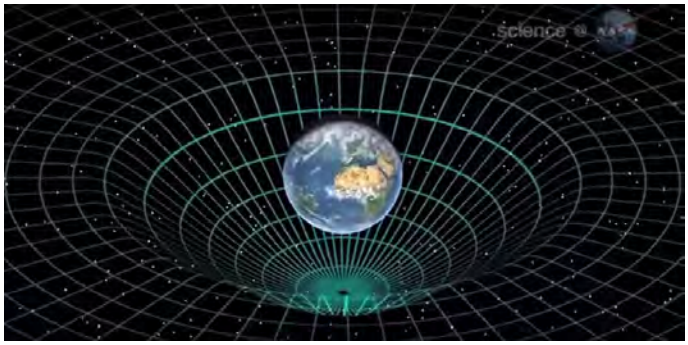

(a)

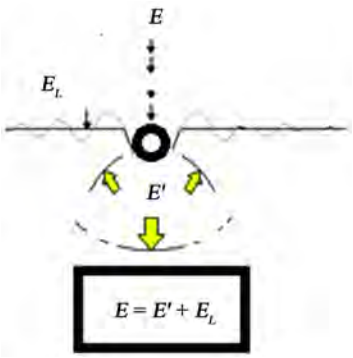

(b)

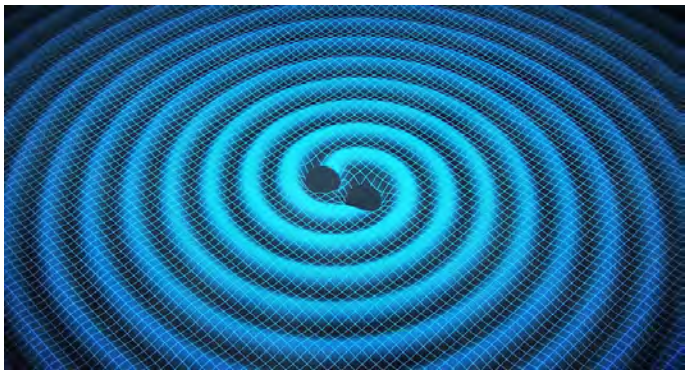

(c)

Figure 1. (a) Curvature of space-time fabric after, einstein [19]; (b) New concept of energy behaviour interacted to space-time fabric after, H. Khelalfa [1]; (c) Gravitational waves [19].

2.1. Space-Time and Energy Interaction Mechanism

Our theory is based to consider the space-time fabric as element volume of a fluid [11] [20] or Continuous media which give us possibility to applied Continuous mechanical environments laws (**Figure 2**) characterized by a vacuum ratio (v). So; The physical Curvature (ΔV) of the Space-Time Fabric caused by Energy pulses (E) will reduce the vacuum ratio (v) by filling the vacuum with energy. Therefore, it can be considered that the energy is a function of the vacuum ratio (e) Equation (2):

$$E = f(v) \tag{2}$$

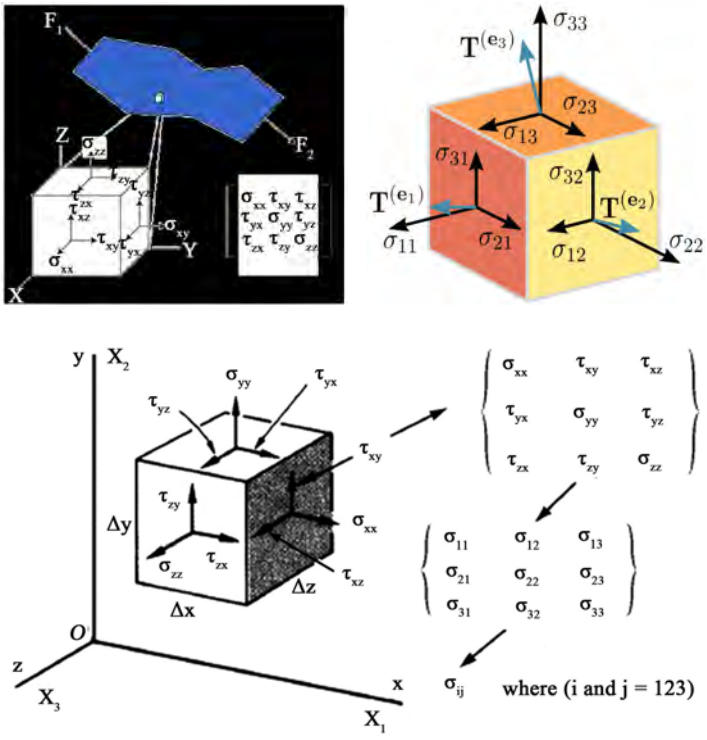

Figure 2. Definition and components of stress of space-time fabric's element volume according to our theory.

When Space-Time Fabric extend in the unknown matter (or dark matter), a high proportion of the Energy impulse is transferred to the porous unknown matter. In this case we will consider that the energy is a function of degree of saturation of unknown matter (S) instead of the vacuum ratio Equation (3).

$$E = f(S) \tag{3}$$

2.2. Case of Space-Time Fabric without Unknown Matter

Without unknown matter, the physical displacement of the Space-Time skeleton (pothole) is the main mechanism of Curvature. During the displacement process (Figure 3), high energy waves propagate through the Space-Time Fabric, Thereby, each Space-Time Fabric element experiences strong impulsion energy for a period of time, resulting from the filling of constituent vacuum ratio in the volume in which they are reduced. Given the Equation (2), we deduce the Equation (4):

$$E' = E \cdot v \tag{4}$$

On the other hand, it is also known that damping (amortization) occurs at infilling of vacuum by energy, which manifests itself as a decrease in the vacuum ratio as a function of time. When the damping (attenuation) in the system exceeds a critical value ($v = 0\%$), there is a starting in the Gravitational waves as a function of time. Given the Equation (2), we deduce the Equation (5):

$$E_p = E \cdot (1 - v) \tag{5}$$

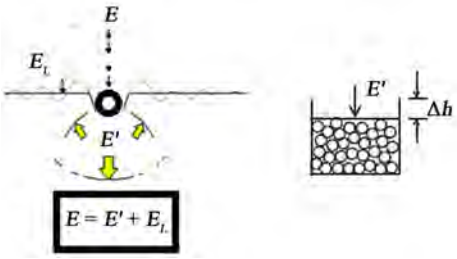

Figure 3. Overall mechanism of space-time fabric and energy interaction in case without unknown matter [1].

2.3. Case of Space-Time Fabric with Unknown (Or Dark) Matter

Space-Time Fabric interaction to Cosmic Energy in saturated Space-Time Fabric with unknown (or dark) matter is different and of course more complex (Figure 4). Its applicability in saturated vacuum is generally considered less effective due to the fact that some of the applied energy is absorbed by interstitial matter (vacuum matter). Considering the Equation (3), we deduce the Equation (6):

$$E' = E \cdot S \tag{6}$$

Moderate levels of energy impulse could cause the displacement of previously vacuum areas in the Space-Time Fabric without unknown matter, Saturation means that these cavities are filled with vacuum matter and that the displacement would be inhibited by unknown matter (vacuum matter) resistance to curvature. However, the really saturated Space-Time Fabric may have few percent of the total vacuum non-occupied by unknown matter. In this condition, the intensity of the Gravitational Waves would be greatly increased due to the low bulk of vacuum matter, but the impact energy still ensure the curvature of the Space-Time Fabric due to the reduction of the rest vacuum volume. Given the Equation (3) we deduce the Equation (7):

$$E_p = E \cdot (1 - S) \tag{7}$$

As mentioned above, the curvature of the rest vacuum volume has a significant effect on the behaviour of saturated Space-Time Fabric with unknown matter under energy impact. It is accepted that unknown matter contains tiny vacuum pockets enclosed in vacuum volume. An accurate assessment of the volume of vacuum pockets trapped in unknown matter is difficult affect the curvature (displacement) of vacuum-matter mixtures and thus significantly alter the process of generating vacuum matter energy. It is therefore essential to take into account the curvature of the vacuum -matter mixture, instead of the curvature of pure matter. Similarly, based on the Equation (3), determining the energy of the vacuum -matter mixture is as follows Equation (8):

$$E_{am} = E_m \cdot S + E_a \cdot (1 - S) \tag{8}$$

where; E_{am} is the energy of the vacuum-matter mixture, E_a is the energy of the vacuum, therefore the lost energy is the energy of the vacuum Equation (9):

$$E_L = E_a = E \cdot (1 - S) \tag{9}$$

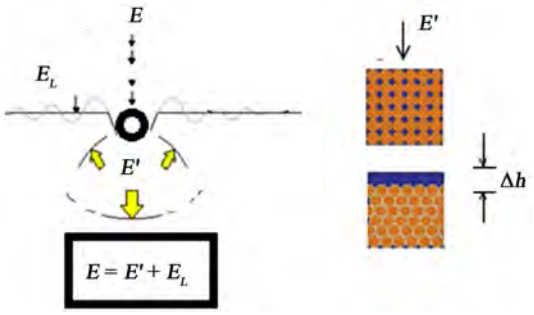

Figure 4. Overall mechanism of Space-Time Fabric and Energy interaction in Case with unknown matter [1].

2.4. Energy Vacuum Diagram

If we take all the equations from 1 to 9 above we can easily obtain the Energy Vacuum Diagram (Figure 5); which is clearly illustrated; that the effective energy is proportional to the degree of saturation and the vacuum ratio as opposed to the lost energy. It can be concluded that the Space-Time Fabric response to the cosmic Energy Interaction depends on the vacuum ratio and degree of saturation. Thus, the level of curvature efficiency depends on the effective energy, too, the lost energy is minimal in saturated Space-Time Fabric with unknown matter (or dark/ others matter).

2.5. Gravitational Waves Intensity

In Space-Time Fabric without unknown matter, the graph of the Gravitational Waves Intensity is divided into four parts (Very Strong, Strong, Low & Limited and Low Gravitational Waves Intensity) as shown in Figure 6(a) to give us an approach to estimate the process of Interaction between cosmic Energy and Space-Time Fabric and its effect (Gravitational Waves). In saturated Space-Time Fabric with unknown (or dark) matter; Assuming the amount of vacuum varies at most between 15% to 25%; which implies a degree of saturation between 75 and at least 85% Figure 6(b), which limits the applicable interaction field of cosmic Energy in saturated Space-Time Fabric, and we can consider the rest as a field not practically interacted. Consequently; The most important remark is that the lost energy in the applicable field is very big.

2.6. Gravity Value from Space-Time Curvature

We proposed a relationship to predict the Space-Time Fabric Curvature is as follows [1]:

$$D = v\sqrt{E} \tag{10}$$

where; D is the Interacted depth of curvature of Space-Time Fabric ($Z = \infty$), E(%) is the cosmic Energy to be interacted, and v (from 0% to 100%/ or 0 to 1) is vacuum ratio that is fundamentally characterised the Space-Time Fabric volume.

If we apply our theory in Space-Time Fabric without unknown matter, given Equation (10), we get Equation (11) [1]:

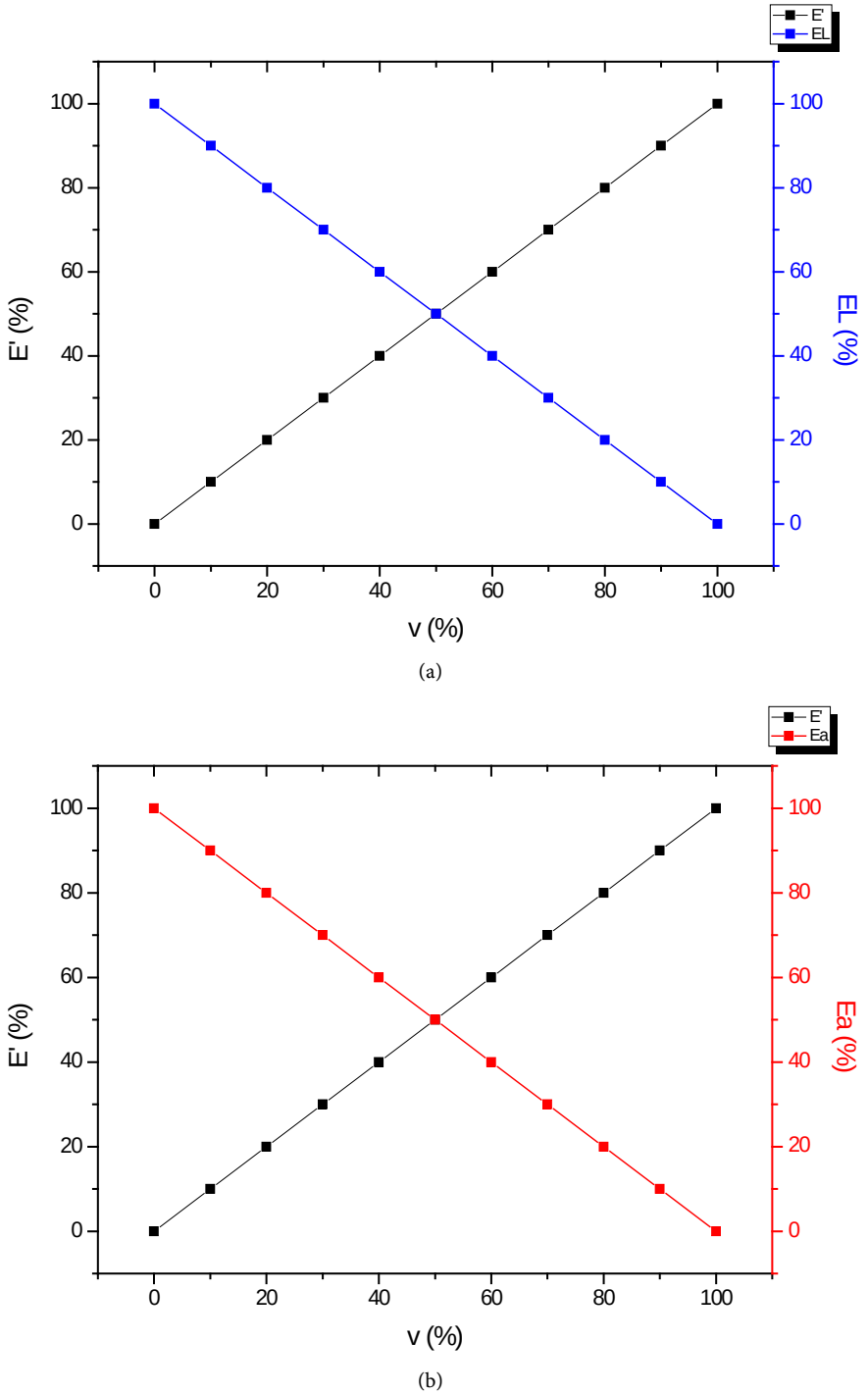

Figure 5. Energy vacuum diagram of interaction of cosmic energy and space-time fabric (a) without unknown matter; (b) with unknown matter [1].

$$D = f(E, v) \tag{11}$$

If we apply our theory in saturated Space-Time Fabric with unknown matter, given Equation (10), we get Equation (12) [1]:

$$D = f(E, S) \tag{12}$$

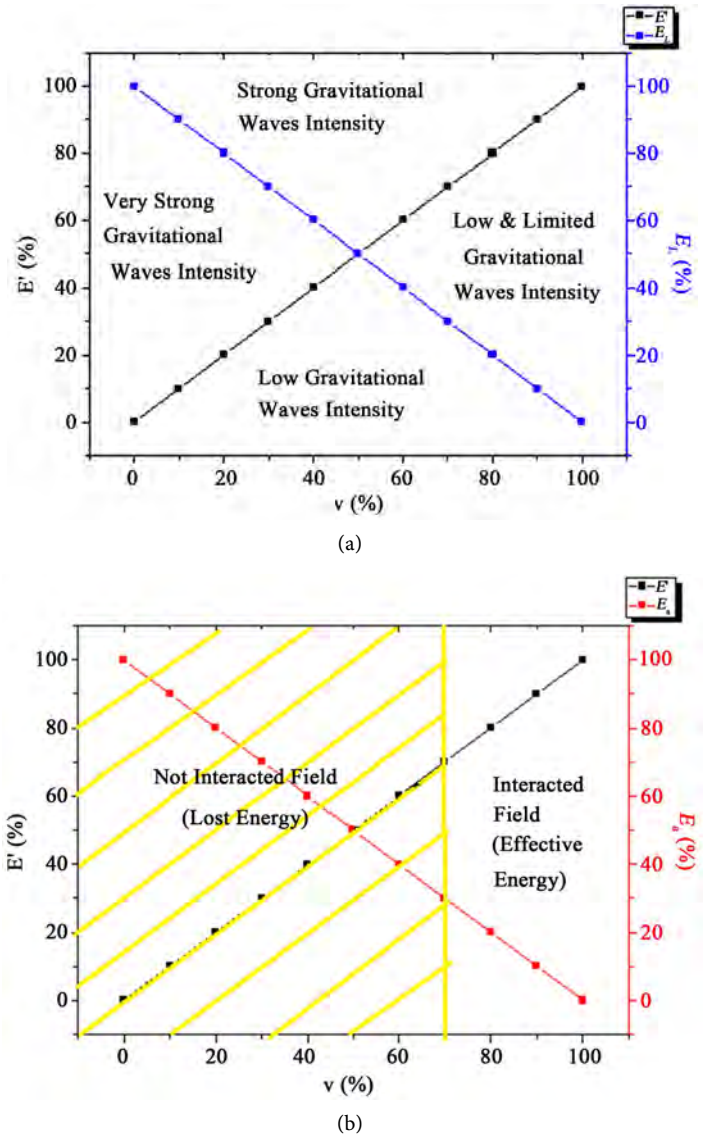

Figure 6. Graph of gravitational waves intensity of interaction of cosmic energy and space-time fabric (a) without unknown matter, (b) with unknown matter [1].

Similarly, for the previous equation, we propose the following equality [1]:

$$v = S \tag{13}$$

When finishes Interaction between a Space-Time Fabric's element volume and Energy, finding a crater which represent Space-Time Curvature (or Gravity from Einstein Relativity) (**Figure 7**) whose volume (ΔV) can be defined by Equation (14) [1]:

$$\Delta V = e \cdot \int_0^D V \cdot \mathrm{d}D \tag{14}$$

where, V is the total volume of the Space-Time Fabric's element, A is the surface/or area of the Interacted Energy, ΔH is the height of the crater (Space-Time Curvature), e is the vacuum ratio (v) and D is the Interacted depth of curvature of Space-Time Fabric mentioned in Equation (10) above.

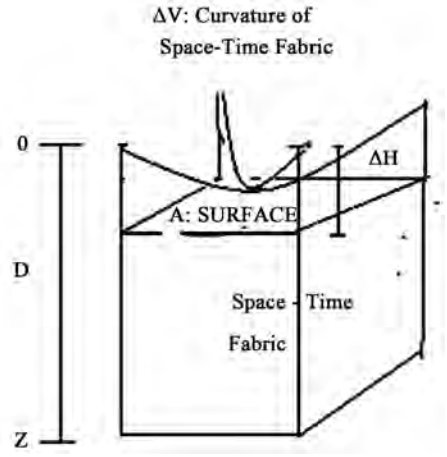

Figure 7. Space-Time Fabric's element volume according to our theory after Energy Interaction [1].

After development of Equation (14) and introducing Equation (11) we deduce Equation (15) [1]:

$$v = \sqrt{\frac{\Delta H}{\sqrt{E}}} \tag{15}$$

after development of Equation (14) and introducing Equation (11) we deduce Equation (15) [1]:

Which implies the Equation (16):

$$\text{Quantum Gravity} = \Delta H = \sqrt{E} \cdot v^2 \tag{16}$$

We found an empirical relationship between the height of the crater (Space-Time Curvature) and interacted depth determined by Equation (17), where we introduce the proposed coefficient K (**Table 1**) [1]:

$$D = K \cdot \Delta H, \quad K = x \cdot v^{-1} \tag{17}$$

$$x = 6.67 \cdot v \tag{18}$$

3. Space-Time Curvature MATRIX

As illustrated in **Figure 8** according to our study; the Space-Time Fabric curvature phenomenon has been summarized in a **curvature cycle** which consists of three basic components, Energy (***E***), times (***T***) and Curvature (***C***), that they are related to each other by three main index properties, over curvature ratio (***OCR***), Curvature index (***Cc***) and anti-gravity index (***Cg***).

If we take all assuming that indexes and components are linearly dependent we can easily obtain a **curvature matrix**, which clearly illustrates that three basic components are the diagonal and the other three main index properties compose the rest of the matrix:

$$\begin{pmatrix} XX & XY & XZ \\ YX & YY & YZ \\ ZX & ZY & ZZ \end{pmatrix} = \begin{pmatrix} T & Cc & OCR \\ Cc & C & Cg \\ OCR & Cg & E \end{pmatrix} \quad \textit{Curvature Matrix}$$

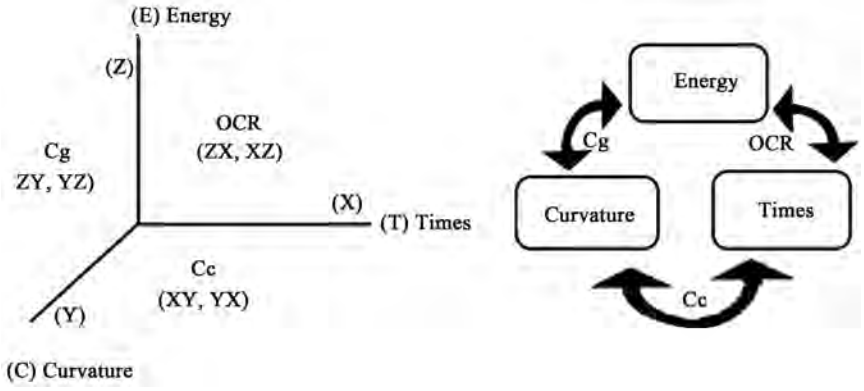

Figure 8. The space-time fabric curvature cycle and its representation on the cartesian coordinate system according to our theory.

Table 1. The values of the coefficient x according to the vacuum ratio.

v	$v < 0.3$	$0.3 < v < 0.5$	$0.5 < v < 0.8$	$v > 0.8$
x	2	3	5	7

Nature of Space-Time Fabric typically display complex concept as a result of missing theory about its interaction with cosmic Energy. A key aspect for the selection of representative Space-Time Fabric parameters is to consider Knowledge of its properties. This nature is based on our theory to determine this characteristics (curvature index ***Cc***, Anti-gravity index ***Cg***, Vacuum ratio ***v***, Over curvature ratio ***OCR***) of the Space-Time Fabric; by using these curvature parameters, it is possible to determine the Curvature (gravity), Times dilation, and amount of interacted Energy etc. While the rigorous selection of Space-Time Fabric parameters requires a deep understanding and proper knowledge of its behaviour. Parameters such as *OCR*, *Cc* and *Cg* play a key role on Curvature and Interacted Energy predictions.

Curvature index (*Cc*) and Anti-gravity index (*Cg*) obtained from our theory are necessary in calculation for Space-Time Fabric curvature. In our hypothesis, we have been looking for a possible relationship between *Cc* and *Cg* indices and general characteristics of Space-Time Fabric. One of these parameters is over curvature ratio (*OCR*). In this study, the effect of *OCR* and vacuum ratio (*v*) on *Cc* and *Cg* indices, was proposed (Figures 9-13). Thus, The hypothesis indicate that *Cc* and *Cg* indices were influenced by *OCR* and *v*, and, a linear relationship between them should be observed. Increasing values of (*v*) will decrease *Cc* and *Cg* values. On the contrary, when *OCR* increases, *Cc* and *Cg* values would also increase. It is possible to say that the *Cc* and *Cg* values are influenced by the same parameters. Therefore it can be concluded that the amount of Curvature depends on the Anti-gravity index, and that the amount of Curvature (*C*) is proportional to the Anti-gravity index (*Cg*) (Figure 14, Table 2). When we compare the time dilation required to stabilize the Curvature, we can talking about *OCR* and *Cc*. Therefore it can be concluded that the time dilation depends on the Curvature index (*Cc*) and over consolidation ratio (*OCR*) (Figure 15,

Table 2), and that the times of Curvature (T) is proportional to the Curvature index (Cc) and over consolidation ratio (OCR), and at the same time that the two latter are proportional.

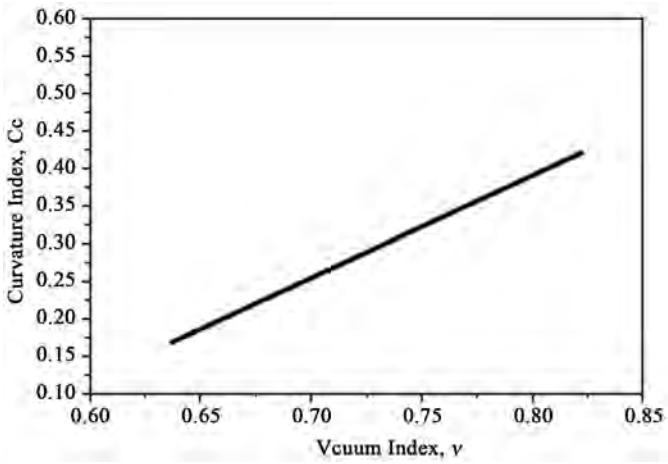

Figure 9. Correlation should be: between Cc and v according to our hypothesis.

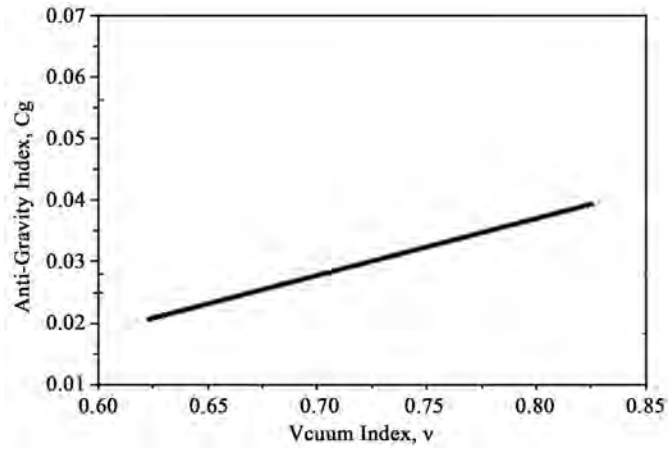

Figure 10. Correlation should be: between Cg and v according to our hypothesis.

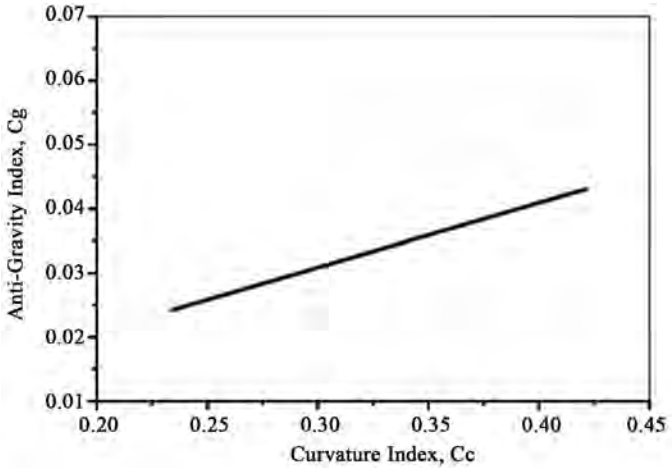

Figure 11. Correlation should be: between Cg and Cc according to our hypothesis.

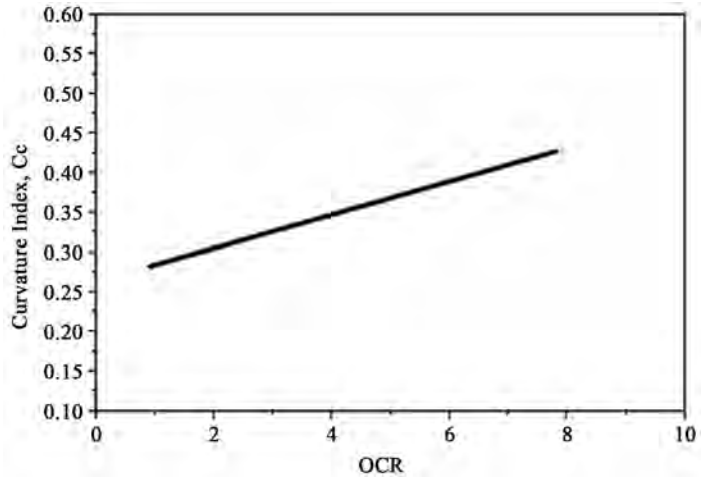

Figure 12. Correlation should be: between Cc and OCR according to our hypothesis.

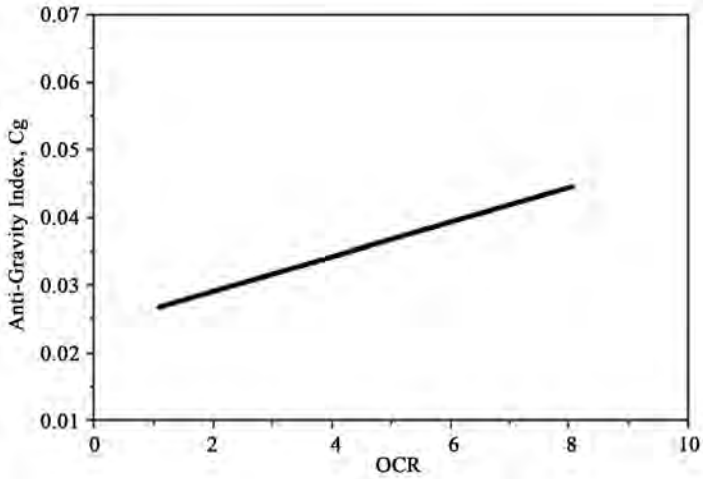

Figure 13. Correlation should be: between Cg and OCR according to our hypothesis.

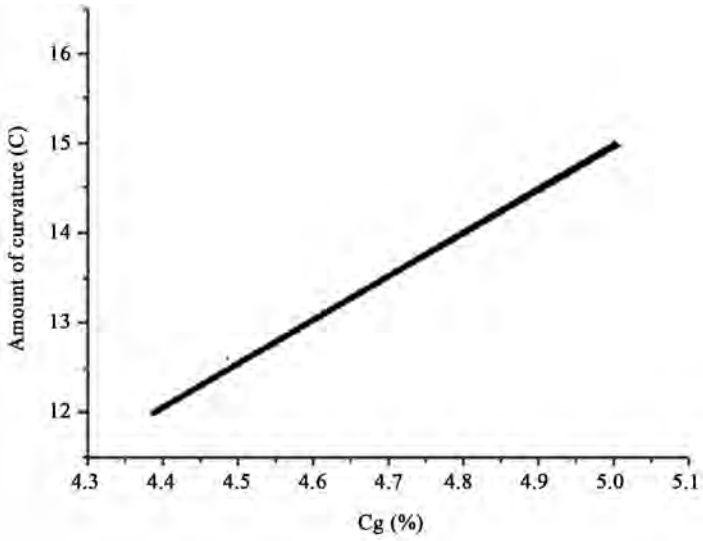

Figure 14. Correlation should be; between Amount of curvature (C) Vs Anti-Gravity index (Cg) according to our hypothesis.

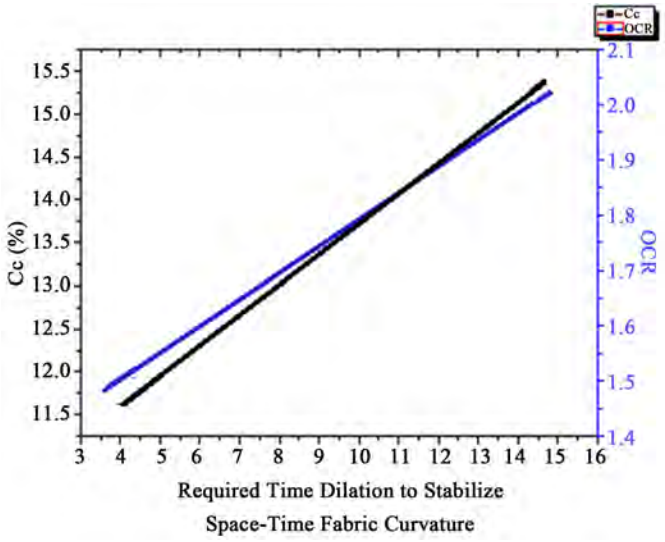

Figure 15. Correlation should be: between Required Time Dilation to Stabilize Space-Time Fabric Curvature Vs. OCR Vs. Cc according to our hypothesis.

Table 2. Correlation parameters of space-time fabric curvature according to our hypothesis.

Parameter	Curvature	Vacuum ratio, v (%)	Energy, E (%)	Curvature Index, Cc	Anti-gravity Index, Cg	Over curvature ratio, OCR
Equation	0 - ∞ (infinity is a black hole)	0 - 100	$=E'+E_L$	$=0.510(v-0.33)$	$=0.15(v+0.007)$	$=E'/E_L$

4. Main Parameters Responsible for Space-Time Fabric Behavior and Time Dilation (*Td*)

Our theory introduced the following factors as the main causes of Time Dilation (*Td*) according to Space-Time Fabric Curvature (**Figure 16**), Equation (19), Equation (20): over curvature ration (*OCR*), Curvature (*C*), and phase (*Phi*) (or time evolution) which depends the Curvature index (*Cc*) as a function of (*t*) and Anti-gravity index (*Cg*) as a function of (*X*). It means that that the change in the value *C* involves changing the value of *Td*.

$$C = OCR \cdot e^{i\varphi} = e^{i(Cc \cdot t + Cg \cdot X)} \tag{19}$$

$$\varphi(X,t) = [0 \sim \Delta H], \ Max.\Delta H = 2\pi \tag{20}$$

In order to carry more than one value and indices to represent the Time Dilation Circle, We used the complex number to explain the curvature characteristics of Space-Time Fabric. We can simply conclude that the final state equals the initial state multiply by the time dilation (*Td*) Equation (21).

$$\varphi(X_1,t_1) = \varphi(X_0,t_0) \cdot Td \tag{21}$$

The most determining factor for the credibility Time Dilation's Circle is its ability to Contain all the characteristics and indices contributing to this phenomenon as illustrates **Figure 16**, Equation (19).

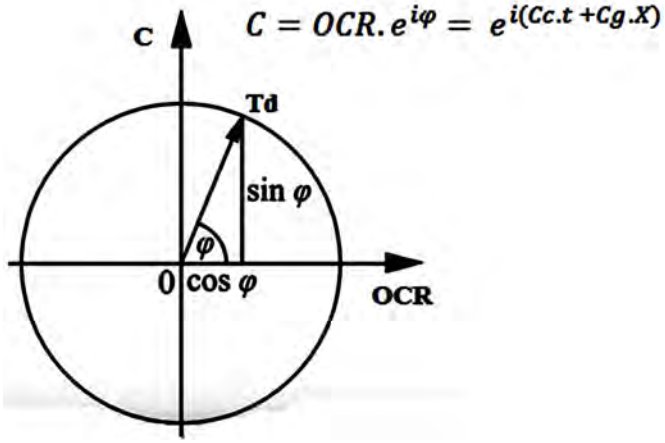

Figure 16. Time dilation's (Td) Circle according to our theory.

5. Conclusions

Is not there yet a complete theory linking Einstein's relativity to quantum mechanics?! Our theory is based on the existence of a relationship between energy and vacuum! So, it can be considered that the energy is a function of the vacuum ratio $E = f(v)$. With simple mathematical formula we can easily obtain the equation of the Energy Vacuum $E = E*v + E*(1-v)$. This gives us the distribution of the energy Vacuum (E) into two parts are inversely proportional from our vacuum energy diagram, the effective energy ($E' = E*v$) that the sole responsible for Curvature of space-time fabric, and the lost energy ($E_L = E*(1-v)$) that the responsible of the Gravitational waves. Therefore, we can say that vacuum ratio which has value from 0% to 100% (or from 0 to 1) is constitutes a part of space-time. From these equations, we can find that the relationship with Energy and Vacuum ratio is linear which are compatible with Quantum Mechanics laws and Maintains the energy conservation principle. It is also observed that the equations obtained through our theory are combining relativity and Quantum Mechanics into one continuum. If we take the equations of our theory, we can easily obtain from Curvature of Space-Time Fabric the Quantum Gravity value equation which equal to the square root of energy multiply times the square of the vacuum ratio ($Quantum\ Gravity = \sqrt{E} * v^2$). From the consequences, we have found after our theory that gravity is energy?! On other hand, our theory consists in considering Space-Time as element volume of a fluid or Continuous media, which gives us possibility for using finite element method (FEM) to resolve and simulate Space-Time Fabric Curvature according to Navier-Stokes equations. Energy Vacuum Diagram as theory can be given new and good explanations in physics about cosmic, quantum and relativity phenomenon, if will make laboratory experiments or cosmic monitoring.

The Interacted Energy consists of displacing Space-Time Fabric and increasing the time dilation. The effectiveness of this hypothesis was demonstrated by the results of the available propositions which verified by curvature matrix. In addition, this matrix gives us a new method to facilitate the calculations of the

parameters involved in the Space-Time Curvature, which gives a great credibility to our hypothesis. Maybe our hypothesis about relationship between Indices involved in curvature cycle based on theoretical results caused by lack of equipments, but can be proved in future by experimental tests in order to compare them by our theory. Indeed, Time Dilation's Circle is considering a good new tool to calculate, interpret and explain this phenomenon; moreover, maybe it can clarify us more other cosmological phenomenon in the future.

Acknowledgements

This work was supported and funded by the K.E.C Laboratory, Department of Engineering & Applied Science of K.E.C Laboratory, Jijel, Algeria, under the project number (PN): KEC.LAB.DEAS.ASTPHY.NCEERQGVP2018N007.

I would like to thank the researchers Dr. Maher Sawaf & Pr. Nidhal Guessoum for his researches and explanation lessons. Also; I would like to thank the Master Khelalfa Hocine & Khalil Agha for their help and support in all steps of this work.

Conflicts of Interest

The author declares no conflicts of interest regarding the publication of this paper.

References

[1] Houssam, K. (2019) New Theory of Soil Response to a High Energy Impact and Its Environmental Consideration. In: Ameen, H. and Sorour, T., Eds., *Sustainability Issues in Environmental Geotechnics*, *Sustainable Civil Infrastructures*, Springer, Cham, 87-104. https://doi.org/10.1007/978-3-030-01929-7_7

[2] Einstein, A. (1920) Relativity: The Special and General Theory. Henry Holt and Company, New York.

[3] Stuver, A.L. (2019) Gravitational Waves. IOP Publishing Ltd., Bristol.

[4] Houssam, K. (2017) New Concept of Physics Energy Behaviour. Department of Engineering & Applied Science of K.E.C. Laboratory, Jijel.

[5] Khelalfa, H. (2019) New Concept of Physics Energy Behaviour and Its Application in Cosmology to Define Gravity Value from Einstein's Relativity. https://www.researchgate.net/publication/330500640_New_Concept_of_physics_energy_behaviour_and_its_application_in_cosmology_to_define_Gravity_value_from_Einstein's_relativity

[6] Torday, J.S. (2018) *Progress in Biophysics and Molecular Biology*, **142**, 23-31.

[7] (1915) Albert Einstein Site. http://www.alberteinsteinsite.com

[8] Einstein, A. (1916) Über die spezielle und die allgemeine Relativitätstheorie. Vieweg, Braunschweig, 1917.
Einstein, A. (1920) Relativity: The Special and General Theory. Methuen & Co. Ltd., London. https://doi.org/10.1007/978-3-663-04964-7_1

[9] Dick, R. (2019) Special and General Relativity: An Introduction to Space-Time and Gravitation. Morgan & Claypool Publishers, San Rafael.
https://doi.org/10.1088/2053-2571/aaf173ch1

[10] Martinetti, P. (2013) *KronoScope*, **13**, 67-84. https://doi.org/10.1163/15685241-12341259

[11] Baryshev, Y.V. (2017) Foundation of Relativistic Astrophysics: Curvature of Riemannian Space versus Relativistic Quantum Field in Minkowski Space.

[12] Hawking, S.W. and Ellis, G.F.R. (1973) The Large-Scale Structure of Space-Time. Cambridge University Press, Cambridge. https://doi.org/10.1017/CBO9780511524646

[13] Minkowski, H. (1952) Space and Time. In: Lorentz, H.A., Einstein, A., Minkowski, H. and Weyl, H., Eds., *The Principle of Relativity*: *A Collection of Original Papers on the Special and General Theory of Relativity*, Dover, New York, 75-91.

[14] https://www.universetoday.com/75705/where-does-gravity-come-from

[15] https://web.archive.org/web/20120206225139/http:/www.alberteinstein.info/gallery/gtext3.html

[16] Hermann Nicolai, H.C. Quantum Gravity and Unified Theories. Max Planck Institute for Gravitational Physics. https://www.aei.mpg.de/18228/03_Quantum_Gravity_and_Unified_Theories

[17] http://www.fnal.gov/pub/today/archive/archive_2012/today12-10-19_NutshellReadMore.html

[18] https://www.quora.com/If-gravitons-are-massless-then-how-can-they-cause-gravity-aforce-dependent-on-mass/answer/Hossein-Javadi-1

[19] Einstein, A. (1930) *Nature*, **125**, 897-898. https://doi.org/10.1038/125897a0

[20] Padmanabhan, T. (2011) *International Journal of Modern Physics*, **20**, 2817-2822.

Journal of Modern Physics, 2019, 10, 1271-1298
https://www.scirp.org/journal/jmp
ISSN Online: 2153-120X
ISSN Print: 2153-1196

Direct Derivation of the Comma 3-Vertex in the Full String Basis

A. Abdurrahman[1], M. Gassem[2]

[1]Department of Physics, Shippensburg University of Pennsylvania, Shippensburg, PA, USA
[2]The Division of Mathematics and Science, South Texas College, McAllen, TX, USA
Email: Ababdu@ship.edu, mgassem@southtexascollege.edu

How to cite this paper: Abdurrahman, A. and Gassem, M. (2019) Direct Derivation of the Comma 3-Vertex in the Full String Basis. *Journal of Modern Physics*, **10**, 1271-1298.
https://doi.org/10.4236/jmp.2019.1010085

Received: August 18, 2019
Accepted: September 26, 2019
Published: September 29, 2019

Abstract

The interacting comma 3-vertex for the bosonic open string in the full string basis is derived using the half string overlap relations directly. Thus avoiding the coherent states technique employed in earlier derivations. The resulting form of the interacting 3-vertex turns out to be precisely the desired expression obtained in terms of the full string oscillator modes. This derivation establishes that the comma 3-vertex and Witten's 3-vertex are identical and therefore are interchangeable.

Keywords

String Theory, Witten's Theory, Open Bosonic String

1. Introduction

Here we are going to give a brief derivation of the transformation matrices between the half string coordinates and the full string coordinates needed for the construction of the half string interacting vertex in terms of the oscillator representation of the full string. For this we shall follow closely the discussion of reference [1] [2] [3] [4] [5]. To make this more concrete, we recall the standard mode expansion for the open bosonic string coordinate

$$x^{\mu}(\sigma)=x_0^{\mu}+\sqrt{2}\sum_{n=1}^{\infty}x_n^{\mu}\cos(n\sigma),\quad \sigma\in[0,\pi] \tag{1}$$

where $\mu=1,2,\cdots,27$ and $x^{27}(\sigma)$ correspond to the ghost part $\phi(\sigma)$. The half string coordinates $x^{L,\mu}(\sigma)$ and $x^{R,\mu}(\sigma)$ for the left and right halves of the string are defined in the usual way

$$\begin{aligned} x^{L,\mu}(\sigma)&=x^{\mu}(\sigma)-x^{\mu}\left(\frac{\pi}{2}\right),\quad \sigma\in\left[0,\frac{\pi}{2}\right]\\ x^{R,\mu}(\sigma)&=x^{\mu}(\pi-\sigma)-x^{\mu}\left(\frac{\pi}{2}\right),\quad \sigma\in\left[0,\frac{\pi}{2}\right]\end{aligned} \tag{2}$$

where both $x^{L,\mu}(\sigma)$ and $x^{R,\mu}(\sigma)$ satisfy the usual Neumann boundary conditions at $\sigma = 0$ and a Dirichlet boundary conditions $\sigma = \pi/2$. Thus they have expansions of the form

$$\begin{aligned} x^{L,\mu}(\sigma) &= \sqrt{2}\sum_{n=1}^{\infty} x_n^{L\mu} \cos(n\sigma), \\ x^{R,\mu}(\sigma) &= \sqrt{2}\sum_{n=1}^{\infty} x_n^{R\mu} \cos(n\sigma) \end{aligned} \tag{3}$$

Comparing Equation (1) and Equation (3) we obtain an expression for the half string modes in terms of the full string modes

$$\begin{aligned} x_n^{L,\mu} &= x_{2n-1}^{\mu} + \sum_{m=1}^{\infty} \sqrt{\frac{2m}{2n-1}} \left[M_{mn}^{1} + M_{mn}^{2} \right] x_{2m}^{\mu}, \\ x_n^{R,\mu} &= -x_{2n-1}^{\mu} + \sum_{m=1}^{\infty} \sqrt{\frac{2m}{2n-1}} \left[M_{mn}^{1} + M_{mn}^{2} \right] x_{2m}^{\mu} \end{aligned} \tag{4}$$

where the change of representation matrices are given by

$$M_{mn}^{1} = \frac{2}{\pi} \sqrt{\frac{2m}{2n-1}} \frac{(-1)^{m+n}}{2m-(2n-1)}, \quad m,n = 1,2,3,\cdots \tag{5}$$

$$M_{mn}^{2} = \frac{2}{\pi} \sqrt{\frac{2m}{2n-1}} \frac{(-1)^{m+n}}{2m+(2n-1)}, \quad m,n = 1,2,3,\cdots \tag{6}$$

Since the transformation in (4) is non singular, one may invert the relation in (4). Inverting (4) we find

$$\begin{aligned} x_{2n-1}^{\mu} &= \frac{1}{2}\left(x_n^{L,\mu} - x_n^{R,\mu} \right), \\ x_{2n}^{\mu} &= \frac{1}{2} \sum_{m=1}^{\infty} \sqrt{\frac{2m-1}{2n}} \left[M_{mn}^{1} - M_{mn}^{2} \right] \left(x_m^{L,\mu} + x_m^{R,\mu} \right) \end{aligned} \tag{7}$$

where $n = 1,2,3,\cdots$.

In the decomposition of the string into right and left pieces in (2), we singled out the midpoint coordinate. Consequently the relationship between x_n^{μ} and $\left(x_n^{L,\mu}, x_n^{R,\mu} \right)$ does not involve the zero mode x_0^{μ} of $x^{\mu}(\sigma)$. At $\sigma = \pi/2$, we have

$$x_M^{\mu} \equiv x^{\mu}\left(\frac{\pi}{2} \right) = x_0^{\mu} + \sqrt{2}\sum_{n=1}^{\infty} x_{2n}^{\mu} \tag{8}$$

and so the center of mass x_0^{μ} may be related to the half string coordinates and the midpoint coordinate

$$x_0^{\mu} = x_M^{\mu} - \frac{\sqrt{2}}{\pi} \sum_{n=1}^{\infty} \frac{(-1)^n}{2n-1} \left(x_n^{L,\mu} + x_n^{R,\mu} \right) \tag{9}$$

Equations (8) and (9) with Equations (4) and (7) complete the equivalence between x_n^{μ}, $n = 0,1,2,\cdots$, and $\left(x_n^{L,\mu}, x_n^{R,\mu}, x_M^{\mu} \right)$, $n = 1,2,3,\cdots$.

For later use we also need the relationships between $\left\{ p_n^{L,\mu}, p_n^{R,\mu}, p_M^{\mu} \right\}_{n=1}^{\infty}$, the half string conjugate momenta and $\left\{ p_n^{\mu} \right\}_{n=0}^{\infty}$, the full string conjugate momenta. Using Dirac quantization procedure

$$\left[x_n^r, p_m^s\right] = i\delta^{rs}\delta_{nm}, \tag{10}$$

we find (thereafter; the space-time index μ is suppressed),

$$p_n^L = \frac{1}{2}p_{2n-1} + \sum_{m=1}^{\infty}\sqrt{\frac{2n-1}{2m}}\left[M_{mn}^1 - M_{mn}^2\right]p_{2m} - \frac{\sqrt{2}}{\pi}\frac{(-1)^n}{2n-1}p_0, \tag{11}$$

$$p_n^R = -\frac{1}{2}p_{2n-1} + \sum_{m=1}^{\infty}\sqrt{\frac{2n-1}{2m}}\left[M_{mn}^1 - M_{mn}^2\right]p_{2m} - \frac{\sqrt{2}}{\pi}\frac{(-1)^n}{2n-1}p_0 \tag{12}$$

and

$$p_M = p_0 \tag{13}$$

To obtain the full string conjugate momenta in terms of the half string conjugate momenta, we need to invert the above relations; skipping the technical details we find

$$\begin{aligned} p_{2n-1} &= p_n^L - p_n^R, \\ p_{2n} &= \sum_{m=1}^{\infty}\sqrt{\frac{2n}{2m-1}}\left[M_{nm}^1 + M_{nm}^2\right]\left(p_m^L + p_m^R\right) + \sqrt{2}(-1)^n p_M \end{aligned} \tag{14}$$

We notice that the existence of the one-to-one correspondence between the half string and the full string degrees of freedom guarantees the existence of the identification

$$\bar{H} = \overline{H_M \otimes H_L \otimes H_R} \tag{15}$$

where $\bar{H}$ stands for the completion of the full string Hilbert space and H_L, H_R, H_M in the tensor product stand for the two half-string Hilbert spaces and the Hilbert space of functions of the mid-point, respectively.

2. The Half-String Overlaps

The half string three interaction vertex of the open bosonic string (V_x^{HS}) have been constructed in the half-string oscillator representation [2] [3]. Here we are interested in constructing the comma three interaction vertex in terms of the oscillator representation of the full string. Here we shall only consider the coordinate piece of the comma three interaction vertex. The ghost part of the vertex (V_ϕ^{HS}) in the bosonic representation is identical to the coordinate piece apart from the ghost mid-point insertions $3i\phi(\pi/2)/2$ required for ghost number conservation at the mid-point. To simplify the calculation we introduce a new set of coordinates and momenta based on a Z_3 Fourier transform[1]

$$\begin{pmatrix} Q^r(\sigma) \\ \bar{Q}^r(\sigma) \\ Q^{3,r}(\sigma) \end{pmatrix} = \frac{1}{\sqrt{3}}\begin{pmatrix} e & \bar{e} & 1 \\ \bar{e} & e & 1 \\ 1 & 1 & 1 \end{pmatrix}\begin{pmatrix} \chi^{1,r}(\sigma) \\ \chi^{2,r}(\sigma) \\ \chi^{3,r}(\sigma) \end{pmatrix} \tag{16}$$

where $e = \exp(2\pi i/3)$ and r refers to the left (L) and right (R) parts of the string. The superscripts 1, 2 and 3 refers to string 1, string 2 and string 3, respectively. Similarly one obtains a new set for the conjugate momenta $\wp^r(\sigma)$,

[1]This technique was first used by D. Gross and A. Jevicki in 1986.

$\bar{\wp}^r(\sigma)$ and $\wp^{3,r}(\sigma)$ as well as a new set for the creation-annihilation operators $\left(B_j^r, B_j^{r\dagger}\right)$. In the Z_3 Fourier space the degrees of freedom in the δ function overlaps equations decouple which result in a considerable reduction of the amount of algebra involved in such calculations as we shall see shortly. Notice that in the Z_3 Fourier space the commutation relations are

$$\left[Q^r(\sigma), \bar{\wp}^s(\sigma')\right] = i\delta^{rs}\delta(\sigma-\sigma') \tag{17}$$

$$\left[\bar{Q}^r(\sigma), \wp^s(\sigma')\right] = i\delta^{rs}\delta(\sigma-\sigma') \tag{18}$$

$$\left[Q^{3,r}(\sigma), \wp^{3,s}(\sigma')\right] = i\delta^{rs}\delta(\sigma-\sigma') \tag{19}$$

Since $\left[Q^r(\sigma), \wp^s(\sigma')\right] \neq i\delta^{rs}\delta(\sigma-\sigma')$, then $Q^r(\sigma)$ and $\wp^r(\sigma)$ are no longer canonical variables. The canonical variables in this case are $Q^r(\sigma)$ and $\bar{\wp}^r(\sigma)$. Thus the Z_3 Fourier transform does not conserve the original commutation relations. The variables $Q^{3,r}(\sigma)$ and $\wp^{3,s}(\sigma)$ are still canonical however. This is a small price to pay for decoupling string three in the Z_3 Fourier space from the other two strings as we shall see in the construction of the comma three interaction vertex. Recall that the overlap equations for the comma three interacting vertex are given by

$$\chi^{j,r}(\sigma) = \chi^{j-1,r-1}(\sigma), \quad 0 \le \sigma \le \pi/2 \tag{20}$$

$$x_M^1 = x_M^2 = x_M^3 \tag{21}$$

for the coordinates (where the mid-point coordinate $x_M \equiv x(\pi/2)$ and the identifications $j-1=0\equiv 3$ and $r-1=0\equiv R$ are understood). The comma coordinates are defined in the usual way [1]

$$\chi^{j,L}(\sigma) = x(\sigma) - x\left(\frac{\pi}{2}\right), \quad 0 \le \sigma \le \pi/2 \tag{22}$$

$$\chi^{j,R}(\sigma) = x(\pi-\sigma) - x\left(\frac{\pi}{2}\right), \quad 0 \le \sigma \le \pi/2 \tag{23}$$

The overlaps for the canonical momenta are given by

$$\wp^{j,r}(\sigma) = -\wp^{j-1,r-1}(\sigma), \quad 0 \le \sigma \le \pi/2 \tag{24}$$

$$\wp_M^1 + \wp_M^2 + \wp_M^3 = 0 \tag{25}$$

where the mid-point momentum is defined in the usual way $\wp_M \equiv -i\partial/\partial x_M = -i\partial/\partial x_0 = p_0$. The comma coordinates and their canonical momenta obey the usual commutation relations

$$\left[\chi^{j,r}(\sigma), \wp^{j,s}(\sigma')\right] = i\delta^{rs}\delta(\sigma-\sigma'), \ r,s = L,R \tag{26}$$

In Z_3 Fourier space of the comma, the overlap equations for the half string coordinates read

$$Q^L(\sigma) = eQ^R(\sigma), \quad 0 \le \sigma \le \pi/2 \tag{27}$$

$$\bar{Q}^L(\sigma) = \bar{e}\bar{Q}^R(\sigma), \quad 0 \le \sigma \le \pi/2 \tag{28}$$

$$Q_M = \bar{Q}_M = 0 \tag{29}$$

$$Q^{3,L}(\sigma)=Q^{3,R}(\sigma),\quad 0\le\sigma\le\pi/2 \tag{30}$$

$$Q_M^3=Q_M^3 \tag{31}$$

where Equation (29) is to be understood as an overlap Equation (*i.e.*, its action on the three vertex is zero). Similarly the canonical momenta of the half string in the Z_3 Fourier space of the comma translate into

$$\wp^L(\sigma)=-e\wp^R(\sigma),\quad 0\le\sigma\le\pi/2 \tag{32}$$

$$\overline{\wp}^L(\sigma)=-\overline{e}\,\overline{\wp}^R(\sigma),\quad 0\le\sigma\le\pi/2 \tag{33}$$

$$\wp^{3,L}(\sigma)=-\wp^{3,R}(\sigma),\quad 0\le\sigma\le\pi/2 \tag{34}$$

$$P_M^3=0 \tag{35}$$

The overlap conditions on $Q^r(\sigma)$ and $\wp^r(\sigma)$ determine the form of the comma three interaction vertex. Thus in the Z_3 Fourier space of the comma the overlap equations separate into two sets. The half string three vertex

$$V_x^{HS}\left(b^{1,r\dagger},b^{2,r\dagger},b^{3,r\dagger}\right)$$

therefore separates into a product of two pieces one depending on $B^{3,r\dagger}$

$$B^{3,r}=\frac{1}{\sqrt{3}}\left(b^{1,r}+b^{2,r}+b^{3,r}\right),\quad r=L,R \tag{36}$$

and the other one depending on $\left(B^{r\dagger},\overline{B}^{r\dagger}\right)$

$$B^r=\frac{1}{\sqrt{3}}\left(eb^{1,r}+\overline{e}b^{2,r}+b^{3,r}\right),\quad r=L,R \tag{37}$$

$$\overline{B}^r=\frac{1}{\sqrt{3}}\left(\overline{e}b^{1,r}+eb^{2,r}+b^{3,r}\right),\quad r=L,R \tag{38}$$

Notice that in this notation we have $B_n^{r\dagger}=\overline{B}_{-n}^r$ and $\overline{B}_n^{r\dagger}=B_{-n}^r$ (where the usual convention $b_{-n}=b_n^\dagger$ applies). Observe that the first of these equations is identical to the overlap equation for the identity vertex. Hence, the comma 3-Vertex takes the form

$$\begin{aligned}\left|V_Q^{HS}\right\rangle=&\int \mathrm{d}Q_M\,\mathrm{d}\overline{Q}_M\,\mathrm{d}Q_M^3\,\delta\left(Q_M\right)\delta\left(\overline{Q}_M\right)\mathrm{e}^{iP_M^3Q_M^3}\\&\times\mathrm{e}^{-\frac{1}{2}\left(B^{3\dagger}|C|B^{3\dagger}\right)-\left(B^\dagger|H|\overline{B^\dagger}\right)}\prod_{r=L,R}\left|0\right\rangle^{3,r}\left|0\right\rangle^r\left|\overline{0}\right\rangle^r\end{aligned} \tag{39}$$

where C and H are infinite dimensional matrices computed in [6] and the integration over Q_M^3 gives $\delta\left(P_M^3\right)$. However $P_M^3=P_0^3$ and so $\delta\left(P_M^3\right)$ is the statements of conservation of momentum at the center of mass of the three strings. Notice that the comma three interaction vertex separates into a product of two pieces as anticipated. The vacuum of the three strings, *i.e.*, $\prod_{j=1}^3\left|0\right\rangle^{j,L}\left|0\right\rangle^{j,R}$, is however invariant under the Z_3 -Fourier transformation. Thus we have $\prod_{r=1}^2\left|0\right\rangle^{3,r}\left|0\right\rangle^r\left|\overline{0}\right\rangle^r=\prod_{j=1}^3\left|0\right\rangle^{j,L}\left|0\right\rangle^{j,R}$. If we choose to substitute the explicit values of the matrices, the above expression reduces to the simple form

$$\left|V_x^{HS}\right\rangle=\int\prod_{i=1}^3\mathrm{d}x_M^i\,\delta\left(x_M^i-x_M^{i-1}\right)\delta\left(\sum_{j=1}^3p_M^j\right)\times\mathrm{e}^{-\sum_{j=1}^3\sum_{n=1}^\infty b_n^{j,L\dagger}b_n^{j-1,R\dagger}}\left|0\right\rangle_{123}^L\left|0\right\rangle_{123}^R \tag{40}$$

where $|0\rangle_{123}^{L,R}$ denotes the vacuum in the left (right) product of the Hilbert space of the three strings. Here $b_n^{j,L(R)}$ denotes oscillators in the $L(R)$ *jth* string Hilbert space. For simplicity the Lorentz index ($\mu = 0,1,\cdots,25$) and the Minkowski metric $\eta_{\mu\nu}$ used to contract the Lorentz indices, have been suppressed in Equation (40). We shall follow this convention throughout this paper.

Though the form of the comma 3-Vertex given in Equation (40) is quite elegant, it is very cumbersome to relate it directly to the *SCSV* 3-Vertex due to the fact that connection between the vacuum in the comma theory and the vacuum in the *SCSV* is quite involved. One also needs to use the change of representation formulas [1] to recast the quadratic form in the half string creation operators in terms of the full string creation-annihilation operators which adds more complications to an already difficult problem. On the other hand the task could be greatly simplified if we express the comma vertex in the full string basis. This may be achieved simply by re expressing the comma overlaps in terms of overlaps in the full string basis. Moreover, the proof of the Ward-like identities will also simplify a great deal if the comma 3-Vertex is expressed in the full string basis. Before we express the half-string 3-Vertex is expressed in the full string basis, we need first to solve the comma overlap equations in (27), (30) and (32), (34) for the Fourier modes of the comma coordinates and momenta, respectively. The modes in the Z_3 Fourier space are given by

$$Q_{2n-1}^r = \frac{1}{\pi\sqrt{2}}\int_{-\pi}^{\pi} Q^r(\sigma)\cos(2n-1)\sigma \mathrm{d}\sigma, \tag{41}$$

$$\bar{Q}_{2n-1}^r = \frac{1}{\pi\sqrt{2}}\int_{-\pi}^{\pi} \bar{Q}^r(\sigma)\cos(2n-1)\sigma \mathrm{d}\sigma, \tag{42}$$

$$Q_{2n-1}^{3,r} = \frac{1}{\pi\sqrt{2}}\int_{-\pi}^{\pi} Q^{3,r}(\sigma)\cos(2n-1)\sigma \mathrm{d}\sigma \tag{43}$$

where $n = 1,2,3,\cdots$, and a similar set for the conjugate momenta. The overlap equations for the coordinates in (27) and (28) and the properties imposed in the Fourier expansion of the comma coordinates

$$Q^r(\sigma) = Q^r(-\sigma) \text{ and } Q^r(\sigma) = -Q^r(\pi-\sigma), \tag{44}$$

$$\bar{Q}^r(\sigma) = \bar{Q}^r(-\sigma) \text{ and } \bar{Q}^r(\sigma) = -\bar{Q}^r(\pi-\sigma), \tag{45}$$

$$Q^{3,r}(\sigma) = Q^{3,r}(-\sigma) \text{ and } Q^{3,r}(\sigma) = -Q^{3,r}(\pi-\sigma) \tag{46}$$

where $0 \le \sigma \le \pi$, imply that their Z_3 Fourier modes in the comma basis satisfy

$$Q_{2n-1}^L = eQ_{2n-1}^R, \tag{47}$$

$$\bar{Q}_{2n-1}^L = \bar{e}\bar{Q}_{2n-1}^R \tag{48}$$

From the overlap in (30) we obtain

$$Q_{2n-1}^{3,L} = Q_{2n-1}^{3,R} \tag{49}$$

For the Fourier modes of the conjugate momenta one obtains

$$\wp_{2n-1}^{L} = -e\wp_{2n-1}^{R}, \tag{50}$$

$$\overline{\wp}_{2n-1}^{L} = -\overline{e}\,\overline{\wp}_{2n-1}^{R} \tag{51}$$

and

$$\wp_{2n-1}^{3,L} = -\wp_{2n-1}^{3,R}, \tag{52}$$

where $n = 1, 2, 3, \cdots$. We see that the comma overlaps in the full string basis separates into a product of two pieces depending on

$$A_n^{3\dagger} = \frac{1}{\sqrt{3}}\left(a_n^{1\dagger} + a_n^{2\dagger} + a_n^{3\dagger}\right) \tag{53}$$

and on

$$A_n^{\dagger} \equiv A_n^{1\dagger} = \frac{1}{\sqrt{3}}\left(\overline{e}a_n^{1\dagger} + ea_n^{2\dagger} + a_n^{3\dagger}\right), \tag{54}$$

$$\overline{A}_n^{\dagger} \equiv A_n^{2\dagger} = \frac{1}{\sqrt{3}}\left(ea_n^{1\dagger} + \overline{e}a_n^{2\dagger} + a_n^{3\dagger}\right), \tag{55}$$

respectively, where the creation and annihilation operators $A_n^{\dagger}$ and A_n in the Z_3-Fourier space are defined in the usual way

$$Q_n = \frac{i}{2}\sqrt{\frac{2}{n}}\left(A_n - A_n^{\dagger}\right), \quad n = 1, 2, 3, \cdots \tag{56}$$

$$Q_0 = \frac{i}{2}\left(A_0 - A_0^{\dagger}\right) \tag{57}$$

$$P_n = -i\frac{\partial}{\partial Q_n} = \sqrt{\frac{n}{2}}\left(A_n + A_n^{\dagger}\right), \quad n = 1, 2, 3, \cdots \tag{58}$$

$$P_0 = -i\frac{\partial}{\partial Q_0} = \left(A_0 + A_0^{\dagger}\right) \tag{59}$$

and similarly for $\overline{A}_n^{\dagger}$, $\overline{A}_n$ and $A_n^{3\dagger}$, A_n^3. Notice that in the Z_3-Fourier space, $A_n^{\dagger} = \overline{A}_{-n}$, $\overline{A}_n^{\dagger} = A_{-n}$. For the matter sector, the comma 3-Vertex would be represented as exponential of quadratic form in the creation operators $A_n^{3\dagger}$, $A_n^{\dagger}$ and $\overline{A}_m^{\dagger}$. Thus the comma 3-Vertex in the full string Z_3-Fourier space takes the form

$$\left|V_Q^{HS}\right\rangle = \int \mathrm{d}Q_M\, \mathrm{d}\overline{Q}_M\, \delta\left(Q_M\right)\delta\left(\overline{Q}_M\right) V^{HS}\left(A_n^{3\dagger}, A_n^{\dagger}, \overline{A}_n^{\dagger}\right)\left|0\right)_{123} \tag{60}$$

where $\left|0\right)_{123}$ denotes the matter part of the vacuum in the Hilbert space of the three strings and

$$V^{HS}\left(A_n^{3\dagger}, A_n^{\dagger}, \overline{A}_n^{\dagger}\right) = \mathrm{e}^{\sum_{n,m=0}^{\infty}\left(-\frac{1}{2}A_n^{3\dagger}C_{nm}A_m^{3\dagger} - A_n^{\dagger}F_{nm}\overline{A}_m^{\dagger}\right)} \tag{61}$$

The ghost piece of the 3-Vertex in the bosonized form has the same structure as the coordinate piece apart from the mid point insertions. In the Z_3-Fourier space $Q_M^{\phi} = \overline{Q^{\phi}}_M = 0$ and only $Q_M^{\phi 3} \neq 0$. Thus the mid-point insertion is given by $3iQ_M^{\phi 3}/2$. The effect of the insertion is to inject the ghost number into the vertex at its mid-point to conserve the ghost number at the string mid-point, where the conservation of ghost number is violated due to the concentration of

the curvature at the mid-point. Thus the ghost part of the 3-Vertex takes the form

$$\left|V_{Q^\phi}^{HS}\right\rangle = \mathrm{e}^{3iQ_M^{\phi,3}/2} V_\phi^{HS}\left(A_n^{\phi,3\dagger}, A_n^{\phi\dagger}, \overline{A^\phi}_n^{\dagger}\right)\left|0\right\rangle_{123}^{\phi} \tag{62}$$

where $\left|0\right\rangle_{123}^{\phi}$ denotes the ghost part of the vacuum in the Hilbert space of the three strings and $V_\phi^{HS}\left(A_n^{\phi,3\dagger}, A_n^{\phi\dagger}, \overline{A^\phi}_n^{\dagger}\right)$ has the exact structure as the coordinate piece $V_Q^{HS}\left(A_n^{3\dagger}, A_n^{\dagger}, \overline{A}_n^{\dagger}\right)$. The mid-point insertion $3iQ_M^{\phi,3}/2$ in (62) may be written in terms of the creation annihilation operators

$$Q_M^{\phi,3} = Q_0^{\phi,3} + i\sum_{n=even=2}^{\infty} \frac{(-1)^{n/2}}{\sqrt{n}}\left(A_n^3 - A_n^{3\dagger}\right) \tag{63}$$

If we now commute the annihilation operators in the mid-point insertion through the exponential of the quadratic form in the creation operators in the three-string ghost vertex ($V_{Q^\phi}^{HS}$), the three-string ghost vertex in (62) takes the form

$$\left|V_{Q^\phi}^{HS}\right\rangle = \mathrm{e}^{3iQ_0^{\phi,3}/2}\mathrm{e}^{3\sum_{n=even=2}^{\infty}\frac{(-1)^{n/2}}{\sqrt{n}}A_n^{3\dagger}} V_\phi^{HS}\left(A_n^{\phi,3\dagger}, A_n^{\phi\dagger}, \overline{A^\phi}_n^{\dagger}\right)\left|0\right\rangle_{123}^{\phi} \tag{64}$$

We note that commuting the annihilation operators in the mid-point insertion $3iQ_M^{\phi,3}/2$ through $V_\phi^{HS}\left(A_n^{\phi,3\dagger}, A_n^{\phi\dagger}, \overline{A^\phi}_n^{\dagger}\right)$ results in the doubling of the creation operator in the mid-point insertion.

3. The Half-String 3-Vertex in the Full String Basis

We now proceed to express the half-string overlaps in the Hilbert space of the full string theory. The change of representation between the half-string modes and the full string modes derived in [1] is given by

$$\begin{aligned} Q_n^r &= (-1)^{r+1} Q_{2n-1} + \sum_{m=1}^{\infty}\sqrt{\frac{2m}{2n-1}}\left[M_{mn}^1 + M_{mn}^2\right]Q_{2m} \\ \wp_n^r &= \frac{(-1)^{r+1}}{2}P_{2n-1} + \frac{1}{2}\sum_{m=1}^{\infty}\sqrt{\frac{2n-1}{2m}}\left[M_{mn}^1 - M_{mn}^2\right]P_{2m} - \frac{\sqrt{2}}{\pi}\frac{(-1)^n}{2n-1}P_0 \end{aligned} \tag{65}$$

where $r = 1, 2 \equiv L, R$; $n = 1, 2, 3, \cdots$; and the matrices M^1 and M^2 are given by

$$M_{mn}^1 = \frac{2}{\pi}\sqrt{\frac{2m}{2n-1}}\frac{(-1)^{m+n}}{2m-(2n-1)}, \quad m, n = 1, 2, 3, \cdots \tag{66}$$

and

$$M_{mn}^2 = \frac{2}{\pi}\sqrt{\frac{2m}{2n-1}}\frac{(-1)^{m+n}}{2m+(2n-1)}, \quad m, n = 1, 2, 3, \cdots \tag{67}$$

Now the overlap equations in (47), (50) and (29) become

$$(1+e)Q_{2n-1} = -(1-e)\sum_{m=1}^{\infty}\sqrt{\frac{2m}{2n-1}}\left[M_{mn}^1 + M_{mn}^2\right]Q_{2m} \tag{68}$$

$$(1-e)\frac{1}{2}P_{2n-1} = -(1+e)\frac{1}{2}\sum_{m=1}^{\infty}\sqrt{\frac{2n-1}{2m}}\left[M^1_{mn} - M^2_{mn}\right]P_{2m} + (1+e)\frac{\sqrt{2}}{\pi}\frac{(-1)^n}{2n-1}P_0 \quad (69)$$

$$Q_M = Q_0 + \sqrt{2}\sum_{n=1}^{\infty}(-1)^n Q_{2n} = 0 \quad (70)$$

respectively. The overlaps for the complex conjugate of the first two equations could be obtained simply by taking the complex conjugation. Similarly from the overlaps in (49), (52) and (35) we obtain

$$Q^3_{2n-1} = 0 \quad (71)$$

$$\sum_{m=1}^{\infty}\sqrt{\frac{2n-1}{2m}}\left[M^1_{mn} - M^2_{mn}\right]P^3_{2m} - \frac{2\sqrt{2}}{\pi}\frac{(-1)^n}{2n-1}P^3_0 = 0 \quad (72)$$

$$\wp^3_M = 0 \quad (73)$$

We have seen in reference [1] the $\wp^3_M = P^3_0$ and so the overlap conditions in (72) and (73) reduce to

$$\sum_{m=1}^{\infty}\sqrt{\frac{2n-1}{2m}}\left[M^1_{mn} - M^2_{mn}\right]P^3_{2m} = 0 \quad (74)$$

$$P^3_0 = 0 \quad (75)$$

It is important to keep in mind that the equality sign appearing in Equations (68) through (75) is an equality between action of the operators when acting on the comma vertex except for Equation (75) which is the conservation of the momentum carried by the third string in the Z_3 Fourier space.

The comma vertex $\left|V^{HS}\left(A^{3\dagger}_n, A^{\dagger}_n, \bar{A}^{\dagger}_n\right)\right\rangle$ in the full string basis now satisfies the comma overlaps in (68), (69), (70), (71), (74) and (74). First let us consider the overlaps in (68), (69) and (70), *i.e.*,

$$\left[(1+e)Q_{2n-1} + (1-e)\sum_{m=1}^{\infty}\sqrt{\frac{2m}{2n-1}}\left(M^1_{mn} + M^2_{mn}\right)Q_{2m}\right]\left|V^{HS}\left(A^{3\dagger}_n, A^{\dagger}_n, \bar{A}^{\dagger}_n\right)\right\rangle = 0, \quad (76)$$

$$\left[(1-e)\frac{1}{2}P_{2n-1} + (1+e)\frac{1}{2}\sum_{m=1}^{\infty}\sqrt{\frac{2n-1}{2m}}\left(M^1_{mn} - M^2_{mn}\right)P_{2m} - (1+e)\frac{\sqrt{2}}{\pi}\frac{(-1)^n}{2n-1}P_0\right]\left|V^{HS}\left(A^{3\dagger}_n, A^{\dagger}_n, \bar{A}^{\dagger}_n\right)\right\rangle = 0, \quad (77)$$

$$\left[Q_0 + \sqrt{2}\sum_{k=1}^{\infty}(-1)^k Q_{2k}\right]\left|V^{HS}\left(A^{3\dagger}_n, A^{\dagger}_n, \bar{A}^{\dagger}_n\right)\right\rangle = 0 \quad (78)$$

(as well as their complex conjugates), where $n = 1, 2, 3, \cdots$. For the remaining overlaps, *i.e.*, equations in (71) and (74), we have

$$Q^3_{2n-1}\left|V^{HS}\left(A^{3\dagger}_n, A^{\dagger}_n, \bar{A}^{\dagger}_n\right)\right\rangle = 0, \quad (79)$$

$$\sum_{m=1}^{\infty}\sqrt{\frac{2n-1}{2m}}\left(M^1_{mn} - M^2_{mn}\right)P^3_{2m}\left|V^{HS}\left(A^{3\dagger}_n, A^{\dagger}_n, \bar{A}^{\dagger}_n\right)\right\rangle = 0, \quad (80)$$

$$P_0^3 \left| V^{HS}\left(A_n^{3\dagger}, A_n^{\dagger}, \bar{A}_n^{\dagger}\right)\right\rangle = 0 \tag{81}$$

where $n = 1,2,3,\cdots$. We notice that these overlaps are identical to the overlap equations for the identity vertex [4] [5] [7] [8]. Thus

$$C_{nm} = (-1)^n \delta_{nm}, \quad n,m = 0,1,2,\cdots \tag{82}$$

The explicit form of the matrix F, may be obtained from the overlap equations given by (76), (77) and (78) as well as their complex conjugates. It will turn out that the matrix F has the following properties

$$F = F^{\dagger}, \quad \bar{F} = CFC, \quad F^2 = 1 \tag{83}$$

which are consistent with the properties of the coupling matrices in Witten's theory of open bosonic strings [7] [8]. This indeed is a nontrivial check on the validity of the comma approach to the theory of open bosonic strings.

Now substituting (61) into (76) and writing Q_n in terms of $A_n^{\dagger}$ and A_n, we obtain the first equation for the matrix F

$$F_{2n-1\,k} + \delta_{2n-1\,k} - i\sqrt{3}\sum_{m=1}^{\infty}\left(M_{mn}^1 + M_{mn}^2\right)\left(F_{2m\,k} + \delta_{2m\,k}\right) = 0 \tag{84}$$

where $k = 0,1,2,\cdots; n = 1,2,3,\cdots$. Next from the overlap equation in (77) we obtain a second condition on the F matrix

$$\begin{aligned} 0 = {} & \left(F_{2n-1\,k} - \delta_{2n-1\,k}\right) + \frac{1}{\sqrt{3}} i \sum_{m=1}^{\infty}\left(M_{mn}^1 - M_{mn}^2\right)\left(F_{2m\,k} - \delta_{2m\,k}\right) \\ & - \frac{4}{\pi}\frac{i}{\sqrt{3}}\frac{(-1)^n}{(2n-1)^{3/2}}\left(F_{0k} - \delta_{0k}\right) \end{aligned} \tag{85}$$

where $k = 0,1,2,\cdots; n = 1,2,3,\cdots$. The overlaps for the mid-point in (78) give

$$\left[\left(F_{0m} + \delta_{0m}\right) + \sqrt{2}\sum_{k=1}^{\infty}(-1)^k\sqrt{\frac{2}{2k}}\left(F_{2k\,m} + \delta_{2k\,m}\right)\right] = 0, \quad m = 0,1,2,\cdots \tag{86}$$

Solving Equations (84) and (85), we have

$$F_{2n\,0} = \frac{1}{\pi}\left(F_{00} - 1\right)\sum_{m=1}^{\infty}\left[\left(M_1^T + \frac{1}{2}M_2^T\right)^{-1}\right]_{nm}\frac{(-1)^m}{(2m-1)^{3/2}} \tag{87}$$

$$\begin{aligned} F_{2n\,2k} = {} & \frac{1}{\pi}F_{0\,2k}\sum_{m=1}^{\infty}\left[\left(M_1^T + \frac{1}{2}M_2^T\right)^{-1}\right]_{nm}\frac{(-)^m}{(2m-1)^{3/2}} \\ & - \sum_{m=1}^{\infty}\left[\left(M_1^T + \frac{1}{2}M_2^T\right)^{-1}\right]_{nm}\left[\frac{1}{2}M_1^T + M_2^T\right]_{mk} \end{aligned} \tag{88}$$

$$\begin{aligned} F_{2n\,2k-1} = {} & -\frac{i\sqrt{3}}{2}\left[\left(M_1^T + \frac{1}{2}M_2^T\right)^{-1}\right]_{nk} \\ & + \frac{1}{\pi}F_{0\,2k-1}\sum_{m=1}^{\infty}\left[\left(M_1^T + \frac{1}{2}M_2^T\right)^{-1}\right]_{nm}\frac{(-)^m}{(2m-1)^{3/2}} \end{aligned} \tag{89}$$

$$F_{2n-1\,2k-1} = \frac{2i}{\sqrt{3}}\sum_{m=1}^{\infty}\left[\frac{1}{2}M_1^T + M_2^T\right]_{nm}F_{2m\,2k-1} + \frac{2i}{\pi\sqrt{3}}\frac{(-)^n}{(2n-1)^{3/2}}F_{0\,2k-1} \tag{90}$$

$$F_{2n-1\,2k}=\frac{2i}{\sqrt{3}}\sum_{m=1}^{\infty}\left[\frac{1}{2}M_1^T+M_2^T\right]_{nm}F_{2m\,2k}+\frac{2i}{\sqrt{3}}\left[M_1^T+\frac{1}{2}M_2^T\right]_{nk}+\frac{2i}{\pi\sqrt{3}}\frac{(-1)^n}{(2n-1)^{3/2}}F_{0\,2k} \tag{91}$$

$$F_{2n-1\,0}=\frac{2i}{\sqrt{3}}\sum_{m=1}^{\infty}\left[\frac{1}{2}M_1^T+M_2^T\right]_{nm}F_{2m\,0}+\frac{2i}{\pi\sqrt{3}}\times\frac{(-)^n}{(2n-1)^{3/2}}(F_{00}-1) \tag{92}$$

where all $n,k=1,2,3,\cdots$. Finally Equation (86) leads to

$$(F_{00}+1)=2\sum_{n=1}^{\infty}\frac{(-1)^{n+1}}{\sqrt{2n}}F_{2n\,0}, \tag{93}$$

$$F_{0\,2m}=2\frac{(-1)^{m+1}}{\sqrt{2m}}+2\sum_{k=1}^{\infty}\frac{(-1)^{k+1}}{\sqrt{2k}}F_{2k\,2m}, \tag{94}$$

$$F_{0\,2m-1}=2\sum_{k=1}^{\infty}\frac{(-1)^{k+1}}{\sqrt{2k}}F_{2k\,2m-1} \tag{95}$$

where $m=1,2,3,\cdots$.

Now the explicit form of the F matrix is completely given by the set of Equations (87), (88), (89), (90), (91), (92), (93), (94) and (95) provided that the inverse of the $\left(M_1^T+\frac{1}{2}M_2^T\right)$ exist. Now we proceed to compute the required inverse.

4. Finding the Inverse

In the half string formulation the combination $\left(M_1^T+\frac{1}{2}M_2^T\right)^{-1}$ is a special case of the more general expression, $M_1^T+\cos(k\pi/N)M_2^T$, where $k=1,2,3,\cdots,2N$ and N is the number of strings[2]. For the case of interest, N corresponds to 3 and $k=1$. It is however more constructive to consider the generic combination $\beta M_1^T+\alpha M_2^T$. Again for the case of interest one has $\beta=1$ and $\alpha=\cos(k\pi/N)=1/2$. For the inverse of $\beta M_1^T+\alpha M_2^T$, we propose the Ansatz

$$\left[\left(\beta M_1^T+\alpha M_2^T\right)^{-1}\right]_{nm}=(-1)^{n+m}\sqrt{2n}\left[\alpha'\frac{u_{2n}^{1-1/p}u_{2m-1}^{1/p}+u_{2n}^{1/p}u_{2m-1}^{1-1/p}}{2n-(2m-1)}+\beta'\frac{u_{2n}^{1-1/p}u_{2m-1}^{1/p}-u_{2n}^{1/p}u_{2m-1}^{1-1/p}}{2n+(2m-1)}\right]\sqrt{2m-1} \tag{96}$$

The coefficients $u_k^{1/p}$ and $u_k^{1-1/p}$ are the modes appearing in the Taylor expansion of the functions $\left(\frac{1+x}{1-x}\right)^{1/p}$ and $\left(\frac{1+x}{1-x}\right)^{1-1/p}$ respectively. For the three interaction vertex $p=3$ and the Taylor modes $u_k^{1/p}$ and $u_k^{1-1/p}$ reduce to $u_k^{1/3}=a_k$ and $u_k^{2/3}=b_k$ found in references [7] [8]. These coefficients are

[2]The reason we are considering this more general expression is that this combination appears in computing the N-interaction vertex which will probe useful in future work and it does not add to the level of difficulty in finding the inverse.

treated in details in appendix A. The free parameters α', β' and p are to be determined by demanding that (96) satisfies the identities

$$\left(\beta M_1^T + \alpha M_2^T\right)^{-1}\left(\beta M_1^T + \alpha M_2^T\right) = I \tag{97}$$

which implies that $\left(\beta M_1^T + \alpha M_2^T\right)^{-1}$ is left inverse and the identity

$$\left(\beta M_1^T + \alpha M_2^T\right)\left(\beta M_1^T + \alpha M_2^T\right)^{-1} = I \tag{98}$$

which implies that $\left(\beta M_1^T + \alpha M_2^T\right)^{-1}$ is right inverse. Here I is the identity matrix in the space of N strings.

Before we proceed to fix the constants α', β' and p, there are two special cases where the inverse could be obtained with ease with the help of the commutation relations of the half string creation annihilation operators $\left(b_n^{(r)}, b_n^{(r)\dagger}\right)$. They are given by $k = 2N$ and $k = N$.

For $k = 2N$, the combination $M_1^T + \cos\left(k\pi/N\right)M_2^T$ reduces to $M_1^T + M_2^T$ and the inverse $\left(M_1^T + M_2^T\right)^{-1} = M_1 - M_2$. To see this we only need to verify that $\left(M_1^T + M_2^T\right)\left(M_1 - M_2\right) = \left(M_1 - M_2\right)\left(M_1^T + M_2^T\right) = I$. We first consider

$$\left(M_1^T + M_2^T\right)\left(M_1 - M_2\right) = \left(M_1^T M_1 - M_2^T M_2\right) - \left(M_1^T M_2 - M_2^T M_1\right) \tag{99}$$

Using the commutation relations

$$\left[b_n^{(r)}, b_{-m}^{(s)}\right] = \delta^{rs}\delta_{n+m\,0} \tag{100}$$

(where $b_{-m}^{(s)} \equiv b_m^{(s)\dagger}$) for the half string creation annihilation modes $\left(b_n^{(r)}, b_n^{(r)\dagger}\right)$, one can show that the the combination inside the first bracket is the identity matrix I and the combination inside the second bracket is identically zero. To see this recall that the change of representation between the full string creation annihilation modes $\left(a_n, a_n^\dagger\right)$ and the half string creation annihilation modes is given by

$$b_n^{(r)} = (-1)^r a_{2n-1} + \frac{1}{2}\sum_{m=1}^{\infty}\left(M_{mn}^1 a_{2m} - M_{mn}^2 a_{-2m}\right),\ n = 1, 2, 3, \cdots \tag{101}$$

and $b_{-n}^{(r)} \equiv b_n^{(r)\dagger}$ is given by the same expression with $a_k \rightleftharpoons a_{-k}$. Substituting (101) into (100) one obtains

$$\begin{aligned} 0 = \left[b_n^{(r)}, b_q^{(s)}\right] &= -\frac{1}{2}\delta^{rs}\sum_{k=1}^{\infty}\left[\left(M_1^T\right)_{nk}\left(M_2\right)_{kq} - \left(M_2^T\right)_{nk}\left(M_1\right)_{kq}\right] \\ &= -\frac{1}{2}\delta^{rs}\left[M_1^T M_2 - M_2^T M_1\right]_{nq} \end{aligned} \tag{102}$$

for $n > 0$ and $m = -q < 0$. Since $\delta^{rs} = 0$ for $r \neq s$, then the above equation does not yield any information about the combination $M_1^T M_2 - M_2^T M_1$ for $r \neq s$. However, for $r = s$, Equation (102) yields

$$M_1^T M_2 - M_2^T M_1 = 0 \tag{103}$$

Similarly one has

$$\begin{aligned} \delta^{rs}\delta_{nm} &= \left[b_n^{(r)}, b_{-m}^{(s)}\right] \\ &= \frac{1}{2}(-1)^{r+s}\delta_{nm} + \frac{1}{2}\sum_{m=1}^{\infty}\left[\left(M_1^T\right)_{nk}\left(M_1\right)_{km} - \left(M_2^T\right)_{nk}\left(M_2\right)_{km}\right] \\ &= \frac{1}{2}(-1)^{r+s} I_{nm} + \frac{1}{2}\left[M_1^T M_1 - M_2^T M_2\right]_{nm} \end{aligned} \tag{104}$$

for $n,m>0$. In this case, the above expression gives the following identity

$$M_1^T M_1 - M_2^T M_2 = I \tag{105}$$

for all possible values of r and s. Substituting Equations (103) and (105) into Equation (99) we arrive at

$$\left(M_1^T + M_2^T\right)\left(M_1 - M_2\right) = I \tag{106}$$

Thus $\left(M_1 - M_2\right)$ is the right inverse of $\left(M_1^T + M_2^T\right)$. To complete the proof one must show that $\left(M_1 - M_2\right)$ is also a left inverse; that is we need to establish the following identity

$$\left(M_1 - M_2\right)\left(M_1^T + M_2^T\right) = I \tag{107}$$

The proof of the above identity follows at once from the change of representation between the half string creation annihilation modes $\left(b_n^{(r)}, b_n^{(r)\dagger}\right)$ and the full string creation annihilation modes $\left(a_n, a_n^\dagger\right)$ given by

$$a_{2n} = \frac{(-1)^n}{\sqrt{2n}} P + \sum_{m=1}^{\infty}\left(M_{nm}^1 b_m^{(+)} - M_{nm}^2 b_{-2m}^{(+)}\right), \quad n = 1,2,3,\cdots \tag{108}$$

(where $b_n^{(+)} = \frac{1}{\sqrt{2}}\left(b_n^{(1)} + b_n^{(2)}\right)$) and the commutation relations

$$\left[a_n, a_{-m}\right] = \delta_{n+m\,0}. \tag{109}$$

Using Equations (108) and (109) and skipping the algebraic details, one obtains the following identities

$$M_1 M_2^T - M_2 M_1^T = 0 \tag{110}$$

$$M_1 M_1^T - M_2 M_2^T = I \tag{111}$$

needed to prove that the combination $\left(M_1 - M_2\right)$ is also a left inverse. This completes the proof.

For $k = N$, the combination $M_1^T + \cos\left(k\pi/N\right) M_2^T$ reduces to $M_1^T - M_2^T$ and the inverse $\left(M_1^T - M_2^T\right)^{-1} = M_1 + M_2$. The proof that $M_1 + M_2$ is the right inverse follows at once simply by taking the transpose of the already established identity in (106). To show that the combination $M_1 + M_2$ is also the left inverse of the combination $M_1^T - M_2^T$ one only needs to take the transpose of (107); thus leading to the desired result.

Now we proceed to fix the constants in (96) for $k \neq N, 2N$. From Equations (66) and (67), we have

$$M_{nm}^1 = \frac{2}{\pi}\sqrt{\frac{2n}{2m-1}}\frac{(-1)^{n+m}}{2n-(2m-1)} \tag{112}$$

and

$$M_{nm}^2 = \frac{2}{\pi}\sqrt{\frac{2n}{2m-1}}\frac{(-1)^{n+m}}{2n+(2m-1)} \tag{113}$$

respectively. First we proceed with the identity in (97). If we could solve for the free parameters α', β', and p in terms of the known parameters α and β then the Ansatz in (96) is the left inverse of the matrix $\beta M_1^T + \alpha M_2^T$. For the off

diagonal elements; that is $q \neq n$, the identity in (97), yields, after much use of the identities in [9],

$$\begin{aligned}
&\alpha'\beta\frac{u_{2n}^{1-1/p}O_{-2n}^{u(1,p)}-u_{2n}^{1-1/p}O_{-2q}^{u(1,p)}+u_{2n}^{1/p}O_{-2n}^{u(p-1,p)}-u_{2n}^{1/p}O_{-2q}^{u(p-1,p)}}{2n-2q}\\
&-\alpha'\alpha\frac{u_{2n}^{1-1/p}O_{-2n}^{u(1,p)}-u_{2n}^{1-1/p}O_{2q}^{u(1,p)}+u_{2n}^{1/p}O_{-2n}^{u(p-1,p)}-u_{2n}^{1/p}O_{2q}^{u(p-1,p)}}{2n+2q}\\
&+\beta'\beta\frac{u_{2n}^{1-1/p}O_{2n}^{u(1,p)}-u_{2n}^{1-1/p}O_{-2q}^{u(1,p)}-u_{2n}^{1/p}O_{2n}^{u(p-1,p)}+u_{2n}^{1/p}O_{-2q}^{u(p-1,p)}}{2n+2q}\\
&-\beta'\alpha\frac{u_{2n}^{1-1/p}O_{2n}^{u(1,p)}-u_{2n}^{1-1/p}O_{2q}^{u(1,p)}-u_{2n}^{1/p}O_{2n}^{u(p-1,p)}+u_{2n}^{1/p}O_{2q}^{u(p-1,p)}}{2n-2q}=0
\end{aligned}$$

where the quantities

$$O_{\pm n=2k}^{u(q,p)}\equiv\sum_{m=2l+1=1}^{\infty}\frac{u_m^{q/p}}{\pm n+m},n\geq 0 \tag{114}$$

have been considered in [9]. The quantities $O_{-n}^{u(q,p)}$ are related to $O_n^{u(q,p)}$ through the identity $O_{-n}^{u(q,p)}=-\cos(q\pi/p)O_n^{u(q,p)}$ [9]. The quantity $O_n^{u(q,p)}$ has the value $\left[\pi/2\sin(q\pi/p)\right]u_{2n}^{q/p}$ [9]. In order for the right hand side of the above expression to vanish, the coefficients of $u_{2n}^{1-1/p}u_{2n}^{1/p}$, $u_{2n}^{1-1/p}u_{2q}^{1/p}$ and $u_{2n}^{1/p}u_{2q}^{1-1/p}$ must vanish separately. The vanishing of the coefficient of the $u_{2n}^{1-1/p}u_{2n}^{1/p}$ can be established explicitly by substituting the explicit values for $O_n^{u(q,p)}$. The vanishing of the coefficient of $u_{2n}^{1-1/p}u_{2q}^{1/p}$ term leads to the following conditions on the free parameters

$$\beta'\alpha+\alpha'\beta\cos\left(\frac{1}{p}\pi\right)=0 \tag{115}$$

$$\alpha'\alpha+\beta'\beta\cos\left(\frac{1}{p}\pi\right)=0 \tag{116}$$

The vanishing of the coefficient of $u_{2n}^{1/p}u_{2q}^{1-1/p}$ does not lead to new conditions on the free parameters but it provides a consistency condition. The equivalence between the half-string field theory and Witten's theory of open bosonic strings will guarantee that this consistency condition will be met. In fact we have verified this requirement explicitly.

For the diagonal elements ($q=n$), the identity in (97), after much use of the various identities in [9], yields

$$\begin{aligned}
1=&\frac{2(-1)^{n+n}}{\pi}(2n)^{1/2}(2n)^{1/2}\left\{\alpha'\beta\left[u_{2n}^{1-1/p}\tilde{O}_{-2n}^{u(1,p)}+u_{2n}^{1/p}\tilde{O}_{-2n}^{u(p-1,p)}\right]\right.\\
&-\alpha'\alpha\frac{u_{2n}^{1-1/p}O_{-2n}^{u(1,p)}-u_{2n}^{1-1/p}O_{2n}^{u(1,p)}+u_{2n}^{1/p}O_{-2n}^{u(p-1,p)}-u_{2n}^{1/p}O_{2n}^{u(p-1,p)}}{2(2n)}\\
&+\beta'\beta\frac{u_{2n}^{1-1/p}O_{2n}^{u(1,p)}-u_{2n}^{1-1/p}O_{-2n}^{u(1,p)}-u_{2n}^{1/p}O_{2n}^{u(p-1,p)}+u_{2n}^{1/p}O_{-2n}^{u(p-1,p)}}{2(2n)}\\
&\left.+\beta'\alpha\left[u_{2n}^{1-1/p}\tilde{O}_{2n}^{u(1,p)}-u_{2n}^{1/p}\tilde{O}_{2n}^{u(p-1,p)}\right]\right\}
\end{aligned} \tag{117}$$

where

$$\tilde{O}^{u(q,p)}_{\pm n=2k}=\sum_{m=2l+1=1}^{\infty}\frac{u_m^{q/p}}{\left(\pm n+m\right)^2} \tag{118}$$

has been considered in [9]. Using the explicit values of $O_n^{u(q,p)}$, $O_{-n}^{u(q,p)}$, $\tilde{O}_n^{u(q,p)}$ and $\tilde{O}_{-n}^{u(q,p)}$ which are given in [9] and imposing the conditions obtained in (116), the above expression reduces, after a lengthy exercise, otherwise a straight forward algebra, to

$$1=\frac{2}{\pi}\left(2n\right)\beta'\alpha\left[u_{2n}^{1-1/p}\tilde{S}_{2n}^{(1,p)}-u_{2n}^{1/p}\tilde{S}_{2n}^{(p-1,p)}\right] \tag{119}$$

where the quantities $\tilde{S}_{\pm n}^{(q,p)}$ were introduced in [9]. The above expression may be reduced further by expressing $\tilde{S}_{-n}^{(q,p)}$ in terms of $\tilde{S}_n^{(q,p)}$ through the relations

$$\tilde{S}_{-2n}^{(1,p)}=\tilde{S}_{2n}^{(1,p)}\cos\frac{\pi}{p}+\left[1+\cos\left(\frac{\pi}{p}\right)\right]\overline{S}_0^{(1,p)}S_{2n}^{(1,p)} \tag{120}$$

$$\tilde{S}_{-2n}^{(p-1,p)}=\tilde{S}_{2n}^{(p-1,p)}\cos\frac{\left(p-1\right)\pi}{p}+\left[1+\cos\left(\frac{\left(p-1\right)\pi}{p}\right)\right]\overline{S}_0^{(p-1,p)}S_{2n}^{(p-1,p)} \tag{121}$$

which have been established in [9]. Hence

$$\begin{aligned}1=\frac{2}{\pi}\left(2n\right)\alpha'\beta\Bigg\{&u_{2n}^{1-1/p}\left[1+\cos\left(\frac{\pi}{p}\right)\right]\overline{S}_0^{(1,p)}S_{2n}^{(1,p)}\\&+u_{2n}^{1/p}\left[1-\cos\left(\frac{\pi}{p}\right)\right]\overline{S}_0^{(p-1,p)}S_{2n}^{(p-1,p)}\Bigg\}\end{aligned} \tag{122}$$

In arriving at the above expression we used the fact that

$$\alpha'\beta\cos\left(\frac{\left(p-1\right)}{p}\pi\right)-\beta'\alpha=\alpha'\beta\cos\left(\frac{1}{p}\pi\right)+\beta'\alpha=0 \tag{123}$$

Further simplification of (122) may be achieved by substituting the explicit values of $\overline{S}_0^{(1,p)}$ and $\overline{S}_0^{(p-1,p)}$ found in [9]. Thus Equation (122) reduces to

$$\begin{aligned}1&=2n\alpha'\beta\Bigg\{u_{2n}^{1-1/p}\left[1+\cos\left(\frac{\pi}{p}\right)\right]\tan\left(\frac{1}{p}\frac{\pi}{2}\right)S_{2n}^{(1,p)}\\&\quad+S_{2n}^{(1,p)}\left[1-\cos\left(\frac{\pi}{p}\right)\right]\cot\left(\frac{1}{p}\frac{\pi}{2}\right)S_{2n}^{(p-1,p)}\Bigg\}\\&=2n\alpha'\beta\sin\left(\frac{\pi}{p}\right)\left[u_{2n}^{1-1/p}S_{2n}^{(1,p)}+S_{2n}^{(1,p)}S_{2n}^{(p-1,p)}\right]\end{aligned} \tag{124}$$

To compute the right-hand side of the above expression we need to evaluate the expression inside the square bracket. We will show that this expression has the explicit value 2/2*n*. Consider the matrix element defined by

$$W_{mn}=\frac{u_m^{1/p}u_n^{1-1/p}+u_m^{1-1/p}u_n^{1/p}}{m+n} \tag{125}$$

The matrix element W_{mn} satisfies the following recursion relationship, which may be verified by direct substitution

$$0=(n+1)W_{n+1\,m}-(n-1)W_{n-1\,m}+(m+1)W_{n\,m+1}-(m-1)W_{n\,m-1} \tag{126}$$

for $m+n=odd$ integer. Letting $n\to 2n-1\geq 1$, $m\to 2m\geq 2$ in (126), we obtain

$$0=2nW_{2n\,2m}-(2n-2)W_{2n-2\,2m}+(2m+1)W_{2n-1\,2m+1}-(2m-1)W_{2n-1\,2m-1} \tag{127}$$

Summing both sides of (127) over m, we have

$$2n\sum_{m=0}^{\infty}W_{2n\,2m}-(2n-2)\sum_{m=0}^{\infty}W_{2n-2\,2m}=2nW_{2n\,0}-(2n-2)W_{2n-2\,0}+W_{2n-1\,1} \tag{128}$$

Substituting the explicit values for $2nW_{2n\,0}$, $W_{2n-2\,0}$ and $W_{2n-1\,1}$ into (128) we obtain

$$\begin{aligned}&2n\sum_{m=0}^{\infty}W_{2n\,2m}-(2n-2)\sum_{m=0}^{\infty}W_{2n-2\,2m}\\&=u_{2n}^{1/p}+u_{2n}^{1-1/p}-u_{2n-2}^{1/p}-u_{2n-2}^{1-1/p}+\frac{2}{2n}u_{2n-1}^{1/p}-\frac{1}{2n}\frac{2}{p}u_{2n-1}^{1/p}+\frac{1}{2n}\frac{2}{p}u_{2n-1}^{1-1/p}\end{aligned} \tag{129}$$

Recalling the recursion relations for the Taylor modes established in [9]

$$u_{k+1}^{1/p}=\frac{1}{k+1}\left[\frac{2}{p}u_{k}^{1/p}+(k-1)u_{k-1}^{1/p}\right] \tag{130}$$

$$u_{k+1}^{1-1/p}=\frac{1}{k+1}\left[\frac{2}{p}(p-1)u_{k}^{1-1/p}+(k-1)u_{k-1}^{1-1/p}\right] \tag{131}$$

If we now set $k=2n-1$ in the recursion relations in (130) and (131) and then rearrange terms, we have

$$\frac{1}{2n}\frac{2}{p}u_{2n-1}^{1/p}=u_{2n}^{1/p}-\frac{1}{2n}(2n-2)u_{2n-2}^{1/p}, \tag{132}$$

$$\frac{1}{2n}\frac{2}{p}u_{2n-1}^{1-1/p}=-u_{2n}^{1-1/p}+\frac{2}{2n}u_{2n-1}^{1-1/p}+\frac{2n-2}{2n}u_{2n-2}^{1-1/p} \tag{133}$$

Substituting (132) and (133) in the above equations into (129), we find

$$2n\sum_{m=0}^{\infty}W_{2n\,2m}=(2n-2)\sum_{m=0}^{\infty}W_{2n-2\,2m} \tag{134}$$

Repeated application of the above identity implies that

$$2n\sum_{m=0}^{\infty}W_{2n\,2m}=2\sum_{m=0}^{\infty}W_{2\,2m} \tag{135}$$

Substituting the explicit form of W_{nm} into the above identity we have

$$\left[u_{2n}^{1/p}S_{2n}^{(p-1,p)}+u_{2n}^{1-1/p}S_{2n}^{(1,p)}\right]=\frac{2}{2n}\left[u_{2}^{1/p}S_{2}^{(p-1,p)}+u_{2}^{1-1/p}S_{2}^{(1,p)}\right] \tag{136}$$

where

$$S_{n}^{(1,p)}\equiv\sum_{n+m=even,m=0}^{\infty}\frac{u_{m}^{1/p}}{n+m}, \tag{137}$$

$$S_{n}^{(p-1,p)}\equiv\sum_{n+m=even,m=0}^{\infty}\frac{u_{m}^{1-1/p}}{n+m} \tag{138}$$

To complete the proof, it remains to show that the expression inside the

square bracket on the right hand side of Equation (136) is equal to unity. This we do by explicit computation. Consider

$$u_2^{1/p} S_2^{(p-1,p)} + u_2^{1-1/p} S_2^{(1,p)} \tag{139}$$

Using the summation formulas for $S_n^{(1,p)}$ and $S_n^{(p-1,p)}$, which are given in [9], the above expression reduces to

$$u_2^{1/p} S_2^{(p-1,p)} + u_2^{1-1/p} S_2^{(1,p)} = 1 \tag{140}$$

and so Equation (136) yields

$$\left[u_{2n}^{1/p} S_{2n}^{(p-1,p)} + u_{2n}^{1-1/p} S_{2n}^{(1,p)} \right] = \frac{2}{2n} \tag{141}$$

Substituting this result for the expression in the square bracket in (124) leads to one more condition on the parameters α' and p

$$\alpha' = \frac{1}{2\sin\left(\frac{1}{p}\pi\right)\beta} \tag{142}$$

Collecting all the conditions on the free parameters, and then solving for the parameters α' and β', and p in terms of the known parameters α and β, we find

$$\frac{\alpha^2}{\beta^2} = \cos^2\left(\frac{1}{p}\pi\right), \alpha' = \frac{1}{2\sin\left(\frac{1}{p}\pi\right)\beta}, \beta' = -\frac{\cos\left(\frac{1}{p}\pi\right)}{2\sin\left(\frac{1}{p}\pi\right)\alpha} \tag{143}$$

The desired expression for the inverse of $\beta M_1^T + \alpha M_2^T$, is therefore given by substituting the values of α' and β' given by the above expressions into the Ansatz for $\left(\beta M_1^T + \alpha M_2^T\right)^{-1}$ in Equation (96). Hence,

$$\begin{aligned} &\left[\left(\beta M_1^T + \alpha M_2^T\right)^{-1}\right]_{nm} \\ &= (-1)^{n+m} \frac{\sqrt{2n}\sqrt{2m-1}}{2\sin\left(\frac{1}{p}\pi\right)} \left[\frac{1}{\beta} \frac{u_{2n}^{1-1/p} u_{2m-1}^{1/p} + u_{2n}^{1/p} u_{2m-1}^{1-1/p}}{2n-(2m-1)} \right. \\ &\left. - \frac{\cos\left(\frac{1}{p}\pi\right)}{\alpha} \frac{u_{2n}^{1-1/p} u_{2m-1}^{1/p} - u_{2n}^{1/p} u_{2m-1}^{1-1/p}}{2n+(2m-1)} \right] \end{aligned} \tag{144}$$

This shows that the above expression is the left inverse. To complete the proof we need to check that the identity in (98) is also satisfied and leads to the same conditions as in Equations (143). This in fact we did verify. The special cases of $k = N$ and $k = 2N$ have been treated earlier. This completes the construction of the inverse for the general case of the $\left(\beta M_1^T + \alpha M_2^T\right)$ matrix.

In the particular case of $\left(M_1^T + \cos\frac{k\pi}{N} M_2^T\right)^{-1}$, the parameters

$\alpha = \cos(k\pi/N)$ and $\beta = 1$ respectively, and the above relations in (143) become

$$\cos^2\left(\frac{\pi}{p}\right) = \alpha^2 = \cos^2\left(\frac{k\pi}{N}\right), \alpha' = \frac{1}{2\sin\frac{\pi}{p}}, \beta' = -\frac{\cos\frac{\pi}{p}}{2\sin\frac{\pi}{p}\cos\frac{k\pi}{N}} \tag{145}$$

For the particular case of $\alpha = \cos(k\pi/N)$ and $\beta = 1$, the relations in (145) yield

$$\alpha' = -\beta' = \frac{1}{2\sin\left(\frac{1}{p}\pi\right)} \tag{146}$$

$$1/p = \begin{cases} k/N, & 1 \le k \le N-1 \\ (2N-k)/N, & N+1 \le k \le 2N-1 \end{cases} \tag{147}$$

If we choose $1 \le k \le N-1$, then we have

$$\begin{aligned} &\left[\left(M_1^T + \cos\left(\frac{k\pi}{N}\right)M_2^T\right)^{-1}\right]_{nm} \\ &= (-1)^{n+m}\frac{\sqrt{2n}\sqrt{2m-1}}{2\sin\left(\frac{1}{p}\pi\right)}\left[\frac{u_{2n}^{1-1/p}u_{2m-1}^{1/p} + u_{2n}^{1/p}u_{2m-1}^{1-1/p}}{2n-(2m-1)} - \frac{u_{2n}^{1-1/p}u_{2m-1}^{1/p} - u_{2n}^{1/p}u_{2m-1}^{1-1/p}}{2n+(2m-1)}\right] \end{aligned} \tag{148}$$

For the case of interest, that is, the three interaction vertex $N = 3$ and $k = 1$ so that $p = 3$. This implies that the Taylor modes $u_n^{1/p}$ and $u_n^{1-1/p}$ in the expansion of $\left(\frac{1+x}{1-x}\right)^{1/p}$ and $\left(\frac{1+x}{1-x}\right)^{1-1/p}$ are a_n and b_n in the expansion of $\left(\frac{1+x}{1-x}\right)^{1/3}$ and $\left(\frac{1+x}{1-x}\right)^{2/3}$ encountered in reference [7] [8]. Thus the inverse of $\left(M_1^T + \frac{1}{2}M_2^T\right)$ now reads

$$\begin{aligned} &\left[\left(M_1^T + \frac{1}{2}M_2^T\right)^{-1}\right]_{nm} \\ &= \frac{1}{\sqrt{3}}(-1)^{n+m}\sqrt{2n}\sqrt{2m-1}\left[\frac{a_{2n}b_{2m-1} + b_{2n}a_{2m-1}}{2n-(2m-1)} + \frac{a_{2n}b_{2m-1} - b_{2n}a_{2m-1}}{2n+(2m-1)}\right] \end{aligned} \tag{149}$$

This is the required inverse needed to finish the construction of the half-string three interaction vertex in terms of the full-string basis. The expression in (149) is indeed the right and left inverse of $M_1^T + \frac{1}{2}M_2^T$ as can be checked explicitly. See ref. [9].

5. Computing the Explicit Values of the Matrix Elements of the *F* Matrix

To complete the construction of the comma 3-Vertex

$$\left|V^{HS}\right\rangle = \int \mathrm{d}Q_M^3 \mathrm{d}Q_M \mathrm{d}\bar{Q}_M \delta(Q_M)\delta(\bar{Q}_M)\mathrm{e}^{iP_0^3 Q_M^3} V^{HS}\left(A_n^{3\dagger}, A_n^{\dagger}, \bar{A}_n^{\dagger}\right)|0,0,0\rangle \tag{150}$$

in the Z_3-Fourier space of the full string, we need the explicit form of the F matrix. Here we shall give the steps involved in the computation of the matrix elements of F and relegate many of the technical details to appendix A. For the purpose of illustration consider F_{2n0}. Substituting the explicit value of $\left(M_1^T+\frac{1}{2}M_2^T\right)^{-1}$ obtained in (149) into Equation (87) gives

$$\begin{aligned}F_{2n\,0}=&\frac{1}{\pi}\left(F_{00}-1\right)\sum_{m=1}^{\infty}\frac{1}{\sqrt{3}}\left(-1\right)^{n+m}\sqrt{2n}\sqrt{2m-1}\cdot\frac{\left(-1\right)^m}{\left(2m-1\right)^{3/2}}\\&\times\left[\frac{a_{2n}b_{2m-1}+b_{2n}a_{2m-1}}{2n-\left(2m-1\right)}+\frac{a_{2n}b_{2m-1}-b_{2n}a_{2m-1}}{2n+\left(2m-1\right)}\right]\end{aligned}\tag{151}$$

where $n=1,2,3,\cdots$. Using partial fractions, the above expression becomes

$$\begin{aligned}F_{2n\,0}=&\frac{1}{\pi}\left(F_{00}-1\right)\frac{1}{\sqrt{3}}\left(-1\right)^n\frac{\sqrt{2n}}{2n}\left[2\left(a_{2n}\right)O_0^b-a_{2n}O_{-2n}^b\right.\\&\left.-b_{2n}O_{-2n}^a-a_{2n}O_{2n}^b+b_{2n}O_{2n}^a\right]\end{aligned}\tag{152}$$

where the quantities appearing in the above expression are defined have been evaluated in [9]. Thus substituting the explicit values of these quantities into (152) and combining terms we find

$$F_{2n\,0}=\left(F_{00}-1\right)\frac{\left(-1\right)^n a_{2n}}{\sqrt{2n}}\tag{153}$$

The explicit value of the F_{00} may be computed by substituting (153) into (93). Doing that and rearranging terms we get

$$\left(F_{00}+1\right)=-2\left(F_{00}-1\right)\sum_{n=1}^{\infty}\frac{a_{2n}}{2n}\tag{154}$$

The sum appearing on the right-hand side has the value $\left(3/2\right)\ln 3-2\ln 2$, so we obtain

$$\frac{1+F_{00}}{1-F_{00}}=\ln\frac{3^3}{2^4}\tag{155}$$

which gives the explicit value of F_{00} at once. This result is consistent with that given in [7] [8]. To obtain the explicit value of $F_{0\,2m}$, we first need to evaluate the sum over k in Equation (94), *i.e.*,

$$\sum_{k=1}^{\infty}\frac{\left(-1\right)^{k+1}}{\sqrt{2k}}F_{2k\,2m}$$

where the explicit expression for $F_{2k\,2m}$ in terms of the change of representation matrices is given by Equation (88). Thus substituting (88) into the above expression we have

$$\begin{aligned}\sum_{k=1}^{\infty}\frac{\left(-1\right)^{k+1}}{\sqrt{2k}}F_{2k\,2m}=&\sum_{k=1}^{\infty}\frac{\left(-1\right)^{k+1}}{\sqrt{2k}}\frac{1}{\pi}F_{0\,2m}\sum_{l=1}^{\infty}\frac{\left(-1\right)^l}{\left(2l-1\right)^{3/2}}\left[\left(M_1^T+\frac{1}{2}M_2^T\right)^{-1}\right]_{kl}\\&-\sum_{k=1}^{\infty}\frac{\left(-1\right)^{k+1}}{\sqrt{2k}}\sum_{l=1}^{\infty}\left[\left(M_1^T+\frac{1}{2}M_2^T\right)^{-1}\right]_{kl}\left[\frac{1}{2}M_1^T+M_2^T\right]_{lm}\end{aligned}\tag{156}$$

If we commute[3] the sums over k and l, we get

$$\sum_{k=1}^{\infty}\frac{(-1)^{k+1}}{\sqrt{2k}}F_{2k\,2m}=\frac{1}{\pi}F_{0\,2m}\sum_{l=1}^{\infty}\sum_{k=1}^{\infty}\frac{(-1)^{l}}{(2l-1)^{3/2}}(\cdots)-\sum_{l=1}^{\infty}\sum_{k=1}^{\infty}\left[\frac{1}{2}M_1^T+M_2^T\right]_{lm}(\cdots) \quad (157)$$

where

$$(\cdots)\equiv\frac{(-1)^{k+1}}{\sqrt{2k}}\left[\left(M_1^T+\frac{1}{2}M_2^T\right)^{-1}\right]_{kl} \quad (158)$$

Substituting Equation (149) for the inverse of the combination $M_1^T+(1/2)M_2^T$ into the above expression and summing over k from 1 to ∞, we obtain

$$\sum_{k=1}^{\infty}\frac{(-1)^{k+1}}{\sqrt{2k}}\left[\left(M_1^T+\frac{1}{2}M_2^T\right)^{-1}\right]_{kl}=-\frac{2}{\sqrt{3}}\frac{(-1)^{l}a_{2l-1}}{(2l-1)^{1/2}} \quad (159)$$

In arriving at the above result we made use of the identities

$$\sum_{k=0}^{\infty}\frac{a_{2k}}{2k-(2l-1)}=-\frac{1}{2}\sum_{k=0}^{\infty}\frac{a_{2k}}{2k+(2l-1)}=-\frac{1}{2}\frac{1}{\sqrt{3}}\pi a_{2l-1} \quad (160)$$

which were derived in [9]. Similar expressions hold for the sums over b_{2k}; see ref. [9]. Now substituting Equation (159) into (157) gives

$$\sum_{k=1}^{\infty}\frac{(-1)^{k+1}}{\sqrt{2k}}F_{2k\,2m}=-\frac{1}{2}\ln\frac{3^3}{2^4}F_{0\,2m}+\sum_{l=1}^{\infty}\frac{(-1)^{l}}{\sqrt{3}}\times\frac{2a_{2l-1}}{\sqrt{2l-1}}\left[\frac{1}{2}M_1^T+M_2^T\right]_{lm} \quad (161)$$

Using the explicit value of M_1 and M_2 and rewriting $\ln(3^3/2^4)$ in terms of F_{00}, the above expression becomes

$$\sum_{k=1}^{\infty}\frac{(-1)^{k+1}}{\sqrt{2k}}F_{2k\,2m}=-\frac{1}{2}\left(\frac{1+F_{00}}{1-F_{00}}\right)F_{0\,2m}+\frac{(-1)^{m}(1-a_{2m})}{(2m)^{1/2}} \quad (162)$$

Substituting this result into (94), we find

$$F_{0\,2m}=(F_{00}-1)\frac{(-1)^{m}a_{2m}}{(2m)^{1/2}} \quad (163)$$

which has the same form as $F_{2m\,0}$ given in (153). Thus in this case we see that the property $F_{even\,0}=\left(F^{\dagger}\right)_{0\,even}$ holds.

Next we consider the evaluation of $F_{2n-1\,0}$. If we replace M_1, M_2 and $F_{2m\,0}$ in (92) by their explicit values, given respectively by Equation (66), (67) and (153), we have

$$\begin{aligned}F_{2n-1\,0}=&\frac{2i}{\sqrt{3}}\frac{2}{\pi}(F_{00}-1)\frac{(-1)^{n}}{\sqrt{2n-1}}\left[\frac{1}{2}\sum_{m=1}^{\infty}\frac{a_{2m}}{2m-(2n-1)}\right.\\&\left.+\sum_{m=1}^{\infty}\frac{a_{2m}}{2m+(2n-1)}\right]+\frac{2i}{\pi\sqrt{3}}\frac{(-1)^{n}}{(2n-1)^{3/2}}(F_{00}-1)\end{aligned} \quad (164)$$

[3]Since both the sums over l and k are uniformly convergent, one may perform the sums in any order. We have carried the sums in the two different orders and found that the result is the same. However, it is much easier to perform the sum over k first followed by the sum over l rather than the reverse. Here we shall follow the former.

In order to benefit from the results obtained in [9] to help carry out the sums we first need to extend the range of the sums to include $m=0$. Hence adding zero in the form $-a_0/(2n-1)+a_0/(2n-1)$, the above expression becomes

$$F_{2n-1\,0}=\frac{2i}{\sqrt{3}}\frac{2}{\pi}(F_{00}-1)\frac{(-1)^n}{\sqrt{2n-1}}\left[\frac{1}{2}\frac{a_0}{(2n-1)}+\frac{1}{2}\sum_{m=0}^{\infty}\frac{a_{2m}}{2m-(2n-1)}\right.$$
$$\left.-\frac{a_0}{(2n-1)}+\sum_{m=0}^{\infty}\frac{a_{2m}}{2m+(2n-1)}+\frac{2i(-1)^n(F_{00}-1)}{\pi\sqrt{3}(2n-1)^{3/2}}\right] \tag{165}$$

The sums in the square brackets have been evaluated in [9]. Thus one finds

$$F_{2n-1\,0}=i(F_{00}-1)\frac{(-1)^n a_{2n-1}}{\sqrt{2n-1}}, \tag{166}$$

where $n=1,2,3,\cdots$. To check if the property $F=F^{\dagger}$ continue to hold, we need to compute explicitly the value of $F_{0\,2n-1}$. It is important to verify that the matrix F is self adjoint for the consistency of our formulation. The matrix element $F_{0\,2n-1}$ involves the matrix element $F_{2n\,2k-1}$ which in turn is expressed in terms of the combination $\left(M_1^T+\frac{1}{2}M_2^T\right)^{-1}$ and the matrix element $F_{0\,2n-1}$ itself. To carry out the calculation, unfortunately we first need to compute the explicit value of $F_{2n\,2k-1}$. The matrix element $F_{2n\,2k-1}$ is given by (89)

$$F_{2n\,2k-1}=-\frac{i\sqrt{3}}{2}\left[\left(M_1^T+\frac{1}{2}M_2^T\right)^{-1}\right]_{nk}$$
$$+\frac{1}{\pi}F_{02k-1}\sum_{m=1}^{\infty}\left[\left(M_1^T+\frac{1}{2}M_2^T\right)^{-1}\right]_{nm}\frac{(-1)^m}{(2m-1)^{3/2}} \tag{167}$$

Substituting the explicit value of $\left(M_1^T+\frac{1}{2}M_2^T\right)^{-1}$ into the above equation and summing over m, we find

$$F_{2n\,2k-1}=\frac{(-1)^{n+k}\sqrt{2n}\sqrt{2k-1}}{2i}\left[\frac{a_{2n}b_{2k-1}+b_{2n}a_{2k-1}}{2n-(2k-1)}\right.$$
$$\left.+\frac{a_{2n}b_{2k-1}-b_{2n}a_{2k-1}}{2n+(2k-1)}\right]+\frac{(-1)^n a_{2n}}{\sqrt{2n}}F_{0\,2k-1} \tag{168}$$

where $n=1,2,3,\cdots$. Combining Equation (168) with Equation (95), leads to

$$F_{0\,2m-1}=i(-1)^m\sqrt{2m-1}\sum_{k=1}^{\infty}\left[\frac{a_{2k}b_{2m-1}+b_{2k}a_{2m-1}}{2k-(2m-1)}\right.$$
$$\left.+\frac{a_{2k}b_{2m-1}-b_{2k}a_{2m-1}}{2k+(2m-1)}\right]-2F_{0\,2m-1}\frac{1}{2}\left(\frac{1+F_{00}}{1-F_{00}}\right) \tag{169}$$

To evaluate the sums appearing in (169) we first need to extend their range to include $k=0$. Doing so and making use of the result of already established identities in appendix A, Equation (169) reduces to

$$F_{0\,2m-1}=2i(-1)^m\frac{a_{2m-1}}{\sqrt{2m-1}}-F_{0\,2m-1}\left(\frac{1+F_{00}}{1-F_{00}}\right) \tag{170}$$

Solving the above equation for $F_{0\,2m-1}$, we obtain

$$F_{0\,2m-1} = -i\left(F_{00}-1\right)\left(-1\right)^{m}\frac{a_{2m-1}}{\sqrt{2m-1}} \tag{171}$$

which is precisely the adjoint of $F_{2m-1\,0}$; see Equation (166). Thus we have

$$F_{0\,odd} = \left(F^{\dagger}\right)_{0\,odd} \tag{172}$$

as expected.

The result obtained in (171) may be now used to find the explicit value of $F_{2n\,2m-1}$. Thus substituting Equation (171) back into Equation (168), we find

$$\begin{aligned} F_{2n\,2m-1} = {} & \frac{\left(-1\right)^{n+m}\sqrt{2n}\sqrt{2m-1}}{2i}\left[\frac{a_{2n}b_{2m-1}+b_{2n}a_{2m-1}}{2n-\left(2m-1\right)}\right. \\ & \left.+\frac{a_{2n}b_{2m-1}-b_{2n}a_{2m-1}}{2n+\left(2m-1\right)}\right]-i\left(F_{00}-1\right)\frac{\left(-1\right)^{n+m}a_{2n}a_{2m-1}}{\sqrt{2n}\sqrt{2m-1}} \end{aligned} \tag{173}$$

where $n,m=1,2,3,\cdots$.

The computation of the matrix element $F_{2n-1\,2m}$ is indeed quite cumbersome. The difficulty arises from the fact that the defining equation of $F_{2n-1\,2m}$, which is given by (91), involves this summing over the matrix $F_{2m\,2k}$ which is potentially divergent when the summing index m takes the k value. The limiting procedures involved in smoothing out the divergence are quite delicate and require careful consideration. Thus here we shall only give the final result; the details may be found in [9],

$$\begin{aligned} F_{2n-1\,2m} = {} & -\frac{\left(-1\right)^{n+m}\sqrt{2m}\sqrt{2n-1}}{2i}\left[\frac{a_{2m}b_{2n-1}+b_{2m}a_{2n-1}}{2m-\left(2n-1\right)}\right. \\ & \left.+\frac{a_{2m}b_{2n-1}-b_{2m}a_{2n-1}}{2m+\left(2n-1\right)}\right]+i\left(F_{00}-1\right)\frac{\left(-1\right)^{n+m}a_{2m}a_{2n-1}}{\sqrt{2m}\sqrt{2n-1}} \end{aligned} \tag{174}$$

Comparing Equations (173) and (174), we see that

$$F_{even\,odd} = \left(F^{\dagger}\right)_{even\,odd} \tag{175}$$

as expected.

To complete fixing the comma interaction vertex in the full-string basis we still need to compute the remaining elements, namely $F_{2n\,2m}$ and $F_{2n-1\,2m-1}$. The computation of the matrices $F_{2n\,2m}$ and $F_{2n-1\,2m-1}$ involve two distinct cases. The off diagonal case is given by $n\neq m$ and the diagonal case is given by $n=m$. Though the off diagonal elements are not difficult to compute, the diagonal elements are indeed quite involved and they can be evaluated by setting $n=m$ in the defining equations for $F_{2n\,2m}$ and $F_{2n-1\,2m-1}$ and then explicitly performing the sums with the help of the various identities we have established in [9]. An alternative way of computing the diagonal elements is to take the limit of $n\to m$ in the explicit expressions for the off diagonal elements. We have computed the diagonal elements both ways and obtained the same result which is a non trivial consistency check on our formalism. For illustration, here we shall compute the diagonal elements by the limiting process we spoke of as we

shall see shortly. But first let us compute the off diagonal elements. We first consider $F_{2n\,2m}$. From Equation (88), we have

$$\begin{aligned} F_{2n\,2k} &= \frac{1}{\pi}F_{0\,2k}\sum_{m=1}^{\infty}\left[\left(M_1^T+\frac{1}{2}M_2^T\right)^{-1}\right]_{nm}\frac{(-1)^m}{(2m-1)^{3/2}} \\ &\quad -\sum_{m=1}^{\infty}\left[\left(M_1^T+\frac{1}{2}M_2^T\right)^{-1}\right]_{nm}\left[\frac{1}{2}M_1^T+M_2^T\right]_{mk} \end{aligned} \tag{176}$$

Substituting the explicit value of $\left(M_1^T+\frac{1}{2}M_2^T\right)^{-1}$ and $\frac{1}{2}M_1^T+M_2^T$ into the above equation, we have

$$\begin{aligned} F_{2n\,2k} &= F_{0\,2k}\frac{(-1)^n a_{2n}}{(2n)^{1/2}}-\frac{(-1)^{n+k}(2k)^{1/2}(2n)^{1/2}}{2}\frac{a_{2n}b_{2k}+b_{2n}a_{2k}}{2n+2k} \\ &\quad -\frac{2}{\pi}\frac{(-1)^{n+k}}{\sqrt{3}}\sqrt{2k}\sqrt{2n}\left\{\frac{1}{2}\sum_{m=1}^{\infty}\frac{a_{2n}b_{2m-1}+b_{2n}a_{2m-1}}{\left[2n-(2m-1)\right]\left[2k-(2m-1)\right]}\right. \\ &\quad \left.+\sum_{m=1}^{\infty}\frac{a_{2n}b_{2m-1}-b_{2n}a_{2m-1}}{\left[2n+(2m-1)\right]\left[2k+(2m-1)\right]}\right\} \end{aligned} \tag{177}$$

The difficulty in evaluating the sums arises from the fact in performing these sums one usually make use of partial fraction to reduce them to the standard sums treated in [9]; however partial fraction in this case fails due to a divergence arising from the particular case when $n=m$. Thus to carry our program through, we first consider the case for which $n\neq k$. For $n\neq k$, partial fraction can be used to reduce the sums in the above expression to the standard results obtained in [9]. Skipping some rather straight forward algebra, we find

$$F_{2n\,2k}=\frac{F_{02k}(-1)^n a_{2n}}{\sqrt{2n}}-\frac{(-1)^{n+k}\sqrt{2k}\sqrt{2n}}{2}\left[\frac{a_{2n}b_{2k}+b_{2n}a_{2k}}{2n+2k}+\frac{a_{2n}b_{2k}-b_{2n}a_{2k}}{2n-2k}\right] \tag{178}$$

where $n,k=1,2,3,\cdots$, and $n\neq k$. Substituting the value of $F_{0\,2k}$, which is given by Equation (163), we have

$$\begin{aligned} F_{2n\,2k} &= (F_{00}-1)\frac{(-1)^{n+k}a_{2n}a_{2k}}{(2n)^{1/2}(2k)^{1/2}}-\frac{(-1)^{n+k}(2k)^{1/2}(2n)^{1/2}}{2} \\ &\quad \times\left[\frac{a_{2n}b_{2k}+b_{2n}a_{2k}}{2n+2k}+\frac{a_{2n}b_{2k}-b_{2n}a_{2k}}{2n-2k}\right] \end{aligned} \tag{179}$$

which is the desired result valid for $n,k=1,2,3,\cdots$,and subject to the condition $n\neq k$. Note that in this case we have

$$F_{even\,even}=\left(F^{\dagger}\right)_{even\,even} \tag{180}$$

as expected. As we pointed earlier the diagonal element $F_{2n\,2k}$ may be obtained by taking the limit of $k\to n$ in Equation (177). Hence

$$\begin{aligned} F_{2n\,2n} &= F_{02n}\frac{(-1)^n a_{2n}}{(2n)^{1/2}}-\frac{a_{2n}b_{2n}+b_{2n}a_{2n}}{4} \\ &\quad -\frac{2}{\pi}\frac{2n}{\sqrt{3}}\left[\frac{1}{2}a_{2n}\tilde{S}^b_{-2n}+\frac{1}{2}b_{2n}\tilde{S}^a_{-2n}+a_{2n}\tilde{S}^b_{2n}-b_{2n}\tilde{S}^a_{2n}\right] \end{aligned} \tag{181}$$

This result may be simplified further with the help of the following identities derived in [9]

$$\tilde{S}^a_{-2n} = \frac{1}{2}\tilde{S}^a_{2n} + \frac{1}{4}\pi\sqrt{3}S^a_{2n}, n > 0 \tag{182}$$

and

$$\tilde{S}^b_{-2n} = -\frac{1}{2}\tilde{S}^b_{2n} + \frac{1}{4}\pi\sqrt{3}S^b_{2n}, n > 0 \tag{183}$$

Hence

$$\begin{aligned} F_{2n\,2n} = F_{0\,2n}\frac{(-1)^n a_{2n}}{(2n)^{1/2}} - \frac{a_{2n}b_{2n} + b_{2n}a_{2n}}{4} \\ -\frac{2n}{\pi}\frac{1}{2}\left[\frac{\pi}{2}\left(a_{2n}S^b_{2n} + b_{2n}S^a_{2n}\right) + \sqrt{3}\left(a_{2n}\tilde{S}^b_{2n} - b_{2n}\tilde{S}^a_{2n}\right)\right] \end{aligned} \tag{184}$$

The generalization of the plus combination in the square bracket has been considered before; its value is given explicitly by setting $p = 1/3$ in Equation (141)

$$b_{2n}S^a_{2n} + a_{2n}S^b_{2n} = \frac{2}{2n} \tag{185}$$

Using this identity, we obtain

$$F_{2n\,2n} = F_{0\,2n}\frac{(-1)^n a_{2n}}{\sqrt{2n}} - \frac{1}{2}b_{2n}a_{2n} - \frac{1}{2} - \frac{2n}{\pi}\frac{\sqrt{3}}{2}\left(a_{2n}\tilde{S}^b_{2n} - b_{2n}\tilde{S}^a_{2n}\right) \tag{186}$$

Using Equation (163) to eliminate $F_{0\,2n}$, the above expression becomes

$$F_{2n\,2n} = \left(F_{00} - 1\right)\frac{a_{2n}a_{2n}}{2n} - \frac{1}{2}b_{2n}a_{2n} - \frac{1}{2} - \frac{2n}{\pi}\frac{\sqrt{3}}{2}\left(a_{2n}\tilde{S}^b_{2n} - b_{2n}\tilde{S}^a_{2n}\right) \tag{187}$$

which satisfies the property

$$F_{even\,even} = \left(F^\dagger\right)_{even\,even} \tag{188}$$

as expected.

Finally we consider the matrix elements $F_{odd\,odd}$. From Equation (90), we have

$$F_{2n-1\,2k-1} = \frac{2i}{\sqrt{3}}\sum_{m=1}^{\infty}\left[\frac{1}{2}M_1^T + M_2^T\right]_{nm}F_{2m\,2k-1} + \frac{2i}{\pi\sqrt{3}}\frac{(-)^n}{(2n-1)^{3/2}}F_{0\,2k-1} \tag{189}$$

The values of $F_{2m\,2k-1}$ and $F_{0\,2k-1}$ are given by Equations (173) and (171) respectively. Hence, substituting the explicit value of M_1^T and M_2^T in (189) and skipping some rather straightforward algebra, we find

$$\begin{aligned} F_{2n-1\,2k-1} = \frac{(-1)^{n+k}(F_{00}-1)}{3}\frac{a_{2k-1}a_{2n-1}}{(2n-1)^{1/2}(2k-1)^{1/2}} \\ + \frac{(-1)^{k+n}\sqrt{2n-1}\sqrt{2k-1}}{2}\frac{a_{2n-1}b_{2k-1} + b_{2n-1}a_{2k-1}}{(2n-1)+(2k-1)} \\ + \frac{2(-1)^{k+n}}{\sqrt{3}}\frac{\sqrt{2k-1}\sqrt{2n-1}}{\pi}\sum_{m=0}^{\infty}\left[\frac{1}{2}\frac{a_{2m}b_{2k-1} + b_{2m}a_{2k-1}}{\left[2m-(2n-1)\right]\left[2m-(2k-1)\right]}\right. \\ \left. - \frac{a_{2m}b_{2k-1} - b_{2m}a_{2k-1}}{\left[2m+(2n-1)\right]\left[2m+(2k-1)\right]}\right] \end{aligned} \tag{190}$$

Now there are two cases to consider $k \neq n$ and $k = n$. For $k \neq n$, Equation (190) becomes

$$F_{2n-1\,2k-1} = \frac{(-1)^{n+k}(F_{00}-1)}{3}\frac{a_{2k-1}a_{2n-1}}{\sqrt{2n-1}\sqrt{2k-1}} + \frac{(-1)^{k+n}\sqrt{2n-1}\sqrt{2k-1}}{2} \times\left[\frac{a_{2n-1}b_{2k-1}+b_{2n-1}a_{2k-1}}{(2n-1)+(2k-1)} + \frac{a_{2n-1}b_{2k-1}-b_{2n-1}a_{2k-1}}{(2n-1)-(2k-1)}\right] \tag{191}$$

where $n,k = 1,2,3$ and we have made use of the results in [9] to evaluate the various sums. Thus for $n \neq k$, we see that

$$F_{odd\ odd} = \left(F^{\dagger}\right)_{odd\ odd}, \text{ for } n \neq k \tag{192}$$

For $k = n$, Equation (190) becomes

$$F_{2n-1\,2n-1} = \frac{1}{3}(F_{00}-1)\frac{a_{2n-1}a_{2n-1}}{2n-1} + \frac{1}{2}a_{2n-1}b_{2n-1} + \frac{2}{\sqrt{3}}\frac{(2n-1)}{\pi}\left\{\frac{b_{2n-1}\tilde{E}^{a}_{-(2n-1)} + a_{2n-1}\tilde{E}^{b}_{-(2n-1)}}{2} - \left[b_{2n-1}\tilde{E}^{a}_{(2n-1)} - a_{2n-1}\tilde{E}^{b}_{(2n-1)}\right]\right\} \tag{193}$$

where we have made use of the results in [9] to evaluate the various sums appearing in the steps leading to the above result. Using the identities

$$\tilde{E}^{a}_{-(2n-1)} = \frac{1}{2}\tilde{E}^{a}_{2n-1} + \frac{1}{4}\pi\sqrt{3}S^{a}_{2n-1} \tag{194}$$

$$\tilde{E}^{b}_{-(2n-1)} = -\frac{1}{2}\tilde{E}^{b}_{2n-1} + \frac{1}{4}\pi\sqrt{3}S^{b}_{2n-1} \tag{195}$$

derived in [9], the above expression becomes

$$F_{2n-1\,2n-1} = \frac{1}{3}(F_{00}-1)\frac{a_{2n-1}a_{2n-1}}{2n-1} + \frac{1}{2}a_{2n-1}b_{2n-1} + \frac{1}{2} + \frac{\sqrt{3}}{2\pi}(2n-1)\left(a_{2n-1}\tilde{E}^{b}_{(2n-1)} - b_{2n-1}\tilde{E}^{a}_{(2n-1)}\right) \tag{196}$$

which is clearly self adjoint. Thus from Equations (191) and (196) it follows that

$$F_{odd\ odd} = \left(F^{\dagger}\right)_{odd\ odd} \tag{197}$$

as expected. With this result we, establish that $F = F^{\dagger}$ as anticipated.

In the original variables, the comma three-string in (60) can be written in the form

$$\left|V^{HS}_{x}\right\rangle = \delta\left(\sum_{r=1}^{3}p_0^r\right)V^{HS}\left(\alpha^{1\dagger},\alpha^{2\dagger},\alpha^{3\dagger}\right)\left|0\right\rangle_{123} \tag{198}$$

where

$$V^{HS}\left(\alpha^{1\dagger},\alpha^{2\dagger},\alpha^{3\dagger}\right) = \mathrm{e}^{-\frac{1}{2}\sum_{r,s=1}^{3}\sum_{n,m=0}^{\infty}a^{r}_{-n}\mathcal{F}^{rs}_{nm}a^{s}_{-m}} \tag{199}$$

The matrix elements $\mathcal{F}^{ij}_{nm}$ may be obtained by comparing (199) to (60). For

example consider the terms involving a^1 and a^2 in (60)

$$\begin{aligned}&-\frac{1}{2}\left(\frac{1}{3}a^1_{-n}C_{nm}a^2_{-m}+\frac{1}{3}a^2_{-n}C_{nm}a^1_{-m}\right)-\left(\frac{1}{3}\bar{e}^2a^1_{-n}F_{nm}a^2_{-m}+\frac{1}{3}e^2a^2_{-n}F_{nm}a^1_{-m}\right)\\&=-\frac{1}{2}a^1_{-n}\left[\frac{1}{3}C-\frac{1}{6}\left(F+F^T\right)+i\frac{1}{6}\sqrt{3}\left(F-F^T\right)\right]_{nm}a^2_{-m}\\&\quad-\frac{1}{2}a^2_{-n}\left[\frac{1}{3}C-\frac{1}{6}\left(F+F^T\right)-i\frac{1}{6}\sqrt{3}\left(F-F^T\right)\right]_{nm}a^1_{-m}\end{aligned}\tag{200}$$

Comparing this result with the terms $-\frac{1}{2}a^1_{-n}\mathcal{F}^{12}_{nm}a^2_{-m}$ and $-\frac{1}{2}a^2_{-n}\mathcal{F}^{21}_{nm}a^1_{-m}$, we obtain

$$\mathcal{F}^{12}=\frac{1}{6}\left[\left(2C-F-\bar{F}\right)+i\sqrt{3}\left(F-\bar{F}\right)\right]\tag{201}$$

$$\mathcal{F}^{21}=\frac{1}{6}\left[\left(2C-F-\bar{F}\right)-i\sqrt{3}\left(F-\bar{F}\right)\right]\tag{202}$$

where we have used the fact that $F^T=\bar{F}$. Likewise one expresses the remaining matrix element $\mathcal{F}^{rs}_{nm}$ in terms of the matrix elements C_{nm} and F_{nm} and their complex conjugates. All in all we have

$$\begin{aligned}\mathcal{F}=\frac{1}{3}\Bigg[&\left(C+F+\bar{F}\right)\begin{pmatrix}1&0&0\\0&1&0\\0&0&1\end{pmatrix}+\left(C-\frac{F+\bar{F}}{2}\right)\begin{pmatrix}0&1&1\\1&0&1\\1&1&0\end{pmatrix}\\&+i\frac{\sqrt{3}}{2}\left(F-\bar{F}\right)\begin{pmatrix}0&1&-1\\-1&0&1\\1&-1&0\end{pmatrix}\Bigg]\end{aligned}\tag{203}$$

which is the same result obtained in ref. [7]. Equation (203) gives completely the comma interaction three vertex in the full string basis in the representation with oscillator zero modes.

Sometimes it is useful to express the comma vertex in the momentum representation. For a single oscillator with momentum p and creation operator $\alpha^\dagger$, the change of basis is accomplished by

$$\left|p\right)=\exp\left(-\frac{1}{2}p_0\bar{p}_0+\bar{p}_0\alpha^\dagger_0+\bar{\alpha}^\dagger_0p_0-\alpha^\dagger\bar{\alpha}^\dagger\right)\left|0\right)\tag{204}$$

with $\left|0\right\rangle$ being the oscillator ground state. Thus using the above identity and Equation (61) one finds the following representation for the Vertex in the momentum space

$$\exp\left[-\frac{1}{2}\sum_{n,m=0}^{\infty}A^{3\dagger}_nC_{nm}A^{3\dagger}_m-\sum_{n,m=1}^{\infty}A^\dagger_nF'_{nm}\bar{A}^\dagger_m-\sum_{n=0}^{\infty}A^\dagger_nF'_{n0}\bar{P}_0-\sum_{n=0}^{\infty}P_0F'_{0m}\bar{A}^\dagger_m+\frac{1}{2}\bar{P}_0F'_{00}P_0\right]\tag{205}$$

where the prime matrices F'_{nm} are related to the unprimed matrices F_{nm} by

$$F'_{00}=\frac{1+F_{00}}{1-F_{00}}\tag{206}$$

$$F'_{0n}=\frac{F_{0n}}{1-F_{00}},\quad n=1,2,3,\cdots\tag{207}$$

$$F'_{nm} = F_{nm} + \frac{F_{n0}F_{0m}}{1-F_{00}}, \quad n,m = 1,2,3,\cdots \tag{208}$$

The property $F^2 = 1$ in Equation (83) implies that in the momentum representation, the F' matrix satisfies

$$\sum_{k=1}^{\infty} F'_{nk}F'_{km} = \delta_{nm}, \quad n,m = 1,2,3,\cdots \tag{209}$$

For $n \neq 0$, we have $a^r_{-n} \equiv \alpha^r_{-n}/\sqrt{n}$, and so Equation (205) may be written as

$$\begin{aligned} \left|V_x^{HS}\right\rangle = \int\prod p_0^r \exp\Bigg[\frac{1}{2}\sum_{r,s=1}^{3}\sum_{n,m=1}^{\infty}\alpha^r_{-n}G^{rs}_{nm}\alpha^s_{-m} + \sum_{r,s=1}^{3}p_0^r G^{rs}_{0m}\alpha^s_{-m} \\ + \frac{1}{2}\sum_{r,s=1}^{3}p^r G^{rs}_{00}p^s_0\Bigg]\left|0,p\right)_{123} \end{aligned} \tag{210}$$

where the matrix G is defined through the relation

$$G^{rs}_{nm} = -\frac{1}{\sqrt{n+\delta_{n0}}}\mathcal{F}'^{rs}_{nm}\frac{1}{\sqrt{m+\delta_{m0}}} \tag{211}$$

The ghost part of the comma vertex in the full string basis has the same structure as the coordinate one apart from the mid-point insertions

$$\left|V_\phi^{HS}\right\rangle = \mathrm{e}^{\frac{1}{2}i\sum_{r=1}^{3}\phi^r(\pi/2)}V_\phi^{HS}\left(\alpha^{\phi,1\dagger},\alpha^{\phi,2\dagger},\alpha^{\phi,3\dagger}\right)0, N_{ghost} = \frac{3}{2} > {}^{\phi}_{123} \tag{212}$$

where the α's are the bosonic oscillators defined by the expansion of the bosonized ghost $\left(\phi(\sigma), p^\phi(\sigma)\right)$ fields and $V_\phi^{HS}\left(\alpha^{\phi,1\dagger},\alpha^{\phi,2\dagger},\alpha^{\phi,3\dagger}\right)$ is the exponential of the quadratic form in the ghost creation operators with the same structure as the coordinate piece of the vertex.

6. Conclusion

We have successfully constructed the comma three interaction vertex of the open bosonic string in terms of the oscillator representation of the full open bosonic string. The form of the vertex we have obtained for both the matter and ghost sectors are those obtained in ref. [7] [8] [10]. This establishes the equivalence between Witten's 3-interaction vertex of open bosonic strings and the half string 3-vertex directly without the need for the coherent state methods employed in ref. [1].

Conflicts of Interest

The authors declare no conflicts of interest regarding the publication of this paper.

References

[1] Bordes, J., Hong-Mo, C., Nellen, L. and Sheung, T. (1991) *Nuclear Physics B*, **351**, 441-473. https://doi.org/10.1016/0550-3213(91)90097-H

[2] Abdurrahman, A., Anton, F. and Bordes, J. (1993) *Nuclear Physics B,* **397**, 260-282. https://doi.org/10.1016/0550-3213(93)90344-O

[3] Abdurrahman, A, Anton, F. and Bordes, J. (1994) *Nuclear Physics B,* **411**, 694-714. https://doi.org/10.1016/0550-3213(94)90467-7

[4] Abdurrahman, A. and Bordes, J. (2001) *Nuovo Cimento B*, **116**, 635.

[5] Abdurrahman, A. and Bordes, J. (2003) *Nuovo Cimento B*, **118**, 641.

[6] Abdurrahman, A. and Bordes, J. (2003) *Nuovo Cimento B*, **116**, 635-658.

[7] Gross, D.J. and Jevicki, A. (1987) *Nuclear Physics B,* **283**, 1-49. https://doi.org/10.1016/0550-3213(87)90260-4

[8] Gross, D.J. and Jevicki, A. (1987) *Nuclear Physics B,* **287**, 225-250. https://doi.org/10.1016/0550-3213(87)90104-0

[9] Gassem, M. (2008) The Operator Connecting the SCSV 3-Vertex and the Comma 3-Vertex. PhD Thesis, The American University, London. https://doi.org/10.1103/PhysRevD.49.2966

[10] Itoh, K., Ogawa, K. and Suchiro, K. (1987) *Nuclear Physics B*, **289**, 127. https://doi.org/10.1016/0550-3213(87)90374-9
Siegel, W. (1984) *Physics Letters B*, **149**, 157-161. https://doi.org/10.1016/0370-2693(84)91574-0
Hata, H., Itoh, K., Kugo, T., Kunimoto, H. and Ogawa, K. (1986) *Physics Letters B*, **172**, 186. https://doi.org/10.1016/0370-2693(86)90834-8
Neveu, A. and West, P. (1986) *Physics Letters B*, **165**, 63-66. https://doi.org/10.1016/0370-2693(85)90691-4
Friedan, D. (1985) *Physics Letters B*, **162**, 102-108.
Gervais, J.L. (1986) l'Ecole Normale Superieure Preprints LPTENS, 85/35. https://doi.org/10.1016/0370-2693(85)91069-X
Gervais, J.L. (1986) l'Ecole Normale Superieure Preprints LPTENS 86/1.
Neveu, A. and West, P. (1986) *Physics Letters B*, **168**, 192. https://doi.org/10.1016/0370-2693(86)90962-7
Chang, N.P., Guo, H.Y., Qiu, Z. and Wu, K. (1986) City College Preprint.
Tseytlin, A.A. (1986) *Physics Letters B*, **168**, 63. https://doi.org/10.1016/0370-2693(86)91461-9

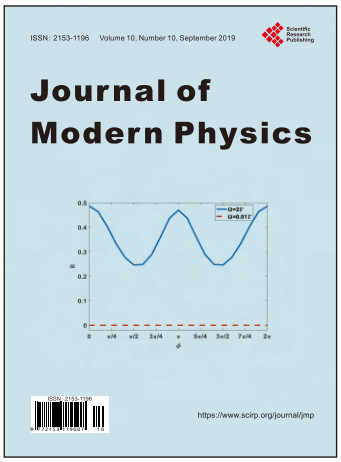

Call for Papers

Journal of Modern Physics

ISSN: 2153-1196 (Print) ISSN: 2153-120X (Online)
https://www.scirp.org/journal/jmp

Journal of Modern Physics **(JMP)** is an international journal dedicated to the latest advancement of modern physics. The goal of this journal is to provide a platform for scientists and academicians all over the world to promote, share, and discuss various new issues and developments in different areas of modern physics.

Editor-in-Chief

Prof. Yang-Hui He City University, UK

Subject Coverage

Journal of Modern Physics publishes original papers including but not limited to the following fields:

Biophysics and Medical Physics
Complex Systems Physics
Computational Physics
Condensed Matter Physics
Cosmology and Early Universe
Earth and Planetary Sciences
General Relativity
High Energy Astrophysics
High Energy/Accelerator Physics
Instrumentation and Measurement
Interdisciplinary Physics
Materials Sciences and Technology
Mathematical Physics
Mechanical Response of Solids and Structures
New Materials: Micro and Nano-Mechanics and Homogeneization
Non-Equilibrium Thermodynamics and Statistical Mechanics
Nuclear Science and Engineering
Optics
Physics of Nanostructures
Plasma Physics
Quantum Mechanical Developments
Quantum Theory
Relativistic Astrophysics
String Theory
Superconducting Physics
Theoretical High Energy Physics
Thermology

We are also interested in: 1) Short Reports—2-5 page papers where an author can either present an idea with theoretical background but has not yet completed the research needed for a complete paper or preliminary data; 2) Book Reviews—Comments and critiques.

Notes for Intending Authors

Submitted papers should not have been previously published nor be currently under consideration for publication elsewhere. Paper submission will be handled electronically through the website. All papers are refereed through a peer review process. For more details about the submissions, please access the website.

Website and E-Mail

https://www.scirp.org/journal/jmp **E-mail: jmp@scirp.org**

What is SCIRP?

Scientific Research Publishing (SCIRP) is one of the largest Open Access journal publishers. It is currently publishing more than 200 open access, online, peer-reviewed journals covering a wide range of academic disciplines. SCIRP serves the worldwide academic communities and contributes to the progress and application of science with its publication.

What is Open Access?

All original research papers published by SCIRP are made freely and permanently accessible online immediately upon publication. To be able to provide open access journals, SCIRP defrays operation costs from authors and subscription charges only for its printed version. Open access publishing allows an immediate, worldwide, barrier-free, open access to the full text of research papers, which is in the best interests of the scientific community.

- High visibility for maximum global exposure with open access publishing model
- Rigorous peer review of research papers
- Prompt faster publication with less cost
- Guaranteed targeted, multidisciplinary audience

Scientific Research Publishing

Website: https://www.scirp.org

Subscription: sub@scirp.org

Advertisement: service@scirp.org